**RĪGAS TEHNISKĀ UNIVERSITĀTE**
Materiālzinātnes un lietišķās ķīmijas fakultāte
Lietišķās ķīmijas institūts

**RIGA TECHNICAL UNIVERSITY**
Faculty of Materials Science and Applied Chemistry
Institute of Applied Chemistry

**Ilze Māliņa**
Doktora studiju programmas "Ķīmija" doktorante
Doctoral Student of the Study Programme "Chemistry"

# HROMOFORI UN LUMINOFORI UZ β,β'-TRIKETONU UN β-DIKETONU BĀZES

**Promocijas darbs**

# CHROMOPHORES AND LUMINOPHORES BASED ON β,β'-TRIKETONES AND β-DIKETONES

**Doctoral Thesis**

Zinātniskais vadītājs
Profesors *Dr. habil. chem.*
VALDIS KAMPARS

Scientific supervisor
Professor Dr. habil. chem.
VALDIS KAMPARS

RTU izdevniecība / RTU Press
Rīga 2020 / Riga 2020

Māliņa, I. Hromofori un luminofori uz β,β'-triketonu un β-diketonu bāzes. Promocijas darbs. Rīga: RTU Izdevniecība, 2020. 124 lpp.

Māliņa, I. Chromophores and Luminophores Based on β,β'-Triketones and β-Diketones. Doctoral Thesis. Riga: RTU Press, 2020. 124 p.

Iespiests saskaņā ar RTU promocijas padomes "P-01" 2020. gada 6. jūlija lēmumu, protokols Nr. 04030-9.1/5.

Published in accordance with the decision of the Promotion Council "P-01" of 6 July 2020, Minutes No. 04030-9.1/5.

# PROMOCIJAS DARBS IZVIRZĪTS ZINĀTNES DOKTORA GRĀDA IEGŪŠANAI RĪGAS TEHNISKAJĀ UNIVERSITĀTĒ

Promocijas darbs zinātnes doktora (*Ph. D.*) grāda iegūšanai tiek publiski aizstāvēts 2020. gada 12. novembrī Rīgas Tehniskās universitātes Materiālzinātnes un lietišķās ķīmijas fakultātē, Rīgā, Paula Valdena iela 3, 272. auditorijā.

OFICIĀLIE RECENZENTI

Profesore *Dr. chem.* Māra Jure,
Rīgas Tehniskā universitāte, Latvija

Vadošais pētnieks *Dr. habil. chem.* Gunārs Duburs,
Latvijas Organiskās sintēzes institūts, Latvija

Vadošais pētnieks *Dr. phys.* Mārtiņš Rutkis,
Latvijas Universitātes Cietvielu fizikas institūts, Latvija

APSTIPRINĀJUMS

Apstiprinu, ka esmu izstrādājusi šo promocijas darbu, kas iesniegts izskatīšanai Rīgas Tehniskajā universitātē zinātnes doktora (*Ph. D.*) grāda iegūšanai. Promocijas darbs zinātniskā grāda iegūšanai nav iesniegts nevienā citā universitātē.

Ilze Māliņa ……. (paraksts)

Datums: ……

Promocijas darbs ir sagatavots kā tematiski vienota zinātnisko publikāciju kopa. Tajā ir kopsavilkums un sešas publikācijas. Publikācijas uzrakstītas angļu valodā, to kopējais apjoms ir 54 lpp.

# SATURS

**LIETOTIE SAĪSINĀJUMI** ..... 5
**PROMOCIJAS DARBA VISPĀRĒJS RAKSTUROJUMS** ..... 7
Tēmas aktualitāte ..... 7
Pētījuma mērķis un uzdevumi ..... 8
Tēzes aizstāvēšanai ..... 9
Zinātniskā novitāte un galvenie rezultāti ..... 9
Darba struktūra un apjoms ..... 9
Darba aprobācija un publikācijas ..... 10
**PROMOCIJAS DARBA GALVENIE REZULTĀTI** ..... 12
$Eu^{3+}$ kompleksu ar β,β'-triketonu ligandiem sintēze un spektroskopisko īpašību raksturojumi ..... 12
$Eu^{3+}$ kompleksu ar β-diketonu ligandiem sintēze un spektroskopisko īpašību raksturojumi17
2-cinnamoil-1,3-indandiona un 2-cinnamoildimedona atvasinājumu sintēze un spektroskopisko īpašību raksturojumi ..... 21
**SECINĀJUMI** ..... 28
**LITERATŪRAS SARAKSTS** ..... 30
**PATEICĪBAS** ..... 32
**PIELIKUMI/PUBLICATIONS** ..... 64

# LIETOTIE SAĪSINĀJUMI

| | |
|---|---|
| $\lambda_{abs}$ | absorbcijas spektra maksimums |
| $\lambda_{em}$ | emisijas spektra maksimums |
| $\lambda_{exc}$ | ierosināšanas spektra maksimums |
| $\Delta\lambda$ | Stoksa nobīde |
| $\tau$ | luminiscences dzīves laiks |
| A | akceptorā grupa |
| AD | 2-acetil-5,5-dimetilcikloheksān-1,3-diona anjons jeb 2-acetildimedona anjons |
| *AEE* | agregācijas pastiprināta emisija |
| AID | 2-acetil-1*H*-indēn-1,3-(2*H*)-diona anjons jeb 2-acetil-1,3-indandiona anjons |
| BD | 2-benzoil-5,5-dimetilcikloheksān-1,3-diona anjons jeb 2-benzoildimedona anjons |
| BID | 2-benzoil-1*H*-indēn-1,3-(2*H*)-diona anjons jeb 2-benzoil-1,3-indandiona anjons |
| BPh | bifenilgrupa |
| Bu | butilgrupa |
| CBZ-HDBM | 1-[4-(9*H*-karbazol-9-il)-fenil]-3-fenilpropān-1,3-dions |
| CBZ-DBM | 1-[4-(9*H*-karbazol-9-il)-fenil]-3-fenilpropān-1,3-diona anjons |
| *CT* | lādiņa pārnese |
| D | donorā grupa |
| DBM | 1,3-difenil-propān-1,3-diona anjons jeb dibenzoilmetāna anjons |
| Et | etilgrupa |
| Fl | fluorescence |
| HAD | 2-acetil-5,5-dimetilcikloheksān-1,3-dions jeb 2-acetildimedons |
| HAID | 2-acetil-1*H*-indēn-1,3-(2*H*)-dions jeb 2-acetil-1,3-indandions |
| HBD | 2-benzoil-5,5-dimetilcikloheksān-1,3-dions jeb 2-benzoildimedons |
| HBID | 2-benzoil-1*H*-indēn-1,3-(2*H*)-dions jeb 2-benzoil-1,3-indandions |
| HDBM | 1,3-difenilpropān-1,3-dions jeb dibenzoilmetāns |
| HMBID | 2-(4-metilbenzoil)-1*H*-indēn-1,3-(2*H*)-dions jeb 2-(4-metilbenzoil)-1,3-indandions |
| *ITO* | indija alvas oksīds |
| Me | metilgrupa |
| MBID | 2-(4-metilbenzoil)-1*H*-indēn-1,3-(2*H*)-diona anjons jeb 2-(4-metilbenzoil)-1,3-indandiona anjons |
| MeCN | acetonitrils |
| Me-DBM | 1-(4-metilfenil)-3-fenilpropān-1,3-diona anjons |
| Me-HDBM | 1-(4-metilfenil)-3-fenilpropān-1,3-dions |
| MeOH | metanols |
| OLED | organiskā gaismu emitējošā diode |
| PEDOT:PSS | poli(3,4-etilēndioksitiofēna):polistirola sulfonāts |

| | |
|---|---|
| Ph | fenilgrupa |
| PHEN | 1,10-fenantrolīns |
| *PLQY* | absolūtais fotoluminiscences kvantu iznākums |
| PMMA | poli-(metilmetaakrilāts) |
| PVK | *N*-polivinilkarbazols |
| $S_1$ | singleta enerģijas līmenis |
| $T_1$ | tripleta enerģijas līmenis |
| THF | tetrahidrofurāns |
| TPBi | 1,3,5-tri-(*N*-fenil-2-benzimidazoil)-benzols |
| UV | ultravioletais |

# PROMOCIJAS DARBA VISPĀRĒJS RAKSTUROJUMS

## Tēmas aktualitāte

β,β'-triketoni un β-diketoni ir plaši pētīti savienojumi dažādu jaunu emitējošu un nelineāru optisko materiālu iegūšanā. Viens no veidiem, kā iegūt luminoforus uz šo savienojumu bāzes, ir izmantot to molekulā esošo, koordinēties spējīgo β-diketona fragmentu. 1,3-diketoni pēc deprotonēšanas izveido β-diketona anjonus, kas viegli koordinējas gan ar metālu, gan nemetālu katjoniem, veidojot dažādus kompleksus, kuriem parasti piemīt izteiktas emisijas īpašības, piemēram, lantanoīdu katjonu β-diketonātu kompleksu luminiscence raksturojas ar izteiktu krāsu tīrību, augstiem luminiscences kvantu iznākumiem un līdz pat vairākiem simtiem μs gariem emisijas dzīves laikiem [1]. Šajā gadījumā enola anjons veido ligandu, kas nodrošina metāla katjonu ar enerģiju gaismas absorbcijas rezultātā. Otrs veids, kā iegūt luminoforus un nelineāros hromoforus, ir izmantot 1,3-diketona fragmentu kā elektronakceptoro grupu (A). Ievadot molekulā donoro grupu (D), iespējams iegūt *push-pull* D-A vai D-π-A tipa luminoforu savienojumus. Šo savienojumu priekšrocība ir salīdzinoši liela izvēle starp D un A grupām, ar kurām var pielāgot vēlamās savienojuma emisijas un citas īpašības.

β,β'-triketoni ir savienojumi, kuru struktūras pamatā ir 1,3-diketona grupu saturošs cikls un 2-acilaizvietotājs, kas novietots pie cikla otrā oglekļa atoma. Šāda tipa savienojumiem, pie kuriem pieder 2-acil-5,5-dimetilciklohekšān-1,3-diona (2-acildimedona) un 2-acil-1*H*-indēn-1,3-(2*H*)-diona (2-acil-1,3-indandiona) atvasinājumi, plaši pētītas dažādas farmakoloģiskās īpašības [2], bet maz datu ir par to fotofizikālajām īpašībām un potenciālu luminoforu savienojumu iegūšanā. Līdz šim ziņots, ka 2-acil-1,3-indandiona atvasinājumi tiek raksturoti ar intensīvu absorbciju tuvajā ultravioletajā (UV) apgabalā ar augstiem absorbcijas koeficientiem, kā arī salīdzinoši augstu stabilitāti UV starojumā [3], kas ir teicami priekšnosacījumi lantanoīdu kompleksos izmantotajiem ligandiem, kā arī prekursoriem D-π-A tipa savienojumiem. Turklāt pētījumi par β,β'-triketonātu izmantošanu luminiscējošu metālu kompleksu iegūšanā šobrīd aprobežojas vien ar dažu $Eu^{3+}$ tris un Lūisa bāzu kompleksu ar 2-acil-1,3-indandiona atvasinājumu ligandiem izmantošanu organisko gaismu emitējošo diožu (OLED) izstrādē [4], [5]. Savukārt par β,β'-triketonu izmantošanu D-π-A tipa savienojumu iegūšanā šobrīd ziņots tikai par vairākiem efektīvi luminiscējošiem 2-cinnamoil-1,3-indandiona [6]–[8] un 2-cinnamoilpirona atvasinājumiem [9]. No otras puses, β-diketoni ir visvairāk pētītā lantanoīdu metālu katjonu kompleksos izmantotā ligandu klase. Uz 1,3-difenilpropān-1,3-diona jeb dibenzoilmetāna (HDBM) atvasinājumu bāzes, kas tiek uzskatīti par ļoti efektīviem aromātiskajiem un simetriskajiem ligandiem, ir iegūti vairāki $Eu^{3+}$ kompleksi ar potenciālu optoelektronisko iekārtu izstrādē [1]. Tādējādi salīdzinājums starp populārā HDBM atvasinājumu β-diketonātu $Eu^{3+}$ kompleksiem un neizpētītajiem β,β'-triketonu ligandus saturošiem $Eu^{3+}$ kompleksiem varētu sniegt ieskatu par ligandu struktūras un simetriskuma ietekmi uz $Eu^{3+}$ kompleksu īpašībām.

Ņemot vērā to, ka promocijas darba izejas savienojumus β,β'-triketonus – 2-acildimedona un 2-acil-1,3-indandiona atvasinājumus – var dažādos virzienos modificēt, promocijas darbs tika dalīts divās neatkarīgās daļās ar diviem dažādiem mērķiem. Par pirmo mērķi tika izvirzīta

β,β'-triketonu – 2-acildimedonāta un 2-acil-1,3-indandionāta atvasinājumu – dažādas struktūras (tris, Lūisa bāzes, tetrakis) eiropija trivalento katjonu ($Eu^{3+}$) kompleksu sintēze. Salīdzināšanas nolūkos tika iegūti arī simetriskākus HDBM atvasinājumu ligandus saturoši $Eu^{3+}$ kompleksi. Pirmais mērķis ietver iegūto kompleksu īpašību izpēti, kuras rezultātā varētu izdarīt secinājumus par kompleksu struktūras un īpašību sakarībām, kā arī, izmantojot eksperimentālos un teorētiski aprēķinātos datus, noteikt, ar kuriem ligandiem iespējams iegūt visefektīvāk emitējošus $Eu^{3+}$ kompleksus.

Otrs mērķis bija izpētīt 2-acetil-5,5-dimetilcikloheksān-1,3-dionu (2-acetildimedonu) un 2-acetil-1*H*-indēn-1,3-(2*H*)-dionu (2-acetil-1,3-indandionu) kā izejas materiālus *push-pull* D-π-A tipa savienojumu (5,5-dimetil-2-[(2*E*)-3-fenil-1-okso-2-propēn-1-il]-cikloheksān-1,3-diona jeb 2-cinnamoildimedona un 2-[(2*E*)-3-fenil-1-okso-2-propēn-1-il]-1*H*-indēn-1,3(2*H*)-diona jeb 2-cinnamoil-1,3-indandiona atvasinājumu) iegūšanā, kas 1,3-indandiona gadījumā ir populārā 4-*N*,*N*-dimetilaminobenzilidēn-1,3-indandiona (DMABI) analogi ar attīstītāku konjugācijas sistēmu. Šis promocijas darba mērķis ietver iegūto jauno D-π-A savienojumu īpašību izpēti un dažādu struktūras elementu (donoro, akceptoro grupu, π-tiltiņa garuma un struktūras) ietekmes noskaidrošanu uz savienojumu īpašībām.

## Pētījuma mērķis un uzdevumi

### Promocijas darba mērķi

1. Dažādas struktūras (tris, Lūisa bāzes, tetrakis) $Eu^{3+}$ kompleksu sintēze ar 2-acildimedona, 2-acil-1,3-indandiona un dibenzoilmetāna atvasinājumu ligandiem un iegūto kompleksu struktūras-īpašību sakarību pētījumi un salīdzinājums.
2. D-π-A savienojumu (2-cinnamoildimedona un 2-cinnamoil-1,3-indandiona atvasinājumu) sintēze uz 2-acetildimedona un 2-acetil-1,3-indandiona bāzes un iegūto savienojumu īpašību izpēte un dažādu struktūras elementu (donoro, akceptoro grupu, π-tiltiņa garuma un struktūras) un savienojumu īpašību sakarību pētījumi.

### Promocijas darba pirmā mērķa sasniegšanai izvirzīti vairāki uzdevumi

1.1. Variējot $Eu^{3+}$ jona un organisko ligandu molārās attiecības kompleksu sintēzes reakcijā, iegūt $Eu^{3+}$ jona tris, Lūisa bāzes un tetrakis kompleksus ar dažādiem 2-acildimedona, 2-acil-1,3-indandiona un dibenzoilmetāna atvasinājumu ligandiem.

1.2. Noskaidrot vides ietekmi uz kompleksu struktūras-emisijas īpašību sakarībām.

1.3. Teorētiski aprēķināt izmantoto ligandu enerģētisko līmeņu vērtības un iegūt katra kompleksa teorētisko enerģijas līmeņu diagrammu.

### Arī promocijas darba otrā mērķa sasniegšanai izvirzīti vairāki uzdevumi

2.1. Iegūt atšķirīgas uzbūves aminogrupas saturošus 2-cinnamoildimedona un 2-cinnamoil-1,3-indandiona atvasinājumus un izpētīt to absorbcijas, emisijas, termiskās, elektroķīmiskās īpašības un ar kvantu ķīmijas aprēķinu programmu "*ORCA*" noteikt to pamatstāvokļa ģeometriju un *HOMO*/*LUMO* orbitāles.

2.2. Izpētīt 2-cinnamoildimedona un 2-cinnamoil-1,3-indandiona atvasinājumu donoro, akceptoro grupu un π-tiltiņa garuma ietekmi uz īpašībām.
2.3. Iegūstot dažus 2-cinnamoil-1,3-indandiona *O*-metilēterus, noskaidrot, kāda ir enolās hidroksilgrupas ietekme uz savienojumu īpašībām.

## Tēzes aizstāvēšanai

1. $Eu^{3+}$ β-diketonātu kompleksu emisijas efektivitāti ietekmē kompleksa struktūra, izmantotā liganda enerģētisko līmeņu izvietojums pret $Eu^{3+}$ jona rezonanses līmeni un – tetrakis kompleksu gadījumā – arī izmantotā tetraalkilamonija jona izmērs.
2. 2-cinnamoildimedona un 2-cinnamoil-1,3-indandiona atvasinājumiem, kā D-π-A tipa savienojumiem, piemīt efektīva emisija, kuru ietekmē savienojuma planaritāte, donoro grupu struktūra, π-tiltiņa garums un uzbūve, kā arī izmantotās vides (šķīdinātāja) polaritāte.

## Zinātniskā novitāte un galvenie rezultāti

Promocijas darba pirmā mērķa pētījumu rezultātā iegūti jauni $Eu^{3+}$ organiskie tris, Lūisa bāzes un tetrakis kompleksi ar dažādiem β,β'-triketonātiem un β-diketonātiem (2-acildimedona, 2-acil-1,3-indandiona un dibenzoilmetāna atvasinājumiem), kuriem noteiktas un salīdzinātas emisijas īpašības ($\lambda_{em}$, *PLQY*, τ) šķīdumos, pulverveidā un polimērplēvītēs. Aprēķinātas izmantoto ligandu ierosināto singleta ($S_1$) un tripleta ($T_1$) līmeņu enerģijas, un iegūtas $Eu^{3+}$ kompleksu enerģijas līmeņu diagrammas. Izpētītas kompleksa struktūras un tetrakis kompleksa katjona izmēra ietekme uz emisijas īpašībām. Izgatavoti divi OLED ar $Eu^{3+}$ kompleksiem ar dibenzoilmetāna atvasinājumu ligandiem. Pirmo reizi novērota agregācijas pastiprinātā emisija $Eu^{3+}$ kompleksiem ar dibenzoilmetāna atvasinājumu ligandiem.

Promocijas darba otrā mērķa pētījumu rezultātā iegūta virkne 2-cinnamoildimedona un 2-cinnamoil-1,3-indandiona atvasinājumu, izpētītas un salīdzinātas to optiskās, elektroķīmiskās, termiskās īpašības. Izmantojot kvantu ķīmijas aprēķinu programmu "*ORCA*", aprēķināta savienojumu pamatstāvokļa ģeometrija un *HOMO*/*LUMO* orbitāles. Sistemātiski izpētīts dažādu amino-donoro grupu, akceptoro grupu un π-tiltiņa garuma ietekme uz D-π-A savienojumu īpašībām.

Promocijas darbs ir pabeigts oriģināls pētījums, kura rezultātiem ir būtiska nozīme ķīmijas nozares organiskās ķīmijas apakšnozarē.

## Darba struktūra un apjoms

Promocijas darbs sagatavots kā tematiski vienota zinātnisko publikāciju kopa par dažādu β,β'-triketonu un β-diketonu (2-acildimedona, 2-acil-1,3-indandiona un dibenzoilmetāna atvasinājumi) izmantošanu jaunu $Eu^{3+}$ kompleksu un D-π-A tipa struktūras savienojumu sintēzē un īpašību pētījumos.

## Darba aprobācija un publikācijas

Promocijas darba galvenie rezultāti apkopoti sešās zinātniskās publikācijās. Pētījuma rezultāti prezentēti sešās konferencēs.

### Zinātniskās publikācijas

1. **Malina I**, Traskovskis K, Lesiņa N, Vembris A. $Eu^{3+}$ ternary and tetrakis complexes with carbazole and methyl group substituted dibenzoylmethane derivatives: Induction of aggregation enhanced emission. *Dyes and Pigments*, **2019**, *163*, 257–266.
2. **Malina I**, Kampars V, Belyakov S. Luminescence properties of 2-benzoyl-1,3-indandione based $Eu^{3+}$ ternary and tetrakis complexes and their polymer films. *Dyes and Pigments*, **2018**, *159*, 655–665.
3. **Malina I**, Kampars V. Comparison of luminescent properties in solid-state and polymer films of Eu(III) complexes containing 2-acylindandione ligands. *Key Eng. Mater.*, **2018**, *762*, 239–243.
4. **Malina I**, Juhnevics N, Kampars V. Study of thermal and optical properties of dibenzoylmethane Eu(III) organic complexes. *Proc. Est. Acad. Sci.*, **2017**, *66* (4), 493–500.
5. **Malina I**, Kampars V, Turovska B, Belyakov S. Novel green-yellow-orange-red light emitting donor-π-acceptor type dyes based on 1,3-indandione and dimedone moieties. *Dyes and Pigments*, **2017**, *139*, 820–830.
6. **Malina I**, Kampars V, Turovska B. Synthesis, optical and electrochemical properties of substituted 2-cinnamoyl-1,3-indandione *O*-methyl ethers. *J. Mol. Struct.*, **2016**, *1115*, 241–249.

### Darba rezultāti prezentēti sešās konferencēs

1. **Malina I**, Kampars V. Comparison of luminescent properties in solid-state and polymer films of Eu(III) complexes containing 2-acylindandione ligands. *58th International Riga Technical University scientific conference "Materials Science and Applied Chemistry"*, Riga, Latvia, October 20, **2017**.
2. **Malina I**, Kampars V. Photoluminescent properties of novel tris, ternary and tetrakis $Eu^{3+}$ organic complexes with 2-acetyl-1,3-indandione ligands. *International conference "Materials, Methods & Technologies 2017*", Elenite, Bulgaria, June 26–30, **2017**.
3. **Malina I**, Juhnevics N, Kampars V. Study of thermal and optical properties of dibenzoyl-methane Eu(III) organic complexes. *International conference "Functional materials and Nanotechnologies-2017"*, Tartu, Estonia, April 24–27, **2017**.
4. **Malina I**, Kampars V. Synthesis and optical properties of red light emitting europium(III) complexes containing 2-acyldimedone and phenantroline ligands. *57th International Riga Technical University scientific conference "Materials Science and Applied Chemistry"*, Riga, Latvia, October 21, **2016**.

5. **Malina I**, Kampars V. Synthesis and optical properties of novel luminophores bearing cyclic β,β'-triketones. *56th International Riga Technical University scientific conference "Materials Science and Applied Chemistry"*, Riga, Latvia October 14–16, **2015**, Abstract book pp. 17.
6. **Neibolte I**, Kampars V, Plotniece M. Synthesis and spectroscopic properties of 2-substituted cinnamoil-1,3-indandione *O*-methyl ethers. *55th International Riga Technical University scientific conference "Materials Science and Applied Chemistry"*, Riga, Latvia October 14–17, **2014**, Abstract book pp. 100.

# PROMOCIJAS DARBA GALVENIE REZULTĀTI

## $Eu^{3+}$ kompleksu ar β,β'-triketonu ligandiem sintēze un spektroskopisko īpašību raksturojumi

Eiropija trivalento katjonu ($Eu^{3+}$) organiskie kompleksi ir visvairāk pētītie lantanoīdu grupas metālu kompleksi, pateicoties to specifiskajām luminiscences īpašībām – vairākām šaurām emisijas joslām dzeltenajā, oranžajā un sarkanajā spektra daļā ($\lambda_{em}$ = 580 nm, 594 nm, 611 nm, 652 nm un 701 nm) un gariem ierosināto stāvokļu dzīves laikiem (līdz simtiem μs). Lai šādiem kompleksiem novērotu metāla luminiscenci, nepieciešams, lai ierosināšanas enerģiju absorbētu tiem piesaistītie organiskie ligandi un pārnestu to uz metāla jonu caur ligandu un metāla jona ierosinātajiem singleta ($S_1$) un tripleta ($T_1$) līmeņiem. Šo procesu sauc par Antenas efektu (*Antenna effect*) (1. att.). Divi no priekšnoteikumiem šādai pārnesei ir liganda augsta absorbcijas spēja tuvajā ultravioletajā (UV) gaismas apgabalā un $T_1$ enerģijas līmeņa atrašanās tuvu vai augstāk par $Eu^{3+}$ jona rezonanses līmeni (17 250 $cm^{-1}$) [1].

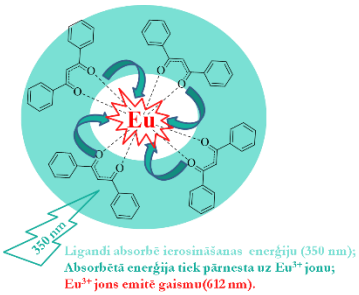


1. att. Antenas efekts.

2-acildimedona atvasinājumi (2-acetil-5,5-dimetilcikloheksān-1,3-dions jeb 2-acetildimedons (HAD) **1** un 2-benzoil-5,5-dimetilcikloheksān-1,3-dions jeb 2-benzoildimedons (HBD) **2**) un 2-acil-1,3-indandiona atvasinājumi (2-acetil-1*H*-indēn-1,3-(2*H*)-dions jeb 2-acetil-1,3-indandions (HAID) **7**, 2-benzoil-1*H*-indēn-1,3-(2*H*)-dions jeb 2-benzoil-1,3-indandions (HBID) **8**, 2-(4-metilbenzoil)-1*H*-indēn-1,3-(2*H*)-dions jeb 2-(4-metilbenzoil)-1,3-indandions) (HMBID) **9**) satur molekulā ar metālu joniem kompleksēties spējīgu β-dikarbonilfragmentu ar enolgrupu. Tiem piemīt arī izteikta gaismas absorbcija UV apgabalā (250–400 nm). Turklāt šie savienojumi attiecībā pret 1,3-dikarbonilfragmentu ir nesimetriski, jo viena karbonilgrupa atrodas ciklā, bet otra – alifātiskajā ķēdē, un pētījumi par šāda tipa $Eu^{3+}$ kompleksiem ir nepilnīgi [4], [5], [10]. Šo iemeslu dēļ promocijas darbā iepriekš nosauktie savienojumi tika pētīti kā ligandi jaunu $Eu^{3+}$ organisko kompleksu iegūšanai.

Dažādas struktūras $Eu^{3+}$ kompleksus ir iespējams iegūt, izmantojot dažādu organisko ligandu un $Eu^{3+}$ molāro attiecību un sekundāros ligandus. Sistemātiska kompleksu sintēze sākās ar vienkāršāko tris kompleksu **3**, **4** (vispārīgā struktūra Eu(β,β'-triketonāts)$_3$($H_2O$)$_2$) ieguvi, izmantojot β,β'-triketonu un $EuCl_3$ molāro attiecību 3 : 1 10 % NaOH klātbūtnē (2. att.). $Eu^{3+}$ jona koordinācijas skaitlis ir 8 un, izmantojot trīs β,β'-triketonātus, neaizpildās visa jona koordinācijas sfēra un no apkārtējās vides piekoordinējas divas šķīdinātāja – ūdens – molekulas, kas parasti nevēlami ietekmē kompleksa luminiscences efektivitāti. Lai izvērtētu

ūdens molekulu ietekmi uz kompleksa īpašībām, tālāk tika iegūti vairāki $Eu^{3+}$ Lūisa bāzes kompleksi **5**, **6** un **10-12**, kuros par sekundāro ligandu izmantots 1,10-fenantrolīns (PHEN) (vispārīgā formula Eu(β,β'-triketonāts)$_3$(PHEN)). Kompleksi iegūti, izmantojot PHEN, β,β'-triketonu un $EuCl_3$ attiecībā 1 : 3 : 1 10 % NaOH klātbūtnē (2. un 3. att.). PHEN tika izvēlēts kā sekundārais ligands, pateicoties tā intensīvajai absorbcijai UV apgabalā ($\lambda_{abs}$ = 270 nm) ar augstu molāro absorbcijas koeficientu (ε ~ 30 000 $cm^{-1}$) un $Eu^{3+}$ jona rezonanses līmenim atbilstošu $S_1$ un $T_1$ enerģijas līmeņu atrašanās vietu [11]. Visbeidzot, izmantojot β,β'-triketonu un $Eu^{3+}$ jonu molārajā attiecībā 4 : 1, iegūti vairāki tetrakis kompleksi **13–17** ar vispārīgo formulu [Eu(β,β'-triketonāts)$_4$]$^-$. $Eu^{3+}$ jonam, kompleksējoties ar četriem β,β'-triketonātiem, izveidojas komplekss ar negatīvu lādiņu, ko stabilizē pievienotie pozitīvie tetraalkilamonija joni ($N^+Et_4$ vai $N^+Bu_4$) (3. att.).

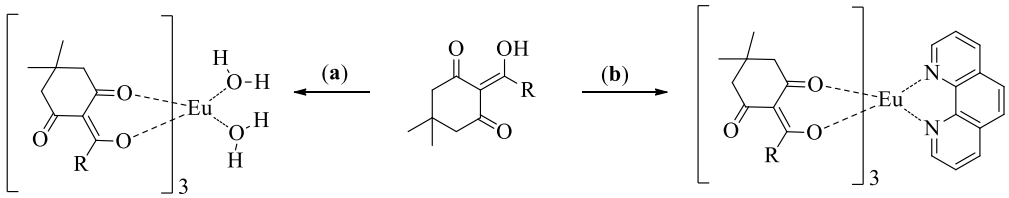


**3:** R = $CH_3$; **Eu(AD)$_3$(H$_2$O)$_2$**
**4:** R = $C_6H_5$; **Eu(BD)$_3$(H$_2$O)$_2$**

**1:** R = $CH_3$; **HAD**
**2:** R = $C_6H_5$; **HBD**

**5:** R = $CH_3$; **Eu(AD)$_3$(PHEN)**
**6:** R = $C_6H_5$; **Eu(BD)$_3$(PHEN)**

2. att. $Eu^{3+}$ tris **3**, **4** un $Eu^{3+}$ Lūisa bāzu kompleksu **5**, **6** ar 2-acildimedona atvasinājumu ligandiem iegūšana.
(**a**) 10 % NaOH/$H_2O$, $EuCl_3 \cdot 6H_2O$; (**b**) 10 % NaOH/$H_2O$, 1,10-fenantrolīns, $EuCl_3 \cdot 6H_2O$.

Iegūto kompleksu struktūras pierādītas, izmantojot elementanalīzi, $^1$H-KMR, FT-IR un masspektru datus. $^1$H-KMR spektri izmantoti $Eu^{3+}$ Lūisa bāzu un tetrakis kompleksiem β,β'-triketonāta:PHEN vai β,β'-triketonāta:amonija jona attiecības pierādīšanai kompleksā. Tetrakis kompleksa **15** kristāliskā struktūra pierādīta arī ar rentgenstruktūranalīzi.

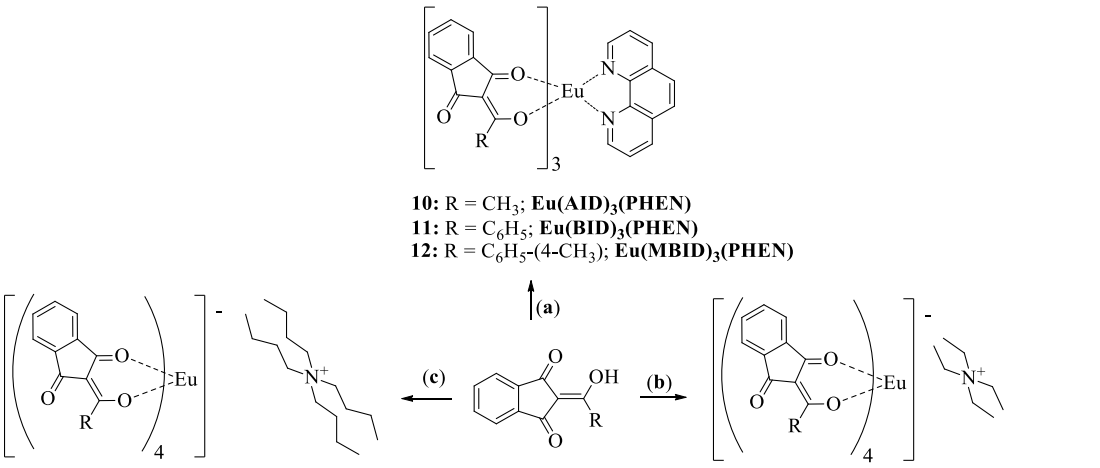


**10:** R = $CH_3$; **Eu(AID)$_3$(PHEN)**
**11:** R = $C_6H_5$; **Eu(BID)$_3$(PHEN)**
**12:** R = $C_6H_5$-(4-$CH_3$); **Eu(MBID)$_3$(PHEN)**

**16:** R = $C_6H_5$; **[Eu(BID)$_4$]$^-$N+Bu$_4$**
**17:** R = $C_6H_5$-(4-$CH_3$); **[Eu(MBID)$_4$]$^-$N$^+$Bu$_4$**

**7:** R = $CH_3$; **HAID**
**8:** R = $C_6H_5$; **HBID**
**9:** R = $C_6H_5$-(4-$CH_3$); **HMBID**

**13:** R = $CH_3$; **[Eu(AID)$_4$]$^-$N$^+$Et$_4$**
**14:** R = $C_6H_5$; **[Eu(BID)$_4$]$^-$N+Et$_4$**
**15:** R = $C_6H_5$-(4-$CH_3$); **[Eu(MBID)$_4$]$^-$N$^+$Et**

3. att. $Eu^{3+}$ Lūisa bāzu **10–12** un tetrakis kompleksu **13–17** ar 2-acil-1,3-indandiona atvasinājumu ligandiem sintēze.
(**a**) 10 % NaOH/$H_2O$, 1,10-fenantrolīns, $EuCl_3 \cdot 6H_2O$; **(b)** 10 % NaOH/$H_2O$, $Et_4NBr$, $EuCl_3 \cdot 6H_2O$;
**(c)** 10 % NaOH/$H_2O$, $Bu_4NBr$, $EuCl_3 \cdot 6H_2O$.

Jauniegūtajiem $Eu^{3+}$ kompleksiem **3–6** un **10–17** izpētītas absorbcijas un emisijas īpašības dažādos agregātstāvokļos. Vispirms, aplūkojot spektroskopiskās īpašības THF vai MeCN šķīdumos ($c$ ~ $1{,}5 \cdot 10^{-5}$ M), konstatēts, ka $Eu^{3+}$ kompleksiem ar 2-acildimedona atvasinājumu ligandiem (**3-6**) gaismas absorbciju novēro starp 210–340 nm ($\lambda_{abs}$ = 259–267 nm), savukārt kompleksiem ar 2-acil-1,3-indandiona ligandiem **10–17** tā ir nobīdīta uz garāku viļņu pusi 260–400 nm robežās ar $\lambda_{abs}$ = 321–333 nm. Neatkarīgi no tā, ka tikai kompleksi ar 2-acil-1,3-indandiona ligandiem **10–17** uzrāda absorbciju $Eu^{3+}$ joniem vēlamajā tuvajā UV apgabalā (300–400 nm), visi $Eu^{3+}$ kompleksi emitē gaismu ar $Eu^{3+}$ jonam raksturīgajām piecām emisijas joslām un maksimumiem pie 580 nm, 594 nm, 611 nm, 652 nm, 701 nm. Jāsecina gan, ka $Eu^{3+}$ kompleksu **3–6** emisija ir vāja un ar zemiem absolūtajiem fotoluminiscences kvantu iznākumiem (*PLQY*) (<0.01) THF šķīdumos. Savukārt $Eu^{3+}$ kompleksi **10–17** ar 2-acil-1,3-indandiona ligandiem uzrāda nedaudz intensīvāku emisiju ar *PLQY* 0,01–0,03. Visticamāk, zemu emisiju šķīdumos izraisa kompleksa disociācija, kā arī nevēlama apkārtējās vides (šķīdinātāja molekulu) ietekme. Šķīdinātāja molekulas darbojas kā augstas frekvences CH vibrāciju oscillatori, kas samazina centrālā metāla jona emisiju pārejas iespējamību. Šķīdumos nenovēro ne kompleksa struktūras, ne izmantotā katjona ietekmi uz emisijas efektivitāti.

Daudz efektīvāku emisiju iegūtajiem $Eu^{3+}$ kompleksiem **10–17** (vājas emisijas šķīdumā dēļ kompleksi **3–6** tālāk pētīti netika) novēro pulverveida stāvoklī (1. tab.). Ierosināšanas spektri, kas uzņemti kompleksiem pulverveida stāvoklī, ir izteikti nobīdīti batohromi (~80–130 nm), salīdzinot ar kompleksu šķīdumu absorbcijas spektriem. Kompleksus ar AID, BID un MBID ligandiem var ierosināt jau ar redzamo gaismu (408–450 nm). Šāda ierosināšanas viļņa garuma nobīde uzskatāma par priekšrocību, jo parasti β-diketoni ir nestabili intensīva UV starojuma ietekmē, kā rezultātā komplekss ilgstošas apstarošanas dēļ degradējas [1]. Tāpat izmantošanai bioloģijas nozarē, piemēram, bioloģisko marķieru vai zonžu izstrādē, ir nepieciešami luminiscējoši savienojumi, kurus var ierosināt redzamā gaisma, nevis UV starojums, kas ir kaitīgs dzīvajiem organismiem.

1. tabula

$Eu^{3+}$ kompleksu **10–17** ierosināšanas spektru maksimumi ($\lambda_{exc}$), absolūtie fotoluminiscences kvantu iznākumi (*PLQY*), luminiscences dzīves laiku ($\tau_1$ un $\tau_2$) dati pulverveida paraugiem un teorētiski aprēķinātie ierosinātā singleta ($S_1$) un tripleta stāvokļa ($T_1$) enerģētiskie līmeņi β,β'-triketoniem

| Savienojums | $\lambda_{exc}$ | *PLQY* | $\tau_1$, μs | $\tau_2$, μs | $S_1$, $cm^{-1}$ | $T_1$, $cm^{-1}$ |
|---|---|---|---|---|---|---|
| **10** $Eu(AID)_3(PHEN)$ | 450 | 0,08 | –[a] | –[a] | 27 834 | 24 547 |
| **13** $[Eu(AID)_4]^-N^+Et_4$ | 450 | 0,34 | –[a] | –[a] | | |
| **11** $Eu(BID)_3(PHEN)$ | 408 | 0,06 | 121 ± 4 (6 %) | 42 ± 1 (94 %) | 27 659 | 22 779 |
| **14** $[Eu(BID)_4]^-N^+Et_4$ | 425 | 0,29 | 233 ± 2 (22 %) | 54 ± 1 (78 %) | | |
| **16** $[Eu(BID)_4]^-N^+Bu_4$ | 408 | 0,12 | 118 ± 4 (4 %) | 37 ± 1 (96 %) | | |
| **12** $Eu(MBID)_3(PHEN)$ | 408 | 0,10 | 122 ± 3 (5 %) | 39 ± 1 (95 %) | 27 802 | 22 525 |
| **15** $[Eu(MBID)_4]^-N^+Et_4$ | 425 | 0,60 | 203 ± 17 (25 %) | 118 ± 5 (75 %) | | |
| **17** $[Eu(MBID)_4]^-N^+Bu_4$ | 408 | 0,11 | 115 ± 6 (2 %) | 34 ± 1 (98 %) | | |

[a] Nav noteikts.

Visu **10–17** kompleksu emisijas spektri cietā stāvoklī – tāpat kā šķīdumos – sastāv no piecām $Eu^{3+}$ jona $^5D_0 \rightarrow {}^7F_J$ ($J$ = 0–4) pārejām ar intensīvāko pie 611 nm ($^5D_0 \rightarrow {}^7F_2$) (4. **(a)** att.). Šī josla ir ~20–30 reizes intensīvāka par pārējām joslām un dod kompleksiem izteikti sarkanu emisijas krāsu. Tik liela pāreju $^5D_0 \rightarrow {}^7F_2$, $^5D_0 \rightarrow {}^7F_1$ attiecība norāda uz stipru koordinācijas mijiedarbību starp metāla jonu un ligandiem, un $Eu^{3+}$ jons kompleksā atrodas bez inversijas simetrijas. Augsta pārejas $^5D_0 \rightarrow {}^7F_2$ attiecība pret pārējām pārejām izraisa arī to, ka kompleksu emisijas krāsu koordinātes (*CIE 1931 chromaticity coordinates*), kas aprēķinātas no emisijas spektriem ($x$ = 0,670–0,673, $y$ = 0,327–0,330) pilnībā atbilst *NTSC* krāsu koordinātu standarta sarkanās krāsas koordinātēm ($x$ = 0,67; $y$ = 0,33). Jāpiebilst, ka zinātniskajā literatūrā ir tikai daži piemēri par iegūtiem $Eu^{3+}$ kompleksiem ar 100 % sarkanās krāsas emisiju [12].

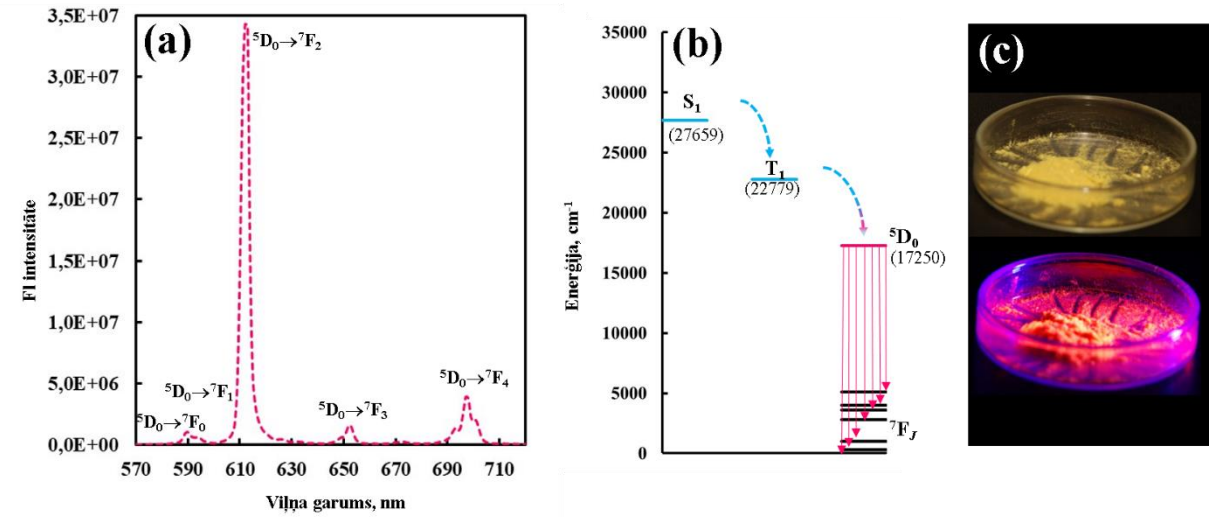


4. att. **(a)** Kompleksa **14** emisijas spektrs cietā stāvoklī ($\lambda_{exc}$ = 425 nm);
**(b)** kompleksa **14** enerģijas līmeņu diagramma ar enerģijas pārneses shēmu;
**(c)** komplekss **14** dienasgaismā un zem UV ($\lambda_{exc}$ = 365 nm) apgaismojuma.

Kompleksu **10-17** $Eu^{3+}$ jona pārejas $^5D_0 \rightarrow {}^7F_2$ (611 nm) luminiscences dzīves laiki $\tau_1$ un $\tau_2$ doti 1. tabulā. Visu kompleksu luminiscences dzīves laiku līknes apstrādātas ar divu eksponenciālu funkcijām, un iegūti divi dzīves laiki $\tau_1$ un $\tau_2$, kas norāda uz divu veidu simetrijām apkārt emitējošajam $Eu^{3+}$ jonam. Dažādas simetrijas ap centrālo metāla jonu var veidoties no dažādiem attālumiem starp emitējošajiem centriem ($Eu^{3+}$–$Eu^{3+}$). Ja attālums starp diviem joniem ir mazs, pastāv iespējamība, ka notiks mijiedarbība starp tiem, kā rezultātā izveidojas dažādas vides ap metālu joniem. Kompleksa **15** rentgenstruktūranalīzes dati apstiprina šādu pieņēmumu un rāda, ka molekulu izvietojums kristālā izsauc dažādu attālumu veidošanos starp emitējošajiem $Eu^{3+}$ joniem. Savukārt otrs svarīgākais emisijas raksturojums – *PLQY* ir robežās 0,06–0,60. Pulverveida stāvoklī ir novērojama kompleksa struktūras ietekme uz emisijas efektivitāti. Tetrakis kompleksi **14–17** uzrāda augstāku luminiscences efektivitāti par $Eu^{3+}$ Lūisa bāzu kompleksiem, pateicoties ievērojami lielākam fotonu absorbcijas laukumam, ko palielina ceturtais β,β'-triketonātu ligands. Jāsecina arī, ka tetrakis kompleksu struktūra, pateicoties piesaistītajam katjonam un četriem β,β'-triketonātu ligandiem, ievērojami labāk aizsargā $Eu^{3+}$ jonu no apkārtējās vides, kas bieži izsauc šī jona ierosinātā stāvokļa

bezizstarojuma pāreju uz pamatstāvokli. Ievērojamu katjona izmēra ($N^+Et_4$ vai $N^+Bu_4$) ietekmi uz *PLQY* novēro tetrakis kompleksu **14**–**17** gadījumā. Tetrakis komplekss **14** ar $N^+Et_4$ katjonu uzrāda trīs reizes augstāku emisijas efektivitāti nekā tā analogs ar $N^+Bu_4$ katjonu **16**. Savukārt tetrakis kompleksa **15** ar $N^+Et_4$ katjonu gadījumā *PLQY* jau ir pat sešas reizes augstāks nekā savienojumam **17** ar $N^+Bu_4$ katjonu. Šādu atšķirību *PLQY* izraisa dažāda garuma katjonu iekļaušana kompleksa kristālrežģī. Tetraalkilamonija jona izmēra palielināšana izteikti samazina kompleksa luminiscences efektivitāti un luminiscences dzīves laiku. Iespējams, iemesls tam ir tāds, ka lielāks katjons ir vairāk spējīgs ietekmēt tuvāko kompleksu $Eu^{3+}$ jonu koordinācijas sfēras apkārtni un, iespējams, stērisku iemeslu dēļ kompleksu molekulas kristālrežģī ir izvietotas neizdevīgākā konformācijā, kas izraisa daļēju $Eu^{3+}$ jona bezizstarojuma deaktivēšanos ierosinātā stāvoklī. Arī zinātniskajā literatūrā ir ziņots par tetrakis kompleksa katjona izmēra palielināšanas negatīvu ietekmi uz tā luminiscences īpašībām [13].

Skaidrojums tam, ka iegūtie jaunie β,β'-triketonātu $Eu^{3+}$ kompleksi raksturojas ar vidējiem kvantu iznākumiem un salīdzinoši īsiem luminiscences dzīves laikiem, meklējams tieši to enerģijas līmeņu $S_1$ un $T_1$ izvietojumos un to attiecībai pret $Eu^*$ ierosināto rezonanses līmeni (17 250 $cm^{-1}$). Savienojumu **1**, **2**, **7**–**9** $S_1$ un $T_1$ enerģētiskie līmeņi aprēķināti ar kvantu ķīmijas aprēķinu programmu "*ORCA*" un doti 1. tabulā (HAD $S_1$ = 31 025 $cm^{-1}$; $T_1$ = 27 653 $cm^{-1}$; HBD $S_1$ = 27 148 $cm^{-1}$; $T_1$ = 24 286 $cm^{-1}$). Vienkāršota enerģijas līmeņu diagramma dota 4. **(b)** attēlā. Literatūrā aprakstīti divi efektīva Antenas efekta priekšnosacījumi: (1) starpībai starp liganda līmeņiem $S_1$–$T_1$ jābūt ~5000 $cm^{-1}$ (*Reinhoudt empirical rule*) [14]; (2) starpībai starp $T_1$–Eu* līmeņiem – 2500–5500 $cm^{-1}$ (*Latva empirical rule*) [15]. Savienojumiem HBID **8** un HMBID **9** izpildās abi noteikumi, tāpēc to kompleksu *PLQY* ir ar augstākiem iznākumiem, kamēr HAD **1** un HBD **2** saturošiem kompleksiem starpība starp $T_1$–Eu* līmeņiem ir >5500 $cm^{-1}$, kas norāda uz iespējamu nepilnīgu enerģijas pārnesi starp šiem līmeņiem un arī izskaidro to zemos *PLQY* šķīdumos.

Pateicoties $Eu^{3+}$ kompleksu ar 2-acil-1,3-indandiona ligandiem **10**–**17** vidējiem kvantu iznākumiem cietā stāvoklī, tālāk tika pētītas iespējas izveidot to luminiscējošas filmiņas. $Eu^{3+}$ kompleksi raksturojas ar sliktu filmiņu veidošanos, tāpēc vislabāk ir veidot to polimērfilmiņas. *N*-Polivinilkarbazols (PVK) kā visvairāk izmantotais polimērs priekš $Eu^{3+}$ kompleksu filmiņām tika izvēlēts kā matrica, un filmiņas ar kompleksiem **10–17** (8 masas %) tika uzklātas ar rotējošā diska (*spin-coating*) metodi. Iegūtās filmiņas raksturojas ar salīdzinoši zemiem *PLQY* (0,02–0,08), un tā iemesls ir polimēra un kompleksu enerģijas līmeņu izkārtojuma neatbilstība. Lai notiktu efektīva enerģijas pārnese no polimēra uz kompleksu, polimēra $T_1$ līmenim jābūt virs izmantoto ligandu $S_1$ un $T_1$ līmeņiem. No literatūras [16] ir zināms, ka PVK $T_1$ = 24 440 $cm^{-1}$. Kā redzams 1. tabulā, savienojumiem HAID, HBID un HMBID $S_1$ līmeņi novietoti virs PVK $T_1$ līmeņa, savukārt $T_1$ līmeņi tuvu polimēra $T_1$ līmenim. Līdz ar to var secināt, ka ierosināšanas enerģija no PVK tikai daļēji pāriet ligandu ierosinātajos enerģijas līmeņos, kas, visticamāk, izraisa zemu kvantu emisijas efektivitāti.

Iegūtie jaunie $Eu^{3+}$ kompleksi ar 2-acil-1,3-indandiona ligandiem raksturojas ar tīru sarkanās gaismas emisiju ($\lambda_{em}$ = 611 nm), lielām Stoksa nobīdēm (161–203 nm), iespēju tos ierosināt gan ar UV, gan redzamo gaismu, vidējiem *PLQY* un vairākiem simtiem μs gariem dzīves laikiem cietā stāvoklī. To filmiņas ar PVK, kas bieži tiek izmantotas OLED izstrādē,

gan uzrāda zemus *PLQY*, un lietojums būtu jāmeklē citā sfērā, piemēram, polimēru optisko šķiedru vai viļņvadu izstrādē, jo kompleksu **11**, **12**, **14–17** poli-(metilmetakrilāta) (PMMA) filmiņas uzrāda jau augstāku kvantu efektivitāti (*PLQY* 0,09–0,14).

## $Eu^{3+}$ kompleksu ar β-diketonu ligandiem sintēze un spektroskopisko īpašību raksturojumi

Iepriekšējā nodaļā aprakstītie $Eu^{3+}$ kompleksi ar nesimetriskajiem 2-acil-1,3-indandiona un 2-acildimedona atvasinājumu ligandiem neuzrādīja pietiekami augstu *PLQY* praktiskam lietojumam OLED, tāpēc, turpinot pētījumus par 1,3-diketonu izmantošanu lantanoīdu kompleksu ieguvē, promocijas darbā tika iegūti arī daži $Eu^{3+}$ kompleksi ar simetriskākiem β-diketoniem – 1,3-difenilpropān-1,3-diona jeb dibenzoilmetāna (HDBM) atvasinājumu ligandiem. HDBM atvasinājumi ir vieni no visvairāk pētītajiem $Eu^{3+}$ kompleksu ligandiem. Iemesls tam ir komerciāla pieejamība, viegla sintēze un fakts, ka šādiem $Eu^{3+}$ kompleksiem parasti piemīt intensīva luminiscence [1]. Analogi kā β,β'-triketonu gadījumā, vispirms tika iegūti vienkāršākie neaizvietota HDBM **18** un 1-(4-metilfenil)-3-fenilpropān-1,3-diona (Me-HDBM) **19** ligandu $Eu^{3+}$ Lūisa bāzu **21**, **22** un tetrakis **24**, **25** kompleksi (5. att.). Zināms, ka aizvietotāji HDBM fenilgredzenos var izteikti izmainīt šī savienojuma enerģētisko līmeņu izvietojumu, īpašības, šķīdību, kā arī tā $Eu^{3+}$ kompleksu īpašības, tāpēc tika iegūts arī sarežģītāks HDBM atvasinājums, kas satur fenilgredzena *para*-pozīcijā karbazolu. Karbazolu bieži izmanto kā aizvietotāju β-diketonu un sekundāro ligandu sintēzē, pateicoties tā īpašībām – labai šķīdībai, caurumu pārneses īpašībām un augstai termiskai stabilitātei. Ievedot karbazolu $Eu^{3+}$ kompleksu izmantotajos ligandos, būtu iespējams uzlabot kompleksa elektriskās īpašības. HDBM gadījumā izpētīti savienojumi, kuros karbazols pievienots fenilgredzena *para*-pozīcijā caur 2. vai 3. karbazola gredzena oglekļa atomu, taču nav pētīti savienojumi, kuros karbazols būtu pievienots caur slāpekļa atomu. Tāpēc tālāk tika sintezēts šāds savienojums – 1-[4-(9*H*-karbazol-9-il)-fenil]-3-fenilpropān-1,3-dions (CBZ-HDBM **20**) un attiecīgi tā $Eu^{3+}$ Lūisa bāzes **23** un tetrakis **26** komplekss.

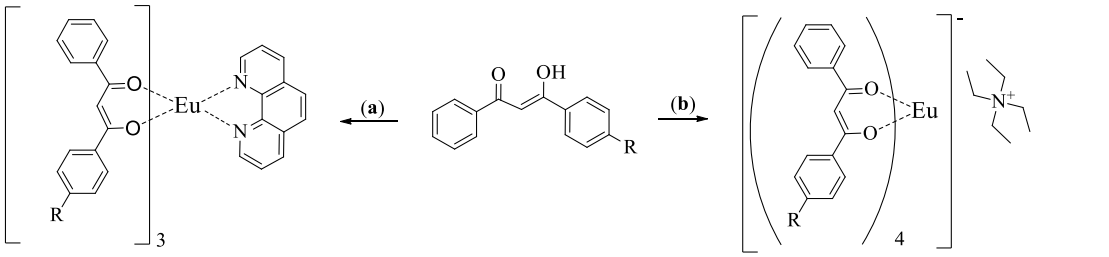


**21:** R = H; **Eu(DBM)$_3$(PHEN)**
**22**: R = $CH_3$; **Eu(Me-DBM)$_3$(PHEN)**
**23**: R = CBZ; **Eu(CBZ-DBM)$_3$(PHEN)**

**18:** R = H; **HDBM**
**19:** R = $CH_3$; **Me-HDBM**
**20:** R = CBZ, **CBZ-HDBM**

**24:** R = H; **[Eu(DBM)$_4$]N$^+$Et$_4$**
**25**: R = $CH_3$; **[Eu(Me-DBM)$_4$]N$^+$Et$_4$**
**26**: R = CBZ; **[Eu(CBZ-DBM)$_4$]N$^+$Et$_4$**

5. att. $Eu^{3+}$ Lūisa bāzu **21–23** un tetrakis kompleksu **24–26** ar HDBM atvasinājumu ligandiem sintēze.
(**a**) 10 % NaOH/$H_2O$, 1,10-fenantrolīns, $EuCl_3 \cdot 6H_2O$; (**b**) 10 % NaOH/$H_2O$, $Et_4NBr$, $EuCl_3 \cdot 6H_2O$.

Iegūtie kompleksi **21–26** raksturoti un to struktūras pierādītas tāpat kā 2-acil-1,3-indandionu kompleksu **10–17** gadījumā. Turklāt β-diketonātu $Eu^{3+}$ kompleksi **21–26**,

salīdzinot ar β,β'-triketonātu $Eu^{3+}$ kompleksiem **10–17**, uzrāda labāku šķīdību organiskajos šķīdinātājos ($CHCl_3$, EtOH, THF).

Vispirms pētītas un salīdzinātas iegūto kompleksu **21–26** absorbcijas un emisijas īpašības $1{,}5\cdot10^{-5}$ M THF šķīdumos. Kompleksu absorbciju var raksturot ar platām absorbcijas joslām tuvajā UV apgabalā (300–400 nm) (6. **(a)** att.). Kompleksu **21**, **22**, **24** un **25** $\lambda_{abs}$ atrodas 352–356 nm robežās, kamēr CBZ ievešana HDBM molekulu *para*-pozīcijā izraisa kompleksu **23** un **26** $\lambda_{abs}$ batohromu nobīdi līdz 369–374 nm. Šī absorbcijas josla ir lādiņa pārneses (*CT – charge transfer*) pāreja, jo CBZ-HDBM ligands satur gan elektrondonoro CBZ grupu, gan elektronakceptorās karbonilgrupas. Kvantu ķīmijas aprēķini, kas veikti, lai iegūtu savienojumu HDBM **18**, Me-HDBM **19** un CBZ-HDBM **20** optimizētu pamatstāvokļa struktūras ģeometriju un *HUMO*/*LUMO* orbitāles, parāda, ka savienojumam **20** ir izteikts lādiņu sadalījums starp *HOMO* un *LUMO* orbitālēm (*HOMO* orbitāle lokalizēta uz CBZ grupas, kamēr LUMO uz DBM daļas), kas norāda uz izteiktu *CT* šajā molekulā. Savienojumu **18** un **19** gadījumā *HOMO*/*LUMO* orbitāles izkliedētas pa visu molekulu.

Kompleksu emisija $1{,}5\cdot10^{-5}$ M THF šķīdumos ir ļoti atšķirīga. β-diketonātu $Eu^{3+}$ kompleksi **21**, **22**, **24** un **25** uzrāda tikai $Eu^{3+}$ jonam raksturīgās emisijas joslas (6. **(b)** att.) ar *PLQY* – 0,02–0,06 (2. tab.). Savukārt kompleksu **23** un **26** gadījumā luminiscences spektrs uzrāda ne tikai metāla jona emisiju. Pateicoties *CT* dabai, savienojumam CBZ-HDBM piemīt izteikta zilās krāsas emisija ar $\lambda_{em}$ pie 478 nm (*PLQY* 0,26), ko var novērot arī kompleksu **23** un **26** luminiscences spektros. $Eu^{3+}$ komplekss **23** luminiscences spektrā uzrāda duālo emisiju – liganda emisiju 400–600 nm robežās un vairākas $Eu^{3+}$ jona emisijas joslas 570–705 nm apgabalā. Abu joslu maksimumu (pie 475 nm un 611 nm) intensitāšu attiecība ir 1 : 2. Duālo emisiju bieži novēro $Eu^{3+}$ kompleksiem, kas satur ligandus ar elektrondonorām un elektronakceptorām grupām [17], un tā norāda uz neefektīvu enerģijas pārnesi starp ligandiem un centrālā metāla jonu. Kompleksa **23** *PLQY* šķīdumā ir 0,10 un tā CIE koordinātes atrodas ciāna zilā reģionā ($x$ = 0,26; $y$ = 0,28) (6. **(c)** att.). Savukārt tetrakis kompleksa **26** gadījumā emisijas spektrā novēro tikai liganda emisiju, ko varētu skaidrot ar šo kompleksu tendenci šķīdumos disociēt tris kompleksos un attiecīgajā tetraetilamonija sālī, kas ietekmē $Eu^{3+}$ jona emisijas intensitāti un pastiprina liganda emisiju.

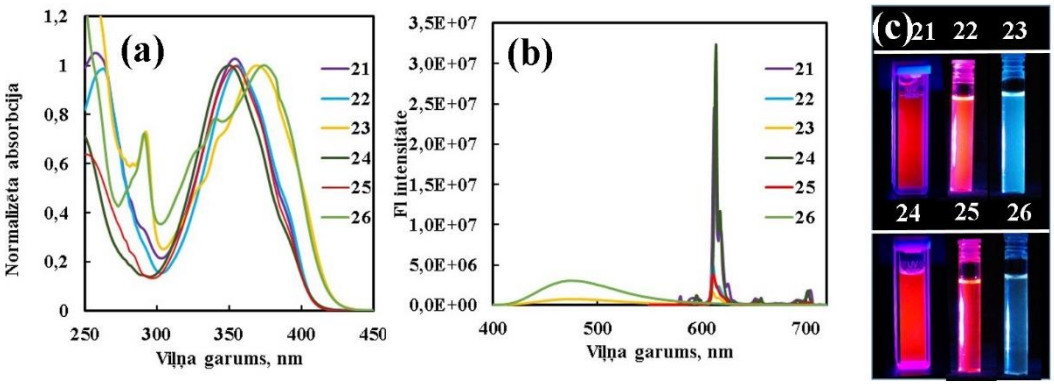


6. att. **(a)** Kompleksu **21–26** absorbcijas spektri $1{,}5\cdot10^{-5}$ M THF šķīdumos;
**(b)** kompleksu **21–26** emisijas spektri $1{,}5\cdot10^{-5}$ M THF šķīdumos;
**(c)** kompleksi **21–26** zem UV ($\lambda_{exc}$ = 365 nm) apgaismojuma.

Tālāk tika pētīta kompleksu emisija cietā stāvoklī. Līdzīgi kā 2-acil-1,3-indandionātu $Eu^{3+}$ kompleksu **10–17** gadījumā, arī kompleksiem **21**–**26** emisija pulverī ir daudz efektīvāka. Kompleksiem ar HDBM ligandiem **21**, **24** un ar Me-HDBM **22**, **25** *PLQY* sasniedz pat 0,53–0,75 (2. tab.). Tik liela starpība starp emisiju šķīdumā un cietā stāvoklī varētu norādīt uz agregācijas pastiprinātu emisiju (*AEE – Aggregation enhanced emission*). Tetrakis kompleksam **25** šis efekts tika pierādīts, izmantojot THF:heksāna šķīdinātāju sistēmu. Palielinot heksāna daļu šķīdumā, veidojas kompleksa daļiņas, kas efektīvi pastiprina emisiju no šķīduma. Līdz šim zinātniskajā literatūrā ir pieejams tikai viens piemērs ar $Eu^{3+}$ kompleksu, kam izpaužas *AEE* efekts [18].

2. tabula

$Eu^{3+}$ kompleksu **21–26** absolūtie fotoluminiscences kvantu iznākumi $1{,}5\cdot10^{-5}$ M THF šķīdumos ($PLQY_{THF}$), pulverī ($PLQY_p$), 8 wt% PVK filmiņās ($PLQY_{PVK}$) un teorētiski aprēķinātie ierosinātā singleta ($S_1$) un tripleta stāvokļa ($T_1$) enerģētiskie līmeņi β-diketoniem

| Komplekss | $PLQY_{THF}$ | $PLQY_p$ | $PLQY_{PVK}$ | $S_1$, $cm^{-1}$ | $T_1$, $cm^{-1}$ |
|---|---|---|---|---|---|
| $Eu(DBM)_3(PHEN)$ **21** | 0,04 | 0,56 | 0,26 | 28 122 | 22 121 |
| $[Eu(DBM)_3]^-N^+Et_4$ **24** | 0,06 | 0,75 | 0,46 | | |
| $Eu(Me\text{-}DBM)_3(PHEN)$ **22** | 0,03 | 0,53 | 0,22 | 28 218 | 21 928 |
| $[Eu(Me\text{-}DBM)_3]^-N^+Et_4$ **25** | 0,02 | 0,57 | 0,18 | | |
| $Eu(CBZ\text{-}DBM)_3(PHEN)$ **23** | 0,10 | 0,09 | 0,07 | 21 929 | 20 973 |
| $[Eu(CBZ\text{-}DBM)_3]^-N^+Et_4$ **26** | 0,26[a] | 0,10 | 0,09 | | 18 416[b] |

[a] Kvantu iznākums ligandam CBZ-HDBM.

[b] Eksperimentāli iegūtais liganda CBZ-HDBM tripletstāvokļa enerģētiskais līmenis.

Kompleksiem **23** un **26**, kuriem ierosinātā šķīdumā izpaudās duālā emisija vai tikai liganda emisija, cietā stāvoklī piemīt tikai $Eu^{3+}$ jona sarkanās gaismas emisija. To varētu skaidrot ar to, ka cietā stāvoklī izpaužas stiprāka saistība starp ligandiem un metāla jonu, kā arī agregācijas dēļ netiek novērota liganda emisija. *PLQY* cietā stāvoklī nepieaug kā kompleksu **21**, **22**, **24**, **25** gadījumā un ir 0,09 (**23**) un 0,10 (**26**).

Cietā stāvoklī kompleksu **21–26** luminiscences dzīves laiks $^5D_0 \rightarrow {}^7F_2$ (611 nm) pārejai, tāpat kā β,β'triketonātu $Eu^{3+}$ kompleksu **10–17** gadījumā, ir diveksponenciāls ($\tau_1$ un $\tau_2$) un arī norāda uz divu veidu simetriju apkārt $Eu^{3+}$ jonam. Jāpiemin, ka THF šķīdumā kompleksiem **22**, **23** un **25** luminiscences dzīves laiks bija monoeksponenciāls, apstiprinot pieņēmumu, ka dažāda emisijas kinētika cietā stāvoklī rodas no $Eu^{3+}$ jonu savstarpējās mijiedarbības, kas šķīdumā atšķaidījuma dēļ netiek novērota.

Tālāk tika pētītas iegūto kompleksu polimēru luminiscējošās filmiņas, par matricu atkal izmantojot PVK. Kompleksiem **21** un **24** tika pētīta kompleksa masas ietekme uz luminiscējošās filmiņas emisijas efektivitāti. Katram kompleksam tika iegūtas četras PVK filmiņas ar dažādu kompleksa masu (1 masas %, 4 masas %, 8 masas % un 15 masas %). Kompleksa **21** PVK filmiņu emisijas spektri attēloti 7. attēlā. Gan **21**, gan **24** kompleksa PVK filmiņu gadījumā emisijas intensitāte un *PLQY* pieaug, palielinot kompleksa masu filmiņā. Filmiņām ar 1 masas % kompleksa masu emisijas apgabalā 360–560 nm novērojama PVK vāja emisija, kas skaidrojams ar to, ka, izmantojot mazu dopēšanas masu, filmiņā ir salīdzinoši liels attālums starp polimēra ķēdi un kompleksu, un enerģijas pārnese starp tiem ir

nepilnīga. Palielinot kompleksa masu, polimēra emisiju vairs nenovēro luminiscences spektrā. *PLQY* kompleksa **21** filmiņu gadījumā doti 7. attēlā, savukārt kompleksa **24** gadījumā tie ir šādi: 0,17, 0,30, 0,46 un 0,48 (1 masas %, 4 masas %, 8 masas % un 15 masas %). No šiem datiem izsecināts, ka visefektīvākā $Eu^{3+}$ kompleksu masa ir 8 masas %. Lai arī ar 15 masas % tika iegūti vēl augstāki *PLQY*, šis palielinājums ir nenozīmīgs, salīdzinot ar to, ka kompleksa masa filmiņā jāpalielina gandrīz uz pusi, salīdzinot ar 8 masas %.

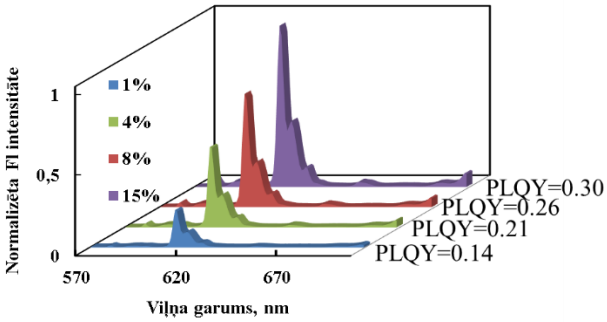


7. att. Kompleksa **21** (1 masas %, 4 masas %, 8 masas % un 15 masas %) PVK filmiņu emisijas spektri.

Pārējo kompleksu **22**, **23**, **25** un **26** PVK filmiņas tika iegūtas ar 8 masas %. Kompleksi **22** un **25** – tāpat kā kompleksi **21** un **24** – uzrāda vidējus *PLQY* – 0,22 un 0,18, savukārt CBZ-HDBM ligandu saturošie kompleksi **23** un **26** – 0,07 un 0,09. Kā redzams, kompleksiem **21**, **22**, **24** un **25** *PLQY* filmiņās ir aptuveni divreiz zemāki nekā pulverveida paraugiem, ko varētu skaidrot ar tiem piemītošo *AEE* efektu. Polimērfilmiņās daļa kompleksa molekulu ietver polimērķēdes, savukārt daļa veido agregātus [19]. Šo kompleksu *PLQY* kritumu varētu skaidrot ar to, ka to PVK filmiņās gaismu emitē tikai agregātus veidojošās molekulas, bet izolēto kompleksu molekulu emisija tiek dzēsta. Savukārt kompleksu **23** un **26** gadījumā PVK filmiņu *PLQY* ir tādi paši kā cietā stāvoklī, jo, visticamāk, šajā gadījumā gaismu emitē gan agregātus veidojošās, gan izolētās kompleksa molekulas.

Lai iegūtu priekšstatu par kompleksu praktisko lietojumu, tika izveidoti divi OLED, izmantojot kompleksu **22** kā emiteri (*Dr. phys.* A. Vembris). Pirmais OLED tika izgatavots, kompleksu **22** iejaucot PVK (10 masas %), un tā struktūra ir šāda: [ITO/PEDOT: PSS(40 nm)/PVK:**22**(50 nm)(10 wt%)/TPBi(20 nm)/LiF(1 nm)/Al(100 nm)]. Otrais OLED tika izgatavots bez polimēra ar struktūru: [ITO/PEDOT:PSS(40 nm)/**22**(50 nm)/ TPBi(20 nm)/LiF(1 nm)/Al(100 nm)]. Pirmais OLED, kas izgatavots, iejaucot kompleksu **22** PVK, elektroluminiscences spektrā neuzrādīja $Eu^{3+}$ emisiju. Savukārt otrais OLED, kurā tikai savienojums **22** izmantots kā emitējošais slānis, uzrādīja vāju $Eu^{3+}$ emisiju (maksimālais spožums (*maximal brightness*) 10 cd/m$^2$ ar strāvas efektivitāti (*current efficiency*) 0,004 cd/A un ieslēgšanas spriegumu (*turn on voltage*) 9 V). Vāju elektroluminiscenci izraisa tas, ka kompleksam **22** nepiemīt lādiņa pārneses īpašības. No iegūto OLED datiem var secināt, ka šie $Eu^{3+}$ kompleksi neuzrāda optoelektroniskajām iekārtām noderīgas īpašības, bet tos varētu izmantot citā nozarē.

Aprēķinātie $S_1$ un $T_1$ līmeņi savienojumiem HDBM, Me-DBM, CBZ-HDBM (2. tab.) arī dod skaidrojumu par $Eu^{3+}$ kompleksu novērotajām spektroskopiskajām īpašībām. Kā redzams, savienojumiem HDBM un Me-HDBM veiksmīgai enerģijas pārnesei no ligandiem uz centrālo metāla jonu izpildās abi empīriskie likumi (13. lpp), jo starpība starp $S_1$ un $T_1$ ir 6001 $cm^{-1}$ (HDBM) un 6290 $cm^{-1}$ (Me-HDBM), bet starp $T_1$–Eu* – 4871 $cm^{-1}$ (HDBM) un 4678 $cm^{-1}$ (Me-HDBM). Savukārt savienojumam CBZ-HDBM karbazola ievešana *para*-pozīcijā ir izraisījusi tuvu $S_1$ un $T_1$ enerģētisko līmeņu novietojumu (starpība 3513 $cm^{-1}$), kā arī tuvu $T_1$–Eu* novietojumu (starpība 1166 $cm^{-1}$), kā rezultātā kompleksā novēro neefektīvu enerģijas pārnesi un zemākus *PLQY*.

## 2-cinnamoil-1,3-indandiona un 2-cinnamoildimedona atvasinājumu sintēze un spektroskopisko īpašību raksturojumi

Iepriekšējā nodaļā pētītie savienojumi – 2-acetildimedons **1** un 2-acetil-1,3-indandions **7** – ar divām elektronakceptorām karbonilgrupām un reaģētspējīgu metilgrupu ir perspektīvi prekursori jaunu hromoforu un luminoforu savienojumu iegūšanā. Relatīvi maz pētītas šo savienojumu reakcijas ar elektrofīliem reaģentiem, piemēram, aromātiskajiem aldehīdiem, kā rezultātā iespējams iegūt savienojumus ar pagarinātu konjugētu sistēmu – 5,5-dimetil-2-[(2*E*)-3-fenil-1-okso-2-propēn-1-il]-cikloheksān-1,3-diona jeb 2-cinnamoildimedona vai 2-[(2*E*)-3-fenil-1-okso-2-propēn-1-il]-1*H*-indēn-1,3(2*H*)-diona jeb 2-cinnamoil-1,3-indandiona atvasinājumus [6]–[8]. Ja sintēzes reakcijā izmantots aromātiskais aldehīds ar donoro grupu (D), tad iegūtais 2-cinnamoil-β-diketons satur molekulā akceptoro grupu A (dimedons vai-1,3-indandions), D grupu, kā arī π-konjugēto sistēmu starp šīm grupām un ir pieskaitāms D-π-A savienojumu klasei. Šādi savienojumi ir unikāli ar tiem piemītošajām absorbcijas un emisijas īpašībām, tos var izmantot fotoelementu un OLED izstrādē, medicīnā fluorescējošo marķieru izveidē un citur. To lielākā priekšrocība, salīdzinot ar iepriekšējās nodaļās aprakstītajiem $Eu^{3+}$ organiskajiem kompleksiem, ir plašs klāsts organisko D un A grupu, kā arī π-tiltiņa izvēlē, kā rezultātā ir iespējams pielāgot vēlamā savienojuma īpašības, piemēram, emisijas krāsu.

Promocijas darbā tika iegūti pieci jauni 2-cinnamoildimedona atvasinājumi **27–31** un pieci jauni 2-cinnamoil-1,3-indandiona atvasinājumi **32–36** savienojumu **1** un **7** kondensācijas reakcijās ar aromātiskajiem aldehīdiem, kas fenilgredzena *para*-pozīcijā satur spēcīgus donoros *N*-alkil- vai *N*-arilamino- aizvietotājus. Tālāk, apstrādājot ar dimetilsulfātu dažus no iegūtajiem 2-cinnamoil-1,3-indandiona atvasinājumiem **32–34**, papildus tika iegūti 2-cinnamoil-1,3-indandiona atvasinājumu *O*-metilēteri **37–39** (8. att.). Izmantojot iegūtos jaunos D-π-A savienojumus **27–39**, tika pētīta dažādu akceptoro grupu (dimedons, 1,3-indandions), donoro (*N*,*N*-dimetilamino- ($NMe_2$), *N*,*N*-difenilamino- ($NPh_2$), julolidil- un *N*,*N*-dibifenilamino- ($N(BPh)_2$) grupu un π-tiltiņa garuma (1-hidroksiallilidēn-, 1-hidroksipenta-2,4-ilidēn-) ietekme uz savienojumu īpašībām. Savukārt, salīdzinot 2-cinnamoil-1,3-indandiona atvasinājumus **32–34** un to *O*-metilēterus **37–39**, iespējams noteikt hidroksilgrupas, kas veido spēcīgu ūdeņražsaiti ar 1,3-indandiona cikla karbonilgrupu, ietekmi uz savienojumu īpašībām.

Iegūto savienojumu **27–39** struktūras ir pierādītas ar $^{1}$H-KMR, $^{13}$C-KMR un FT-IR spektriem, elementanalīžu un masspektru datiem. Neapstrīdams pierādījums tam, ka savienojumi **27–36** pastāv tieši eksocikliskajā enolformā, ko stabilizē spēcīga iekšmolekulārā ūdeņražsaite, iegūts, veicot savienojumu **27** un **34** kristāliem rentgenstruktūranalīzi (*Dr. phys.* S. Beļakovs). Iegūtie dati parāda, ka abiem savienojumiem ir iekšmolekulāra ūdeņražsaite starp cikla (dimedons, 1,3-indandions) karbonilgrupu un allilidēnfragmentā atrodošās enolgrupas ūdeņraža atomu ar garumiem 2,386(7) Å (**27**) un 1,66(8) Å (**34**). Iegūtie saišu garumi un leņķi starp atomiem β,β'-triketona fragmentā norāda arī uz konjugētas π-elektronu sistēmas veidošanos, ko stabilizē iekšmolekulāra ūdeņražsaite. Savukārt kvantu ķīmijas aprēķini savienojumiem **27–39** (optimizēta pamatstāvokļa struktūra) parāda, ka savienojumi ar *N*,*N*-alkilamino- aizvietotājiem (**27**, **29**, **31**, **32**, **34**, **36**, **37** un **39**) ir pilnībā planāri, savukārt atvasinājumi **28**, **30**, **33**, **35** un **38** uzrāda fenil- un bifenil- grupu ārpus plaknes izgriešanos.

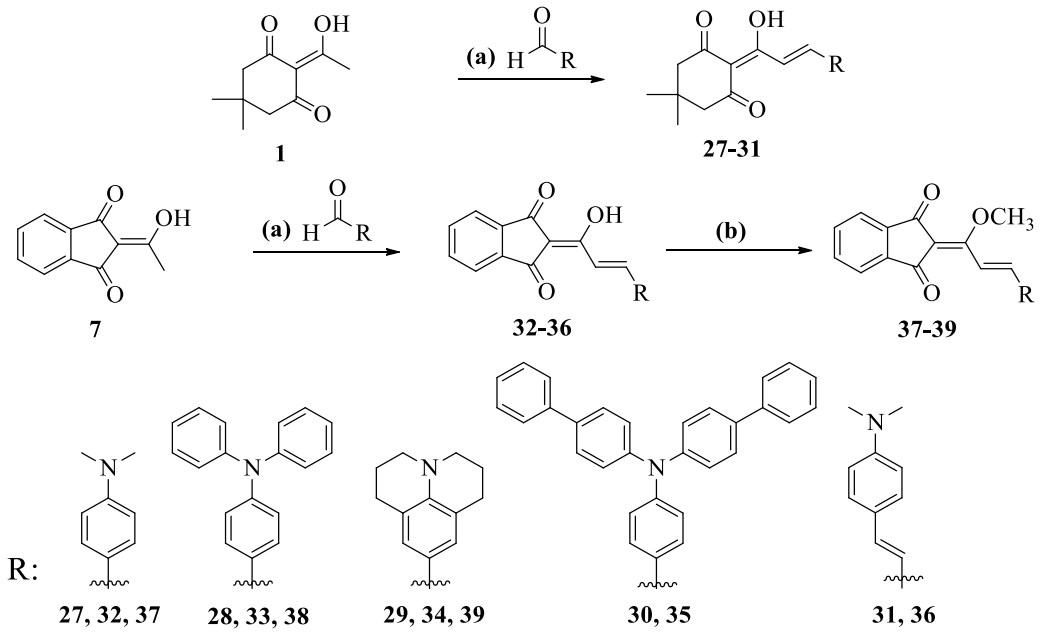


8. att. D-π-A tipa savienojumu **27-39** sintēze uz 2-acetildimedona **1** un 2-acetil-1,3-indandiona **7** bāzes.

(**a**) – (1) piperidīns, 100 °C, 4 h; (2) etanols, 80 °C, 0,5 h; (**b**) – dimetilsulfāts, $K_2CO_3$, acetons, 56 °C, 4 h.

*O*-Metilēteru **37–39** $^{1}$H-KMR un $^{13}$C-KMR spektros novēro tikai divas atšķirības no 2-cinnamoil-1,3-indandiona atvasinājumu **32–34** spektriem: **(1)** -$CH_3$ signāls (4,35 ppm) ir aizstājis uz vājiem laukiem (~13,20 ppm) nobīdīto -OH grupas signālu; **(2)** $^{13}$C-KMR spektros 1,3-indandiona benzola cikla oglekļa atomu pāri (C8 un C9; C4 un C7; C5 un C6) uzrāda vienādas ķīmiskās nobīdes, kas norāda uz vienādu ķīmisko apkārtni šiem atomiem (2-cinnamoil-1,3-indandiona atvasinājumu **32–34** gadījumā iekšmolekulārā ūdeņražsaite starp enolgrupas ūdeņraža atomu un 1,3-indandiona cikla karbonilgrupas skābekļa atomu izraisa dažādas ķīmiskās nobīdes šiem atomu pāriem) – metilēšana ir padarījusi simetriskāku molekulas akceptoro daļu.

Jauniegūtajiem D-π-A savienojumiem izpētītas absorbcijas un emisijas īpašības dažādas polaritātes šķīdinātājos (toluols, THF, $CHCl_3$, MeCN, MeOH), un 3. tabulā doti savienojumu

**27–39** spektroskopiskie raksturojumi $1{,}5\cdot10^{-5}$ M $CHCl_3$ šķīdumos, kā arī *PLQY* toluolā, $CHCl_3$ un MeOH. 2-cinnamoildimedona **27–31** un 2-cinnamoil-1,3-indandiona atvasinājumi **32–36** uzrāda intensīvu redzamās gaismas absorbciju ar viļņu garumu maksimumiem ($\lambda_{abs}$) robežās 466–540 nm. Šīs platās absorbcijas joslas izsauc *CT* molekulā starp D un A grupām ($\pi$(D) $\rightarrow$ $\pi^*$(A)). 2-cinnamoil-1,3-indandiona *O*-metilēteru **37–39** absorbcijas joslas ir batohromi nobīdītas par 7–22 nm, salīdzinot ar to nemetilētajiem analogiem **32–34**, ko izraisa vājas donorās grupas -$OCH_3$ atrašanās $\pi$-tiltiņā, kas pastiprina lādiņa sadalījumu starp 1,3-indandiona ciklu un cinnamoil- fragmentā novietoto donoro aminogrupu. Visi jauniegūtie savienojumi **27–39** ir fluorescenti $CHCl_3$ šķīdumos, un to emisijas spektri atrodas ļoti plašā spektrālajā apgabalā, sākot no zaļās līdz pat sarkanās gaismas reģionam (9. att.) ar $\lambda_{em}$ 548–647 nm robežās.

3. tabula

D-$\pi$-A savienojumu **27–39** absorbcijas, emisijas spektru maksimumi $1{,}5\cdot10^{-5}$ M $CHCl_3$ šķīdumos un *PLQY* $1{,}5\cdot10^{-5}$ M $CHCl_3$, toluola un MeOH šķīdumos, cikliskās voltametrijas oksidēšanās ($E_{ox}$) un reducēšanās ($E_{red}$) potenciāli, aprēķinātie *HOMO*/*LUMO* enerģijas līmeņi un *HOMO–LUMO* spraugas ($E_g^{DFT}$)

| Savienojums | $\lambda_{abs}$, nm | $\lambda_{em}$, nm | *PLQY* | | | $E_{ox}$, V | $E_{red}$, V | *HOMO*, eV | *LUMO*, eV | $E_g^{DFT}$, eV[b] |
|---|---|---|---|---|---|---|---|---|---|---|
| | | | Toluols | $CHCl_3$ | MeOH | | | | | |
| **27** | 467 | 548 | 0,05 | 0,15 | 0,01 | 0,81 | –1,32 | –5,38 | –2,16 | 3,22 |
| **28** | 466 | 612 | 0,40 | 0,78 | <0,01 | 1,07 | –1,19 | –5,33 | –2,37 | 2,96 |
| **29** | 509 | 577 | 0,31 | 0,36 | <0,01 | 0,61 | –1,36 | –5,16 | –2,11 | 3,05 |
| **30** | 476 | 654 | 0,79 | 0,16 | –[a] | 0,96 | –1,18 | –5,26 | –2,40 | 2,86 |
| **31** | 487 | 624 | 0,05 | 0,15 | 0,05 | 0,67 | –1,15 | –5,21 | –2,34 | 2,87 |
| **32** | 503 | 566 | 0,12 | 0,03 | <0,01 | 0,80 | –1,17 | –5,37 | –2,28 | 3,09 |
| **33** | 502 | 621 | 0,52 | 0,76 | –[a] | 1,05 | –1,07 | –5,34 | –2,47 | 2,87 |
| **34** | 540 | 595 | 0,15 | <0,01 | –[a] | 0,60 | –1,21 | –5,11 | –2,19 | 2,92 |
| **35** | 512 | 663 | 0,93 | 0,21 | –[a] | 0,98 | –1,04 | –5,27 | –2,50 | 2,77 |
| **36** | 520 | 647 | 0,12 | 0,25 | <0,01 | 0,66 | –1,04 | –5,22 | –2,43 | 2,79 |
| **37** | 514 | 597 | <0,01 | 0,02 | <0,01 | 0,77 | –1,11 | –5,26 | –2,25 | 3,01 |
| **38** | 509 | 647 | 0,01 | 0,06 | <0,01 | 0,97 | –0,97 | –5,27 | –2,57 | 2,70 |
| **39** | 562 | 634 | 0,02 | 0,32 | 0,01 | 0,57 | –1,14 | –5,02 | –2,30 | 2,73 |

[a] Nešķīstošs.
[b] $E_g^{DFT}$ = *HOMO–LUMO*.

2-cinnamoildimedona un 2-cinnamoil-1,3-indandiona atvasinājumu struktūras ietekme uz $\lambda_{abs}$ un $\lambda_{em}$ atrašanās vietu ir šāda:

**(1)** akceptorās grupas (dimedons vai 1,3-indandions) vairāk ietekmē absorbcijas joslas atrašanās vietu. Savienojumiem ar 1,3-indandionu, kas uzskatāms par spēcīgāku akceptoro grupu, pateicoties tā aromātiskajai uzbūvei, novēro $\lambda_{abs}$ un $\lambda_{em}$ nobīdi uz garākiem viļņiem. Salīdzinot abu atvasinājumu rindas (**27/32**, **28/32**, **29/34**, **30/35**, **31/36**), redzams, ka *CT* joslas maksimums 466–509 nm (dimedona atvasinājumi **27–31**) ir nobīdīts batohromi līdz 502–540 nm (1,3-indandiona atvasinājumi **32–36**). Emisijas spektru $\lambda_{em}$, pārejot no dimedona uz 1,3-indandiona atvasinājumiem, nobīdās batohromi tikai par 9–23 nm;

**(2)** pretēji donorās aminogrupas uzrāda nelielu ietekmi uz $\lambda_{abs}$ un izteiktu ietekmi uz $\lambda_{em}$. $NMe_2$ un $NPh_2$ grupu saturošie savienojumi uzrāda vienādu $\lambda_{abs}$. Šeit ir jāņem vērā tas, ka $NPh_2$ grupai slāpekļa atoma nedalītais elektronu pāris konjugējas ar fenilgrupu π-elektroniem, kas, visticamāk, mazina grupas donoro stiprumu. Savienojumi ar $N(BPh)_2$ grupu uzrāda jau par 10 nm batohromi nobīdītu absorbcijas spektru, ko var izskaidrot, aplūkojot to optimizēto pamatstāvokļa ģeometriju. Kvantu ķīmiskie aprēķini parāda, ka savienojumiem ar $N(BPh)_2$ grupu (**30** (–32,1°), **35** (–31,2°)) novērojama lielāka fenilgrupu ārpusplaknes izgriešanās nekā savienojumiem ar $NPh_2$ grupu (**28** (–30,1 °), **33** (–30,3 °)), līdz ar to donorā grupa ir mazāk planāra. Lielākas izgriešanās dēļ slāpekļa atoma nedalītais elektronu pāris konjugējas daudz vājāk ar bifenilgrupu π-elektroniem nekā tas bija savienojumos **28** un **33**, un donorās grupas stiprums pieaug. Visbeidzot julolidilaizvietotājs ievērojami nobīda hromoforu **29** un **34** *CT* absorbcijas joslas uz garākiem viļņiem ar mazāku enerģiju. Jāmin, ka literatūrā aprakstītie D-π-A savienojumi ar julolidilaizvietotāju vienmēr uzrāda batohromi nobīdītu absorbciju, salīdzinot ar analogiem savienojumiem ar citām aminogrupām, un šo novērojumu skaidro ar julolidilgrupas donoro raksturu, kas padara molekulu vieglāk polarizējamu [20]. Turpretī, apskatot savienojumu **27–36** emisijas spektrus, donorās grupas pēc to ietekmes uz $\lambda_{em}$ (batohroma nobīde) var sarindot šādā secībā: $NMe_2$ < julolidil < $NPh_2$ < $N(BPh)_2$. Pēc to struktūras ietekmes uz $\lambda_{em}$ sintezētie hromofori ir dalāmi divās grupās: pirmā grupa ir savienojumi ar alkilaizvietotājiem pie slāpekļa atoma ($NMe_2$ un julolidilfragments); otrā grupa – savienojumi ar fenilgrupām pie slāpekļa atoma ($N(BPh)_2$, $NPh_2$). Šīm abām grupām dažādos šķīdinātājos ir izteikta atšķirība Stoksa nobīdēs (Δλ). Savienojumiem ar alkilaizvietotājiem pie slāpekļa atoma (**27**, **29**, **31**, **32**, **34**, **36**) Δλ ir gandrīz uz pusi mazākas (2005–4273 $cm^{-1}$ dimedona atvasinājumiem un 1466–2779 $cm^{-1}$ 1,3-indandiona atvasinājumiem) nekā savienojumiem ar fenilaizvietotājiem pie slāpekļa atoma (3715–7487 $cm^{-1}$ dimedona atvasinājumiem un 2434–4815 $cm^{-1}$ 1,3-indandiona atvasinājumiem). Vismazākās Δλ tika iegūtas tieši savienojumiem **29** un **34** ar julolidilaizvietotāju. To varētu skaidrot ar šo savienojumu līdzīgiem pamatstāvokļa un ierosinātā stāvokļa dipolmomentiem, ko bieži min literatūrā [21]. Savukārt savienojumu **28**, **30**, **33** un **35** lielās Stoksa nobīdes skaidrojamas ar iespējamu struktūras pārorientāciju ierosinātā stāvoklī, piemēram, ierosinātā stāvokļa iekšmolekulāru protonu pārnesi, ko bieži novēro savienojumiem ar stiprām iekšmolekulārām ūdeņraža saitēm [22];

**(3)** π-tiltiņa pagarināšana starp D un A grupu (**27** → **31** un **32** → **36**), kā paredzams, nobīda gan absorbcijas (17 nm un 20 nm), gan emisijas joslas batohromi (76 nm un 81 nm) garākas konjugētās sistēmas dēļ.

Solvatohromisma pētījumi parāda, ka savienojumu **27–39** absorbciju maz ietekmē šķīdinātāju polaritātes maiņa un $\lambda_{abs}$ izmainās tikai par 1–12 nm. Šāds rezultāts liek secināt, ka jauno D-π-A savienojumu pamatstāvokli neietekmē vides polaritātes maiņa. Pretēji, savienojumu emisijas īpašības ievērojami ietekmē šķīdinātāja polaritāte. Visiem savienojumiem novērojams spēcīgs pozitīvs solvatofluorohromisms un, pārejot no nepolārā toluola uz polāro MeOH, $\lambda_{em}$ izmainās par 24–126 nm. Vislielāko batohromo $\lambda_{em}$ nobīdi novēro tieši savienojumiem ar apjomīgajiem un ārpusplaknes izgrieztajiem difenil- un

bidifenil- aizvietotājiem pie slāpekļa atoma (94–126 nm). Šo novērojumu var skaidrot ar to, ka izteiktu jutību pret vides polaritāti novēro tieši savienojumiem, kuriem ierosinātā stāvoklī ir spēcīga lādiņa pārnese no D grupas uz A grupu [23].

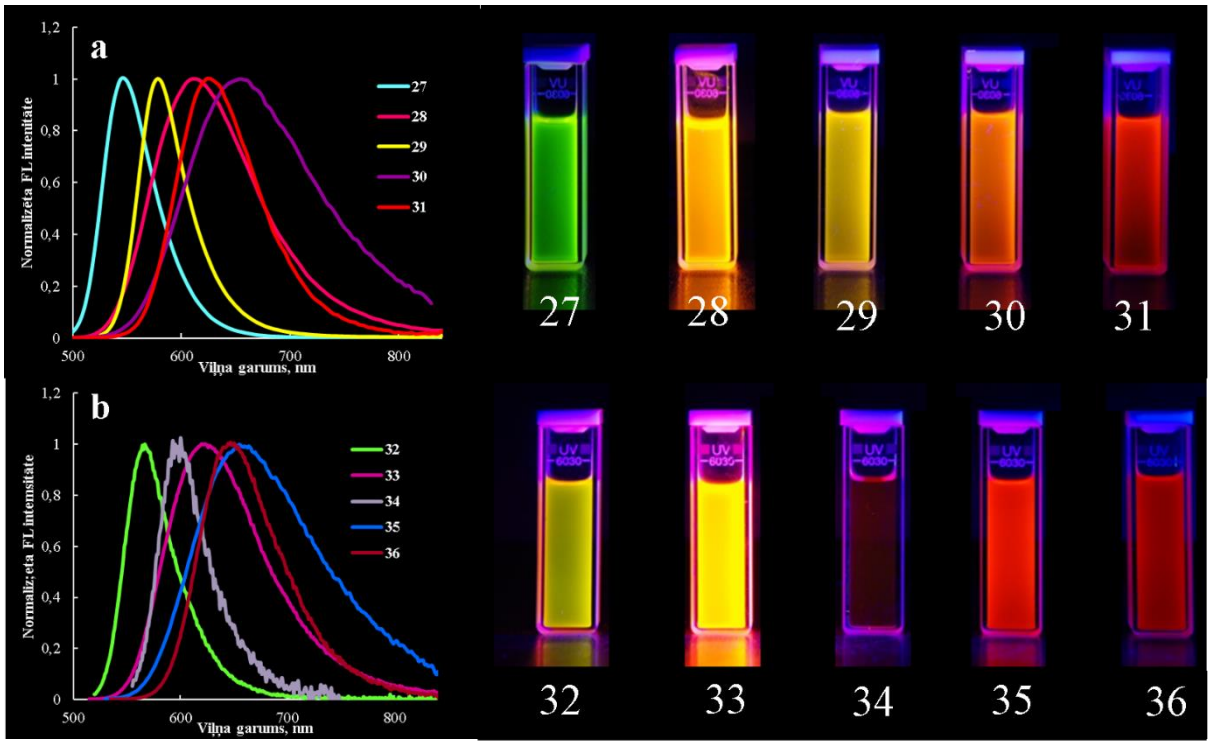


9. att. **(a)** – dimedona atvasinājumu **27–31** emisijas spektri un to $CHCl_3$ šķīdumu emisija zem UV gaismas; **(b)** – 1,3-indandiona atvasinājumu **32–36** emisijas spektri un to $CHCl_3$ šķīdumu emisija zem UV gaismas.

Emisijas efektivitātes noskaidrošanai iegūtajiem savienojumiem tika izmērīti *PLQY* dažādos šķīdinātājos (3. tab.). Palielinot šķīdinātāja polaritāti (toluols, $CHCl_3$ → MeOH),visiem savienojumiem **27–39** strauji krītas *PLQY*. Šajā gadījumā jāņem vērā, ka polāros šķīdinātājos pētāmo D-π-A savienojumu emisijas joslas tiek ievērojami nobīdītas uz garākiem viļņiem, tas ir, polārs šķīdinātājs pazemina savienojumu ierosinātā stāvokļa enerģiju [23]. Iespējams, šis pazemināts ierosinātais stāvoklis ir nefluorescējošs vai tajā savienojuma-šķīdinātāja molekulu mijiedarbības rezultātā tiek pastiprināta molekulu bezizstarojuma pāreja pamatstāvoklī. Apskatot literatūru par D-π-A tipa savienojumiem, jāsecina, ka pārsvarā šādiem savienojumiem novēro fluorescences efektivitātes izzušanu vai samazināšanos polāros šķīdinātājos, piemēram, cinnamoilpironu atvasinājumu gadījumā [9]. 2-cinnamoildimedona **27–31** un 2-cinnamoil-1,3-indandiona atvasinājumu **32–36** rindās visaugstākie *PLQY* iegūti toluolā. Savienojumi **28**, **30**, **33** un **35** ar fenilaizvietotājiem pie slāpekļa atoma uzrāda augstus *PLQY* (0,40–0,93), savukārt savienojumiem ar alkilaizvietotājiem, kā paredzams, novēro ievērojami zemākus iznākumus (0,05–0,31). Tāpat nepolārā $CHCl_3$ *PLQY* ir pietiekami augsti (0,15–0,78), atskaitot 1,3-indandiona atvasinājumus **32** un **34**, kas uzrāda zemas intensitātes emisiju šajā šķīdinātājā (0,03, <0,01). Savukārt 2-cinnamoil-1,3-indandiona *O*-metilēteri **37–39** uzrāda zemus *PLQY* toluolā (<0,01–0,02) un $CHCl_3$ (0,02–0,06), izņemot savienojumu **39** ar julolidilaizvietotāju, kas $CHCl_3$

uzrāda vidēju *PLQY* – 0,32. Acīmredzot 2-cinnamoil-1,3-indandiona atvasinājumu hidroksilgrupas metilēšana un spēcīgas iekšmolekulāras ūdeņraža saites izjaukšana izraisa izteiktu emisijas efektivitātes samazināšanos.

Ar kvantu ķīmijas aprēķinu programmu "*ORCA*" noteikta savienojumu **27–39** pamatstāvokļa ģeometrija un *HOMO*/*LUMO* orbitāļu enerģijas (3. tab.) un izvietojums (10. att.). Sintezētajiem savienojumiem **27-39** *HOMO* orbitāle novietota donorajā daļā un cinnamoilfragmentā, turpretī *LUMO* orbitāle – akceptorajā daļā un cinnamoilfragmentā. Šāds orbitāļu izvietojums izsauc ievērojamu *CT* šiem savienojumiem. Aprēķinātās *HOMO*/*LUMO* līmeņu enerģijas parāda, ka atkal novērojama atšķirība starp savienojumiem ar dažāda izmēra donorajām grupām. Savienojumiem **27**, **29**, **32** un **34** ar $NMe_2$ un julolidilaizvietotājiem *HOMO–LUMO* orbitāļu enerģiju spraugas ($E_g^{DFT}$) ir platākas (2,90–3,22 eV) nekā savienojumiem ar apjomīgajām $NPh_2$ un $N(BPh)_2$ grupām (2,77–2,96 eV) un norāda, ka pēdējiem ir spēcīgāka *CT* molekulā, kas arī rada augstāku kvantu efektivitāti. Pēc iegūtajiem $E_g^{DFT}$ donorās grupas pēc stipruma var sarindot šādā secībā (stiprākai donorai grupai atbilst šaurāka $E_g^{DFT}$ sprauga): $NMe_2$ < julolidil < $NPh_2$ < $N(BPh)_2$, kas atbilst iepriekš izvirzītajai secībai pēc $\lambda_{em}$. Tiltiņa pagarināšana starp D un A grupu (**27** → **31** un **32** → **36**) izraisa izteiktu $E_g^{DFT}$ samazinājumu (3,22 eV → 2,87 eV; 3,09 eV → 2,79 eV). *O*-Metilēteriem **37–39** aprēķinātās *HOMO* orbitāļu enerģijas ir augstākas, savukārt *LUMO* – zemākas nekā atbilstošajiem 2-cinnamoil-1,3-indandiona atvasinājumiem **32–36** un rezultātā to $E_g^{DFT}$ spraugas ir šaurākas. Iespējams, enerģijas starpības samazinājums starp *HOMO* un *LUMO* līmeņiem ir iemesls, kāpēc *O*-metilēterim **39** novēro vidēju *PLQY* (0,32), kamēr nemetilētajam atvasinājumam **34** – ļoti zemu *PLQY* (<0,01) $CHCl_3$ šķīdumos. Toties starp 2-cinnamoil-1,3-indandiona atvasinājumu **34** un tā *O*-metilēteri **39** nenovēro izmaiņas pamatstāvokļa ģeometrijā un *HOMO*/*LUMO* orbitāļu izvietojumā (10. att.).

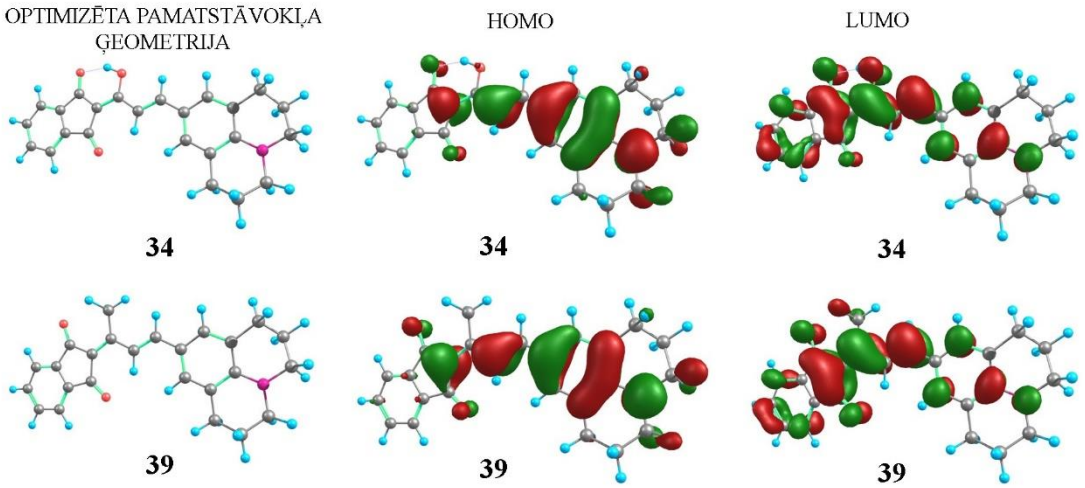


10. att. 2-cinnamoil-1,3-indandiona atvasinājuma **34** un tā *O*-metilētera **39** optimizētā pamatstāvokļa ģeometrija un *HOMO*/*LUMO* orbitāles.

Tālāk ar cikliskās voltmetrijas palīdzību pētītas savienojumu **27–39** elektroķīmiskās īpašības MeCN šķīdumos ($1{,}5\cdot10^{-5}$ M) un elektroķīmiskās oksidēšanās un reducēšanās potenciāli ($E_{ox}$, $E_{red}$) doti 3. tabulā (*Dr. chem.* B. Turovska). Visi savienojumi MeCN šķīdumos uzrāda elektroķīmiski neatgriezenisku katodisko reducēšanos un anodisko oksidēšanos. Apskatot iegūtos potenciālus, var secināt, ka $E_{ox}$ pārsvarā ietekmē savienojumu donorās grupas, jo akceptoro grupu maiņa no dimedona uz 1,3-indandionu (**27/32**, **28/33**, **29/34**, **30/35**, **31/36**) izraisa tikai nelielu potenciāla vērtības izmaiņu par 0,01–0,02 V. Iegūtās $E_{ox}$ vērtības rāda, ka donorās grupas pēc aizvietotājiem pie slāpekļa atoma, atkal iedalāmas divās grupās – ar alkilaizvietotājiem ($NMe_2$ un julolidilaizvietotājs) un fenilaizvietotājiem ($NPh_2$ un $N(BPh)_2$). Savienojumiem ar alkilaizvietotājiem (**27**, **29**, **31**, **32**, **34**, **36**, **37**, **39**) $E_{ox}$ atrodas robežās 0,57–0,81 V, savukārt savienojumiem ar fenilaizvietotājiem – 0,96–1,07 V. Tiltiņa pagarināšana starp donoro un akceptoro daļu (**27** → **31**; **32** → **36**) izraisa $E_{ox}$ vērtības palielināšanos par 0,14 V. Turpretī elektroķīmiskais reducēšanās potenciāls $E_{red}$ ir vairāk atkarīgs no akceptorās grupas un, pārejot no dimedona atvasinājumiem (**27–31**) uz 1,3-indandiona atvasinājumiem (**32–39**), novēro potenciāla samazinājumu par 0,11–0,22 V.

Termiskās īpašības tika pētītas 2-cinnamoildimedona **27–31** un 2-cinnamoil-1,3-indandiona atvasinājumiem **32–36**. Termogrammas iegūtas, karsējot paraugus 30–550 °C ar ātrumu 10 °C/min $N_2$ atmosfērā (*Dr. chem.* K. Lazdoviča), un parāda, ka visi 10 savienojumi ir termiski stabili līdz 200 °C, un to $T_{5\%}$ ($T_{5\%}$ – temperatūra, kurā savienojuma masa samazinājusies par 5 %) ir robežās 216–290 °C. Arī termiskās īpašības ievērojami ietekmē donorās grupas struktūra. Savienojumi ar alkilaizvietotājiem pie slāpekļa atoma uzrāda zemāku $T_{5\%}$ (216–238 °C) par savienojumiem ar telpiski lielākām $NPh_2$ un $N(BPh)_2$ grupām (271–290 °C) cinnamoilfragmentā. Savienojumu **30** un **35** ar $N(BPh)_2$ aizvietotāju augsto termisko stabilitāti var izskaidrot ar to lielo molekulāro masu un papildu π-π sadarbību un novietojumu.

No struktūras un īpašību pētījumiem par 2-cinnamoildimedona un 2-cinnamoil-1,3-indandiona atvasinājumiem **27–39** var secināt, ka šāda tipa savienojumu īpašības visvairāk ietekmē tieši donorās grupas struktūra. Apjomīgu ārpusplaknes izgrieztu difenil- un bidifenilamino- grupu izmantošana, kas padara savienojumu (**28**, **30**, **33** un **35**) struktūru neplanāru, rada jaunus savienojumus ar batohromi nobīdītu emisiju ($\lambda_{em}$ > 612 nm), neierasti lielām Stoksa nobīdēm (3715–7487 $cm^{-1}$ dimedona atvasinājumiem un 2434–4815 $cm^{-1}$ 1,3-indandiona atvasinājumiem) un augstiem *PLQY* (0,16–0,93) nepolāros šķīdinātājos, šaurākām HOMO–LUMO spraugām (2,77–2,96 eV) un paaugstinātu termisko stabilitāti ($T_{5\%}$ > 270 °C), salīdzinot ar savienojumiem, kas satur *N*-alkil- aizvietototājus (**27**, **29**, **32** un **34**). Potenciālu lietošanai OLED uzrāda savienojums **28** ar dimedona ciklu kā akceptoru, donoro *N*,*N*-difenilaminogrupu un 1-hidroksiallilidēn- π-tiltiņu, kura emisiju $CHCl_3$ var raksturot šādi: $\lambda_{abs}$ = 466 nm, $\lambda_{em}$ = 612 nm (*PLQY* = 0,78), $\Delta\lambda$ = 5119 $cm^{-1}$.

# SECINĀJUMI

1. Uz β,β'-triketonu – 2-acil-1,3-indandiona un 2-acildimedona – atvasinājumu bāzes ir iespējams iegūt divu dažādu veidu efektīvi luminiscējošus savienojumus: **(1)** eiropija trivalento jonu ($Eu^{3+}$) kompleksus, deprotonējot un izmantojot β,β'-triketonātus, piemēram, ligandus; **(2)** D-π-A savienojumus, β,β'-triketonu kondensācijas reakciju rezultātā ar donoru grupu saturošiem benzaldehīda atvasinājumiem.
2. 2-acil-1,3-indandionātu $Eu^{3+}$ kompleksu emisijas īpašības cietā stāvoklī ievērojami ietekmē kompleksu struktūra: (1) tetrakis kompleksi ar vispārīgo formulu [Eu(β,β'-triketonāts)$_4$]$^-$ uzrāda augstākus *PLQY* un emisijas dzīves laikus nekā analogie $Eu^{3+}$ Lūisa bāzu kompleksi (Eu(β,β'-triketonāts)$_3$(PHEN)), pateicoties ievērojami lielākam fotonu absorbcijas laukumam, ko palielina ceturtais β,β'-triketonāta ligands; (2) tetrakis kompleksu katjona izmēra ietekmes izpēte uz emisijas īpašībām rāda, ka īsāka $N^+Et_4$ katjona gadījumā *PLQY* ir 3–6 reizes augstāki un to emisijas dzīves laiki – divas reizes ilgāki, nekā izmantojot garāku $N^+Bu_4$ katjonu.
3. $Eu^{3+}$ kompleksi ar 2-acildimedona ligandiem uzrāda zemus *PLQY* šķīdumos, pateicoties to ligandu ierosinātā stāvokļa enerģētisko līmeņu izkārtojumam pret $Eu^{3+}$ jona rezonanses līmeni. 2-acildimedona atvasinājumiem starpība starp ierosināto tripleta līmeni un $Eu^{3+}$ jona rezonanses līmeni ir pārāk liela (>7000 $cm^{-1}$), lai notiktu efektīva enerģijas pārnese kompleksā.
4. Salīdzinot β-diketonātu (dibenzoilmetāna atvasinājumu ligandi) $Eu^{3+}$ kompleksu *PLQY* cietā stāvoklī un PVK filmiņā ar β,β'-triketonātu $Eu^{3+}$ kompleksu datiem, novērojams, ka pirmajiem *PLQY* plēvītē samazinās tikai divas reizes, savukārt otrajiem *PLQY* var samazināties 3–7 reizes. Šādi dati norāda uz dibenzoilmetāna atvasinājumiem kā efektīvākiem $Eu^{3+}$ kompleksu ligandiem.
5. $Eu^{3+}$ kompleksi ar dibenzoilmetāna un 4-metildibenzoilmetāna ligandiem uzrāda 5–7 reizes augstākus *PLQY* cietā stāvoklī nekā kompleksi, kas satur karbazolu aizvietotu dibenzoilmetāna atvasinājumu ligandus. Emisijas efektivitātes pieaugumu izraisa šiem kompleksiem piemītošā agregācijas pastiprinātā emisija.
6. Izgatavotie OLED, kuros kā emiteris izmantots $Eu^{3+}$ komplekss ar 4-metildibenzoilmetāna ligandiem, uzrāda vāju elektroluminiscenci sakarā ar to, ka kompleksam nepiemīt lādiņa pārneses īpašības, kas norāda, ka sintezētajiem $Eu^{3+}$ kompleksiem nepiemīt OLED iekārtām nepieciešamās īpašības.
7. 2-cinnamoildimedona un 2-cinnamoil-1,3-indandiona atvasinājumu spektroskopiskās, elektroķīmiskās un termiskās īpašības izteiktāk ietekmē izvēlētās donorās grupas struktūra. Apjomīgās ārpus plaknes izgrieztas *N,N*-difenilamino- ($NPh_2$) un *N,N*-bidifenilaminogrupas ($N(BPh)_2$), kas padara savienojumu struktūru neplanāru, noved pie batohromi nobīdītas emisijas ($\lambda_{em} > 612$ nm), neierasti lielām Stoksa nobīdēm (2434-7487 $cm^{-1}$) un augstiem *PLQY* (0,16–0,93) nepolāros šķīdinātājos, šaurākām *HOMO–LUMO* spraugām (2,77–2,96 eV) un paaugstinātas termiskās stabilitātes ($T_{5\%} > 270$ °C), salīdzinot ar planāriem savienojumiem, kas satur *N,N*-alkilamino-aizvietotājus.

8. 2-cinnamoil-1,3-indandiona atvasinājumu un to *O*-metilēteru īpašību salīdzinājums liecina, ka metilēšanas rezultātā iegūtajiem savienojumiem strauji krītas emisijas efektivitāte nepolāros šķīdinātājos, savukārt pārējām īpašībām izteiktas izmaiņas nenovēro.
9. π-tiltiņa pagarināšana par diviem oglekļa atomiem starp donoro un akceptoro grupu 2-cinnamoildimedonu un 2-cinnamoil-1,3-indandiona atvasinājumu rindās izraisa absorbcijas (17–20 nm) un emisijas joslu (76–81 nm) batohromas nobīdes, augstākus *PLQY* un šaurākas *HOMO–LUMO* spraugas (3,22 eV; 3,09 eV → 2,87 eV; 2,79 eV).

# LITERATŪRAS SARAKSTS


[1] Binnemans K. Lanthanide-based luminescent hybrid materials. *Chem. Rev.*, **2009**, *109*, 4283–4374.

[2] Pluskota R, Koba M. Indandione and its derivatives - chemical compounds with high biological potential. *Mini Rev. Med. Chem.*, **2018**, *18* (15), 1321–1330.

[3] Ahmedova A, Mantarevay V, Enchev V, Mitewa V. 2-Acetylindan-1,3-dione and its $Cu^{2+}$ and $Zn^{2+}$ complexes as promising sunscreen agents. *Int. J. Cosmet. Sci.*, **2002**, *24*, 103–110.

[4] Teotonio EES, Brito HF, Cremona M, Quirino WG., Legnani C, Felinto MCFC. Novel electroluminescent devices containing $Eu^{3+}$-(2-acyl-1,3-indandionate) complexes with TPPO ligand. *Opt. Mater.*, **2009**, *32*, 345–349.

[5] Teotonio EES, Brito HF, Viertler H, Faustino WM, Malta OL, de Sá GF. Synthesis and luminescent properties of $Eu^{3+}$-complexes with 2-acyl-1,3-indandionates (ACIND) and TPPO ligands: the first X-ray structure of Eu–ACIND complex. *Polyhedron*, **2006**, *25*, 3488–3494.

[6] Ahmedova A, Marinova P, Pavlovic G, Guncheva M, Stoyanov N, Mitewa M. Structure and properties of a series of 2-cinnamoyl-1,3-indandiones and their metal complexes. *J. Iran. Chem. Soc.*, **2012**, *9*, 297–306.

[7] Ahmedova A, Atanasov V, Marinova P, Stoyanov N, Mitewa M. Synthesis, characterization and spectroscopic properties of some 2-substituted 1,3-indandiones and their metal complexes. *Cent. Eur. J. Chem.*, **2009**, *7*, 429–438.

[8] Ahmedova A, Pavlovic G, Zhiryakova D, Šišak D, Stoyanov N, Springborg M, Mitewa M. Experimental and theoretical study on the structure and optical properties of 2-acyl-1,3-indandiones – Conformational effects. *J. Mol. Struct.*, **2010**, *981*, 10–20.

[9] Tykhanov DA, Serikova II, Yaremenko FG, Roshal AD. Structure and spectal properties of cinnamoyl pyrones and their vinylogs. *Cent. Eur. J. Chem.*, **2010**, *8*(2), 347–355.

[10] Li W, Yan P, Hou G, Li H, Li G. Efficient red emission from PMMA films doped with 5,6-DTFI europium(III) complexes: synthesis, structure and photophysical properties. *Dalton. Trans.*, **2013**, *42*, 11537–11547.

[11] Accorsi G, Listorti A, Yoosaf K, Armaroli N. 1,10-Phenanthrolines: versatile building blocks for luminescent molecules, materials and metal complexes. *Chem. Soc. Rev.*, **2009**, *38*, 1690–1700.

[12] Adati RD, Lima SAM, Davolos MR, Jafelicci M. A new β-diketone complex with high color purity, *J. Alloys Compd.*, **2006**, *418*, 222–225.

[13] Mech A, Karbowiak M, Görller-Walrand C, Van Deun R. The luminescence properties of three tetrakis dibenzoylmethane europium(III) complexes with different counter ions. *J. Alloys Compd.*, **2008**, *451*, 215–219.

[14] Steemers FJ, Verboom W, Reinhoudt DN, Van der Tal JEB, Verhoeven JW. New sensitizer-modified calix[4]arenes enabling near-UV Excitation of complexed luminescent lanthanide ions. *J. Am. Chem. Soc.*, **1995**, *117*, 9408–9414.

[15] Latva M, Takalo H, Mukkala VM, Matachescu C, Rodriguez-Ubis JC, Kankare J. Correlation between the lowest triplet state energy level of the ligand and lanthanide(II1) luminescence quantum yield. *J. Lumin*., **1997**, *75*, 149–169.

[16] Pina J, Seixas de Melo J, Burrows HD, Monkman AP, Navaratnam S. On the triplet state of poly(*N*-vinylcarbazole). *Chem. Phys. Lett.*, **2004**, *400*, 441–445.

[17] Li L, Liu Y, Guo H, Wang Y, Cao Y, Liang A, Tan H, Qi H, Zhu M, Zhu W. Synthesis, optophysical and electrochemical properties of bipolar-transporting europium(III) complexes with carbazole and oxadiazole units. *Tetrahedron*, **2010**, *66*, 7411–7417.

[18] Zhu Z, Song B, Yuan J, Yang C. Enabling the triplet of tetraphenylethene to sensitize the excited state of europium(III) for protein detection and time-resolved luminescence imaging. *Adv. Sci.*, **2016**, *3*, 1600146.

[19] Xu X, Yang X , Zhao J, Zhou G, Wong W-Y. Recent advances in solution-processible dendrimers for highly efficient phosphorescent organic light-emitting diodes (PHOLEDs). *Asian J. Org. Chem.*, **2015**, *4*, 394–429.

[20] Zhou XH, Luo J, Davies JA, Huang S, Jen AK. Push–pull tetraene chromophores derived from dialkylaminophenyl, tetrahydroquinolinyl and julolidinyl moieties: optimization of second-order optical nonlinearity by fine-tuning the strength of electron-donating groups. *J. Mater. Chem.*, **2012**, *32*, 16390–16398.

[21] Fulopova A, Magdolen P, Sigmundova I, Zahradnik P, Rakovsky E, Cigan M. Benzotristhiazole based chromophores for nonlinear optics. *J. Mol. Struct*., **2012**, *1027*, 70–80.

[22] Enchev V, Bakalova S, Ivanova G, Stoyanov N. Excited state intramolecular proton transfer of 2-acetylindan-1,3-dione. *Chem. Phys. Lett.*, **1999**, *314*, 234–238.

[23] Lakowicz JR. Principles of fluorescence spectroscopy, 3rd edition, Springer, US, **2006**, 954.

# PATEICĪBAS

Izsaku pateicību promocijas darba vadītājam profesoram *Dr. habil. chem.* Valdim Kamparam par atbalstu un veltīto laiku promocijas darba tapšanā.

Liels paldies arī visiem Lietišķās ķīmijas institūta darbiniekiem par palīdzību zinātniskā darba tapšanā, it seviški Rūtai Kamparei par KMR spektru uzņemšanu, Kristīnei Lazdovičai par FT-IR, TG analīžu veikšanu, Laumai Laipniecei par apmācību ar AEŠH, Kasparam Traskovskim par konsultācijām, idejām un palīdzību pēdējās publikācijas tapšanā un Zanei Ābelniecei par uzklausīšanu un atbalstīšanu!

Paldies arī kolēģiem no OSI – *Dr. chem.* Baibai Turovskai par elektroķīmisko analīžu veikšanu un *Dr. phys.* Sergejam Beļakovam par savienojumu rentgenstruktūranalīžu uzņemšanu! Vislielākā pateicība arī kolēģiem no CFI – *Dr. phys.* Aivaram Vembrim par apmācību darbā ar luminiscences spektrometru un savienojumu OLED izgatavošanu un mērīšanu, un Igoram Mihailovam par iepazīstināšanu un apmācību ar teorētisko kvantu ķīmijas aprēķinu programmu "*ORCA*".

Paldies SIA "*Grindex*" par 2014. gadā piešķirto "Sudraba pūces apbalvojumu"!

Vislielākais paldies manam vīram Kristapam Māliņam par iedrošināšanu, atbalstu un nerimtīgām sarunām par zinātni! Paldies arī manai pārejai ģimenei un draudzenēm par uzmundrināšanu un atbalstu!

# DOCTORAL THESIS PROPOSED TO RIGA TECHNICAL UNIVERSITY FOR THE PROMOTION TO THE SCIENTIFIC DEGREE OF DOCTOR OF SCIENCE

To be granted the scientific degree of Doctor of Science (Ph. D.), this Doctoral Thesis has been submitted for the defence at the open meeting of RTU Promotion Council on 12 November, 2020 at the Faculty of Materials Science and Applied Chemistry of Riga Technical University, 3 Paula Valdena Street, Room 272.

OFFICIAL REVIEWERS

Professor Dr. chem. Māra Jure
Riga Technical University, Latvia

Lead researcher Dr. habil. chem. Gunārs Duburs
Latvian Institute of Organic Synthesis, Latvia

Lead researcher Dr. phys. Mārtiņš Rutkis
Institute of Solid State Physics, University of Latvia, Latvia

DECLARATION OF ACADEMIC INTEGRITY

I hereby declare that the Doctoral Thesis submitted for the review to Riga Technical University for the promotion to the scientific degree of Doctor of Science (Ph. D.) is my own. I confirm that this Doctoral Thesis had not been submitted to any other university for the promotion to a scientific degree.

Ilze Māliņa ……. (signature)

Date: ……

The Doctoral Thesis has been prepared as a thematically united collection of scientific publications. It consists of summary and six publications. Publications have been written in English. The total number of publication pages is 54.

# CONTENTS

**ABBREVATIONS** ..... 35
**GENERAL OVERVIEW OF THE THESIS** ..... 37
Introduction ..... 37
Aims and Objectives ..... 38
Thesis for Defence ..... 39
Scientific Novelty and Main Results ..... 39
Structure of the Thesis ..... 40
Publications and Approbation of the Thesis ..... 40
**MAIN RESULTS OF THE THESIS** ..... 42
Synthesis and Characterization of Spectroscopic Properties of $Eu^{3+}$ Complexes With β,β'-Triketone Ligands ..... 42
Synthesis and Characterization of Spectroscopic Properties of $Eu^{3+}$ Complexes With β-Diketone Ligands ..... 47
Synthesis and Characterization of Spectroscopic Properties of Derivatives of 2-Cinnamoyldimedones and 2-Cinnamoyl-1,3-Indandiones ..... 51
**CONCLUSIONS** ..... 59
**REFERENCES** ..... 61
**ACKNOWLEDGEMENTS** ..... 63
**PIELIKUMI/PUBLICATIONS** ..... 64

# ABBREVATIONS

| | |
|---|---|
| $\lambda_{abs}$ | absorption spectra maximum |
| $\lambda_{em}$ | emission spectra maximum |
| $\lambda_{exc}$ | excitation spectra maximum |
| $\Delta\lambda$ | Stokes shifts |
| $\tau$ | luminescence lifetime |
| A | acceptor group |
| AD | 2-acetyl-5,5-dimethylcyclohexane-1,3-dione anion or 2-acetyldimedone anion |
| AEE | aggregation enhanced emission |
| AID | 2-acetyl-1*H*-indene-1,3(2*H*)-dione anion or 2-acetyl-1,3-indandione anion |
| BD | 2-benzoyl-5,5-dimethylcyclohexane-1,3-dione anion or 2-benzoyldimedone anion |
| BID | 2-benzoyl-1*H*-indene-1,3(2*H*)-dione anion or 2-benzoyl-1,3-indandione anion |
| BPh | biphenylgroup |
| Bu | butyl group |
| CBZ-HDBM | 1-[4-(9*H*-carbazol-9-yl)-phenyl]-3-phenylpropane-1,3-dione |
| CBZ-DBM | 1-[4-(9*H*-carbazol-9-yl)-phenyl]-3-phenylpropane-1,3-dione anion |
| CT | charge transfer |
| D | donor group |
| DBM | 1,3-diphenylpropane-1,3-dione anion or dibenzoylmethane anion |
| Et | ethylgroup |
| Fl | fluorescence |
| HAD | 2-acetyl-5,5-dimethylcyclohexane-1,3-dione or 2-acetyldimedone |
| HAID | 2-acetyl-1*H*-indene-1,3(2*H*)-dione or 2-acetyl-1,3-indandione |
| HBD | 2-benzoyl-5,5-dimethylcyclohexane-1,3-dione or 2-benzoyldimedone |
| HBID | 2-benzoyl-1*H*-indene-1,3(2*H*)-dione or 2-benzoyl-1,3-indandione |
| HDBM | 1,3-diphenylpropane-1,3-dione or dibenzoylmethane |
| HMBID | 2-(4-methylbenzoyl)-1*H*-indene-1,3(2*H*)-dione or 2-(4-methylbenzoyl)-1,3-indandione |
| ITO | indium tin oxide |
| Me | methyl group |
| MBID | 2-(4-methylbenzoyl)-1*H*-indene-1,3(2*H*)-dione anion or 2-(4-methylbenzoyl)-1,3-indandione anion |
| MeCN | acetonitrile |
| Me-DBM | 1-(4-methylphenyl)-3-phenylpropane-1,3-dione anion |
| Me-HDBM | 1-(4-methylphenyl)-3-phenylpropane-1,3-dione |
| MeOH | methanol |
| OLED | organic light emitting dione |
| PEDOT:PSS | poly(3,4-ethylenedioxythiophene):poly(styrene sulfonate) |
| Ph | phenyl group |

| | |
|---|---|
| PHEN | 1,10-phenathroline |
| PLQY | absolute photoluminiscence quantum yield |
| PMMA | poly(methyl metaacrylate) |
| PVK | *N*-polyvinylcarbazole |
| $S_1$ | singlet energy level |
| $T_1$ | triplet energy level |
| THF | tetrahydrofuran |
| TPBi | 1,3,5-tri-(*N*-phenylbenzimidazol-2-yl)-benzene |
| UV | ultraviolet |

# GENERAL OVERVIEW OF THE THESIS

## Introduction

β,β'-triketones and β-diketones are widely investigated compounds for synthesis of new emitting and non-linear optical materials. One of the ways, how to obtain luminophores on the basis of these compounds, is to use their coordinated capable β-diketone fragment. After deprotonation, 1,3-diketones form β-diketone anions, which easily coordinate with metal and non-metal cations, forming different complexes, which usually are characterized with strong emission properties, for example, luminescence of lanthanide cation β-diketonate complexes are described with pronounced colour purity, high luminescence quantum yields and more than few hundred μs long lifetimes [1]. In this case, enolate is used as ligand, which provides metal cation with energy, obtained from light absorption. The second way of obtaining luminophores and non-linear chromophores, is by using 1,3-diketone fragment as electron acceptor group (A). By introducing donor group (D) in these compounds, it is possible to obtain luminescent compounds with push-pull D-A or D-π-A structures. The main advantage of compounds with D-π-A structure is the variety of D and A groups, which allows to adjust desirable emission and other properties of compound.

β,β'-triketones are compounds with 1,3-diketone group containing cycle and 2-acyl substituent, which is located at second carbon atom of the cycle. Investigations of this type of compounds, which includes derivatives of 2-acyl-5,5-dimethylcyclohexane-1,3-dione (2-acyldimedone) and 2-acyl-1*H*-indene-1,3(2*H*)-dione (2-acyl-1,3-indandione), are mainly focused on their pharmacological properties [2], however, information about their photophysical properties and potential for synthesis of new luminophores are poorly documented. Till now, it has been reported that derivatives of 2-acyl-1,3-indandiones exhibit intense ultraviolet (UV) light absorption with high molar absorption coefficients as well as high stability under UV light [3], which are desirable properties for ligands of lanthanide complexes and precursors of D-π-A compounds. Moreover, till now information about lanthanide β,β'-triketonate complexes is limited only to synthesis of some $Eu^{3+}$ tris and $Eu^{3+}$-Lewis base complexes with derivatives of 2-acyl-1,3-indandione ligands and their application in the fabrication of organic light emitting diodes (OLED) [4], [5]. In turn, there are also only few investigations about utilization of β,β'-triketones in synthesis of D-π-A compounds, and only derivatives of 2-cinnamoyl-1,3-indandiones [6]–[8] and 2-cinnamoylpyrones [9] are reported. On the other hand, β-diketones are the most investigated class of ligands for lanthanide cation complexes. Derivatives of 1,3-diphenylpropane-1,3-dione (dibenzoylmethane HDBM) are considered as very effective aromatic and symmetric ligands for lanthanide complexes, and many $Eu^{3+}$ complexes with these ligands have shown potential in fabrication of optoelectronic devices [1]. Thereby comparison between $Eu^{3+}$ complexes with popular β-diketone (derivatives of HDBM) and unexplored β,β'-triketone ligands could give insight about the influence of structure and symmetry of ligands on the properties of $Eu^{3+}$ complex.

The Doctoral Thesis is divided in two separate sections with two different aims considering the fact that it is possible to modify β,β'-triketones (derivatives of 2-acyldimedone and 2-acyl-1,3-indandione) in different ways. The first aim was the synthesis of different structures (tris, Lewis base, tetrakis) of $Eu^{3+}$ complexes with derivatives of 2-acyldimedonates and 2-acyl-1,3-indandionates. For comparison purposes $Eu^{3+}$ complexes with more symmetrical derivatives of HDBM ligands were synthesized. The first aim also includes property investigation of the obtained complexes, which would lead to conclusions about complex relationships of structure-complex properties, as well as by using experimental and theoretical calculated data of ligands and complexes, determining which ligands give $Eu^{3+}$ complexes with most efficient emission.

The second aim was directed towards investigation of 2-acetyl-5,5-dimethylcyclohexane-1,3-dione (2-acetyldimedone) and 2-acetyl-1*H*-indene-1,3(2*H*)-dione (2-acetyl-1,3-indandione) as precursors to obtain push-pull D-π-A type compounds (derivatives of 5,5-dimethyl-2-[(2*E*)-3-phenyl-1-oxo-2-propen-1-yl]-cyclohexane-1,3-dione or 2-cinnamoyldimedone and 2-[(2*E*)-3-phenyl-1-oxo-2-propen-1-yl]-1*H*-indene-1,3(2*H*)-dione or 2-cinnamoyl-1,3-indandione), which in the case of 1,3-indandione derivatives are popular 4-*N*,*N*-dimethylaminobenzylidene-1,3-indandione (DMABI) analogues with more prolonged conjugation system. This aim also includes property investigations of newly synthesized D-π-A type compounds and influence of different structural fragments (donor, acceptor group, π-bridge length and structure) on these properties.

## Aims and Objectives

### The aims of the Thesis

1. Synthesis of different structures (tris, Lewis base, tetrakis) of $Eu^{3+}$ complexes with derivatives of 2-acyldimedone, 2-acyl-1,3-indandione and dibenzoylmethane ligands and investigation of structure-property relationship for the obtained complexes.
2. Synthesis of D-π-A (derivatives of 2-cinnamoyldimedone and 2-cinnamoyl-1,3-indandione) compounds on the bases of 2-acetyldimedone and 2-acetyl-1,3-indandione and property investigation of the obtained compounds, as well as investigation of relationships of properties of different structural element (donor, acceptor group, π-bridge length and structure)-compounds.

### The following tasks were set to reach the first aim

1.1. To obtain $Eu^{3+}$ ion tris, Lewis base and tetrakis complexes with derivatives of 2-acyldimedone, 2-acyl-1,3-indandione and dibenzoylmethane ligands by varying molar ratio of $Eu^{3+}$ ion and organic ligands in the synthesis reaction.

1.2. To investigate environment influence on relationships of complex structures-emission properties.

1.3. To obtain theoretical energy level diagrams of all complexes, by theoretically calculating excited state energy levels of used ligands.

**The following tasks were set to reach the second aim**

2.1. To obtain derivatives of 2-cinnamoyldimedone and 2-cinnamoyl-1,3-indandione, which contain amino groups with different structures, and investigate absorption, emission, thermal and electrochemical properties and to determin their ground state geometry and HOMO/LUMO orbitals by using quantum chemistry program "ORCA".

2.2. To investigate donor and acceptor group and π-bridge length influence on the properties of compounds.

2.3. To investigate enol group influence on the properties of D-π-A compounds by synthesizing some derivatives of 2-cinnamoyl-1,3-indandione *O*-methylethers.

## Thesis for Defence

1. Complex structure, adjustment of excited state energy levels of used ligands to resonance level of the $Eu^{3+}$ ion, and the size of tetraalkyl ammonium ion in the case of tetrakis complexes influence the emission efficiency of $Eu^{3+}$ β-diketonate complexes.
2. Being D-π-A type compounds, derivatives of 2-cinnamoyldimedone and 2-cinnamoyl-1,3-indandione exhibit effective emission, which is influenced by compound's planarity, structure of donor groups, length and structure of π-bridge as well as polarity of the surrounding environment (solvent).

## Scientific Novelty and Main Results

As a result of the research towards the first aim of the Doctoral Thesis, new $Eu^{3+}$ organic tris, Lewis base, and tetrakis complexes with different β,β'-triketonates and β-diketonates (derivatives of 2-acyldimedone, 2-acyl-1,3-indandione and dibenzoylmethane) were obtained and their emission properties ($\lambda_{em}$, PLQY, τ) in solvents, powder state, and polymer films were investigated and compared. Energies of excited states of ligands were calculated theoretically and energy level diagrams of $Eu^{3+}$ complexes were determined. Impact of complex structure and cation size of tetrakis complexes on emission properties were investigated. Two OLEDs with $Eu^{3+}$ β-diketonate complex were fabricated. For the first time, aggregation enhanced emission was present for $Eu^{3+}$ complexes with derivatives of dibenzoylmethane ligands.

As a result of the research towards the second aim of the Doctoral Thesis, series of derivatives of 2-cinnamoyldimedone and 2-cinnamoyl-1,3-indandione were synthesized and their optical, electrochemical and thermal properties were investigated. Ground state geometries and HOMO/LUMO orbitals of all compounds were theoretically calculated using quantum chemistry program "ORCA". Systematic investigation of different amino donor group, acceptor group, and length of π-bridge impact on properties of obtained D-π-A compounds were conducted.

Doctoral Thesis is a finished original investigation, which shows significant importance in organic chemistry subbranch of chemistry.

## Structure of the Thesis

The Thesis is a collection of scientific publications focussed on synthesis and property invetigation of new $Eu^{3+}$ complexes and compounds with D-π-A type structure on the basis of different β,β'-triketones and β-diketones (derivatives of 2-acyldimedone, 2-acyl-1,3-indandione and dibenzoylmethane).

## Publications and Approbation of the Thesis

Main results of the Thesis are summarized in six scientific publications. Results of the research were presented in six conferences.

**Scientific publications**

1. **Malina I**, Traskovskis K, Lesiņa, N., Vembris A. $Eu^{3+}$ ternary and tetrakis complexes with carbazole and methyl group substituted dibenzoylmethane derivatives: Induction of aggregation enhanced emission. *Dyes and Pigments*, **2019**, *163*, 257–266.
2. **Malina I**, Kampars V, Belyakov S. Luminescence properties of 2-benzoyl-1,3-indandione based $Eu^{3+}$ ternary and tetrakis complexes and their polymer films. *Dyes and Pigments*, **2018**, *159*, 655–665.
3. **Malina I**, Kampars V. Comparison of luminescent properties in solid-state and polymer films of Eu(III) complexes containing 2-acylindandione ligands. *Key Eng. Mater.*, **2018**, *762*, 239–243.
4. **Malina I**, Juhnevics N, Kampars V. Study of thermal and optical properties of dibenzoylmethane Eu(III) organic complexes. *Proc. Est. Acad. Sci.*, **2017**, *66*(4), 493–500.
5. **Malina I**, Kampars V, Turovska B, Belyakov S. Novel green-yellow-orange-red light emitting donor-π-acceptor type dyes based on 1,3-indandione and dimedone moieties. *Dyes and Pigments*, **2017**, *139*, 820–830.
6. **Malina I**, Kampars V, Turovska B. Synthesis, optical and electrochemical properties of substituted 2-cinnamoyl-1,3-indandione *O*-methyl ethers. *J. Mol. Struct.*, **2016**, *1115*, 241–249.

**Results of the Thesis were presented in the following conferences**

1. **Malina I**, Kampars V. Comparison of luminescent properties in solid-state and polymer films of Eu(III) complexes containing 2-acylindandione ligands. *58th International Riga Technical University scientific conference "Materials Science and Applied Chemistry"*, Riga, Latvia, October 20, **2017**.
2. **Malina I**, Kampars V. Photoluminescent properties of novel tris, ternary and tetrakis $Eu^{3+}$organic complexes with 2-acetyl-1,3-indandione ligands. *International conference "Materials, Methods & Technologies 2017*", Elenite, Bulgaria, June 26–30, **2017**.

3. **Malina I**, Juhnevics N, Kampars V. Study of thermal and optical properties of dibenzoyl-methane Eu(III) organic complexes. *International conference "Functional materials and Nanotechnologies-2017"*, Tartu, Estonia, April 24–27, **2017**.
4. **Malina I**, Kampars V. Synthesis and optical properties of red light emitting europium(III) complexes containing 2-acyldimedone and phenantroline ligands. *57th International Riga Technical University scientific conference "Materials Science and Applied Chemistry"*, Riga, Latvia, October 21, **2016**.
5. **Malina I**, Kampars V. Synthesis and optical properties of novel luminophores bearing cyclic β,β'-triketones. *56th International Riga Technical University scientific conference "Materials Science and Applied Chemistry"*, Riga, Latvia, October 14–16, **2015**, Abstract book p. 17.
6. **Neibolte I**, Kampars V, Plotniece, M. Synthesis and spectroscopic properties of 2-substituted cinnamoil-1,3-indandione *O*-methyl ethers. *55th International Riga Technical University scientific conference "Materials Science and Applied Chemistry"*, Riga, Latvia, October 14–17, **2014**, Abstract book p. 100.

# MAIN RESULTS OF THE THESIS

## Synthesis and Characterization of Spectroscopic Properties of $Eu^{3+}$ Complexes With β,β'-Triketone Ligands

Due to specific luminescence properties, such as several narrow emission lines in yellow, orange and red spectral range ($\lambda_{em}$ = 580 nm, 594 nm, 611 nm, 652 nm un 701 nm) and long excited state lifetimes (more than hundred μs), europium trivalent cation ($Eu^{3+}$) organic complexes are the most investigated ones from lanthanide group metal complexes. In order for the complex to exhibit metal luminescence, it is necessary that excited energy is absorbed by attached organic ligands and transferred to metal ion through excited singlet and triplet levels of ligands and $Eu^{3+}$ ion. This process is called Antenna effect (Fig. 1). High absorption ability in near ultraviolet (UV) light range of the ligands as well as excited triplet energy level location near or above resonance level (17 250 $cm^{-1}$) of $Eu^{3+}$ ion are the main preconditions for efficient energy transfer between ligands and $Eu^{3+}$ ion [1].

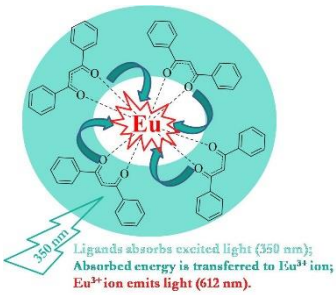


Fig. 1. Antenna effect.

Derivatives of 2-acyldimedone (2-acetyl-5,5-dimethylcyclohexane-1,3-dione or 2-acetyldimedone (HAD) **1** and 2-benzoyl-5,5-dimethylcyclohexane-1,3-dione or 2-benzoyldimedone (HBD) **2**) and 2-acyl-1,3-indandione (2-acetyl-1*H*-indene-1,3(2*H*)-dione or 2-acetyl-1,3-indandione (HAID) **7**, 2-benzoyl-1*H*-indene-1,3(2*H*)-dione or 2-benzoyl-1,3-indandione (HBID) **8**, 2-(4-methylbenzoyl)-1*H*-indene-1,3(2*H*)-dione or 2-(4-methylbenzoyl)-1,3-indandione) (HMBID) **9**) contains β-dicarbonyl fragment with enol group, which easily coordinates with metal cations. Also these compounds exhibit intense absorption in the UV range (250–400 nm) and show asymmetry towards 1,3-dicarbonylfragment due to location of one carbonyl group into 1,3-indandione cycle and other in aliphatic chain. Furthermore, investigations about application of these β,β'-triketones in metal complexes are documented poorly [4], [5], [10], therefore, in the Doctoral Thesis they were investigated as ligands for $Eu^{3+}$ organic complexes.

Different structure of $Eu^{3+}$ complexes can be obtained using different ratio of ligands to $Eu^{3+}$ ion and utilization of secondary ligands. Systematic synthesis of complexes started with synthesis of tris complexes **3**, **4** (general structure of Eu(β,β'-triketonate)$_3$($H_2O$)$_2$) by using molar ratio of β,β'-triketone and $EuCl_3$ 3 : 1 in the presence of 10 % NaOH (Fig. 2). Coordination number of $Eu^{3+}$ is 8, therefore, when using three anions of β,β'-triketones in the

synthesis reaction, coordination sphere of $Eu^{3+}$ ion is partly filled and two solvent ($H_2O$) molecules are attached to the complex, which usually negatively affect emission efficiency of complex. The coordination of these undesirable solvent molecules to $Eu^{3+}$ ion can divert using secondary ligands – *N*- or *O*-donor containing compounds, such as 1,10-phenanthroline (PHEN), therefore obtaining $Eu^{3+}$-Lewis base complexes **5**, **6** and **10–12** with general structure of Eu(β,β'-triketonate)$_3$(PHEN). $Eu^{3+}$-Lewis base complexes were obtained using PHEN, β,β'-triketone and $EuCl_3$ with molar ratio 1 : 3 : 1 in the presence of 10 % NaOH (Figs. 2 and 3). PHEN was used as secondary ligand, due to its intense UV light absorption ($\lambda_{abs}$ = 270 nm) and high molar absorption coefficient (ε ~ 30 000 $cm^{-1}$), and its excited singlet and triplet energy level location regard to resonance level of $Eu^{3+}$ ion [11]. Finally, several tetrakis complexes **13–17** were synthesized by using β,β'-triketone and $EuCl_3$ with molar ratio 4 : 1 with general formula [Eu(β,β'-triketonate)$_4$]$^-$. In this case $Eu^{3+}$ ion is coordinated with four β,β'-triketonates and negatively charged complex is obtained and stabilized with positively charged tetraalkylammonium ions ($N^+Et_4$ or NBu)$_4$) (Fig. 3).

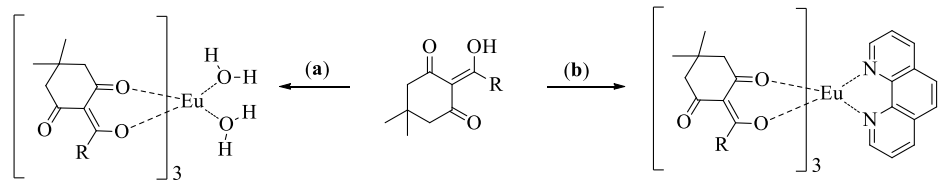


Fig. 2. Synthesis of $Eu^{3+}$ tris **3**, **4** and $Eu^{3+}$-Lewis base complexes **5**, **6** with 2-acyldimedone ligands.

(**a**) 10 % NaOH/$H_2O$, $EuCl_3 \cdot 6H_2O$; (**b**) 10 % NaOH/$H_2O$, 1,10-phenanthroline, $EuCl_3 \cdot 6H_2O$.

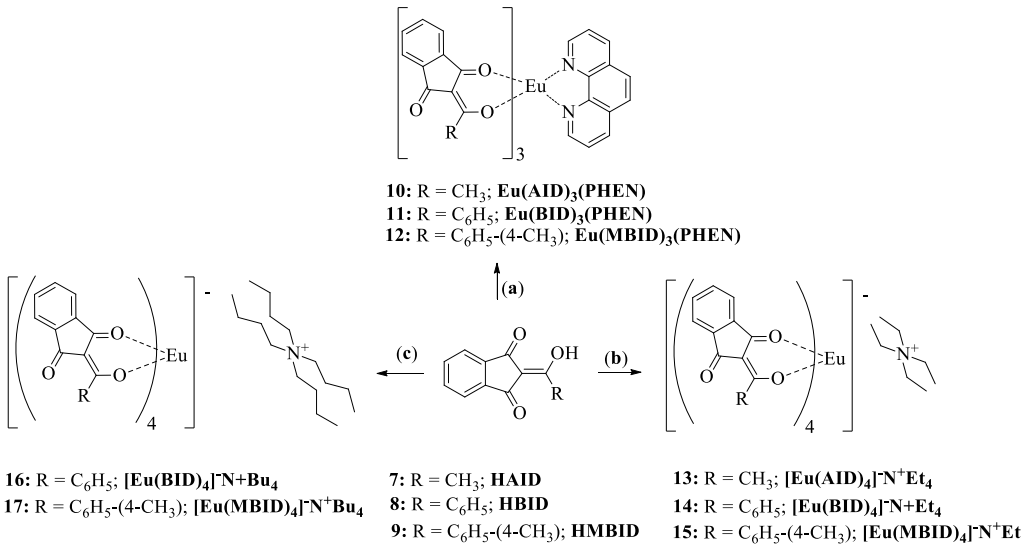


Fig. 3. Synthesis of $Eu^{3+}$-Lewis base **10–12** and tetrakis complexes **13–17** with 2-acyl-1,3-indandione ligands.

(**a**) 10 % NaOH/$H_2O$, 1,10-phenanthroline, $EuCl_3 \cdot 6H_2O$; (**b**) 10 % NaOH/$H_2O$, $Et_4NBr$, $EuCl_3 \cdot 6H_2O$; (**c**) 10 % NaOH/$H_2O$, $Bu_4NBr$, $EuCl_3 \cdot 6H_2O$.

To establish the structures of synthesized complexes, element analysis, $^1$H-NMR, FT-IR spectroscopy, and mass spectroscopy were employed. $^1$H-NMR spectroscopy was used to

prove the ratio of β,β'-triketonate:PHEN or β,β'-triketonate:ammonium cation in the synthesized $Eu^{3+}$-Lewis base and tetrakis complexes. The structure of tetrakis complex **15** crystal was established by X-Ray diffraction analysis.

Absorption and emission properties of newly synthesized $Eu^{3+}$ complexes **3–6** and **10–17** were investigated in different states. First, when looking at the spectroscopic properties in THF or MeCN solutions ($c \sim 1.5 \cdot 10^{-5}$ M), it was found that $Eu^{3+}$ complexes with derivatives of 2-acyldimedone ligands (**3–6**) exhibit light absorption between 210–340 nm ($\lambda_{abs}$ = 259–267 nm), while for complexes with derivatives of 2-acyl-1,3-indandione ligands **10–17** it is shifted to the longer wavelengths at 260–400 nm with $\lambda_{abs}$ = 321–333 nm. Apart from the fact that only complexes with derivatives of 2-acyl-1,3-indandione ligands **10–17** show absorption in the desired near UV region (300–400 nm), all $Eu^{3+}$ complexes emit five characteristic $Eu^{3+}$ ion bands with maxima at 580 nm, 594 nm, 611 nm, 652 nm, 701 nm. However, it can be concluded, that emission of $Eu^{3+}$ complexes **3–6** is weak and characterized with low PLQY (<0.01) in THF solutions. $Eu^{3+}$ complexes **10–17** with derivatives of 2-acyl-1,3-indandione ligands exhibit somewhat intense emission with higher PLQY 0.01–0.03. Low intensity emission in solutions is most likely caused by complex dissociation as well as undesirable environmental (solvent molecules) effects. Solvent molecules act as high-frequency oscillators of CH vibrations, which reduce the possibility of emission transition of central metal ion. In the solutions the effect of complex structures or the used cation impact on emission efficiency are not observed.

More efficient emission of the obtained $Eu^{3+}$ complexes **10–17** (due to the weak emission in solution, complexes **3–6** were not studied further) are observed in the powdered state (Table 1). The excitation spectra taken for complexes **10–17** in the powdered state are strongly shifted bathochromic (~80–130 nm) compared to the absorption spectra of the complexes solutions. Complexes with AID, BID, and MBID ligands can be excited by visible light (408–450 nm). Such a shift in the excitation wavelength is considered to be an advantage, since β-diketones are generally unstable under intense UV radiation, resulting in degradation of the complex by prolonged irradiation [1]. It is known, that many applications in the biological field, such as biomarkers or probes, require luminescent compounds that can be excited by visible light rather than UV radiation, which is harmful to living organisms.

The emission spectra of all complexes **10–17** in the solid-state, as in solutions, consist of five $Eu^{3+}$ ion transitions $^5D_0 \rightarrow {}^7F_J$ ($J$ = 0–4) with the most intense at 611 nm ($^5D_0 \rightarrow {}^7F_2$) (Fig. 4 **(a)**). This band is ~20–30 times more intense than the other bands and gives the complexes a distinctly red emission colour. Such a high ratio of transitions $^5D_0 \rightarrow {}^7F_2$, $^5D_0 \rightarrow {}^7F_1$ indicates that there is a strong coordination interaction between the metal ion and the ligands, and the $Eu^{3+}$ ion in the complex is present without inversion symmetry. The high ratio of the transition $^5D_0 \rightarrow {}^7F_2$ to other transitions also leads to complete match between the complex emission colour coordinates (*CIE 1931 chromaticity coordinates*) calculated from the emission spectra ($x$ = 0.670–0.673, $y$ = 0.327–0.330) to the NTSC standard red colour coordinates ($x$ = 0.67; $y$ = 0.33). It should be noted, that there are only a few examples in the scientific literature of obtained $Eu^{3+}$ complexes with 100 % red colour emission [12].

Table 1

Excitation Spectra Maxima ($\lambda_{exc}$), Absolute Photoluminescence Quantum Yields (PLQY), Luminescence Lifetimes ($\tau_1$ and $\tau_2$ ) of Powdered Samples of $Eu^{3+}$ Complexes **10–17**, and Theoretically Calculated Excited Singlet $S_1$ and Triplet $T_1$ Energetic Levels of β,β'-triketones

| Complex | $\lambda_{exc}$ | PLQY | $\tau_1$, μs | $\tau_2$, μs | $S_1$, $cm^{-1}$ | $T_1$, $cm^{-1}$ |
|---|---|---|---|---|---|---|
| **10** $Eu(AID)_3(PHEN)$ | 450 | 0.08 | –[a] | –[a] | 27 834 | 24 547 |
| **13** $[Eu(AID)_4]^-N^+Et_4$ | 450 | 0.34 | –[a] | –[a] | | |
| **11** $Eu(BID)_3(PHEN)$ | 408 | 0.06 | 121 ±4 (6%) | 42±1 (94%) | 27 659 | 22 779 |
| **14** $[Eu(BID)_4]^-N^+Et_4$ | 425 | 0.29 | 233±2 (22%) | 54±1 (78%) | | |
| **16** $[Eu(BID)_4]^-N^+Bu_4$ | 408 | 0.12 | 118 ±4 (4%) | 37±1 (96%) | | |
| **12** $Eu(MBID)_3(PHEN)$ | 408 | 0.10 | 122±3 (5%) | 39±1 (95%) | 27 802 | 22 525 |
| **15** $[Eu(MBID)_4]^-N^+Et_4$ | 425 | 0.60 | 203±17 (25%) | 118±5 (75%) | | |
| **17** $[Eu(MBID)_4]^-N^+Bu_4$ | 408 | 0.11 | 115±6 (2%) | 34±1 (98%) | | |

[a] Not determined

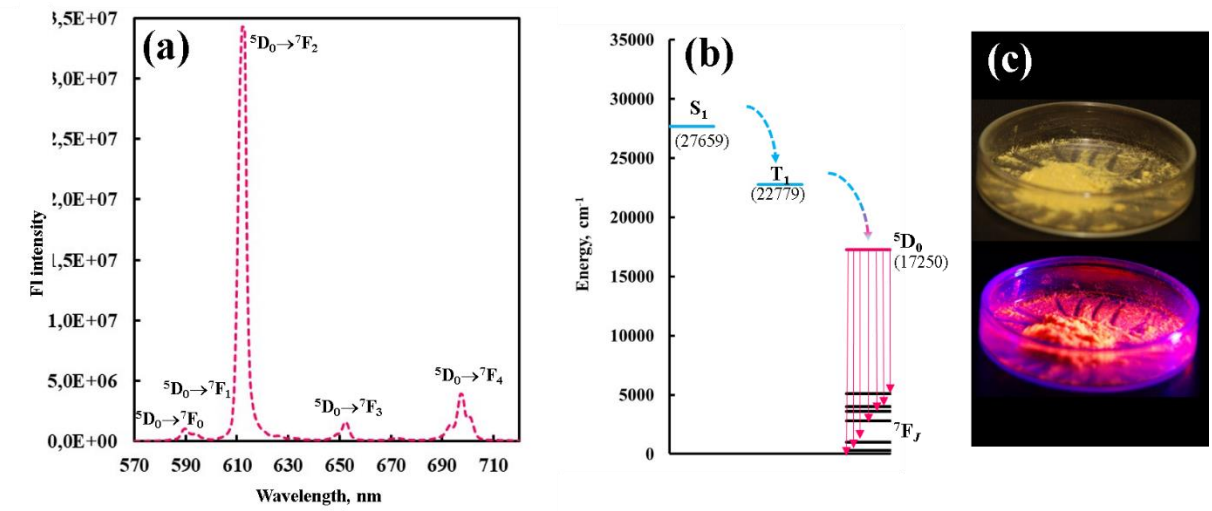


Fig. 4. **(a)** Emission spectra of complex **14** in solid-state ($\lambda_{exc}$ = 425 nm); **(b)** energy level diagram of complex **14** with the energy transfer process; **(c)** complex **14** in daylight and under UV ($\lambda_{exc}$=365 nm) light.

The luminescence lifetimes $\tau_1$ and $\tau_2$ of $Eu^{3+}$ ion transition $^5D_0 \rightarrow {}^7F_2$ (611 nm) for complexes **10–17** are given in Table 1. The luminescence lifetime curves were fitted with bi-exponential functions and two lifetime components $\tau_1$ and $\tau_2$ were obtained, indicating the presence of two sites of symmetry around the $Eu^{3+}$ ion. Different symmetry around $Eu^{3+}$ ions probably form from diferent distances between emitting $Eu^{3+}$ ions in the solid-state. When the distance between two emitting $Eu^{3+}$ ion sites is short, some interactions between $Eu^{3+}$–$Eu^{3+}$ centres take place, which could lead to two different chemical environment formations around $Eu^{3+}$ ions. X-ray structure analysis data of complex **15** confirm this assumption and show that the arrangement of the molecules in the crystal causes the formation of different distances between the emitting $Eu^{3+}$ ions. In turn, the second most important emission characteristic – PLQY – is in the range from 0.06 to 0.60. In the powder state, the effect of the complex structure on the emission efficiency is observed. Tetrakis complexes **14–17** show higher

luminescence efficiency than $Eu^{3+}$-Lewis base complexes due to a significantly larger photon absorption area increased by the fourth β, β'-triketonate ligand. It should also be concluded that the structure of tetrakis complexes due to the attached cation and four β,β'-triketonate ligands significantly better protects the $Eu^{3+}$ ion from the environment, which often causes the non-radiative transition of this ion to its ground state. A significant effect of cation size ($N^+Et_4$ or $N^+Bu_4$) on PLQY is observed for tetrakis complexes **14–17**. Tetrakis complex **14** with $N^+Et_4$ cation shows 3 times higher emission efficiency than its analogue **16** with $N^+Bu_4$ cation. Moreover, in the case of tetrakis complex **15** with $N^+Et_4$ cation PLQY is already 6 times higher than for compound **17** with $N^+Bu_4$ cation. This difference in PLQY is caused by the inclusion of cations with different lengths in the crystal lattice of the complex. Increasing the size of the tetraalkylammonium ion significantly reduces the luminescence efficiency and the luminescence lifetime of the complex. This is probably due to the fact that the larger cation is abler to influence the coordination sphere of the nearest complex $Eu^{3+}$ ions and, possibly for steric reasons, the complex molecules are located in the crystal lattice in an unfavourable conformation, which could lead to partial non-radiative deactivation of $Eu^{3+}$ ion in the excited state. The negative effect of increasing the size of the cation of the tetrakis complex on its luminescence properties has also been reported in the scientific literature [13].

The explanation for the fact that the obtained new β,β'-triketonate $Eu^{3+}$ complexes are characterized by average quantum yields and relatively short luminescence lifetimes can be found in the locations of their energy levels $S_1$ and $T_1$ and their relation to the Eu* excited resonance level (17 250 $cm^{-1}$). The energy levels $S_1$ and $T_1$ of compounds **1**, **2**, and **7–9** were calculated with the quantum chemistry program "ORCA" and are given in Table 1 (HAD $S_1$ = 31 025 $cm^{-1}$; $T_1$ = 27 653 $cm^{-1}$; HBD $S_1$ = 27 148 $cm^{-1}$; $T_1$ = 24 286 $cm^{-1}$). A simplified diagram of energy levels is given in Fig. 4 **(b)**. Two preconditions for an effective Antenna effect have been described in the literature: (1) the difference between ligand levels $S_1$–$T_1$ must be ~5000 $cm^{-1}$ (*Reinhoudt empirical rule*) [14]; (2) the difference between $T_1$–Eu* levels – 2500–5500 $cm^{-1}$ (*Latva empirical rule*) [15]. For HBID **8** and HMBID **9** both conditions are fulfilled and therefore PLQYs of their complexes are higher, while for compounds HAD **1** and HBD **2** the difference between $T_1$–Eu* levels is >5500 $cm^{-1}$, indicating of incomplete energy transfer between these levels and also explaining low PLQY of their complexes in solutions.

Due to average quantum yields of $Eu^{3+}$ complexes with 2-acyl-1,3-indanedione ligands **10–17** in the solid-state, the possibilities of forming their luminescent films were further investigated. $Eu^{3+}$ complexes are characterized by poor film formation, so it is best to form their polymer films. *N*-Polyvinylcarbazole (PVK) owing excellent hole transporting properties as well as good match between its triplet energy state and energy levels of most $Eu^{3+}$ β-diketone complexes is one of the most used host materials for metal organic complexes. PVK polymer films doped with 8 wt% of $Eu^{3+}$ complexes **10–17** were prepared by spin coating technique from THF solutions. The obtained films are characterized by relatively low PLQY (0.02–0.08), which is due to the discrepancy between the arrangement of polymer and complex energy levels. For efficient energy transfer from polymer to complex, the $T_1$ level of polymer must be above the levels $S_1$ and $T_1$ of used ligands. It is known from the literature

[16] that PVK $T_1$ = 24 440 $cm^{-1}$. As can be seen from Table 1, for the compounds HBID and HMBID the $S_1$ levels are located above the PVK $T_1$ level, but the $T_1$ levels are close to the polymer $T_1$ level. Thus, it can be concluded that the excitation energy from the PVK is only partially transferred to the excited energy levels of the ligands, which likely leads to low emission efficiency.

The obtained new $Eu^{3+}$ complexes with 2-acyl-1,3-indanedione ligands are characterized with pure red light emission ($\lambda_{em}$ = 611 nm), long Stokes shifts (161–203 nm), possibility to excite them with both UV and visible light, average PLQY, and several hundred μs long lifetime in the solid-state. Their PVK films, which are often used in OLED development, show low PLQY and should find application in different fields, such as polymer optical fiber or waveguides development, as complex **11**, **12**, and **14–17** poly(methyl methacrylate) (PMMA) films of complexes already show higher quantum efficiencies (PLQY 0.09–0.14).

## Synthesis and Characterization of Spectroscopic Properties of $Eu^{3+}$ Complexes With β-Diketone Ligands

The $Eu^{3+}$ complexes with asymmetric 2-acyl-1,3-indanedione and 2-acyldimedone derivative ligands, described in the previous section, did not show high enough PLQY for practical application in OLEDs, therefore, the research was continued on the use of 1,3-diketones in lanthanide complexes, some $Eu^{3+}$ complexes with more symmetrical β-diketones – ligands of 1,3-diphenylpropane-1,3-dione or dibenzoylmethane (HDBM) derivatives. HDBM derivatives are one of the most studied ligands of $Eu^{3+}$ complexes. This is due to the commercial availability, ease of synthesis, and the fact that such $Eu^{3+}$ complexes usually have intense luminescence [1]. Analogous to β,β'-triketones, the simplest $Eu^{3+}$-Lewis base **21**, **22** and tetrakis **24**, **25** complexes of unsubstituted HDBM **18** and 1-(4-methylphenyl)-3-phenylpropane-1,3-dione (Me-HDBM) **19** were first obtained (Fig. 5). It is known that substituents on HDBM phenyl rings can significantly alter the energy level distribution, properties, as well as the properties of its $Eu^{3+}$ complexes, therefore, a more complex HDBM derivative containing carbazole in the *para*-position of the phenyl ring was also obtained. Carbazole is often used as a substitute in the synthesis of β-diketones and secondary ligands due to its excellent properties as good solubility, hole transport properties and high thermal stability. Therefore, including carbazole in the structure of ligands for $Eu^{3+}$ complexes could impove their electrical properties. In the case of HDBM, compounds, where carbazole is attached to β-diketone phenyl ring *para*- position through 2- and 3- position, are reported. However, compounds, where carbazole has been attached through the nitrogen atom have not been studied. Therefore, the following compound was further synthesized – 1-[4-(9*H*-carbazol-9-yl)-phenyl]-3-phenylpropane-1,3-dione (CBZ-HDBM **20**) and its $Eu^{3+}$-Lewis base **23** and tetrakis **26** complexes, respectively.

The obtained complexes **21–26** are described and their structures are proved in the same way as in the case of 2-acyl-1,3-indanedionate complexes **10–17**. In addition, β-diketonate $Eu^{3+}$ complexes **21–26** show better solubility in organic solvents ($CHCl_3$, EtOH, THF) compared to β,β'-triketonate $Eu^{3+}$ complexes **10–17**.

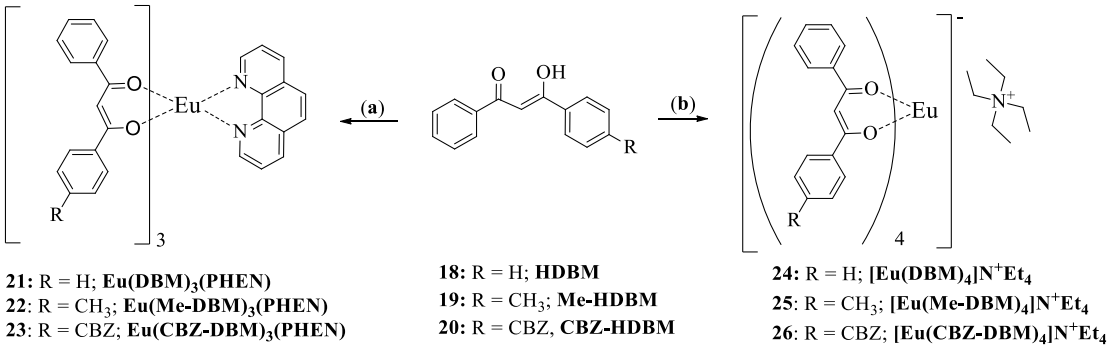


Fig. 5. Synthesis of $Eu^{3+}$-Lewis base **21–23** and tetrakis complexes **24–26** with derivatives of HDBM ligands.

(**a**) 10 % $NaOH/H_2O$, 1,10-phenanthroline, $EuCl_3 \cdot 6H_2O$; **(b)** 10 % $NaOH/H_2O$, $Et_4NBr$, $EuCl_3 \cdot 6H_2O$.

First, the absorption and emission properties of complexes **21–26** in $1.5 \cdot 10^{-5}$ M THF solutions were studied and compared. The absorption of complexes can be characterized by wide absorption bands in the near UV range (300–400 nm) (Fig. 6 **(a)**). The $\lambda_{abs}$ of complexes **21**, **22**, **24**, and **25** is in the range of 352–356 nm, while the introduction of CBZ into the *para*-position of HDBM molecules causes bathochromic shift of $\lambda_{abs}$ to 369–374 nm for complexes **23** and **26**. This absorption band is the charge transfer (CT) transition, because the CBZ-HDBM ligand contains both an electron-donating CBZ group and an electron-accepting carbonyl group. Quantum chemical calculations performed to obtain the optimized ground state geometry and HUMO/LUMO orbitals of compounds HDBM **18**, Me-HDBM **19**, and CBZ-HDBM **20** show, that compound **20** has a pronounced charge distribution between HOMO and LUMO orbitals (HOMO localized on the CBZ group, while LUMO on the DBM moiety), indicating to strong CT in this molecule. For compounds **18** and **19**, the HOMO/LUMO orbitals are located throughout the molecule.

The emission of complexes in $1.5 \cdot 10^{-5}$M THF solutions is very different. The β-diketonate $Eu^{3+}$ complexes **21**, **22**, **24**, and **25** show only the emission bands characteristic of the $Eu^{3+}$ ion (Fig. 6 **(b)**) with PLQY – 0.02–0.06 (Table 2). In the case of complexes **23** and **26**, the luminescence spectrum shows not only the metal ion emission. Due to the nature of CT, CBZ-HDBM has a pronounced blue emission with $\lambda_{em}$ at 478 nm (PLQY 0.26), which can also be observed in the luminescence spectra of complexes **23** and **26**. $Eu^{3+}$-Lewis base complex **23** in the luminescence spectrum shows dual emission – ligand emission in the range of 400–600 nm and several $Eu^{3+}$ ion emission bands in the range of 570–705 nm. The ratio of the intensities of the maximums of both bands (at 475 nm and 611 nm) is 1 : 2. Dual emission is often observed for $Eu^{3+}$ complexes containing ligands with electron donor and electron acceptor groups [17], and indicates that there is inefficient energy transfer between ligands and the central metal ion. The PLQY of complex **23** solution is 0.10 and its CIE coordinates are located in the cyan blue region ($x$ = 0.26; $y$ = 0.28) (Fig. 6 **(c)**). In the emission spectra of tetrakis complex **26** no characteristic $Eu^{3+}$ ion emission bands are observed and only the emission of the ligand is present. This could be explained by a known tendency of tetrakis complexes to dissociate into tris complexes and the corresponding tetraethylammonium salt,

which could greatly affect the emission intensity of the $Eu^{3+}$ ion and intensify the emission of ligand.

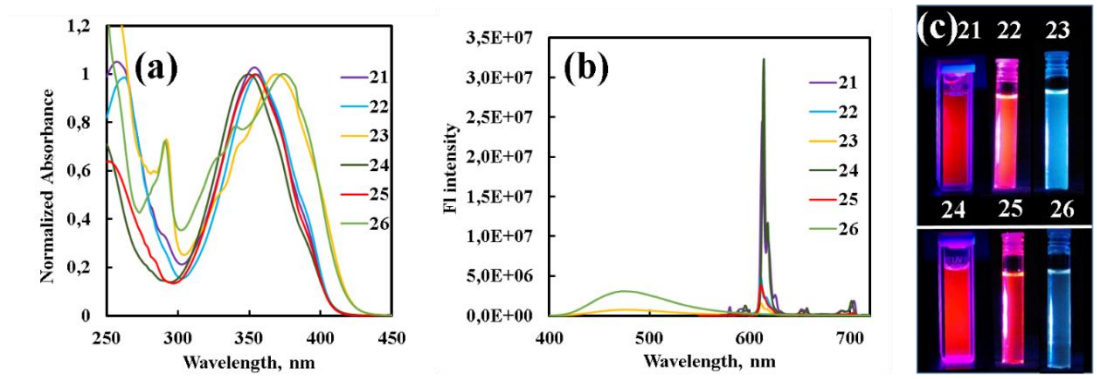


Fig. 6. **(a)** Absorption spectra of complexes **21–26** in THF solutions ($1.5 \cdot 10^{-5}$ M); **(b)** emission spectra of complexes **21–26** in THF solutions ($1.5 \cdot 10^{-5}$ M); (**c**) complexes **21–26** under UV ($\lambda_{exc}$ = 365 nm) light.

The solid-state emission of complexes was further investigated. As in the case of 2-acyl-1,3-indanedionate $Eu^{3+}$ complexes **10–17**, the emission in powders for **21–26** is much more efficient. For complexes with HDBM ligands **21**, **24** and with Me-HDBM **22**, **25** PLQY reaches even 0.53–0.75 (Table 2). Such a difference between emissions in solution and in the solid-state could indicate to aggregation enhanced emission (AEE). This effect was demonstrated for tetrakis complex **25** using a THF:hexane solvent system. By increasing the proportion of hexane in the solution, complex particles are formed, which effectively enhances the emission from the solution. To date, only one example of an $Eu^{3+}$ complex with an AEE effect is available in the scientific literature [18].

Table 2

Absolute Photoluminescence Quantum Yields of $Eu^{3+}$ Complexes **21–26** in $1.5 \cdot 10^{-5}$ M THF Solutions ($PLQY_{THF}$), Powder State ($PLQY_p$), 8 wt% PVK Films ($PLQY_{PVK}$) and Theoretically Calculated Excited Singlet ($S_1$) and Triplet ($T_1$) Energy Levels of β-Diketones

| Complex | $PLQY_{THF}$ | $PLQY_p$ | $PLQY_{PVK}$ | $S_1$, $cm^{-1}$ | $T_1$, $cm^{-1}$ |
|---|---|---|---|---|---|
| $Eu(DBM)_3(PHEN)$ **21** | 0.04 | 0.56 | 0.26 | 28 122 | 22 121 |
| $[Eu(DBM)_3]^-N^+Et_4$ **24** | 0.06 | 0.75 | 0.46 | | |
| $Eu(Me\text{-}DBM)_3(PHEN)$ **22** | 0.03 | 0.53 | 0.22 | 28 218 | 21 928 |
| $[Eu(Me\text{-}DBM)_3]^-N^+Et_4$ **25** | 0.02 | 0.57 | 0.18 | | |
| $Eu(CBZ\text{-}DBM)_3(PHEN)$ **23** | 0.10 | 0.09 | 0.07 | 21 929 | 20 973<br>18 416[b] |
| $[Eu(CBZ\text{-}DBM)_3]^-N^+Et_4$ **26** | 0.26[a] | 0.10 | 0.09 | | |

[a] Quantum yield of CBZ-HDBM.

[b] Experimentally obtained $T_1$ level of ligand CBZ-HDBM.

Complexes **23** and **26**, which exhibited dual emission or only ligand emission in the solution, show only $Eu^{3+}$ ion red light emission in the solid-state. This could be explained by the stronger bond between ligands and metal ions in the solid-state and the lack of ligand emission due to aggregation. PLQY in the solid-state does not grow as for complexes **21**, **22**, **24**, and **25** and are 0.09 (**23**) and 0.10 (**26**).

The luminescence lifetime of complexes **21–26** for the $^5D_0 \rightarrow {}^7F_2$ (611 nm) transition in the solid-state, as in the case of β,β'-triketonate $Eu^{3+}$ complexes **10–17**, is two-exponential ($\tau_1$ and $\tau_2$) and also indicates that there are two types of symmetry around $Eu^{3+}$ ion. It should be noted, that the luminescence lifetimes of complexes **22**, **23**, and **25** in THF solution were monoexponential, confirming the assumption that different emission kinetics in the solid-state result from the interaction of $Eu^{3+}$ ions, which is not observed in solution due to dilution.

The luminescent PVK films containing obtained complexes were further studied. The effect of the complex mass on the emission efficiency of the luminescent film was studied for complexes **21** and **24**. For each complex, four PVK films with different complex masses (1 wt%, 4 wt%, 8 wt% and 15 wt%) were obtained. The emission spectra of the PVK films of complex **21** are shown in Fig. 7. The emission intensity and PLQY increase with increasing complex mass in the film. Films with 1 wt% complex mass show low PVK emission in the range of 360 nm to 560 nm, which can be explained by the relatively large distance between the polymer chain and the complex. Larger distance between PVK and the complex leads to incomplete energy transfer between them. With increasing doping mass, polymer emission is no longer observed in the luminescence spectrum. PLQY of PVK films containing complex **21** are given in Fig. 7, but in the case of PVK films with complex **24** are following: 0.17, 0.30, 0.46, and 0.48 (1 wt%, 4 wt%, 8 wt%, and 15 wt%). From these data it is concluded that the most effective doping mass for $Eu^{3+}$ complexes is 8 wt%. Although even higher PLQYs were obtained with 15 wt%, this increase is insignificant compared to the fact that the mass of the complex in the film has to be increased almost by half compared to 8 wt%.

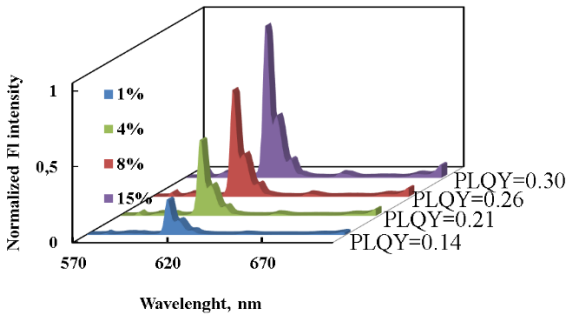


Fig. 7. Emission spectra of PVK films containing complex **21** (1 wt%, 4 wt%, 8 wt%, and 15 wt%).

PVK films of other complexes **22**, **23**, **25**, and **26** were obtained with 8 wt% doping mass. Complexes **22** and **25**, similar to complexes **21** and **24**, show average PLQYs of 0.22 and 0.18, while PVK films with complexes **23** and **26** containing CBZ-HDBM ligands show 0.07 and 0.09. As can be seen, PLQY of PVK films with complexes **21**, **22**, **24**, and **25** are about twice as low as in the powder samples, which could be explained by the AEE effect. In polymer films some molecules of the complex are encapsulated by the host material, while some form aggregates [19]. Decrease of PLQY of PVK films with complexes **21**, **22**, **24**, and **25** can be explained by the fact that only the aggregated fraction of the molecules emits light, while the emission of the isolated molecules is quenched. However, PVK films with

complexes **23** and **26** exhibit identical PLQY to solid-state samples. In this case, both fractions of the molecules are able to emit, hence no apparent change in PLQY is observed.

Taking into the consideration the previously discussed results, two OLEDs were prepared containing complex **22** as the emitter (Dr. phys. A.Vembris). The first OLED was prepared by dispersing complex **22** in PVK host with structure: [ITO/PEDOT:PSS(40 nm)/ PVK:**22**(50 nm)(10 wt%)/TPBi(20 nm)/LiF(1 nm)/Al(100 nm)]. The second OLED was prepared by using complex **22** in a host-free layer with structure: [ITO/PEDOT:PSS (40nm)/C1(50nm)/TPBi (20nm)/LiF(1nm)/Al(100nm)]. In the presence of the host material (first OLED) no characteristic $Eu^{3+}$ emission band was observed in the spectra of the device, as it emitted only blue light, associated with the electroluminescence of the charge transporting compounds. On the other hand, the host-free OLED showed only red $Eu^{3+}$ related emission. The lack of the host and the poor charge transporting characteristics of the compound determines that the device exhibits low maximal brightness of 10 cd/m$^2$, with current efficiency 0.004 cd/A and turn-on voltage 9 V. It was concluded, that the obtained $Eu^{3+}$ complexes do not exhibit valuable properties for optoelectronic devices, therefore application should be found in another field.

Calculated $S_1$ and $T_1$ levels of compounds HDBM, Me-DBM, CBZ-HDBM (Table 2) also give an explanation of observed spectroscopic properties of $Eu^{3+}$ complexes. For compounds HDBM and Me-HDBM both empirical rules discussed previously are fulfilled, because difference between $S_1$–$T_1$ are 6001 (HDBM) and 6290 cm$^{-1}$ (Me-HDBM), and between $T_1$–Eu* – 4871 cm$^{-1}$ (HDBM) and 4678 cm$^{-1}$ (Me-HDBM), therefore their energy transfer process is effective and PLQY is high. However, for compound CBZ-HDBM, carbazole introduction in the molecule has led to closely situated $S_1$ and $T_1$ levels (difference 3513 cm$^{-1}$) and $T_1$–Eu* levels (difference 1166 cm$^{-1}$), and in the result these complexes show inefficient energy transfer process and low PLQY.

## Synthesis and Characterization of Spectroscopic Properties of Derivatives of 2-Cinnamoyldimedones and 2-Cinnamoyl-1,3-Indandiones

In the previous sections described compounds 2-Acetyldimedone **1** and 2-acetyl-1,3-indandione **7**, which contain two electron withdrawing carbonyl groups and a reactive methylene group, are very perspective starting materials for synthesis of new chromophore and luminophore compounds. Relatively low amount of scientific publications is dedicated to investigation of reactions between these compounds and electrophilic reagents, for example, aromatic aldehydes, and forming products with extending conjugation system – derivatives of 5,5-dimethyl-2-[(2*E*)-3-phenyl-1-oxo-2-propen-1-yl]-cyclohexane-1,3-dione or 2-cinnamoyldimedone and 2-[(2*E*)-3-phenyl-1-oxo-2-propen-1-yl]-1*H*-indene-1,3(2*H*)-dione or 2-cinnamoyl-1,3-indandione [6]–[8]. If the aromatic aldehyde used in synthesis reaction contains donor group (D), then obtained 2-cinnamoyl-β-diketone has acceptor group A (dimedone or 1,3-indandione), D group, and π-conjugated system between them and therefore are categorized as D-π-A type compound. These compounds have great absorption and emission properties and they have found a wide application range in

development of photoelements and OLEDs, in medicine for fluorescent markers, etc. The main advantage of compounds with D-π-A structure is the variety of donor, acceptor and π-bridge groups, which allows to adjust the fluorescent material desirable properties, for example emission colour.

Within the framework of the dissertation, five new derivatives of 2-cinnamoyldimedone **27–31** and five new derivatives of 2-cinnamoyl-1,3-indanedione **32–36** were obtained in the condensation reactions between compounds **1** or **7** and aromatic aldehydes, which contain strong *N*-alkyl or *N*-arylamino donor substituents in the *para*-position of the phenyl ring. Further treatment of some of the obtained 2-cinnamoyl-1,3-indanedione derivatives **32–34** with dimethyl sulfate gave additional derivatives of 2-cinnamoyl-1,3-indanedione *O*-methyl ethers **37–39** (Fig. 8). Various acceptor (dimedone, 1,3-indanedione), donor (*N*,*N*-dimethylamino ($NMe_2$), *N*,*N*-diphenylamino ($NPh_2$), julolidyl and *N*,*N*-dibiphenylamino ($N(BPh)_2$) groups, and π-bridge length (1-hydroxyallylidene, 1-hydroxypenta-2,4-ylidene) effect on the properties of compounds were investigated using the obtained new D-π-A compounds **27–39**. Furthermore, by comparing 2-cinnamoyl-1,3-indanedione derivatives **32–34** and their *O*-methyl ethers **37–39**, it is possible to determine the effect of hydroxyl group, which forms a strong hydrogen bond with carbonyl group of 1,3-indandione ring, on the properties of compounds.

The structures of the obtained compounds **27–39** have been proved by $^{1}$H-NMR, $^{13}$C-NMR and FT-IR spectra, elemental analyses, and mass spectral data. Unquestionable proof that compounds **27–36** exist in the exocyclic enol form, which is stabilized by a strong intramolecular hydrogen bond, was obtained by X-ray structure analysis of crystals of compounds **27** and **34** (Dr. phys. S. Belyakov). The obtained data show that both compounds have an intramolecular hydrogen bond between the carbonyl group of the ring (dimedone, 1,3-indanedione) and the hydrogen atom of the enol group in the allylidene moiety with lengths of 2.386 (7) Å (**27**) and 1.66 (8) Å (**34**). The obtained bond lengths and angles between the atoms in the β,β'-triketone fragment also indicate that there is a formation of a conjugated π-electron system, which is stabilized by an intramolecular hydrogen bond. In turn, quantum chemical calculations for compounds **27–39** (optimized ground state geometry) show, that compounds with *N*,*N*-alkylamino substituents (**27**, **29**, **31**, **32**, **34**, **36**, **37**, and **39**) are completely planar, while derivatives **28**, **30**, **33**, **35**, and **38** show out-of-plane twisting of phenyl and biphenyl groups.

The $^{1}$H-NMR and $^{13}$C-NMR spectra of *O*-methyl ethers **37–39** show only two differences from the spectra of 2-cinnamoyl-1,3-indanedione derivatives **32–34**: **(1)** the $-CH_3$ signal (4.35 ppm) has replaced -OH group signal (~13.20 ppm); **(2)** carbon atoms of the 1,3-indanedione benzene ring (C8 and C9; C4 and C7; C5 and C6) show the same chemical shifts in the $^{13}$C-NMR spectra, indicating the same chemical environment for these atoms (in the case of 2-cinnamoyl-1,3-indanedione derivatives **32–34**, the intramolecular hydrogen bond between the hydrogen atom of the enol group and the oxygen atom of the carbonyl group of the 1,3-indanedione ring causes different chemical shifts for these atom pairs) – methylation has made the acceptor part of the molecule more symmetrical.

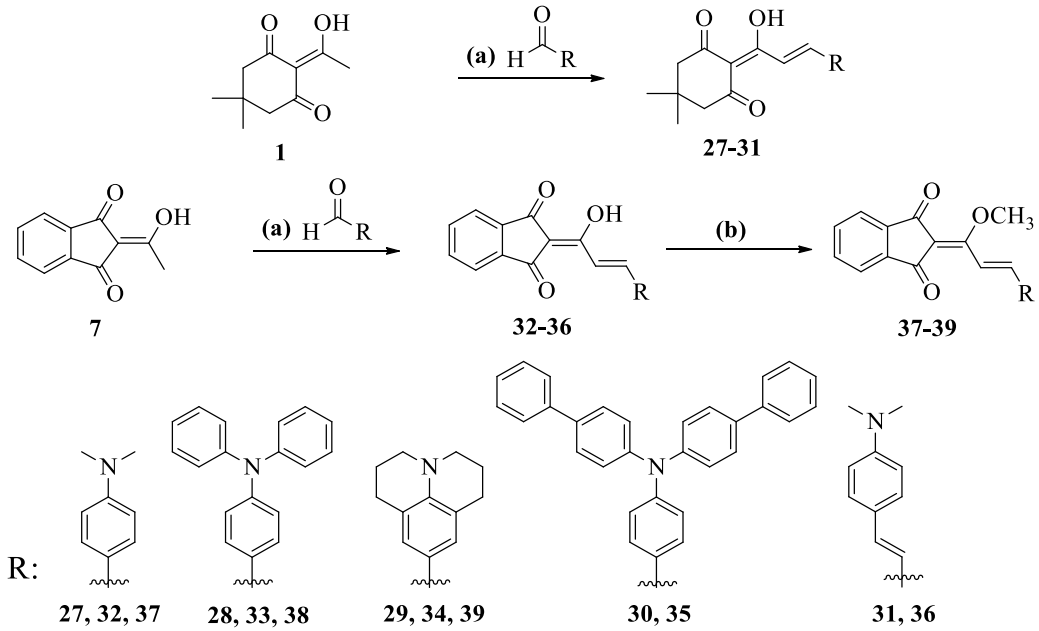


Fig. 8. Synthesis of D-π-A compounds **27–39** on the bases of 2-acetyldimedone **1** and 2-acetyl-1,3-indandione **7**.

(**a**) (1) piperidine, 100 °C, 4 h; (2) ethanol, 80 °C, 0.5 h; (**b**) dimethyl sulfate, $K_2CO_3$, acetone, 56 °C.

The absorption and emission properties of the newly obtained D-π-A compounds were studied in solvents with different polarity (toluene, THF, $CHCl_3$, MeCN, MeOH), and Table 3 gives the spectroscopic characteristics of compounds **27–39** in $1.5 \cdot 10^{-5}$ M $CHCl_3$ solutions, as well as PLQY in toluene, $CHCl_3$, and MeOH.

Table 3

Absorption, Emission Spectra Maxima in $1.5 \cdot 10^{-5}$ M $CHCl_3$ Solutions and PLQY in $1.5 \cdot 10^{-5}$ M $CHCl_3$, Toluene and MeOH Solutions, Oxidation ($E_{ox}$) and Reduction ($E_{red}$) Potentials of Cyclic Voltammetry, Calculated HOMO/LUMO Energy Levels and HOMO–LUMO Gaps ($E_g^{DFT}$) of D-π-A Compounds **27–39**

| Compound | $\lambda_{abs}$, nm | $\lambda_{em}$, nm | PLQY | | | $E_{ox}$, V | $E_{red}$, V | HOMO, eV | LUMO, eV | $E_g^{DFT}$, eV[b] |
|---|---|---|---|---|---|---|---|---|---|---|
| | | | Toluene | $CHCl_3$ | MeOH | | | | | |
| **27** | 467 | 548 | 0.05 | 0.15 | 0.01 | 0.81 | –1.32 | –5.38 | –2.16 | 3.22 |
| **28** | 466 | 612 | 0.40 | 0.78 | <0.01 | 1.07 | –1.19 | –5.33 | –2.37 | 2.96 |
| **29** | 509 | 577 | 0.31 | 0.36 | <0.01 | 0.61 | –1.36 | –5.16 | –2.11 | 3.05 |
| **30** | 476 | 654 | 0.79 | 0.16 | –[a] | 0.96 | –1.18 | –5.26 | –2.40 | 2.86 |
| **31** | 487 | 624 | 0.05 | 0.15 | 0.05 | 0.67 | –1.15 | –5.21 | –2.34 | 2.87 |
| **32** | 503 | 566 | 0.12 | 0.03 | <0.01 | 0.80 | –1.17 | –5.37 | –2.28 | 3.09 |
| **33** | 502 | 621 | 0.52 | 0.76 | –[a] | 1.05 | –1.07 | –5.34 | –2.47 | 2.87 |
| **34** | 540 | 595 | 0.15 | <0.01 | –[a] | 0.60 | –1.21 | –5.11 | –2.19 | 2.92 |
| **35** | 512 | 663 | 0.93 | 0.21 | –[a] | 0.98 | –1.04 | –5.27 | –2.50 | 2.77 |
| **36** | 520 | 647 | 0.12 | 0.25 | <0.01 | 0.66 | –1.04 | –5.22 | –2.43 | 2.79 |
| **37** | 514 | 597 | <0.01 | 0.02 | <0.01 | 0.77 | –1.11 | –5.26 | –2.25 | 3.01 |
| **38** | 509 | 647 | 0.01 | 0.06 | <0.01 | 0.97 | –0.97 | –5.27 | –2.57 | 2.70 |
| **39** | 562 | 634 | 0.02 | 0.32 | 0.01 | 0.57 | –1.14 | –5.02 | –2.30 | 2.73 |

[a] Insoluble.

[b] $E_g^{DFT}$ = HOMO–LUMO.

The derivatives of 2-cinnamoyldimedone **27–31** and 2-cinnamoyl-1,3-indanedione **32–36** show intense visible light absorption with wavelength maximums ($\lambda_{abs}$) ranging from 466 to 540 nm. These broad absorption bands are induced by CT in the molecule between D and A groups ($\pi$(D) $\rightarrow$ $\pi^*$(A)). The absorption bands of 2-cinnamoyl-1,3-indanedione *O*-methyl ethers **37–39** are bathochromic shifted by 7–22 nm compared to their unmethylated analogues **32–34** due to the presence of a weak donor group $–OCH_3$ in the $\pi$-bridge, which enhances charge distribution between the 1,3-indanedione ring and the amino donor group in the cinnamoyl moiety. All newly obtained compounds **27–39** are fluorescent in $CHCl_3$ solutions and their emission spectra are in a very wide spectral range, from the green to the red light region (Fig. 9) with $\lambda_{em}$ in the range of 548 nm to 647 nm.

The effect of the structure of derivatives of 2-cinnamoyldimedone and 2-cinnamoyl-1,3-indanedione on the location of $\lambda_{abs}$ and $\lambda_{em}$ is as follows.

**1.** Acceptor groups (dimedone or 1,3-indanedione) have a greater effect on the location of the absorption band. For compounds with 1,3-indanedione moiety, which is considered to be a stronger acceptor group due to its aromatic structure, a shift of $\lambda_{abs}$ and $\lambda_{em}$ to longer wavelength is observed. Comparing the series of both derivatives (**27/32**, **28/32**, **29/34**, **30/35**, **31/36**) it can be seen that the peak of the CT band from 466–509 nm (dimedone derivatives **27**–**31**) is shifted to 502–540 nm (1,3-indanedione derivatives **32**–**36**). $\lambda_{em}$ of the emission spectrum is shifted only by 9–23 nm switching from dimedone to 1,3-indanedione derivatives.

**2.** In contrast, amino donor groups show a small effect on $\lambda_{abs}$ and a strong effect on $\lambda_{em}$. Compounds containing $NMe_2$ and $NPh_2$ groups show the same $\lambda_{abs}$. It should be noted, that for the $NPh_2$ group, the undivided electron pair of the nitrogen atom is conjugated to the $\pi$-electrons of the phenyl group, which is more likely to reduce the strength of this donor group. Furthermore, change of the donor unit from $NPh_2$ to $N(BPh)_2$ results in bathochromic shift of $\lambda_{abs}$ (+10 nm), which can be explained by looking at their optimized ground state geometry. Quantum chemical calculations show that compounds with $N(BPh)_2$ group (**30** (–32.1°), **35** (–31.2 °)) show greater out-of-plane twisting of phenyl groups than compounds with $NPh_2$ group (**28** (–30.1 °), **33** (–30.3 °)), therefore it is less planar. Due to the higher twisting, nitrogen atom lone pair conjugation with biphenyl group is weaker, which results in enhanced donor character for $N(BPh)_2$. Finally, the julolidyl substituent significantly shifts the CT absorption bands of chromophores **29** and **34** to longer waves with lower energy. It should be noted that D-$\pi$-A compounds with a julolidyl substituent described in the literature always show bathochromic shift of absorption spectra compared to analogous compounds with other amino groups, and this observation is explained by the donor nature of the julolidyl group, which makes the molecule more polarizable [20]. In contrast, looking at the emission spectra of compounds **27**–**36**, the donor groups can be ranked in the following order according to their effect on $\lambda_{em}$ (bathochromic shift): $NMe_2$ < julolidyl < $NPh_2$ < $N(BPh)_2$. Due to their structural effect on $\lambda_{em}$, all synthesized compounds based on their amino donor structures can be divided into two groups – compounds owing amino donors with alkyl chains (julolidyl, $NMe_2$) and phenyl groups ($N(BPh)_2$, $NPh_2$). There is essential difference in the Stokes shifts ($\Delta\lambda$) for these groups. The first group shows smaller $\Delta\lambda$ (in the range from 1466–2779 $cm^{-1}$

for 1,3-indandione derivatives, and 2005–4273 $cm^{-1}$ for dimedone derivatives) than the second group (3715–7487 $cm^{-1}$ for dimedone derivatives and 2434–4815 $cm^{-1}$ for 1,3-indandione derivatives). The smallest $\Delta\lambda$ was obtained for the julolidyl group containing compounds **29** and **34** and can be explained by a similar dipole moment from ground and excited state for these dyes [21]. Observed relatively large $\Delta\lambda$ for compounds **28**, **30**, **33**, and **35** indicates that after excitation these molecules undergo some structural reorientation, for example, excited state intramolecular proton transfer, which is common for compounds with strong intramolecular hydrogen bond in the molecules [22].

**3.** The π-bridge prolongation between D and A groups (**27** → **31** and **32** → **36**) as expected shifts both the absorption (17 and 20 nm) and emission band to longer wavelength (76 and 81 nm) due to the longer conjugate system.

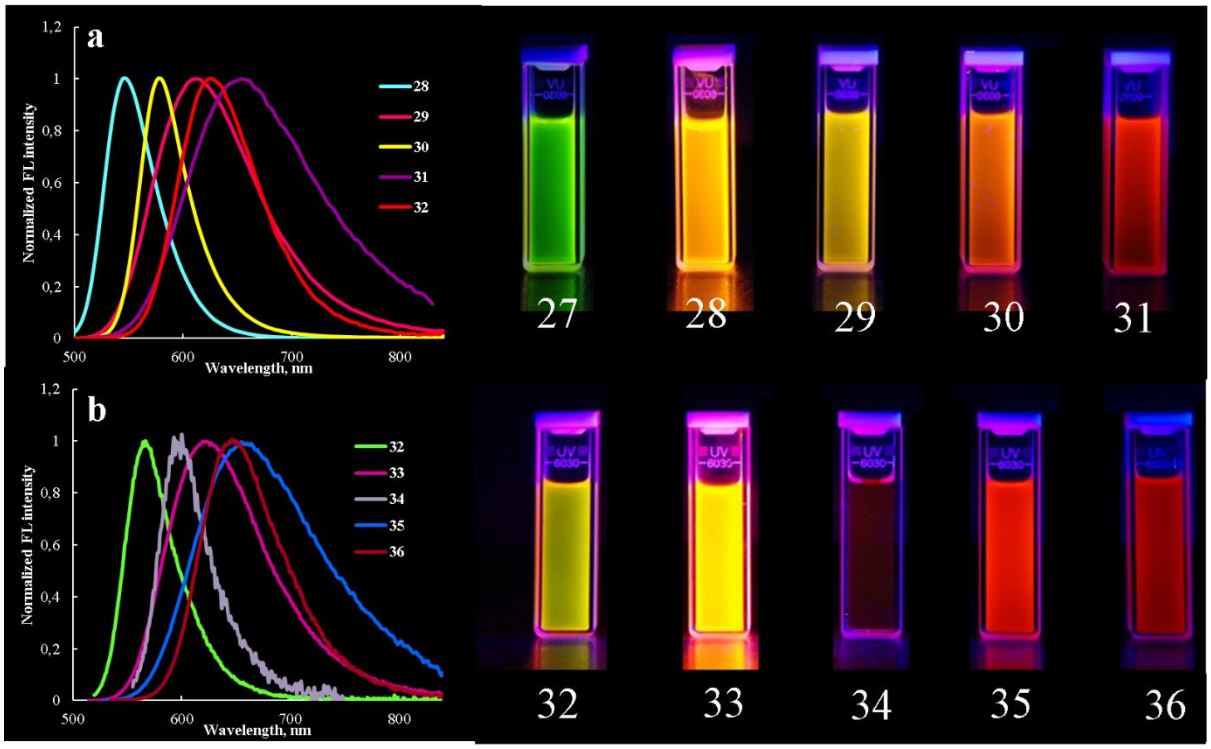


Fig. 9. **(a)** Emission spectra and emission under UV light of dimedone derivatives **27**–**31** in $CHCl_3$ solutions; **(b)** Emission spectra and emission under UV light of 1,3-indandione derivatives **32**–**36** in $CHCl_3$ solutions.

Solvatochromism studies show, that the absorption of compounds **27**–**39** is only lightly affected by the change in solvent polarity and that $\lambda_{abs}$ changes only by 1–12 nm. This result leads to the conclusion that the ground state of the new D-π-A compounds is not affected by the change in environmental polarity. In contrast, the emission properties of the compounds are significantly influenced by the polarity of the solvent. All compounds show a strong positive solvatofluorochromism and change of $\lambda_{em}$ from 24 to 126 nm, when switching from non-polar toluene to polar MeOH. The largest bathochromic shift of $\lambda_{em}$ is observed for compounds with bulky and out-of-plane twisted diphenyl and bidiphenyl substituents (94–126 nm). This observation can be explained by the fact that a strong sensitivity to environmental

polarity is observed directly for compounds that have a strong charge transfer from D to A group in the excited state [23].

To determine the emission efficiency of the obtained compounds, PLQY was measured in different solvents (Table 3). By increasing the polarity of the solvent (toluene, $CHCl_3 \rightarrow$ MeOH), PLQY decreases rapidly for all compounds **27**–**39**. In this case, it should be taken into account that in polar solvents the emission band are significantly shifted to longer waves, that is, the polar solvent lowers the energy of the excited state of the compounds [23]. It is possible that this reduced excited state is non-fluorescent or that the non-radiative transition of the molecules to the ground state is enhanced as a result of the compound-solvent molecule interaction. From the literature on D-π-A type compounds it can be concluded that mostly such compounds show a disappearance or decrease of fluorescence efficiency in polar solvents, for example, in the case of cinnamoylpyrone derivatives [9]. In series of derivatives of 2-cinnamoyldimedone **27**–**31** and 2-cinnamoyl-1,3-indanedione **32**–**36**, the highest PLQYs were obtained in toluene. Compounds **28**, **30**, **33**, and **35** with phenyl substituents at the nitrogen atom show high PLQY (0.40–0.93), while compounds with alkyl substituents, as expected, have significantly lower yields (0.05–0.31). Also, in the non-polar $CHCl_3$, PLQY is sufficiently high (0.15–0.78) except for 1,3-indanedione derivatives **32** and **34**, which show low intensity emission in this solvent (0.03, <0.01). In turn, 2-cinnamoyl-1,3-indanedione *O*-methyl ethers **37**–**39** show low PLQY in toluene (<0.01–0.02) and $CHCl_3$ (0.02-0.06), except for compound **39** with a julolidyl substituent, which shows a medium PLQY – 0.32 in $CHCl_3$. Apparently, methylation of the hydroxyl group of 2-cinnamoyl-1,3-indanedione derivatives and disruption of a strong intramolecular hydrogen bond lead to a pronounced decrease in the emission efficiency.

The ground state geometry of compounds **27**–**39** and HOMO and LUMO orbital energies (Table 3), and location (Fig. 10) were determined with quantum chemistry program "ORCA". For synthesized compounds **27**–**39**, the HOMO orbital is located on the donor and the cinnamoyl moiety, while the LUMO orbital is located in the acceptor moiety and the cinnamoyl moiety. This arrangement of orbitals causes significant CT for the given compounds. The calculated energies of HOMO and LUMO levels show that again there is a difference between compounds with different sizes of donor groups. For compounds **27**, **29**, **32**, and **34** with $NMe_2$ and julolidyl substituents, the HOMO and LUMO orbital energy gaps ($E_g^{DFT}$) are wider (2.90–3.22 eV) than for the compounds with $NPh_2$ and $N(BPh)_2$ groups (2.77–2.96 eV) and indicate, that the latter have a stronger CT in the molecule, which also leads to higher quantum efficiency. According to the obtained $E_g^{DFT}$ the donor groups can be ranked in order of strength in the following order (a narrower $E_g^{DFT}$ gap correspond to stronger donor group): $NMe_2$ < julolidyl < $NPh_2$ < $N(BPh)_2$, which corresponds to the sequence by $\lambda_{em}$. The prolongation of the π-bridge between D and A groups (**27** → **31** and **32** → **36**) causes a marked decrease in $E_g^{DFT}$ (3.22 eV → 2.87 eV; 3.09 eV → 2.79 eV). The calculated HOMO orbital energies for *O*-methyl ethers **37**–**39** are higher and the LUMO is lower than that of the corresponding 2-cinnamoyl-1,3-indanedione derivatives **32**–**36**, resulting in narrower $E_g^{DFT}$ gaps. It is possible that the decrease in the energy difference between HOMO and LUMO levels is the reason why *O*-methyl ether **39** has a medium PLQY (0.32), while the

unmethylated derivative **34** has a very low PLQY (<0.01) in $CHCl_3$ solutions. In contrast, no changes in ground state geometry and HOMO and LUMO orbital arrangement were observed between the 2-cinnamoyl-1,3-indanedione derivative **34** and its *O*-methyl ether **39** (Fig. 10).

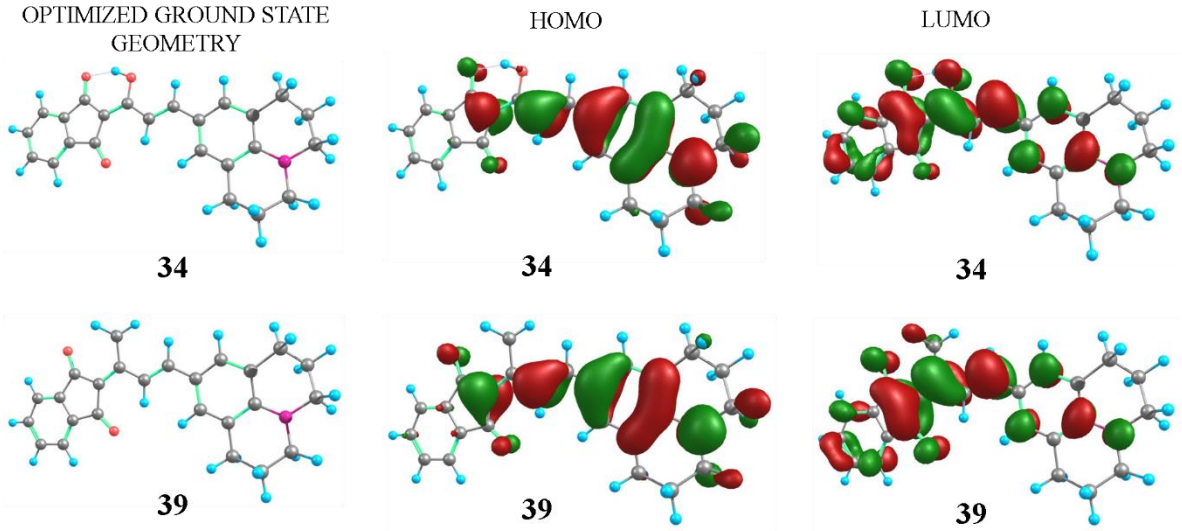


Fig. 10. Optimized ground state geometry and HOMO and LUMO orbitals of derivative of 2-cinnamoyl-1,3-indanedione **34** un its *O*-methyl ether **39**.

Further, the electrochemical properties of compounds **27**–**39** in MeCN solutions ($1.5 \cdot 10^{-5}$ M) were studied by cyclic voltammetry and electrochemical oxidation, and reduction potentials ($E_{ox}$, $E_{red}$) are given in Table 3 (Dr. chem. B. Turovska). All compounds in MeCN solutions show electrochemically irreversible cathodic reduction and anodic oxidation. Examining the obtained potentials, it can be concluded that $E_{ox}$ is mainly affected by the donor groups of compounds, because the change of acceptor groups from dimedone to 1,3-indanedione (**27**/**32**, **28**/**33**, **29**/**34**, **30**/**35**, **31**/**36**) causes only a small change in the potential value by 0.01–0.02 V. The obtained $E_{ox}$ values show that the donor groups according to the substituents at the nitrogen atom can again be divided into two groups – with alkyl substituents ($NMe_2$ and julolidyl substituent) and phenyl substituents ($NPh_2$ and $N(BPh)_2$). For compounds with alkyl substituents (**27**, **29**, **31**, **32**, **34**, **36**, **37**, **39**) $E_{ox}$ is in the range from 0.57 V to 0.81 V, while for compounds with phenyl substituents – 0.96–1.07 V. The extension of the π-bridge between the donor and acceptor parts (**27** → **31**; **32** → **36**) leads to an increase of the $E_{ox}$ value by 0.14 V. In contrast, the electrochemical reduction potential $E_{red}$ is more dependent on the acceptor group and when switching from dimedone derivatives (**27**–**31**) to 1,3-indanedione derivatives (**32**–**39**), a decrease in potential of 0.11–0.22 V is observed.

Thermal properties were studied for derivatives of 2-cinnamoyldimedone **27**–**31** and 2-cinnamoyl-1,3-indanedione **32**–**36**. Thermograms were obtained by heating samples from 30–550 °C at a rate of 10 °C /min in an $N_2$ atmosphere (Dr. chem. K. Lazdoviča) and show that all 10 compounds are thermally stable up to 200 °C and their $T_{5\%}$ ( $T_{5\%}$ – temperature at which the mass of the compound has decreased by 5 %) is in the range of 216–290 °C.

Thermal properties are also significantly influenced by the structure of the donor group. Compounds with alkyl substituents at the nitrogen atom show lower $T_{5\%}$ (216–238 °C) than the compounds with spatially larger $NPh_2$ and $N(BPh)_2$ groups (271–290 °C) in the cinnamoyl moiety. The high thermal stability of compounds **30** and **35** with $N(BPh)_2$ substituents can be explained by their high molecular weight and additional π-π interaction and location.

From the structure-property studies of derivatives of 2-cinnamoyldimedone and 2-cinnamoyl-1,3-indanedione **27**–**39**, it can be concluded that the properties of this type of compounds are most influenced by the structure of the donor group. The use of large out-of-plane twisted diphenyl and bidiphenylamino groups, which make the structure of the compounds (**28**, **30**, **33**, and **35**) non-planar, leads to new compounds with batochrome shifted emission ($\lambda_{em}$ > 612 nm), unusually large Stokes shifts (3715–7487 $cm^{-1}$ for dimedone derivatives and 2434–4815 $cm^{-1}$ for 1,3-indanedione derivatives) and high PLQY (0.16–0.93) in non-polar solvents, narrower HOMO–LUMO gaps (2.77–2.96 eV), and increased thermal stability ($T_{5\%}$ > 270 °C) compared to compounds containing *N*-alkyl substituents (**27**, **29**, **32**, and **34**). Potential for use in OLEDs is shown by compound **28** with a dimedone ring as acceptor, *N*,*N*-diphenylamino donor group and 1-hydroxyallylidene as π-bridge. The emission of this compound in $CHCl_3$ can be characterized as follows $\lambda_{abs}$ = 466 nm, $\lambda_{em}$ = 612 nm (PLQY = 0.78), $\Delta\lambda$ = 5119 $cm^{-1}$.

# CONCLUSIONS

1. It is possible to obtain two different types of effectively luminescent compounds on the bases of β,β'-triketones – derivatives of 2-acyl-1,3-indanedione and 2-acyldimedone: (1) europium trivalent ion ($Eu^{3+}$) complexes by using β,β'-triketonates as ligands; (2) D-π-A compounds as a result of condensation reactions between β,β'-triketone and donor group containing benzaldehyde derivatives.
2. The emission properties of 2-acyl-1,3-indanedione $Eu^{3+}$ complexes in the solid-state are significantly influenced by the structure of the complexes: (1) tetrakis complexes with the general formula $[Eu(\beta,\beta'\text{-triketonate})_4]^-$ show higher PLQY and emission lifetimes than analogous $Eu^{3+}$-Lewis base complexes ($Eu(\beta,\beta'\text{-triketonate})_3(PHEN)$) due to a significantly larger photon absorption area increased by the fourth β,β'-triketonate ligand; (2) a study of the effect of cation size of tetrakis complexes on emission properties shows, that PLQY is 3–6 times higher and their emission lifetimes are 2 times longer in the case of a shorter $N^+Et_4$ cation than in the case of a longer $N^+Bu_4$ cation.
3. $Eu^{3+}$ complexes with 2-acyldimedone ligands show low PLQY in solutions due to the arrangement of the excited state energy levels of their ligands against the $Eu^{3+}$ ion resonance level. For 2-acildimedone derivatives, the difference between the excited triplet level and the $Eu^{3+}$ ion resonance level is too large (>7000 $cm^{-1}$) for efficient energy transfer in the complex.
4. Comparing PLQY in the solid-state and PVK films of the β-diketonate (ligands of dibenzoylmethane derivatives) $Eu^{3+}$ complexes with the data of β,β'-triketonate $Eu^{3+}$ complexes, it is observed that for the first, PLQY in the film decreases only 2 times, while PLQY for the latter ones can decrease from 3–7 times. Such data point to dibenzoylmethane derivatives as more efficient ligands for $Eu^{3+}$ complexes.
5. $Eu^{3+}$ complexes with dibenzoylmethane and 4-methyldibenzoylmethane ligands show 5–7 times higher PLQY in the solid-state than the complexes containing carbazole substituted dibenzoylmethane ligands. The increase in emission efficiency is caused by the aggregation enhanced emission effect for these complexes.
6. OLEDs manufactured using an $Eu^{3+}$ complex with 4-methyldibenzoylmethane ligands as an emitter show weak electroluminescence due to the fact that the complex does not have charge transfer properties, which indicates that the synthesized $Eu^{3+}$ complexes do not have the properties required for OLED.
7. The spectroscopic, electrochemical and thermal properties of derivatives of 2-cinnamoyldimedone and 2-cinnamoyl-1,3-indanedione are strongly influenced by the structure of the selected donor group. The large out-of-plane twisted *N*,*N*-diphenylamino ($NPh_2$) and *N*,*N*-bidiphenylamino groups ($N(BPh)_2$), which make the structure of the compounds non-planar, lead to batchochrome-shifted emissions ($\lambda_{em}$ > 612 nm), unusually large Stokes shifts (2434–7487 $cm^{-1}$) and high PLQY (0.16–0.93) in non-polar solvents, narrower HOMO–LUMO gaps (2.77–2.96 eV), and increased thermal stability ($T_{5\%}$ > 270 °C) compared to planar compounds containing *N*,*N*-alkylamino- substituents.

8. A comparison of the properties of derivatives of 2-cinnamoyl-1,3-indanedione and their *O*-methyl ethers shows that the emission efficiency of the compounds obtained by methylation decreases rapidly in non-polar solvents, while no significant changes are observed for the other properties.
9. Extension of the π-bridge by two carbon atoms between the donor and acceptor groups in the series of derivatives of 2-cinnamoyldimedone and 2-cinnamoyl-1,3-indanedione leads to a bathochromic shift of the absorption (17–20 nm) and emission bands (76–81 nm), higher PLQY and narrower HOMO–LUMO gaps (3.22 eV; 3.09 eV → 2.87 eV; 2.79 eV).

# REFERENCES


[1] Binnemans K. Lanthanide-based luminescent hybrid materials. *Chem. Rev*., **2009**, *109*, 4283–4374.

[2] Pluskota R, Koba M. Indandione and its derivatives - chemical compounds with high biological potential. *Mini Rev. Med. Chem.*, **2018**, *18* (15), 1321–1330.

[3] Ahmedova A, Mantarevay V, Enchev V, Mitewa V. 2-Acetylindan-1,3-dione and its $Cu^{2+}$ and $Zn^{2+}$ complexes as promising sunscreen agents. *Int. J. Cosmet. Sci.*, **2002**, *24*, 103–110.

[4] Teotonio EES, Brito HF, Cremona M, Quirino WG., Legnani C, Felinto MCFC. Novel electroluminescent devices containing $Eu^{3+}$-(2-acyl-1,3-indandionate) complexes with TPPO ligand. *Opt. Mater.*, **2009**, *32*, 345–349.

[5] Teotonio EES, Brito HF, Viertler H, Faustino WM, Malta OL, de Sá GF. Synthesis and luminescent properties of $Eu^{3+}$-complexes with 2-acyl-1,3-indandionates (ACIND) and TPPO ligands: the first X-ray structure of Eu–ACIND complex. *Polyhedron*, **2006**, *25*, 3488–3494.

[6] Ahmedova A, Marinova P, Pavlovic G, Guncheva M, Stoyanov N, Mitewa M. Structure and properties of a series of 2-cinnamoyl-1,3-indandiones and their metal complexes. *J. Iran. Chem. Soc*., **2012**, *9*, 297–306.

[7] Ahmedova A, Atanasov V, Marinova P, Stoyanov N, Mitewa M. Synthesis, characterization and spectroscopic properties of some 2-substituted 1,3-indandiones and their metal complexes. *Cent. Eur. J. Chem.*, **2009**, *7*, 429–438.

[8] Ahmedova A, Pavlovic G, Zhiryakova D, Šišak D, Stoyanov N, Springborg M, Mitewa M. Experimental and theoretical study on the structure and optical properties of 2-acyl-1,3-indandiones – Conformational effects. *J. Mol. Struct.*, **2010**, *981*, 10–20.

[9] Tykhanov DA, Serikova II, Yaremenko FG, Roshal AD. Structure and spectal properties of cinnamoyl pyrones and their vinylogs. *Cent. Eur. J. Chem*., **2010**, *8*(2), 347–355.

[10] Li W, Yan P, Hou G, Li H, Li G. Efficient red emission from PMMA films doped with 5,6-DTFI europium(III) complexes: synthesis, structure and photophysical properties. *Dalton. Trans.*, **2013**, *42*, 11537–11547.

[11] Accorsi G, Listorti A, Yoosaf K, Armaroli N. 1,10-Phenanthrolines: versatile building blocks for luminescent molecules, materials and metal complexes. *Chem. Soc. Rev*., **2009**, *38*, 1690–1700.

[12] Adati RD, Lima SAM, Davolos MR, Jafelicci M. A new β-diketone complex with high color purity, *J. Alloys Compd.*, **2006**, *418*, 222–225.

[13] Mech A, Karbowiak M, Görller-Walrand C, Van Deun R. The luminescence properties of three tetrakis dibenzoylmethane europium(III) complexes with different counter ions. *J. Alloys Compd.*, **2008**, *451*, 215–219.

[14] Steemers FJ, Verboom W, Reinhoudt DN, Van der Tal JEB, Verhoeven JW. New sensitizer-modified calix[4]arenes enabling near-UV Excitation of complexed luminescent lanthanide ions. *J. Am. Chem. Soc*., **1995**, *117*, 9408–9414.

[15] Latva M, Takalo H, Mukkala VM, Matachescu C, Rodriguez-Ubis JC, Kankare J. Correlation between the lowest triplet state energy level of the ligand and lanthanide(II1) luminescence quantum yield. *J. Lumin.*, **1997**, *75*, 149–169.

[16] Pina J, Seixas de Melo J, Burrows HD, Monkman AP, Navaratnam S. On the triplet state of poly(*N*-vinylcarbazole). *Chem. Phys. Lett.*, **2004**, *400*, 441–445.

[17] Li L, Liu Y, Guo H, Wang Y, Cao Y, Liang A, Tan H, Qi H, Zhu M, Zhu W. Synthesis, optophysical and electrochemical properties of bipolar-transporting europium(III) complexes with carbazole and oxadiazole units. *Tetrahedron*, **2010**, *66*, 7411–7417.

[18] Zhu Z, Song B, Yuan J, Yang C. Enabling the triplet of tetraphenylethene to sensitize the excited state of europium(III) for protein detection and time- resolved luminescence imaging. *Adv. Sci.*, **2016**, *3*, 1600146.

[19] Xu X, Yang X , Zhao J, Zhou G, Wong W-Y. Recent advances in solution-processible dendrimers for highly efficient phosphorescent organic light-emitting diodes (PHOLEDs). *Asian J. Org. Chem.*, **2015**, *4*, 394–429.

[20] Zhou XH, Luo J, Davies JA, Huang S, Jen AK. Push–pull tetraene chromophores derived from dialkylaminophenyl, tetrahydroquinolinyl and julolidinyl moieties: optimization of second-order optical nonlinearity by fine-tuning the strength of electron-donating groups. *J. Mater. Chem.*, **2012**, *32*, 16390–16398.

[21] Fulopova A, Magdolen P, Sigmundova I, Zahradnik P, Rakovsky E, Cigan M. Benzotristhiazole based chromophores for nonlinear optics. *J. Mol. Struct*., **2012**, *1027*, 70–80.

[22] Enchev V, Bakalova S, Ivanova G, Stoyanov N. Excited state intramolecular proton transfer of 2-acetylindan-1,3-dione. *Chem. Phys. Lett.*, **1999**, *314*, 234–238.

[23] Lakowicz JR. Principles of fluorescence spectroscopy, 3rd edition, Springer, US, **2006**, 954.

# ACKNOWLEDGEMENTS

I would like to express my gratitude to the supervisor of the dissertation, Professor Dr. habil. chem. Valdis Kampars for support and time devoted to the creation of the Doctoral Thesis.

Many thanks also to all the staff of the Institute of Applied Chemistry for their help in creating scientific work, especially to Rūta Kampare for taking NMR spectra, Kristīne Lazdoviča for performing FT-IR, TG analyses, Lauma Laipniece for training with HPLC, Kaspars Traskovskis for consultations, ideas, and help with latest publication, and Zane Ābelniece for encouragement and support.

Thanks also to colleagues from OSI – Dr. Chem. Baiba Turovska for performing electrochemical analyses and Dr. phys. Sergejs Beļakovs for taking X-ray structure analyses. Also the biggest thanks to colleagues from CFI – Dr. phys. Aivars Vembris for training in working with luminescence spectrometer and OLED manufacturing and measurement, and Igors Mihailovs for introduction and training of theoretical quantum chemistry calculation program “ORCA”.

Thanks to “Grindex” Ltd. for the “Silver Owl Award” awarded in 2014.

Many thanks also to my husband Kristaps Māliņš for his encouragement, support and constant conversations about science. Thanks also to my family and friends.

# PIELIKUMI/PUBLICATIONS

1.pielikums

**Malina I**, Kampars V, Turovska B. Synthesis, optical and electrochemical properties of substituted 2-cinnamoyl-1,3-indandione *O*-methyl ethers. *J. Mol. Struct.*, **2016**, *1115*, 241-249.

DOI: 10.1016/j.molstruc.2016.02.090

© 2016, Elsevier. This manuscript version is made available under the CC-BY-NC-ND 4.0 license http://creativecommons.org/licenses/by-nc-nd/4.0

Journal of Molecular Structure 1115 (2016) 241–249

Contents lists available at ScienceDirect

Journal of Molecular Structure

journal homepage: http://www.elsevier.com/locate/molstruc

# Synthesis, optical and electrochemical properties of substituted 2-cinnamoyl-1, 3-indandione O-methyl ethers

Ilze Malina [a, *], Valdis Kampars [a], Baiba Turovska [b]

[a] Riga Technical University, Institute of Applied Chemistry, P. Valdena 3/7, Riga, LV-1048, Latvia
[b] Latvian Institute of Organic Synthesis, Aizkraukles 21, Riga, LV-1006, Latvia

ARTICLE INFO

*Article history:*
Received 23 August 2015
Received in revised form
9 December 2015
Accepted 24 February 2016
Available online 2 March 2016

*Keywords:*
O-methyl ethers
2-Cinnamoyl-1,3-indandione
Methylation
Optical properties

ABSTRACT

Seven new 2-cinnamoyl-1,3-indandione (2CID) O-methyl ethers with different substituents (R = –H, $-CH_3$, $-OCH_3$, $-N(C_6H_5)_2$, $-N(CH_2CH_2CN)_2$, julolidyl, $-N(CH_3)_2$) in 4-position of the cinnamoyl moiety were synthesized. The methylation with dimethylsulfate occurred at the oxygen atom of the exocyclic enol group with high selectivity.

The synthesized compounds were characterized by $^1H$, $^{13}C$ NMR, IR, UV–Vis and luminescence spectroscopy, their electrochemical properties were investigated by cyclic voltammetry. The obtained results indicates that introducing an electron donating substituents in the 4-position of cinnamoyl moiety facilitates electrochemical oxidation, remarkably shifts absorption and emission bands to longer wavelengths, simultaneously increases extinction coefficient (ε). O-methyl ethers with strong electron donating groups (R = $-N(C_6H_5)_2$, $-N(CH_2CH_2CN)_2$, julolidyl, $-N(CH_3)_2$) in molecule are characterized by luminescence with maximum in range from 547 to 647 nm and absolute photoluminescence quantum yields from 0.02 to 0.32. Quantum yield (QY) of chromophore containing julolidyl fragment is solvent dependent. It was 0.32 in chloroform and decreased in other polar (ethanol, acetone) solvents.

© 2016 Elsevier B.V. All rights reserved.

## 1. Introduction

1,3-Indandione and its derivatives have been intensively studied over years due to their wide range of potential applications. First studies were devoted to investigate biological activity for derivatives of 1,3-indandione. Rat-extermination [1], anti-inflammatory [2,3] and other properties were discovered for several 1,3-indandione compounds. But in the last few decades 1,3-indandione moiety has been used as structural element in synthesis of new chromophores and luminophores with non-linear optical (NLO) properties [4–10]. 1,3-Indandione is well known as strong electron acceptor moiety and, when it is bounded with electron donating substituents, the molecules with potential applications as photoactive organic materials can be obtained [5].

The most studied derivative of 1,3-indandione is 4-*N*,*N*-dimethylaminobenzylidene-1,3-indandione (DMABI) whose crystals and films are characterized with efficient photoconductivity [11] and non-linear luminescence [7].

In recent years particular interest has been focused to 2-acyl-derivatives of 1,3-indandione. Due to the β,β'-triketone fragment, which has strong intramolecular hydrogen bond in the enol form, some compounds from this class are characterized with high stability upon UV-irradiation [12], large Stokes shift [13] and complexation ability with transition [14–16] and rare earth metal ions [17,18]. As a result compounds with excellent emission and thermal properties can be obtained, for example, 2-benzoyl-1,3-indandione complex with europium(III) ion has been proposed as potential molecular light converter material for new organic light emitting diodes (OLED) [18]. Whereas 2-acetyl-1,3-indandione complexes with transition metal ions such as silver(I) ion has shown proper thermal decomposition temperature and it can be used as precursor for silver films [16]. Only few studies have been devoted to 2-acyl derivatives of 1,3-indandione with prolonged π-conjugate system in molecule – 2-cinnamoyl-1,3-indandiones (2CID). 2CID similar as 2-acyl-1,3-indandiones exist in exocyclic enolic form, which is stabilized by intramolecular hydrogen bond. If the benzene ring of cinnamoyl part contains strong electron donating substituent in *para*-position, push–pull type molecules on the basis of 2CID can be obtained with excellent electronic and optical properties. Ahmedova et al. [19–22] have investigated optical and complexation properties of some 2CID and their

* Corresponding author.

http://dx.doi.org/10.1016/j.molstruc.2016.02.090
0022-2860/© 2016 Elsevier B.V. All rights reserved.

analogues. The authors characterized obtained compounds as chromophores with high molar absorptivity, large Stokes shift, good photostability upon UV-irradiance, however due to low solubility in organic solvents transition metal ion complexes with 2CID ligands does not have practical application.

Due to relatively low number of the studies devoted to 2CID and their analogues, our work was directed towards investigation of new chromophores derived from 2CID – their O-methyl ethers. In some papers also O-methylation of β,β'-triketone fragment containing compounds were discussed [23–25], although the properties of O-methyl ethers up till now have not been reported. We are presenting here the synthesis of new chromophores, which contains 1,3-indandione moiety as electron acceptor and with different electron donating substituents derived methylated cinnamoyl fragment. These easily obtainable organic chromophores - 2CID O-methyl ethers consisting of π-conjugated system between electron donor and acceptor could possess pronounced emission characteristics and therefore could find an application in optoelectronic devices, for example in OLED. Newly synthesized 2CID O-methyl ethers are characterized by $^{1}$H, $^{13}$C NMR, FT-IR, UV–Vis and luminescence spectroscopy methods and electrochemical measurement. Furthermore, to investigate the structure modifying effects on the electrochemical and optical properties, 2-cinnamoyl-1,3-indandione O-methyl ether with $-N(CH_3)_2$ substituent is compared with the well investigated "push–pull" chromophore 4-*N*,*N*-dimethylaminobenzylidene-1,3-indandione (DMABI).

## 2. Experimental procedures

### 2.1. General

The FT-IR spectra in the range from 4000 to 650 cm$^{-1}$ were recorded on a Perkin–Elmer Spectrum 100 FT-IR spectrometer using KBr pellets.

The $^{1}$H and $^{13}$C NMR spectra were recorded in $CDCl_3$ or DMSO-$d_6$ solutions on a Brucker Avance 300 MHz spectrometer at 300 MHz for $^{1}$H- and 75 MHz for $^{13}$C- nuclei. Chemical shifts were expressed in parts per million (ppm) relative to solvent signal.

Diffraction data were collected on a Bruker-Nonius Kappa CCD diffractometer using graphite monochromated Mo-Kα radiation (λ = 0.71073 Å). The crystal structure was solved by direct methods [26,27] and refined by full-matrix least squares [28]. The crystal data, details of data collection and refinement are given in Table 1.

The purity of prepared organic compounds was established on Waters 2695 HPLC using Waters 2996 Photodiode array UV–Vis detector. The chromatographic analyses were performed using XTerra® MS C18 (5 μm 2.1 × 100 mm) column, 50% Acetonitrile/0.1% formic acid solution as mobile phase and flow rate 0.2 ml/min. MS spectra were acquired on a Waters EMD 1000MS mass detector. Mass spectra were obtained in ESI + mode, voltage 30 V.

The UV–Vis absorption spectra in $CHCl_3$ solutions were acquired using Perkin–Elmer 35 UV/Vis spectrometer with a 1 cm path length quartz cell.

Emission spectra in $CHCl_3$ solutions were measured on Quanta Master 40 steady state spectrofluorometer (Photon Technology International, Inc.) using 1 cm path length quartz cuvettes. Absolute photoluminescence quantum yields in $CHCl_3$ solutions were determined using QuantaMaster 40 steady state spectrofluorometer (Photon Technology International, Inc.) equipped with 6 inch integrating sphere by LabSphere.

The cyclic voltammograms were recorded using a computer controlled electrochemical system PARSAT 2273. The measurements were carried out using a three-electrode cell configuration. Stationary glassy carbon disk (Ø 0.5 cm) was used as a working electrode, Pt wire - as an auxiliary electrode. Potentials were measured *vs* saturated calomel electrode (SCE) and recalculated *vs* normal hydrogen electrode (NHE). The potential scan rate was 100 mV/s. Electrochemical redox reactions were studied in 0.1 M tetrabutyl-ammonium tetrafluorophosphate ($TBAPF_6$) acetonitrile solution under Ar atmosphere. Acetonitrile (Merck, puriss. grade) was distilled over phosphorus pentoxide, stored over calcium hydride and distilled just before use.

**Table 1**
Crystal data and refinement parameters for compound **3f**.

| Compound | 3f |
|---|---|
| Molecular formula | $C_{24}H_{21}NO_3$ |
| Molecular weight | 371.42 |
| Crystal system | Monoclinic |
| Space group | $P\,2_1/n$ |
| *a* (Å) | 8.5990 (4) |
| *b* (Å) | 21.7570 (5) |
| *c* (Å) | 10.5800 (14) |
| β (°) | 108.692 (3) |
| *V* (Å$^3$) | 1875.0 (3) |
| *Z* | 4 |
| $D_c$ (Mg•m$^{-3}$) | 1.316 |
| *T* (K) | 293 |
| μ (mm$^{-1}$) | 0.09 |
| *F*(000) | 784 |
| $2\theta_{max}$ (°) | 54.2 |
| h, k, l range | −10 to 10, -27 to 26, -12 to 13 |
| No. measured reflections | 11204 |
| No. independent reflections ($R_{int}$) | 4089 (0.139) |
| No. observed reflections (I > 2σ(I)) | 1399 |
| No. refined parameters/restraints | 257/0 |
| *R*, *wR* [$I > 2\sigma(I)$] | 0.0936, 0.2348 |
| *R*, *wR* [all data] | 0.2702, 0.3341 |
| Goodness of Fit on $F^2$, S | 0.902 |
| Max., Min electron density (e Å$^{-3}$) | 0.23, −0.21 |
| Maximum Δ/σ | 0.021 |

Melting points were determined using Stuart SMP101 apparatus and are uncorrected. TLC analyses were performed on MERCK silica gel plates and were detected with EURO-BST-203LS UV detector.

All solvents were purchased from Acros Organics with purity of ≥99%. Dimethylsulphate was purchased from Sigma–Aldrich with purity of ≥99%. Acetone was dried and distilled over $K_2CO_3$. Piperidine was purified by distillation before use. 2-Acetyl-1,3-indandione was synthesized as described in the literature [17] and 4-*N*,*N*-dimethylaminobenzylidene-1,3-indandione as in the study [29]. The synthetic route of compounds **3a-g** and **4a-g** are shown in Scheme 1.

### 2.2. Synthesis of compounds 3a-g

2-Acetyl-1,3-indandione **1** (0.010 mol), derivative of benzaldehyde **2a-g** (0.010 mol) and piperidine (0.005 mol) was refluxed at 110 °C for 2 h. Then reaction mixture was cooled to 80 °C and 8 ml of ethanol was added. Solution was boiled for 30 min, and after cooling, the formed crystals were filtered off and washed with ethanol. Products were recrystallized from $CH_2Cl_2$ and EtOH mixture.

*(E)-2-(1-hydroxy-3-phenylallylidene)-2H-indene-1,3-dione* (**3a**), Yield 32%, M.P. = 186–187 °C. $^{1}$H NMR ($CDCl_3$), δ, [ppm]: 13.20 (s, 1H), 8.04 (d, *J* = 15.0 Hz, 1H), 7.92 (d, *J* = 15.0 Hz, 1H), 7.89 (m, 2H), 7.74 (m, 4H), 7.46 (m, 3H). $^{13}$C NMR ($CDCl_3$), δ, [ppm]: 197.59, 188.60, 173.25, 145.04, 138.65, 134.25, 134.25, 134.00, 133.50, 131.00, 129.03, 122.94, 122.50, 118.14, 108.02. IR, (KBr), ν, [cm$^{-1}$]: 3400-3200 ($\nu_{OH}$), 3027 ($\nu_{CH}$), 1704 ($\nu_{C=O}$), 1620 ($\nu_{C=O}$, $_{C=C}$), 1579, 1564 ($\nu_{C=C(Ph)}$). MS (ES+) *m/z*: 277.00 ($M^+$ requires 277.08), (ES-) *m/z*: 275.20 ($M^-$ requires 275.08).

*(E)-2-(1-hydroxy-3-(p-tolyl)allylidene)-2H-indene-1,3-dione* (**3b**),

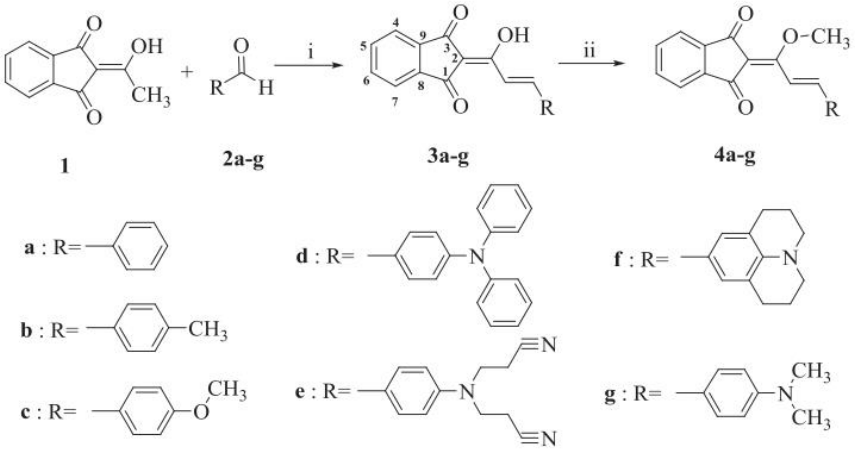


**Scheme 1.** Reagents and conditions: (i) Piperidine, 110 °C, 2 h; (ii) dimethylsulphate, K2CO3, acetone, 56 °C, 4 h.

Yield 43%, M.P. = 184–185 °C. $^1$H NMR ($CDCl_3$), δ, [ppm]: 13.30 (s, 1H), 7.97 (d, $J$ = 13.5 Hz, 1H), 7.89 (m, 3H), 7.73 (m, 2H), 7.62 (d, $J$ = 6.0 Hz, 2H), 7.27 (d, $J$ = 6.0 Hz, 2H), 2.43 (s, 3H). $^{13}$C NMR ($CDCl_3$), δ, [ppm]: 197.81, 188.60, 173.68, 145.27, 142.25, 141.13, 138.64, 134.90, 134.70, 132.14, 129.90, 128.98, 122.50, 122.23, 116.79, 107.57. IR, (KBr), ν, [cm$^{-1}$]: 3200-3000 ($\nu_{OH}$), 2962, 2917 ($\nu_{CH}$), 1699 ($\nu_{C=O}$), 1646, 1625 ($\nu_{C=O}$, $\nu_{C=C}$), 1583 ($\nu_{C=C(Ph)}$). MS (ES+) $m/z$: 291.10 (M$^+$ requires 291.09), (ES-) $m/z$: 289.30 (M$^-$ requires 289.09).

*(E)-2-(1-hydroxy-3-(4-methoxyphenyl)allylidene)-2-H-indene-1,3-dione* (**3c**), Yield 39%, M.P. = 193–194 °C. $^1$H NMR ($CDCl_3$), δ, [ppm]: 13.30 (s, 1H), 7.93 (d, $J$ = 15.0 Hz, 1H), 7.88 (m, 3H), 7.82 (m, 2H), 7.69 (d, $J$ = 9.0 Hz, 2H), 6.98 (d, $J$ = 9.0 Hz, 2H), 3.90 (s, 3H). $^{13}$C NMR ($CDCl_3$), δ, [ppm]: 197.51, 188.80, 173.66, 162.30, 145.04, 140.82, 138.70, 134.74, 133.98, 131.03, 127.67, 122.64, 122.15, 115.33, 114.53, 107.17, 55.42. IR, (KBr), ν, [cm$^{-1}$]: 3100-2600 ($\nu_{OH}$), 3070, 2942, 2845 ($\nu_{CH}$), 1698 ($\nu_{C=O}$), 1624 ($\nu_{C=O}$, $_{C=C}$), 1565 ($\nu_{C=C(Ph)}$), 1258, 1210 ($\nu_{COC}$). MS (ES+) $m/z$: 307.13 (M$^+$ requires 307.09), (ES-) $m/z$: 305.28 (M$^-$ requires 305.09).

*(E)-2-(3-(4-N,N-(diphenylamino)phenyl)-1-hydroxyallylidene)-2H-indene-1,3-dione* (**3d**), Yield 60%, M.P. = 220–222 °C. $^1$H NMR ($CDCl_3$), δ, [ppm]: 13.25 (s, 1H), 7.90 (d, $J$ = 13.5 Hz, 1H), 7.82 (m, 3H), 7.70 (m, 2H), 7.55 (d, $J$ = 7.5 Hz, 2H), 7.33 (m, 4H), 7.17 (m, 6H), 7.04 (d, $J$ = 7.5 Hz, 2H). $^{13}$C NMR ($CDCl_3$), δ, [ppm]: 197.59, 188.83, 173.92, 151.01, 145.30, 145.00, 139.10, 138.85, 133.80, 133.50, 130.30, 129.61, 126.00, 124.58, 122.50, 122.06, 120.90, 114.73, 107.33. IR, (KBr), ν, [cm$^{-1}$]: broad 3200-2800 ($\nu_{OH}$), 3049, 3033 ($\nu_{CH}$), 1696 ($\nu_{C=O}$), 1632, 1617, 1548 ($\nu_{C=O}$, $\nu_{C=C}$, $\nu_{C=C(Ph)}$), 1504, 1489 ($\nu_{C=C(Ph)}$). MS (ES+) $m/z$: 444.20 (M$^+$ requires 444.15), (ES-) $m/z$: 442.30 (M$^-$ requires 442.15).

*(E)-2-(3-(4-N,N-(bis-(2-cyanoethyl))-amino)-phenyl)-1-hydroxy-allylidene)-2H-inde-ne-1,3-dione* (**3e**), Yield 32%, M.P. = 219–220 °C. $^1$H NMR (DMSO), δ, [ppm]: 13.30 (s, 1H), 7.91 (d, $J$ = 15.0 Hz, 1H), 7.85 (m, 3H), 7.72 (m, 2H), 7.70 (d, $J$ = 7.5 Hz, 2H), 6.73 (d, $J$ = 7.5 Hz, 2H), 3.93 (t, $J$ = 4.6 Hz, 4H), 2.74 (t, $J$ = 4.6 Hz, 4H). $^{13}$C NMR (DMSO), δ, [ppm]: 197.23, 188.30, 173.08, 149.87, 146.17, 141.50, 141.00, 133.77, 133.63, 132.15, 124.30, 124.15, 123.51, 122.46, 119.78, 113.36, 106.64, 45.98, 15.75. IR, (KBr), ν, [cm$^{-1}$]: 3200-2600 ($\nu_{OH}$), 3072, 3020, 2965 ($\nu_{CH}$), 2935 ($\nu_{CN}$), 1698 ($\nu_{C=O}$), 1625 ($\nu_{C=O}$, $_{C=C}$), 1587, 1560, 1547 ($\nu_{C=C(Ph)}$). MS (ES+) $m/z$: 398.13 (M$^+$ requires 398.14), (ES-) $m/z$: 396.21 (M$^-$ requires 396.14).

*(E)-2-(3-(1,2,3,5,6,7-hexahydropyrido[3,2,1-ij]quinolin-9-yl)-1-hydroxyallylidene)-2H-indene-1,3-dione* (**3f**), Yield 50%, M.P. = 225–226 °C. $^1$H NMR ($CDCl_3$), δ, [ppm]: 13.25 (s, 1H), 7.84 (d, $J$ = 14.3 Hz, 1H), 7.79 (m, 2H), 7.69 (d, $J$ = 14.3 Hz, 1H), 7.66 (m, 2H), 7.20 (m, 2H), 3.31 (t, $J$ = 2.6 Hz, 4H), 2.78 (4H, t, $J$ = 2.6 Hz, 4H), 1.99 (t, $J$ = 2.6 Hz, 4H). $^{13}$C NMR ($CDCl_3$), δ, [ppm]: 197.51, 189.00, 174.58, 147.30, 147.00, 140.80, 139.00, 133.93, 133.54, 129.70, 122.30, 122.20, 122.00, 121.95, 110.00, 106.30, 50.00, 27.10, 21.35. IR, (KBr), ν, [cm$^{-1}$]: broad 3200-2600 ($\nu_{OH}$), 3014, 2939, 2843 ($\nu_{CH}$), 1693 ($\nu_{C=O}$), 1627, 1567, 1543 ($\nu_{C=O}$, $\nu_{C=C}$, $\nu_{C=C(Ph)}$), 1513, 1463 ($\nu_{C=C(Ph)}$). MS (ES+) $m/z$: 372.40 (M$^+$ requires 372.43).

*(E)-2-(3-(4-N,N-(dimethylamino)phenyl)-1-hydroxyallylidene)-2H-indene-1,3-dione* (**3g**), Yield 67%, M.P. = 210–211 °C. $^1$H NMR ($CDCl_3$), δ, [ppm]: 13.30 (s, 1H), 7.93 (d, $J$ = 15.0 Hz, 1H), 7.82 (m, 2H), 7.80 (d, $J$ = 15.0 Hz, 1H), 7.70 (m, 2H), 7.65 (d, $J$ = 7.5 Hz, 2H), 6.81 (d, $J$ = 7.5 Hz, 2H), 3.10 (s, 6H). $^{13}$C NMR ($CDCl_3$), δ, [ppm]: 197.31, 189.01, 174.35, 152.52, 146.30, 140.95, 138.76, 134.31, 133.51, 131.40, 122.67, 122.07, 111.83, 106.49, 40.23. IR, (KBr), ν, [cm$^{-1}$]: broad 3200-2600 ($\nu_{OH}$), 3019, 2904 ($\nu_{CH}$), 1698 ($\nu_{C=O}$), 1631, 1588, 1567 ($\nu_{C=O}$, $\nu_{C=C}$, $\nu_{C=C(Ph)}$), 1523 ($\nu_{C=C(Ph)}$). MS (ES+) $m/z$: 320.20 (M$^+$ requires 320.12), (ES-) $m/z$: 318.20 (M$^-$ requires 318.12).

### 2.3. Synthesis of compounds **4a-g**

Under an argon atmosphere to a stirred solution of compounds **3a-g** (0.001 mol) and $K_2CO_3$ (0.015 mol) in 25 ml anhydrous acetone was added dimethylsulfate (0.015 mol) and the resulting mixture was heated at reflux for 4 h. After cooling at room temperature, $K_2CO_3$ was filtered off and washed with acetone. Filtrate was cooled at 5 °C, and formed precipitate was filtered off. After drying the precipitate was purified with column chromatography (mobile phase ethyl acetate: $CH_2Cl_2$ 1:2).

*(E)-2-(1-metoxy-3-phenylallylidene)-2H-indene-1,3-dione* (**4a**), Yield 49%, M.P. = 151–152 °C. $^1$H NMR ($CDCl_3$), δ, [ppm]: 8.18 (d, $J$ = 13.8 Hz, 1H), 7.90 (m, 2H), 7.76 (d, $J$ = 13.8 Hz, 1H), 7.71 (m, 4H), 7.44 (m, 3H). 4.35 (s, 3H). $^{13}$C NMR ($CDCl_3$), δ, [ppm]: 191.65, 188.84, 173.91, 145.02, 144.60, 140.45, 134.15, 132.00, 128.52, 122.31, 121.58, 112.39, 65.34. IR, (KBr), ν, [cm$^{-1}$]: 3028, 2941, 2855 ($\nu_{CH}$), 1705 ($\nu_{C=O}$), 1664, 1614, 1593 ($\nu_{C=O}$, $\nu_{C=C}$, $\nu_{C=C(Ph)}$), 1525, 1450 ($\nu_{C=C(Ph)}$). MS (ES+) $m/z$: 291.20 (M$^+$ requires 290.31).

*(E)-2-(1-methoxy-3-(p-tolyl)allylidene)-2H-indene-1,3-dione* (**4b**), Yield 56%, M.P. = 139–140 °C. $^1$H NMR ($CDCl_3$), δ, [ppm]: 8.10 (d, $J$ = 13.8 Hz, 1H), 7.85 (m, 2H), 7.72 (m, 3H), 7.57 (d, $J$ = 5.0 Hz, 2H), 7.21 (d, $J$ = 5.0 Hz, 2H), 4.35 (s, 3H), 2.38 (s, 3H). $^{13}$C NMR ($CDCl_3$), δ, [ppm]: 192.40, 188.85, 174.19, 144.58, 141.49, 140.68, 134.68, 134.00, 133.14, 126.56, 122.23, 120.73, 112.40, 65.35, 21.63. IR, (KBr), ν, [cm$^{-1}$]: 3023, 2926, 2847 ($\nu_{CH}$), 1715 ($\nu_{C=O}$), 1670, 1612,

1598 ($\nu_{C=O}$, $\nu_{C=C}$, $\nu_{C=C(Ph)}$), 1524 ($\nu_{C=C(Ph)}$). MS (ES+) *m/z*: 305.30 ($M^+$ requires 305.11).

*(E)-2-(1-methoxy-3-(4-methoxyphenyl)allylidene)-2-H-indene-1,3-dione* (**4c**), Yield 34%, M.P. = 148–151 °C. $^1$H NMR ($CDCl_3$), δ, [ppm]: 8.05 (d, *J* = 15.0 Hz, 1H), 7.87 (m, 2H), 7.78 (d, *J* = 15.0 Hz, 1H), 7.73 (m, 2H), 7.67 (d, *J* = 8.3 Hz, 2H), 6.97 (d, *J* = 8.3 Hz, 2H), 4.36 (s, 3H), 3.89 (s, 3H). $^{13}$C NMR ($CDCl_3$), δ, [ppm]: 192.31, 188.07, 175.00, 162.50, 141.10, 134.90, 134.50, 132.00, 128.00, 122.50, 119.00, 114.00, 112.00, 65.55, 55.55. IR, (KBr), ν, [$cm^{-1}$]: 3029, 2965, 2838 ($\nu_{CH}$), 1705 ($\nu_{C=O}$), 1663, 1593($\nu_{C=O}$, $\nu_{C=C}$, $\nu_{C=C(Ph)}$), 1524, 1509 ($\nu_{C=C(Ph)}$). MS (ES+) *m/z*: 321.40 ($M^+$ requires 321.34).

*(E)-2-(3-(4-N,N-(diphenylamino)phenyl)-1-methoxyallylidene)-2H-indene-1,3-dione* (**4d**), Yield 53%, M.P. = 186–188 °C. $^1$H NMR ($CDCl_3$), δ, [ppm]: 8.00 (d, *J* = 13.6 Hz, 1H), 7.86 (m, 2H), 7.73 (d, *J* = 13.6 Hz, 1H), 7.70 (m, 2H), 7.54 (d, *J* = 7.5 Hz, 2H), 7.32 (m, 4H), 7.15 (m, 6H), 7.03 (d, *J* = 7.5 Hz, 2H), 4.34 (s, 3H). $^{13}$C NMR ($CDCl_3$), δ, [ppm]: 193.00, 189.03, 174.66, 150.54, 147.89, 144.59, 134.29, 131.59, 130.00, 128.20, 125.51, 124.44, 122.27, 121.15, 119.09, 111.70, 65.13. IR, (KBr), ν, [$cm^{-1}$]: 3027, 2970, 2847 ($\nu_{CH}$), 1738 ($\nu_{C=O}$), 1662, 1581 ($\nu_{C=O}$, $\nu_{C=C}$, $\nu_{C=C(Ph)}$), 1521 ($\nu_{C=C(Ph)}$). MS (ES+) *m/z*: 458.30 ($M^+$ requires 458.17).

*(E)-2-(3-(4-N,N-(bis-(2-cyanoethyl))-amino)-phenyl)-1-metyoxyallylidene)-2H-indene -1,3-dione* (**4e**), Yield 54%, M.P. = 159–160 °C. $^1$H NMR ($CDCl_3$), δ, [ppm]: 8.00 (d, *J* = 13.1 Hz, 1H), 7.85 (m, 2H), 7.72 (m, 3H), 7.76 (d, *J* = 6.9 Hz, 2H), 6.70 (d, *J* = 6.9 Hz, 2H), 4.34 (s, 3H), 3.90 (t, *J* = 5.0 Hz, 4H), 2.72 (t, *J* = 5.0 Hz, 4H). $^{13}$C NMR ($CDCl_3$), δ, [ppm]: 192.03, 188.20, 174.67, 147.07, 144.34, 140.91, 134.21, 131.45, 125.98, 122.27, 118.00, 117.90, 112.44, 111.94, 65.36, 47.68, 15.75. IR, (KBr) ν, [$cm^{-1}$]: 3007, 2851 ($\nu_{CH}$), 2949 ($\nu_{CN}$), 1737 ($\nu_{C=O}$), 1655, 1586 ($\nu_{C=O}$, $\nu_{C=C}$, $\nu_{C=C(Ph)}$), 1516, 1465 ($\nu_{C=C(Ph)}$) 1217 ($\nu_{COC}$). MS (ES+) *m/z*: 412.30 ($M^+$ requires 412.16.)

*(E)-2-(3-(1,2,3,5,6,7-hexahydropyrido[3,2,1-ij]quinolin-9-yl)-1-methoxyallylidene)-2H-indene-1,3-dione* (**4f**), Yield 74%, M.P. = 178–180 °C. $^1$H NMR ($CDCl_3$), δ, [ppm]: 7.85 (d, *J* = 15.0 Hz, 1H), 7.82 (m, 2H), 7.73 (d, *J* = 15.0 Hz, 1H), 7.66 (m, 2H), 7.18 (s, 2H), 4.28 (s, 3H), 3.30 (t, *J* = 3.0 Hz, 4H), 2.76 (t, *J* = 3.0 Hz, 4H), 1.97 (dt, *J* = 3.0 Hz, 4H). $^{13}$C NMR ($CDCl_3$), δ, [ppm]: 197.22, 188.50, 175.52, 147.34, 146.31, 140.60, 133.72, 129.40, 122.27, 121.65, 121.13, 114.50, 110.27, 54.66, 50.10, 27.60, 21.37. IR, (KBr), ν, [$cm^{-1}$]: 2940, 2842, 2812 ($\nu_{CH}$), 1702 ($\nu_{C=O}$), 1660, 1578, ($\nu_{C=O}$, $\nu_{C=C}$, $\nu_{C=C(Ph)}$), 1501, 1434 ($\nu_{C=C(Ph)}$), 1195 ($\nu_{COC}$). MS (ES+) *m/z*: 386.30 ($M^+$ requires 386.16).

*(E)-2-(3-(4-N,N-(dimethylamino)phenyl)-1-methoxyallylidene)-2H-indene-1,3-dione* (**4g**), Yield 34%, M.P. = 133–134 °C. $^1$H NMR ($CDCl_3$), δ, [ppm]: 7.95 (d, *J* = 14.1 Hz, 1H), 7.85 (m, 2H), 7.79 (d, *J* = 14.1 Hz, 1H), 7.68 (m, 2H), 7.61 (d, *J* = 7.1 Hz, 2H), 6.70 (d, *J* = 7.1 Hz, 2H), 4.32 (s, 3H), 3.09 (s, 6H). $^{13}$C NMR ($CDCl_3$), δ, [ppm]: 192.09, 188.28, 175.40, 152.31, 146.29, 140.67, 133.71, 131.39, 123.37, 121.85, 116.15, 111.89, 111.06, 64.90, 40.24. IR, (KBr), ν, [$cm^{-1}$]: 3072, 3024, 2959, 2869 ($\nu_{CH}$), 1697 ($\nu_{C=O}$), 1652, 1576 ($\nu_{C=O}$, $\nu_{C=C}$, $\nu_{C=C(Ph)}$), 1531, 1499 ($\nu_{C=C(Ph)}$) 1278 ($\nu_{COC}$). MS (ES+) *m/z*: 334.20 ($M^+$ requires 333.14).

## 3. Results and discussion

### 3.1. Synthesis and characterization of substituted 2-cinnamoyl-1,3-indandiones

Substituted 2-cinnamoyl-1,3-indandiones (2CID) **3a-g** were obtained in Claisen–Schmidt condensation reaction (Scheme 1) between 2-acetyl-1,3-indandione **1** and derivative of benzaldehyde **2a-g** in the presence of piperidine. The chemical structures of the compounds **3a-g** were identified with $^1$H, $^{13}$C NMR and FT-IR spectroscopy, compound **3f** was also characterized by X-ray diffraction data.

$^1$H NMR spectra of compounds **3a-g** are characterized with broad singlet near 13.20 ppm, which attributes to proton from enol hydroxyl group. Two doublets appears at ~8.00 and 7.90 ppm, which corresponds to protons from double bound of allylidene fragment and their spin coupling constants are in the range from 13.5 to 15.0 Hz indicating that all substituted 2CID **3a-g** exist in trans form. In the $^{13}$C NMR spectra of compounds **3a-g** chemical shifts for 1,3-indandione cycle carbon atoms C(9) and C(8) (see Scheme 1) are not equal, thus meaning that chemical environment are not identical for these atoms. This could be explained with hydrogen bond formation between hydroxyl group and one of the two carbonyl groups of the 1,3-indandione moiety.

FT-IR spectra for compounds **3a-g** shows broad band between 3200 and 3400 $cm^{-1}$, which is assigned to enol hydroxyl group stretching vibrations. Non-bonded hydroxyl group vibrations usually appears as a sharp absorption band near 3670-3580 $cm^{-1}$, therefore such shift to lower region of inverse centimeters and band broadening indicate that the intramolecular hydrogen bond exist in 2-cinnamoyl-1,3-indandione molecules.

By slow evaporation of saturated dichloromethane solution good quality single crystals of 2-cinnamoyl-1,3-indandione **3f** were obtained for crystallographic analysis. The crystal structure of compound **3f** is shown in Fig 1 and selected geometrical parameters are listed in Table 2.

X-ray diffraction data confirms, that compound **3f** in solid state exist in exocyclic enol form, which is stabilized by intramolecular hydrogen bond between carbonyl group oxygen atom (O11) from 1,3-indandione moiety and hydroxyl group (H13–O13) from allylidene fragment. Hydrogen bond O13–H13···O11 is characterized by bond length of 1.66(8) Å (O11···H13) and 2.606(7) Å (O11···O13), and angle of 160(6)° (O13–H13···O11). Interestingly, comparing bonds C2–C3 (1.432(7) Å) and C1–C2 (1.461(7) Å), the latter ones are longer, showing less double bound character. Moreover, bond C3–O11 (1.252(6) Å) are significantly longer than bond C1–O10 (1.222(6) Å), showing more single bond character. These data indicate that the conjugated π-electron system stabilized by the intramolecular hydrogen bond is present in the molecule of **3f**. The angles between atoms O10–C1–C2 (128.7(5)°) are wider than for O11–C3–C2 (125.3(5)°), confirming that hydrogen bond causes carbonyl group (C3–O11) positioning closer to hydroxyl group and therefore pseudoaromatic six-membered system is formed in molecule. Similar data were obtained for other 2-acyl-1,3-indandiones, for examples, 2-acetyl-1,3-indandione [14,30], 2-(3-thiophen-2-yl-1-hydroxy-allylidene)-2H-inden-1,3-dione [21], 2-(3-furan-2-yl-1-hydroxy-allylidene)-2H-inden-1,3-dione [21], 2-(1-hydroxy-3-(p-tolyl)allylid-ene)-2H-indene-1,3-dione [22].

Dihedral angle between 1,3-indandione moiety and julolidyl substituent plane is 9.60°, meaning that molecule are almost planar. Interestingly, 2-acyl-1,3-indandiones with 2-thiophene or 2-furan rings in the molecule are planar [21], but on the contrary 2-(1-hydroxy-3-(p-tolyl)allylidene)-2H-indene-1,3-dione (compound **3b**) is not planar and has larger dihedral angle (11.34°) than **3f** [22]. Planarity of the 1,3-indandione moiety approves dihedral angle (0.96°) between cyclopentane and benzene rings planes.

Compound **3f** also exhibits weak intermolecular hydrogen bonds between carbonyl group oxygen atom (O10) as proton acceptor and $CH_2$ group (C25–H25) from julolidyl substituent as proton donor. Contrary to the compound **3b** [22] cinnamoyl-1,3-indandione **3f** does not show π-π stacking between aromatic rings.

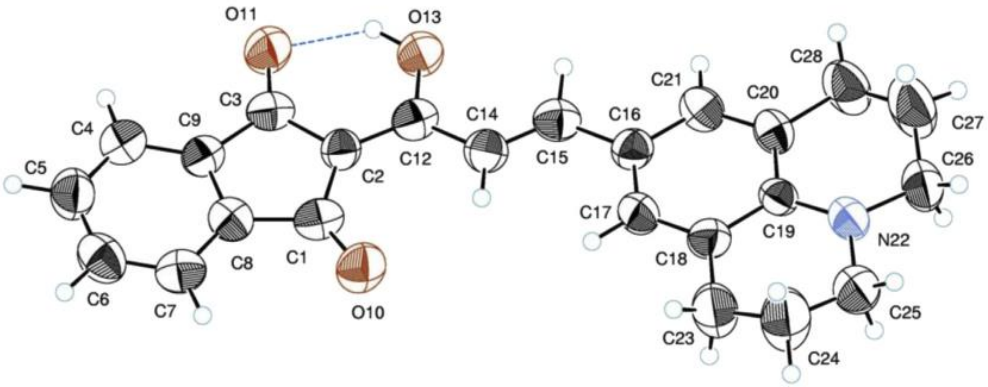


**Fig. 1.** ORTEP drawing of compound 3f with the atom numbering scheme. All non-hydrogen atoms are drawn as 50% probability ellipsoids.

**Table 2**
Selected geometry of compound **3f**.

| Bond distances | | | | Bond angles | |
|---|---|---|---|---|---|
| C1–O10 | 1.222 (6) | C14–C15 | 1.347 (7) | C1–C2–C3 | 107.7 (4) |
| C1–C2 | 1.461 (7) | C15–C16 | 1.447 (7) | C1–C2–C12 | 129.7 (5) |
| C1–C8 | 1.488 (7) | C16–C17 | 1.392 (7) | C2–C12–O13 | 118.4 (5) |
| C2–C3 | 1.432 (7) | C16–C21 | 1.391 (7) | C3–C2–C12 | 122.5 (5) |
| C2–C12 | 1.385 (7) | C17–C18 | 1.367 (7) | O10–C1–C2 | 128.7 (5) |
| C3–O11 | 1.252 (6) | C18–C19 | 1.425 (7) | O10–C1–C8 | 125.1 (5) |
| C3–C9 | 1.477 (7) | C19–C20 | 1.407 (7) | O11–C3–C2 | 125.3 (5) |
| C12–O13 | 1.340 (6) | C20–C21 | 1.380 (7) | O11–C3–C9 | 126.3 (5) |
| C12–C14 | 1.414 (7) | | | | |
| Hydrogen bond geometry | | | | | Symmetry code |
| D-H···A | D-H | H···A | D···A | ∠D-H···A | |
| O13–H13···O11 | 0.98 (7) | 1.66 (8) | 2.606 (7) | 160 (6) | intramolecular |
| C25–H25···O10 | 0.96 | 2.49 | 3.422 (8) | 162 | $-1/2 + x, 1/2-y, 1/2 + z$ |

### 3.2. Synthesis and characterization of substituted 2-cinnamoyl-1,3-indandione O-methyl ethers

Methylation of compounds **3a-g** was carried out in acetone under argon atmosphere with dimethylsulfate as alkylating agent in the presence of potassium carbonate (Scheme 1).

Methylation of β,β'-triketones can lead to two different O-methyl ethers [25]. It is possible to add methyl group to carbonyl group of 1,3-indandione moiety or to enol hydroxyl group of cinnamoyl fragment, and the result mainly depends from the used alkylation agent. In the case of substituted 2-cinnamoyl-1,3-indandiones the theoretically possible methylation products - O-methyl ethers **A** and **B** are shown in Fig. 2. It was confirmed by $^{13}C$ NMR, that all O-methyl ethers **4a-g** have a structure **A**. In the case of structure **B** the symmetry of 1,3-indandione moiety would be lowered, which would lead to different chemical shifts for carbon atoms C(9) and C(8) near to methoxy group. However obtained compounds **4a-g** showed identical chemical shifts for these atoms in $^{13}C$ NMR spectra.

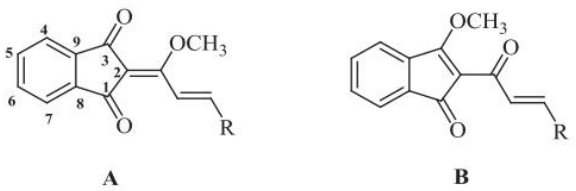


**Fig. 2.** Structures of possible methylation products of substituted 2-cinnamoyl-1,3-indandiones.

The chemical structures of the compounds **4a-g** were confirmed with $^{1}H$ and $^{13}C$ NMR spectroscopy, and FT-IR spectroscopy. $^{1}H$ NMR spectra of compounds **4a-g** shows minor changes from **3a-g** spectra – a singlet for methoxy group protons appears at 4.35 ppm and broad singlet for hydroxyl group proton disappears. $^{13}C$ NMR spectra shows more differences. The comparison of $^{13}C$ NMR spectra chemical shifts for **3a** and O-methyl ether **4a** are given in

**Table 3**
Comparison of 13C NMR chemical shifts for 2-cinnamoyl-1,3-indandione **3a** and O-methyl ether **4a**.

| $^{13}C$ atom | δ, ppm | |
|---|---|---|
| | 3a | 4a |
| C(1) | 188.61 | 188.84 |
| C(2) | 108.02 | 112.39 |
| C(3) | 197.59 | 191.65 |
| C(4) | 122.50 | 132.00 |
| C(5) | 133.50 | 134.15 |
| C(6) | 134.25 | 134.15 |
| C(7) | 122.94 | 132.00 |
| C(8) | 138.65 | 145.02 |
| C(9) | 134.25 | 145.02 |
| =C–OH | 173.25 | – |
| -CH=CH-Ph | 145.04 | 144.60 |
| 1-C-Ph | 134.00 | 140.45 |
| 2,6-C-Ph | 131.00 | 122.31 |
| 3,4,5-C-Ph | 129.03 | 128.52 |
| -CH=CH-Ph | 118.14 | 121.58 |
| =C–$OCH_3$ | – | 173.91 |
| -OCH3 | – | 65.34 |

Table 3. Firstly chemical shifts of carbon atoms C(8) and C(9) from 1,3-indandione moiety became identical, thus indicating that chemical environment around these two atoms are identical. Secondly chemical shifts for atom pairs C(4) and C(7), as well as C(5) and C(6) are identical, which could be explained with more symmetrical structure for O-methyl ethers **4a-g** than for 2CID **3a-g**. Compounds **3a-g** have a strong hydrogen bond between hydroxyl group and carbonyl group from 1,3-indandione moiety in the molecule, which could make molecule less symmetrical. Furthermore, in the IR spectra of compounds **4a-g** a broad band around 3200 $cm^{-1}$, corresponding to hydroxyl group vibrations, was not observed.

### 3.3. Electrochemical properties

Redox properties of the synthesized chromophores **4a-g** were investigated by cyclic voltammetry. Both electrode processes - cathodic reduction as well as anodic oxidation - are electrochemically irreversible (Fig. 3).

In acetonitrile electrochemical reduction of the investigated compounds proceeds in one step at potentials close to −1 V and are practically unaffected by the substituent R (Table 4). On the contrary, electrochemical oxidation potential $E_{ox}$ values are greatly affected by the substituents and are lowered with an increase of their electron donating properties in the line −H, $-CH_3$, $-OCH_3$, $-N(CH_2CH_2CN)_2$, $-N(C_6H_5)_2$, $-N(CH_3)_2$, julolidyl (Table 4). It can be concluded that the peak potentials $E_{ox}$ and $E_{red}$ represents the energies of the frontal molecular orbitals, which are localized on the different parts of chromophore molecules - the oxidation process is localized on the cinnamoyl part of the molecules, while 1,3-indandione moiety undergoes electrochemical reduction.

### 3.4. Optical properties

In order to explore the effect of different substituents in cinnamoyl moiety on the optical properties of compounds **4a-g**, absorption spectra were investigated in $1.5 \cdot 10^{-5}$ M chloroform solution. The absorption bands of the chromophores **4a-g** are presented in the Fig. 4 and the values of its maxima ($\lambda_{abs}$) and molar extinction coefficients ($\varepsilon$) are summarized in Table 4.

As shown in Fig. 4, unsubstituted O-methyl ether **4a** exhibit a broad absorption band with $\varepsilon$ value 22392 $cm^{-1}$ $M^{-1}$ and maximum at 389 nm, which could be assigned to an intramolecular charge transfer (ICT) transitions from cinnamoyl fragment to 1,3-indandione moiety. Introduction of the donor groups in the benzene ring of cinnamoyl moiety shifts absorption bands to longer wavelength and increases its molar absorptivity. Red shift of absorption band increases in the following sequence - **4b**, **4c**, **4e**, **4d**, **4g**, and **4f**. Introducing weak electron donor groups (methyl and methoxy) in the benzene ring (chromophores **4b** and **4c)** exhibits the smallest red shift for 11 and 35 nm of absorption band maxima, but their molar absorptivity increases two times compared to unsubstituted O-methyl ether **4a**. Other O-methyl ethers **4d-g** contains electron rich dialkylamino, diphenylamino or polycyclic amino - julolidine substituents, which possess larger electron donating strength. Therefore large bathochromic shifts of 72–125 nm and higher $\varepsilon$ values more than two times are observed for compounds **4d,e,g**. Similar observations were reported to analogues of substituted 2-cinnamoyl-1,3-indandiones [22]. Julolidyl donor causes the largest bathochromic shift (173 nm), probably due to nitrogen atom location in the donor group. In julolidyl fragment nitrogen is in fixed position, due to polycyclic structure, which promotes the overlap between p-orbital of the amino group and benzene ring. This structure facilitates nitrogen lone pair electron conjugation with the $\pi$-electron system of molecule and increase the electron-donating strength of substituent. Similar observation was reported in the study [31].

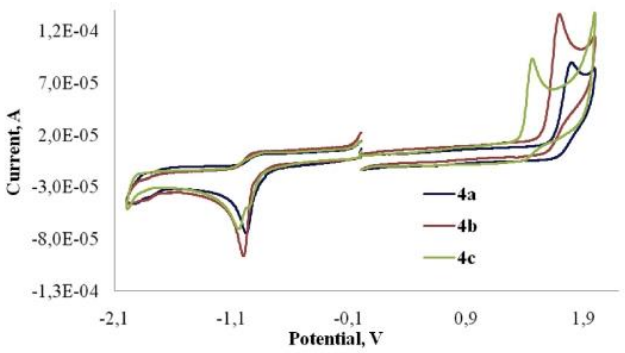


**Fig. 3.** Cyclic voltammogramms of chromophores 4a-c.

The absorption wavelengths of chromophores **4a-g** (the charge–transfer transition energy) linearly depends on the difference between the electrochemical oxidation and reduction peak potentials ($E_{ox}$-$E_{red}$), which indicates that the absorption is connected with charge transfer from cinnamoyl fragment to 1,3-indandione moiety (Fig. 5).

The emission properties of newly synthesized chromophores **4a-g** were also studied in $1.5 \cdot 10^{-5}$ M chloroform solutions; emission bands maxima ($\lambda_{em}$), Stokes shifts ($\Delta\lambda_{sts}$) and absolute photoluminescence quantum yields (QY) are depicted in Table 4.

Unsubstituted and methyl and methoxy group substituted O-methyl ethers **4a-c** does not show emission properties, probably due to weak donating group presence in molecule. The luminescence are observed only for compounds **4d-g**, which have both strong electron acceptor (1,3-indandione) and electron donor ($-N(C_6H_5)_2$, $-N(CH_2CH_2CN)_2$, julolidyl, $-N(CH_3)_2$) groups in molecule. Red shift for emission bands increases in the following sequence - **4e**, **4g**, **4d**, and **4f**, respectively. Emission bands are wide with maximum in range from 547 to 647 nm (Fig. 6), but photoluminescence quantum yields (QY) varies from 0.02 to 0.06 for **4g** and **4d**, to 0.32 for compound **4f**. Interestingly, the replacement of the electron donor $N(CH_3)_2$ by $-N(CH_2CH_2CN)_2$ leads to decrease in QY value below 0.01. This fact could be explained with cyano group location in the donor substituent in chromophore **4e** molecule. Cyano group act as an electron acceptor and therefore decrease the donating strength of diethylamino group to 1,3-indandione. High quantum yield of **4f** in chloroform solution cause a great interest. We assumed, that high quantum yield of O-methyl ether **4f** could be explained with its rigid donor substituent, which prevents amino group from rotation in excited state. Other luminescent O-methyl ethers **4d,e,g** have dialkyl or diphenyl amino groups as donors, which could easily twist in the excited state and therefore lead to the fast non-radiative excited-state deactivation of the whole molecule, likewise it was observed for structurally similar compound - DMABI [32].

However, it was observed, that emission properties for compound **4f** were solvent dependent. QY of **4f** was relatively low in polar solvents, for example, in $1.5 \cdot 10^{-5}$ M ethanol solution QY was only 0.01 and in $1.5 \cdot 10^{-5}$ M acetone solution - 0.03. To explore ethanol influence on the emission properties of **4f**, several chloroform-ethanol mixtures with different ethanol volume were prepared for **4f** (concentration $1.5 \cdot 10^{-5}$ M) and their QY were determined. Obtained data are shown in Fig. 7. As it was expected ethanol has a quenching effect on fluorescence of **4f**. QY lowers for 0.1, when ethanol volume is 6% in mixed ethanol-chloroform solution and decreases for half (0.16), when ethanol volume is 15%.

**Table 4**
Absorption, emission and electrochemical properties of compounds **4a-g**.

| Compound | $\lambda_{abs}$, nm | $\varepsilon$, $cm^{-1} \cdot M^{-1}$ | $\lambda_{em}$, nm | QY | $\Delta\lambda_{sts}$, nm | $E_{ox}$, V | $E_{red}$, V |
|---|---|---|---|---|---|---|---|
| 4a | 389 | 22392 | – | – | – | 1.80 | −0.98 |
| 4b | 401 | 41841 | – | – | – | 1.69 | −1.00 |
| 4c | 424 | 46904 | – | – | – | 1.46 | −1.05 |
| 4d | 509 | 50456 | 647 | 0.06 | 131 | 0.97 | −0.97 |
| 4e | 461 | 57520 | 547 | <0.01 | 101 | 1.02 | −0.97 |
| 4f | 562 | 54367 | 634 | 0.32 | 80 | 0.57 | −1.14 |
| 4g | 514 | 44642 | 597 | 0.02 | 83 | 0.77 | −1.11 |

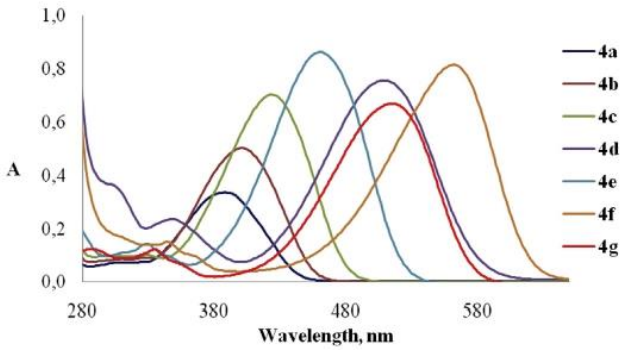


**Fig. 4.** Absorption spectra of compounds 4a-g in $1{,}5 \cdot 10^{-5}$ M chloroform solutions.

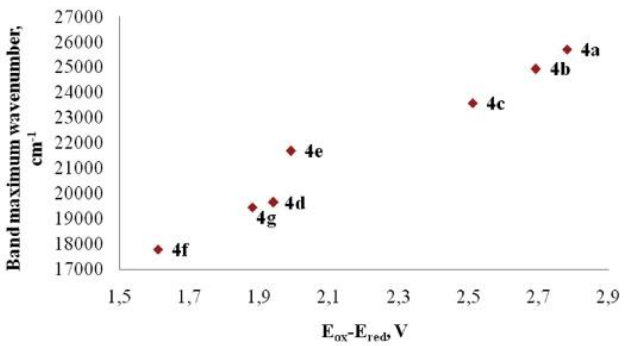


**Fig. 5.** Correlation of the absorption band maxima with the difference of the electrochemical oxidation and reduction peak potentials.

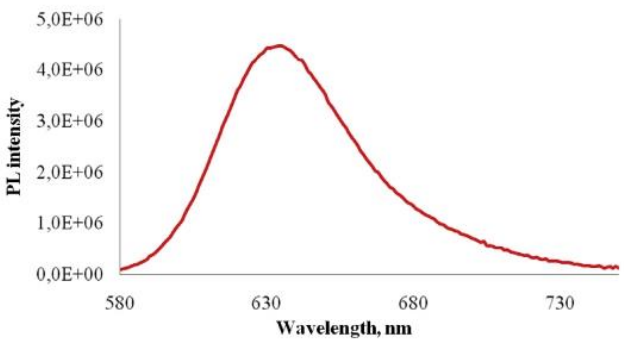


**Fig. 6.** Emission spectrum of O-methyl ether 4f in $1.5 \cdot 10^{-5}$ M chloroform solution.

Polar solvents probably increase non-radiative processes in the excited state of compound **4f** molecules. This could mean that several factors, including structure geometry, interactions of ground and excited states with environment could influence the O-methyl ether **4f** emission properties. To explain clearly O-methyl ether **4f** emission properties further experimental and theoretical investigations are needed.

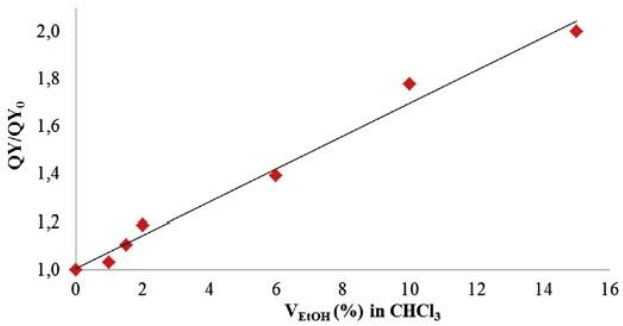


**Fig. 7.** Stern-Volmer-like plot of quenching of compound 4f by ethanol.

In conclusion for practical application only O-methyl ether **4f** with julolidyl substituent presents valuable red light emission with high QY and therefore should be further investigated for use in the optolectronic materials.

Similarly to 2-cinnamoyl-1,3-indandione analogues with heterocyclic ring in molecule [21] large Stokes shift ($\Delta\lambda_{sts}$) were observed for O-methyl ethers **4d-g**, what can be explained with intramolecular rearrangements in excited state for these molecules.

Absorption and emission spectra of compounds **4a-g** in non-polar (cyclohexane, MTBE), polar aprotic (acetone, DMF) and protic (ethanol) solvents were registered in room temperature, data of $\lambda_{abs}$ and $\lambda_{em}$ are depicted in Table 5. Since the dipole moments of the ground and the excited states are different, the change of solvent polarity leads to the different stabilization of these states and cause the solvatochromic effect. For chromophores **4a-c** solvents polarity has an insignificant effect on absorption properties and red shift in DMF compared to cyclohexane by 5–10 nm are observed. Other chromophores **4d-g** shows larger bathochromic shift by 18–47 nm, thus meaning that these chromophores have more polar character than **4a-c**. Impact of solvents polarity on emission properties is similar to those for absorption properties. By changing solvents from cyclohexane to DMF the compounds **4d-g** shows large red shift by 77–99 nm of $\lambda_{em}$ in DMF compared to one in cyclohexane (or MTBE for **4e**).

### *3.5. Comparison of the characteristics for substituted cinnamoyl-1,3-indandione O-methyl ethers and benzylidene-1,3-indandiones*

To gain clearer information about the difference in properties for benzylidene and cinnamoyl derivatives of 1,3-indandione, the compound **4g** with $-N(CH_3)_2$ substituent in cinnamoyl fragment was compared to well-known chromophore 4-*N*,*N*-dimethylaminobenzylidene-1,3-indandione (DMABI). The properties of DMABI

**Table 5**
Absorption ($\lambda_{abs}$) and emission ($\lambda_{em}$) band maxima of compounds **4a-g** in various solvents.

| Compound | Cyclohexane | | MTBE | | Acetone | | Ethanol | | DMF | |
|---|---|---|---|---|---|---|---|---|---|---|
| | $\lambda_{abs}$,nm | $\lambda_{em}$, nm | $\lambda_{abs}$, nm | $\lambda_{em}$, nm | $\lambda_{abs}$, nm | $\lambda_{em}$, nm | $\lambda_{abs}$, nm | $\lambda_{em}$, nm | $\lambda_{abs}$, nm | $\lambda_{em}$, nm |
| 4a | 374 | – | 375 | – | 378 | – | 382 | – | 382 | – |
| 4b | 391 | – | 389 | – | 391 | – | 396 | – | 396 | – |
| 4c | 410 | – | 410 | – | 413 | – | 423 | – | 420 | – |
| 4d | 478, 498sh | 524, 555 | 484 | 597 | 488 | 649 | 506 | 645 | 496 | 654 |
| 4e | -[a] | -[a] | 455 | 526 | 474 | 593 | 483 | 608 | 488 | 611 |
| 4f | 500sh, 522 | 558, 600 | 529 | 610 | 551 | 651 | 573 | 655 | 564 | 662 |
| 4g | 471, 491sh | 545 | 487 | 576 | 505 | 619 | 524 | 628 | 518 | 634 |

Sh – shoulder.
[a] insoluble in cyclohexane.

**Table 6**
Absorption, emission and electrochemical properties of DMABI.

| Characteristics | DMABI |
|---|---|
| $E_{ox}$, V | 1.00 |
| $E_{red}$, V | −1.26 |
| $E_{ox}$− $E_{red}$, V | 2.26 |
| $\lambda_{abs}$, nm in chloroform | 482 |
| $\lambda_{em}$, nm in chloroform | 531 |
| $\Delta\lambda_{sts}$, nm | 49 |
| Photoluminescence quantum yield in chloroform | <0.01 |
| Solvatochromic shift of absorption band by changing solvent from cyclohexane to DMF, nm | 27 |
| $\varepsilon$, $cm^{-1}\cdot M^{-1}$ | 68900 |
| Half width of absorption band in chloroform, nm | 47 |

are given in Table 6. Comparison of absorption properties between DMABI and **4g**, showed that latter one has a red shift of absorption band maximum for 32 nm, due to more extended π-conjugate system in the molecule. Though the DMABI exhibit more intensive absorption band, it is not so wide as absorption band of compound **4g** (89 nm). Furthermore, chromophore **4g** relative strongly emits yellow light at 597 nm, whereas DMABI has a weak luminescence with quantum yield <0.01.

## 4. Conclusions

A series of new substituted 2-cinnamoyl-1,3-indandione O-methyl ethers were synthesized in methylation reaction between substituted 2-cinnamoyl-1,3-indandiones and dimethylsulfate. Obtained O-methyl ether structures were confirmed by $^{1}H$, $^{13}C$ NMR, FT-IR spectroscopy.

Investigation of electrochemical properties by cyclic voltammetry shows that all obtained compounds are "push–pull" chromophores with a location of highest occupied molecular orbital on cinnamoyl and lowest vacant molecular orbital on 1,3-indandione moieties. All 2-cinnamoyl-1,3-indandione O-methyl ethers exhibit strong absorption in 350–600 nm range with high molar absorptivity (22000-57000 $cm^{-1}$ $M^{-1}$). Linear dependence of absorption wavelength on difference between oxidation and reduction peak potentials establishes that absorption is connected with charge transfer from cinnamoyl fragment to 1,3-indandione moiety.

Luminescence for three newly synthesized compounds with no or weak electron donor substituents (R = −H, $-CH_3$, $-OCH_3$) were not observed, but other O-methyl ethers with strong electron donor substituents (R = $-N(C_6H_5)_2$, $-N(CH_2CH_2CN)_2$, julolidyl, $-N(CH_3)_2$) in chloroform solutions shows emission with maximum at 647, 547, 634, 597 nm and with absolute photoluminescence quantum yields - 0.06, <0.01, 0.32, 0.02, respectively. High photoluminescence quantum yield in the case of julolidyl derivative is influenced by several factors, including structure geometry and interactions with environment in the ground and excited states. To elucidate emission properties for the compound with julolidyl substituent, further investigations are necessary.

## Supplementary material

The deposition number CCDC 1439051 for compound **3f** contains the supplementary crystallographic data for this paper. These data can be obtained free of charge at www.ccdc.cam.ac.uk/data_request/cif or from the Cambridge Crystallographic Data Centre (CCDC), 12 Union Road, Cambridge CB2 1EZ, UK; fax: +44 (0) 1223 336033; email:deposit@ccdc.cam.ac.uk.

## Acknowledgments

This work was supported by the National research program of Latvia "Imis2". The authors thanks Dr.phys. S. Belyakov for his help with X-ray diffraction analysis.

## References

[1] L.B. Kilgore, J.H. Ford, W.C. Wolfe, Ind. Eng. Chem. 34 (1942) 494.
[2] J. de Vries, C.N. Verboom, E.J. Groot, W.T. Nauta, E. Wattel, Eur. J. Drug Metab. Pharmacokinet. 4 (1979) 225.
[3] G. Vanden Berg, W.T.H. Nauta, Biochem. Pharmacol. 24 (1975) 815.
[4] M. Rutkis, A. Vembris, V. Zauls, A. Tokmakovs, E. Fonavs, A. Jurgis, V. Kampars, SPIE Proc. 6192 (2006), 61922Q.
[5] B. Stiller, M. Saphiannikova, K. Morawetz, J. Ilnytskyi, D. Neher, I. Muzikante, P. Pastors, V. Kampars, Thin Solid Films 516 (2008) 8893.
[6] R. Karpicz, V. Getautis, K. Kazlauskas, S. Jursenas, V. Gulbinas, Chem. Phys. 351 (2008) 147.
[7] G. Kodis, R. Gulbinas, L. Valkunas, Adv. Mater. Opt. Electron 6 (1996) 391.
[8] G. Seniutinas, R. Tomašiunas, R. Czaplicki, B. Sahraoui, M. Daškevičiene, V. Getautis, Z. Balevicius, Dyes Pigm 95 (2012) 33.
[9] K. Traskovskis, K. Lazdovica, A. Tokmakovs, V. Kokars, M. Rutkis, Dyes Pigm 99 (2013) 1044.
[10] R.M. El-Shishtawy, F. Borbone, Z.M. Al-amshany, A. Tuzi, A. Barsella, A.M. Asiri, A. Roviello, Dyes Pigm 96 (2013) 45.
[11] S. Jursenas, V. Gulbinas, T. Gustavsson, S. Pommeret, J.C. Mialocq, L. Valkunas, Chem. Phys. 27 (2002) 231.
[12] A. Ahmedova, V. Mantareva, V. Enchev, M. Mitewa, Int. J. Cosmet. Sci. 24 (2002) 103.
[13] V. Enchev, S. Bakalova, G. Ivanova, N. Stoyanov, Chem. Phys. Lett. 314 (1999)

234.
[14] V. Enchev, A. Ahmedova, G. Ivanova, I. Wawer, N. Stoyanov, M. Mitewa, J. Mol. Struct. 597 (2001) 67.
[15] A. Ahmedova, V. Rusanov, A. Hazell, J.A. Wolny, G. Gochev, A.X. Trautwein, M. Mitewa, Inorg. Chim. Acta 359 (2006) 3123.
[16] N. Wang, X. Tao, F.L. Du, M. Feng, L.N. Jiang, Y.Z. Shen, Polyhedron 29 (2010) 1687.
[17] E.E.S. Teotonio, H.F. Brito, H. Viertler, W.M. Faustino, O.L. Malta, G.F. de Sa, M.C.F.C. Felinto, R.H.A. Santos, M. Cremona, Polyhedron 25 (2006) 3488.
[18] E.E.S. Teotonio, H.F. Brito, M. Cremona, W.G. Quirino, C. Legnani, M.C.F.C. Felinto, Opt. Mater 32 (2009) 345.
[19] A. Ahmedova, V. Atanasov, P. Marinova, N. Stoyanov, M. Mitewa, Cent. Eur. J. Chem. 7 (2009) 429.
[20] A. Ahmedova, P. Marinova, S. Ciattini, N. Stoyanov, M. Springerborg, M. Mitewa, Struct. Chem. 20 (2009) 101.
[21] A. Ahmedova, G. Pavlovic, D. Zhiryakova, D. Šišak, N. Stoyanov, M. Springborg, M. Mitewa, J. Mol. Struct. 981 (2010) 10.
[22] A. Ahmedova, P. Marinova, G. Pavlovic, M. Guncheva, N. Stoyanov, M. Mitewa, J. Iran. Chem. Soc. 9 (2012) 297.
[23] D.B. Rubinov, I.L. Rubinova, A.A. Akhrem, Chem. Rev. 99 (1999) 1047.
[24] X.C. Li, D. Ferreira, M.R. Jacob, Q. Zhang, S.I. Khan, H.N. Elsohyl, D.G. Nagle, T.J. Smilley, I.A. Khan, L.A. Walker, A.M. Clark, J. Am. Chem. Soc. 126 (2004) 6872.
[25] Y.S. Chen, P.Y. Kuo, T.L. Shie, D.Y. Yang, Tetrahedron 62 (2006) 9410.
[26] A. Altomare, M. Burla, M. Cammali, G. Cascarano, C. Giacovazzo, A. Guagliardi, A. Moliterni, R. Spagna, J. Appl. Cryst. 32 (1999) 115.
[27] G.M. Sheldrick, Acta Cryst. A64 (2008) 112.
[28] S. Mackay, W. Dong, C. Edwards, A. Henderson, C.J. Gilmore, N. Stewart, K. Shankland, A. Donald, maXus, Integrated Crystallography Software, Bruker-Nonius and University of Glasgow, 2003.
[29] V. Kampars, M. Utinans, P. Pastors, E. Kalnina, V. Grazulevicius, Sci. Proc. Riga. Tech. Univ. Mater. Appl. Chem. 9 (2004) 154.
[30] J.D. Korp, I. Bernal, Acta Cryst. B36 (1980) 428.
[31] E. Hendrickx, D. Van Steenwinckel, A. Persoons, C. Samyn, D. Beljonne, J.L. Brédas, J. Chem. Phys. 113 (2000) 5439.
[32] V. Gulbinas, G. Kodis, S. Jursenas, L. Valkunas, A. Gruodis, J.C. Mialocq, S. Pommeret, T. Gustavson, J. Phys. Chem. A 103 (1999) 3969.

2.pielikums

**Malina I**; Kampars V; Turovska B; Belyakov S. Novel green-yellow-orange-red light emitting donor-π-acceptor type dyes based on 1,3-indandione and dimedone moieties. *Dyes and Pigments*, **2017**, *139*, 820-830.

DOI: 10.1016/j.dyepig.2017.01.017

© 2017, Elsevier. This manuscript version is made available under the CC-BY-NC-ND 4.0 license http://creativecommons.org/licenses/by-nc-nd/4.0

Grafiskais abstrakts/graphical abstract

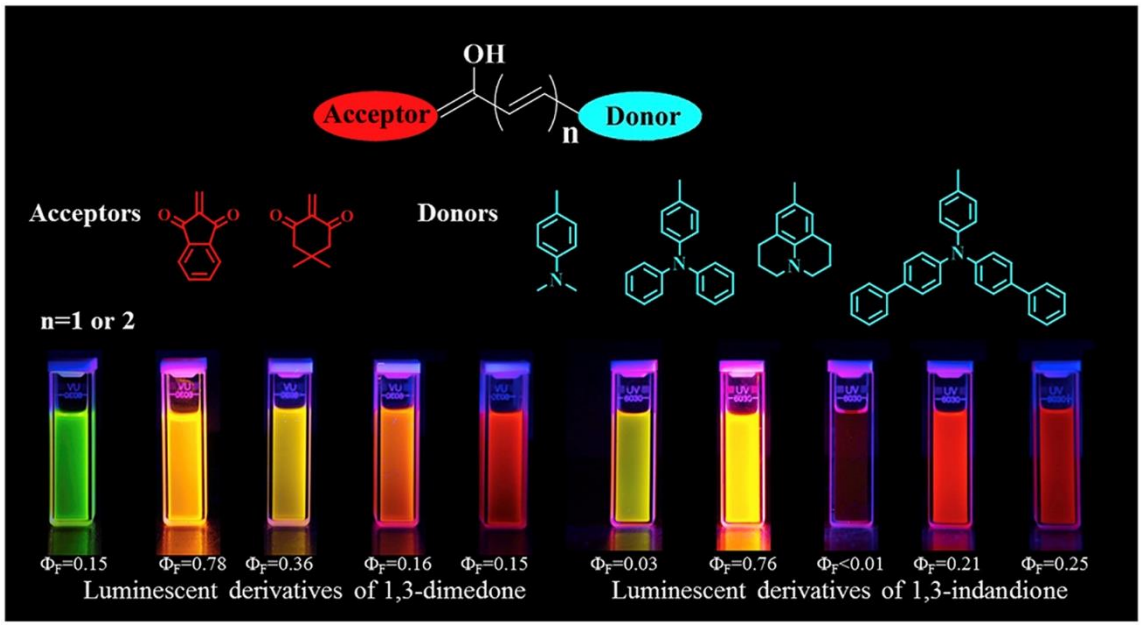

Dyes and Pigments 139 (2017) 820–830

Contents lists available at ScienceDirect

Dyes and Pigments

journal homepage: www.elsevier.com/locate/dyepig

# Novel green-yellow-orange-red light emitting donor-π-acceptor type dyes based on 1,3-indandione and dimedone moieties

Ilze Malina [a, *], Valdis Kampars [a], Baiba Turovska [a, b], Sergey Belyakov [a, b]

[a] Riga Technical University, Institute of Applied Chemistry, Paula Valdena Str. 3, Riga, LV-1048, Latvia
[b] Latvian Institute of Organic Synthesis, Aizkraukles Str. 21, Riga, LV-1006, Latvia

ARTICLE INFO

*Article history:*
Received 27 October 2016
Received in revised form
5 January 2017
Accepted 9 January 2017
Available online 10 January 2017

*Keywords:*
D-π-A dyes
2-Cinnamoyl-1,3-indandione
2-Cinnamoyldimedone
Fluorescent dyes
Amino donors
Positive solvatofluorochromism

ABSTRACT

Ten novel luminescent dyes containing 1,3-indandione or dimedone as electron acceptors, amino derivatives (dimethylamino, diphenylamino, julolidine and dibiphenylamino) as electron donor units and different length olefinic linkers (1-hydroxyallylidene or 1-hydroxypenta-2,4-dien-1-ylidene) are reported in this study. Newly synthesized compound structures are proven with X-ray analysis, $^{1}H$, $^{13}C$ NMR spectroscopy and elemental analysis. The UV–Vis absorption, emission, solvatochromism, solvatofluorochromism, redox properties, as well as thermal stabilities and quantum chemical calculations of these dyes were systematically investigated to outline relation between structure and properties. These dyes exhibit moderate thermal decomposition temperatures above 200 °C, insignificant solvatochromism and positive, significant solvatofluorochromism, large Stokes shifts and green, yellow, orange and red light emission with quantum yields in range from 0.03 to 0.93 in non-polar solvents and in thin films.

Quantum-chemical calculations (DFT) shows, that all dyes exhibit small HOMO/LUMO gaps from 2.77 to 3.22 eV, which is in agreement with experimental data.

© 2017 Elsevier Ltd. All rights reserved.

## 1. Introduction

Among many types of fluorescent organic materials, compounds with π-conjugated system between electron donor (D) and electron acceptor (A) have been intensively investigated and found applications in several fields, including medicine for fluorescent markers [1], photovoltaic technologies for dye-sensitized solar cells [2] and optoelectronic devices for example, in organic light emitting diodes (OLEDs) [3–6], which can be utilized in full-color flat-panel displays for mobile phones and television. The main advantage for compounds with D-π-A structure is the variety of donor, acceptor and π-bridge groups, which allows to adjust the fluorescent material desirable properties, for example emission color. The commonly investigated D-π-A compounds consist of *N,N*-dialkyl, *N,N*-diphenyl substituted anilines [3–9], *N*-substituted carbazoles [8] as D parts and dicyanomethylene pyran [3,6,10], dicyanomethylene furan [11], pyridine [8,12] and benzothiadiazole [13] as electron A groups. As for the π-bridge, it is possible to use olefinic linkers, such as vinyl or butadienyl fragments [8,10] or different cyclic linkers as thiophene bridge [14]. However, there are not a sufficient data in the literature about comprehension of organic compound structure-luminescence property relationship, which would facilitate new suitable material derivation. Some studies deals with the comparison of different donor [3,4,9], acceptor [14] group or π-linker length [14,15] effect on luminescence properties, however continuous work to understand structure-property relationships is necessary.

2-Acyl-β-diketones, for example, 2-acetyl-1,3-indandione or 2-acetyldimedone containing three electron withdrawing carbonyl groups are excellent starting materials for D-π-A luminophores. These compounds easily react in aldol condensation reactions with electrophiles, thus forming compounds with extending conjugation system. The most interesting are the 2-acetyl-β-diketone condensation with aromatic aldehydes, which results in 2-cinnamoyl-β-diketone compounds, but only a few studies deal with the investigation of their physical and chemical properties [16–21]. Continuing our previous research work about derivatives of 2-cinnamoyl-1,3-indandione O-methyl ethers [22], we investigate new luminophores on the basis of two well-known cyclic β-diketones - 1,3-indandione and dimedone. These acceptor units are linked to various amino donors – *N,N*-dimethyl ($N(Me)_2$) and *N,N*-

* Corresponding author.
*E-mail address:* malina.ilze1@gmail.com (I. Malina).

http://dx.doi.org/10.1016/j.dyepig.2017.01.017
0143-7208/© 2017 Elsevier Ltd. All rights reserved.

diphenyl ($N(Ph)_2$), *N,N*-dibiphenyl ($N(BPh)_2$) and julolidine through different length of olefinic linkers, such as 1-hydroxyallylidene or 1-hydroxypenta-2,4-dien-1-ylidene. Our goal is to examine structure-property relationship of these luminophores to gain clearer understanding of how π-bridge length, different donor and acceptor units influences the thermal, electrochemical, absorption and fluorescent properties. DFT calculations were performed to gain understanding about electronic structures of newly synthesized compounds.

## 2. Experimental

### 2.1. Materials and instrument

All chemicals used in synthesis and analysis are commercially available and are used without further purification unless otherwise stated. The $^1H$ and $^{13}C$ NMR spectra were recorded in $CDCl_3$ solutions on a Bruker Avance 300 MHz spectrometer at 300 MHz for $^1H$- and 75 MHz for $^{13}C$- nuclei. Chemical shifts were expressed in parts per million (ppm) relative to solvent signal. The IR spectra in the range from 4000 to 650 $cm^{-1}$ were recorded on a Perkin-Elmer Spectrum 100 FTIR spectrometer using KBr pellets. Elemental analyses were performed on Euro Vector EA 3000 analyzer. Thermal properties were determinated on a Perkin Elmer STA 6000 instrument. Each sample was heated from 30 to 550 °C with heating rate 10 °C/min in nitrogen atmosphere. The purity of prepared organic compounds was established on Waters 2695 HPLC using Waters 2996 Photodiode array UV–Vis detector. The chromatographic analyses were performed using XTerra® MS C18 (5 μm 2.1 × 100 mm) column, 50% Acetonitrile/0,1% formic acid solution as mobile phase and flow rate 0.2 ml/min. Low resolution mass spectra were acquired on a Waters EMD 1000MS mass detector (ESI + mode, voltage 30 V). The UV–Vis absorption spectra of all compounds in solutions and in thin films were acquired using Perkin-Elmer 35 UV/Vis spectrometer. Emission spectra in solutions and in thin films were measured on QuantaMaster 40 steady state spectrofluorometer (Photon Technology International, Inc.). Absolute photoluminescence quantum yields in solutions and in thin films were determined using QuantaMaster 40 steady state spectrofluorometer (Photon Technology International, Inc.) equipped with 6 inch integrating sphere by LabSphere. The cyclic voltammograms were recorded using a computer controlled electrochemical system PARSAT 2273. The measurements were carried out using a three-electrode cell configuration. Stationary glassy carbon disk (Ø 0.5 cm) was used as a working electrode, Pt wire - as an auxiliary electrode. Potentials were measured *vs* saturated calomel electrode (SCE) and recalculated *vs* normal hydrogen electrode (NHE). The potential scan rate was 100 mV/s. Electrochemical redox reactions were studied in 0,1 M tetra butylammonium tetrafluorophosphate ($TBAPF_6$) solution in acetonitrile under Ar atmosphere. Density functional theory (DFT) has been performed using ORCA program [23] and Gaussian 09 [24] package. For auxiliary tasks Avogadro program [25] was used. The geometry optimization of all compounds were obtained using non-local functional B3LYP with 6-311G** [26] basis set. Diffraction data was collected on a Bruker-Nonius KappaCCD diffractometer using graphite monochromated Mo-Kα radiation (λ = 0.71073 Å). The crystal structure was solved by direct methods [27] and refined by full-matrix least squares [28] using maXus complex of programs [29]. Crystal data or compound **16**: monoclinic, $a$ = 12.6089(2), $b$ = 10.5952(2), $c$ = 25.3021(5) Å; β = 104.0991(8)°; $V$ = 3278.33 (10) $Å^3$; $Z$ = 8, μ = 0.09 $mm^{-1}$; $d_{calc}$ = 1.270 $g/cm^3$; space group – $P2_1/a$. For structure refinement 5716 independent reflections with $I > 2\sigma(I)$ were used; the final $R$-factor is 0.137.

### 2.2. Synthesis

2-Acetyl-1,3-indandione (**8**) was synthesized as described in the literature [30], 2-acetyldimedone (**9**) as in Ref. [31], 4-(bis(4-iodophenyl)amino)benzaldehyde (**5**) and 4-(di([1,1'-biphenyl]-4-yl)amino)benzaldehyde (**7**) as in Ref. [32]. Synthesis of starting materials **3**, **7** are shown in Scheme 1 and in Scheme 2 the synthesis of D-π-A compounds **11**–**20** are depicted.

#### 2.2.1. Synthesis of (E)-3-(4-(N,N-dimethylamino)phenyl) acrylaldehyde (3)

A mixture of 4-*N,N*-dimethylaminobenzaldehyde (**1**) (5.00 g, 34 mmol) and 25 ml concentrated sulfuric acid was cooled to 0 °C. Then 1 ml distilled water was added slowly. The solution was cooled to 0 °C and acetaldehyde (**2**) (5.6 ml, 102 mmol) was added dropwise. During the addition temperature of reaction mixture was not allowed to exceed 2 °C. After that dark colored reaction mixture was stirred at 0 °C for 0.5 h and then poured into ice water and neutralized with 10% NaOH solution until pH 7. The obtained brown solution was filtered and crude product was washed with distilled water, crystallized from ethanol twice to give orange solid. Yield: 56%, m.p. = 134–136 °C. FT-IR (KBr, $cm^{-1}$): 2921, 2801, 2738, 1662, 1599, 1527, 1456, 1373. $^1H$ NMR (300 MHz, $CDCl_3$, ppm): δ = 9.62 (1H, d, $J$ = 7.5 Hz), 7.48 (2H, d, $J$ = 7.5 Hz), 7.41 (1H, d, $J$ = 13.1 Hz), 6.71 (2H, d, $J$ = 7.5 Hz), 6.57 (1H, dd, $J$ = 7.5 Hz, 13.1 Hz), 3.08 (6H, s). MS ($C_{11}H_{13}NO$), $m/z$: 176.2 ($M^+$).

#### 2.2.2. Synthesis of derivatives of 2-cinnamoyl-1,3-indandiones (11–15)

To 2-acetyl-1,3-indandione **8** (1.88 g, 10 mmol) and corresponding derivative of benzaldehyde **1**,**3**,**4**,**7**,**10** (10 mmol) piperidine (5 mmol) was added. Reaction mixture was refluxed at 110 °C for 4 h, then it was cooled to 80 °C and 8 ml of ethanol was added. Solution was boiled for 30 min, and after cooling, the formed crystals were filtered off and washed with ethanol. Products were recrystallized from $CH_2Cl_2$ and EtOH mixture.

*(E)*-2-(3-(4-(*N,N*-dimethylamino)phenyl)-1-hydroxyallylidene)-1H-indene-1,3(2H)-dione (**11**), purple crystals, Yield 67%, m.p. = 210–211 °C. FT-IR, (KBr, $cm^{-1}$): 3019, 2904, 1698, 1631, 1588, 1567, 1523. $^1H$ NMR (300 MHz, $CDCl_3$, ppm): δ = 13.30 (1H, s), 7.93 (1H, d, $J$ = 15.0 Hz), 7.88–7.78 (2H, m), 7.80 (1H, d, $J$ = 15.0 Hz), 7.73–7.67 (2H, m), 7.65 (2H, d, $J$ = 7.5 Hz), 6.81 (2H, d, $J$ = 7.5 Hz), 3.10 (6H, s). $^{13}C$ NMR (75 MHz, $CDCl_3$, ppm): δ = 197.31, 189.01, 174.35, 152.52, 146.30, 140.95, 138.76, 134.31, 133.51, 131.40, 122.67, 122.07, 111.83, 106.49, 40.23. MS, $m/z$: 320.2 ($M^+$), 318.2 ($M^-$). Anal. Calcd. (%) for $C_{20}H_{17}NO_3$: C, 75.22; H, 5.37; N, 4.39; found: C, 75.22; H 5.33; N, 4.31.

*(E)*-2-(3-(4-(*N,N*-diphenylamino)phenyl)-1-hydroxyallylidene)-1H-indene-1,3(2H)-dione (**12**), purple crystals, Yield 60%, m.p. = 220–222 °C. FT-IR, (KBr, $cm^{-1}$): 3049, 3033, 1696, 1632, 1617, 1548, 1504, 1489. $^1H$ NMR (300 MHz, $CDCl_3$, ppm): δ = 13.25 (1H, s), 7.90 (1H, d, $J$ = 13.5 Hz), 7.85–7.80 (3H, m), 7.75–7.66 (2H, m), 7.55 (2H, d, $J$ = 7.5 Hz), 7.37–7.32 (4H, m), 7.20–7.13 (6H, m), 7.04 (2H, d, $J$ = 7.5 Hz). $^{13}C$ NMR (75 MHz, $CDCl_3$, ppm): δ = 197.59, 188.83, 173.92, 151.01, 145.30, 145.00, 139.10, 138.85, 133.80, 133.50, 130.30, 129.61, 126.00, 124.58, 122.50, 122.06, 120.90, 114.73, 107.33. MS, $m/z$: 444.2 ($M^+$), 442.3 ($M^-$). Anal. Calcd. (%) for $C_{30}H_{21}NO_3$: C, 81.25; H, 4.77; N, 3.16; found: C 81.64; H, 4.82; N, 3.54.

*(E)*-2-(3-(1,2,3,5,6,7-hexahydropyrido[3,2,1-ij]quinolin-9-yl)-1-hydroxyallylidene)-1H-indene-1,3(2H)-dione (**13**), dark green crystals, Yield 50%, m.p. = 225–226 °C. FT-IR, (KBr, $cm^{-1}$): 3014, 2939, 2843, 1693, 1627, 1567, 1543, 1513, 1463. $^1H$ NMR (300 MHz, $CDCl_3$, ppm): δ = 13.25 (1H, s), 7.84 (1H, d, $J$ = 14.3 Hz), 7.82–7.76 (2H, m), 7.69 (1H, d, $J$ = 14.3 Hz), 7.67–7.61 (2H, m), 7.20 (2H, s), 3.31 (4H, t, $J$ = 2.6 Hz), 2.78 (4H, t, $J$ = 2.6 Hz), 1.99 (4H, quint,

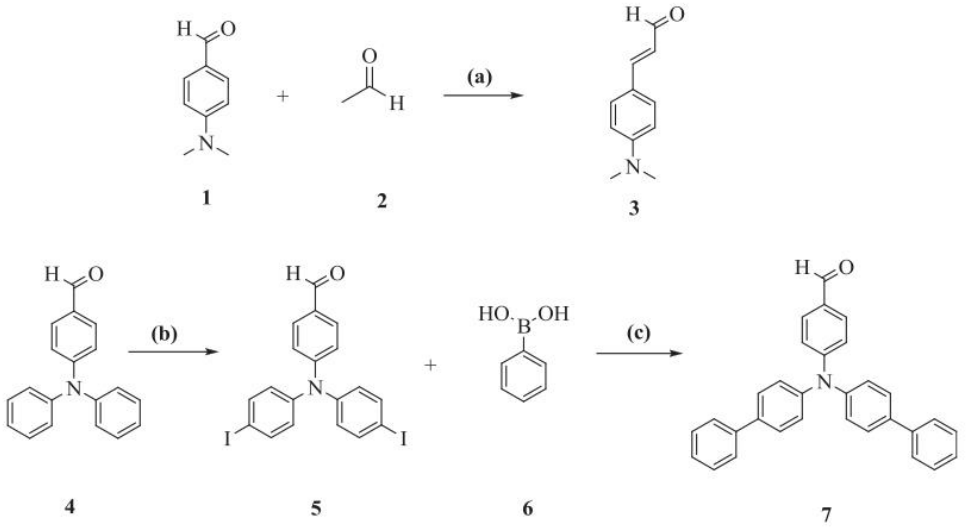


**Scheme 1.** Reagents and conditions: (**a**) – concentrated $H_2SO_4$, 0 °C, 0.5 h; 10% NaOH. (**b**) KI, $KIO_3$, $(CH_3COO)_2O$, 80 °C, 4 h. (**c**) – 2 M $Na_2CO_3$, $Pd(PPh_3)_4$, dry toluene, 80 °C, 24 h.

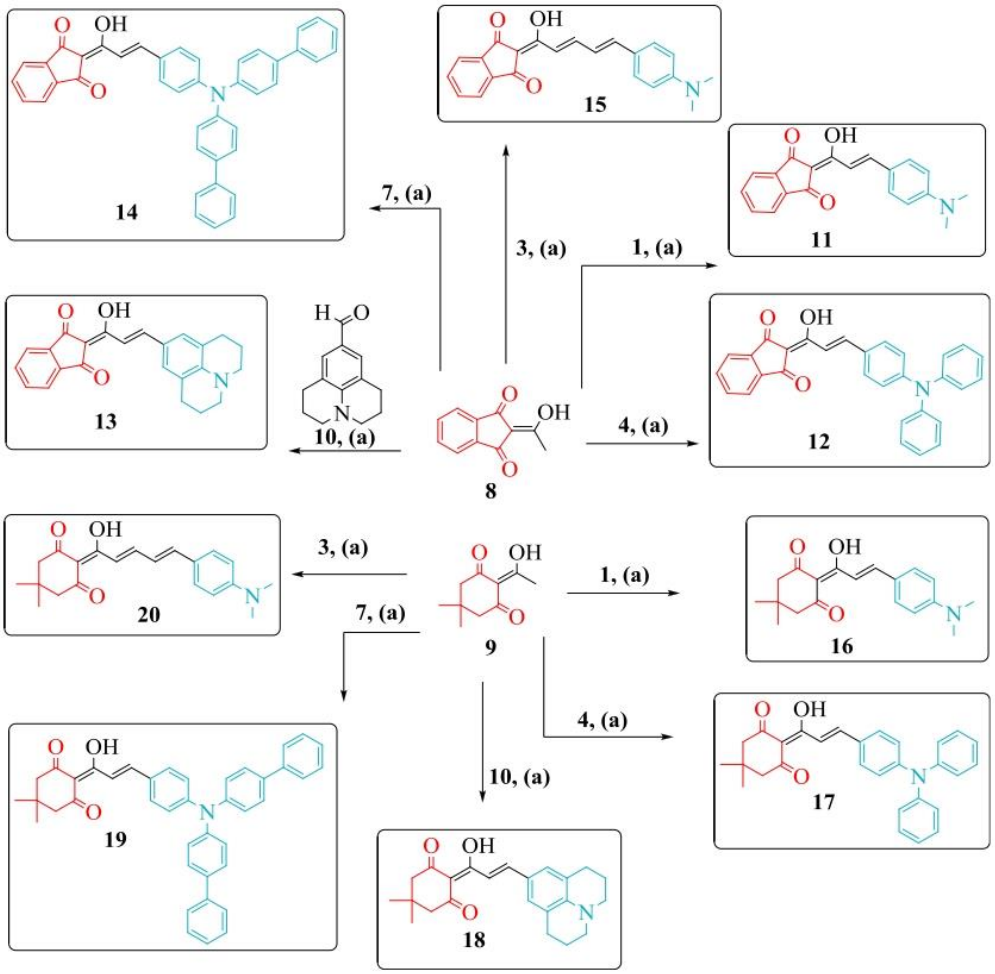


**Scheme 2.** Reagents and conditions: (**a**) – piperidine, 100 °C, 4 h; ethanol, 80 °C, 0,5 h.

$J$ = 2.6 Hz). $^{13}$C NMR (75 MHz, $CDCl_3$, ppm): δ = 197.51, 189.00, 174.58, 147.30, 147.00, 140.80, 139.00, 133.93, 133.54, 129.70, 122.30, 122.20, 122.00, 121.95, 110.00, 106.30, 50.00, 27.10, 21.35. MS, *m/z*: 372.4 ($M^+$). Anal. Calcd. (%) for $C_{24}H_{21}NO_3$: C, 77.61; H, 5.70; N, 3.77; found: C, 77.62; H, 5.72; N, 3.99.

(*E*)-2-(3-(4-(*N*,*N*-di([1,1'-biphenyl]-4-yl)amino)phenyl)-1-hydroxyallylidene)-1H-indene-1,3(2H)-dione (**14**), dark red solid, Yield: 40%, m.p. = 202–203 °C. FT-IR (KBr, $cm^{-1}$): 3063, 3027, 1700, 1622, 1584, 1558, 1505, 1483. $^1$H NMR (300 MHz, $CDCl_3$, ppm): δ = 13.28 (1H, s), 7.96–7.83 (4H, m), 7.73–7.66 (3H, m), 7.73–7.69 (2H, m), 7.64–7.58 (10H, m), 7.50–7.45 (4H, m), 7.37 (2H, d, $J$ = 6.0 Hz), 7.30–7.27 (4H, m), 7.16 (2H, d, $J$ = 6.0 Hz). $^{13}$C NMR (75 MHz, $CDCl_3$, ppm): δ = 197.39, 188.73, 173.65, 150.57, 145.69, 144.83, 141.05, 140.33, 138.81, 137.38, 134.65, 133.81, 130.66, 128.85, 128.23, 127.95, 127.23, 126.84, 122.45, 122.08, 121.58, 114.96, 107.26. MS, *m/z*: 596.3 ($M^+$), 594.6 ($M^-$). Anal. Calcd. (%) for $C_{42}H_{29}NO_3$: C, 84.68; H, 4.91; N, 2.35; found: C, 84.23; H, 4.92; N, 2.52.

2-((2*E*,4*E*)-5-(4-(*N*,*N*-dimethylamino)phenyl)-1-hydroxypenta-2,4-dien-1-ylidene)-1H-indene-1,3(2H)-dione (**15**), purple solid, Yield: 30%, m.p. = 230–231 °C. FT-IR (KBr, $cm^{-1}$): 3017, 2913, 2903, 2821, 1690, 1634, 1618, 1572, 1572, 1554, 1522. $^1$H NMR (300 MHz, $CDCl_3$, ppm): δ = 13.19 (1H, s), 7.85–7.78 (2H, m), 7.73–7.66 (3H, m), 7.45 (2H, d, $J$ = 7.5 Hz), 7.40 (1H, d, $J$ = 13.5 Hz), 7.06–6.92 (2H, m), 6.70 (2H, d, $J$ = 7.5 Hz) 3.09 (6H, s). $^{13}$C NMR (75 MHz, $CDCl_3$, ppm): δ = 197.41, 188.82, 173.72, 151.51, 147.30, 144.83, 140.93, 138.82, 134.43, 133.61, 129.61, 124.02, 122.98, 122.34, 121.88, 118.01, 112.01, 106.63, 40.15. MS, *m/z*: 346.3 ($M^+$), 344.3 ($M^-$). Anal. Calcd. (%) for $C_{22}H_{19}NO_3$: C, 76.50; H, 5.54; N, 4.06; found: C, 76.45; H, 5.54; N, 4.20.

### 2.2.3. Synthesis of derivatives of 2-cinnamoyl-1,3-dimedones (**16**–**20**)

Compounds **16**–**20** were synthesized by same procedure as for compounds **11**–**15**, except 2-acetyldimedone (**9**) was used instead of 2-acetyl-1,3-indandione (**8**).

(*E*)-2-(3-(4-(*N*,*N*-dimethylamino)phenyl)-1-hydroxyallylidene)-5,5-dimethylcyclohexane-1,3-dione (**16**), pink crystals, Yield 56%, m.p. = 154–155 °C. FT-IR, (KBr, $cm^{-1}$): 3093, 2957, 2923, 2866, 2807, 1647, 1612, 1580, 1532, 1280, 1160. $^1$H NMR (300 MHz, $CDCl_3$, ppm): δ = 8.17 (1H, d, $J$ = 15.0 Hz), 8.00 (1H, d, $J$ = 15.0 Hz), 7.60 (2H, d, $J$ = 6.4 Hz), 6.69 (2H, d, $J$ = 6.4 Hz), 3.08 (6H, s), 2.56 (2H, s), 2.44 (2H, s), 1.11 (6H, s). $^{13}$C NMR (75 MHz, $CDCl_3$, ppm): δ = 201.85, 196.08, 186.76, 152.51, 147.93, 131.50, 122.94, 116.34, 111.75, 53.37, 49.27, 40.09, 30.42, 28.27.MS, *m/z*: 314.5 ($M^+$), 312.4 ($M^-$). Anal. Calcd. (%) for $C_{19}H_{23}NO_3$: C, 72.82; H, 7.40; N, 4.47; found: C, 72.90; H, 7.38; N, 4.41.

(*E*)-2-(3-(4-(*N*,*N*-diphenylamino)phenyl)-1-hydroxyallylidene)-5,5-dimethylcyclohexane-1,3-dione (**17**), orange crystals, Yield 45%, m.p. = 162–164 °C. FT-IR, (KBr, $cm^{-1}$): 3099, 3033, 2960, 2949, 2869, 1653, 1602, 1582, 1554, 1266, 1173. $^1$H NMR (300 MHz, $CDCl_3$, ppm): δ = 8.20 (1H, d, $J$ = 13.7 Hz), 7.95 (1H, d, $J$ = 13.7 Hz), 7.52 (2H, d, $J$ = 6.7 Hz), 7.35–7.30 (4H, m), 7.18–7.11 (6H, m), 7.01 (2H, d, $J$ = 6.9 Hz), 2.58 (2H, s), 2.44 (2H, s), 1.12 (6H, s). $^{13}$C NMR (75 MHz, $CDCl_3$, ppm): δ = 201.83, 195.97, 187.12, 150.67, 146.64, 146.31 130.56, 129.55, 127.89, 125.70, 124.38, 121.08, 119.49, 110.67, 53.27, 49.01, 30.45, 28.27. MS, *m/z*: 438.4 ($M^+$), 436.6 ($M^-$). Anal. Calcd. (%) for $C_{29}H_{27}NO_3$: C, 79.61; H, 6.22; N, 3.20; found: C, 79.44; H, 6.27; N, 3.29.

(*E*)-2-(3-(1,2,3,5,6,7-hexahydropyrido[3,2,1-ij]quinolin-9-yl)-1-hydroxyallylidene)-5,5-dimethylcyclohexane-1,3-dione (**18**), purple solid, Yield 52%, m.p. = 186–187 °C FT-IR, (KBr, $cm^{-1}$): 3105, 2940, 2888, 2862, 2837, 1647, 1577, 1523, 1509, 1273, 1137. $^1$H NMR (300 MHz, $CDCl_3$, ppm): δ = 8.10 (1H, d, $J$ = 13.3 Hz), 7.93 (1H, d, $J$ = 13.3 Hz), 7.16 (2H, s), 3.28 (4H, t, $J$ = 1.8 Hz), 2.75 (4H, t, $J$ = 3.5 Hz), 2.54 (2H, s), 2.43 (2H, s), 1.97 (4H, quint, $J$ = 1.8 Hz, 3.5 Hz), 1.10 (6H, s). $^{13}$C NMR (75 MHz, $CDCl_3$, ppm): δ = 201.97, 196.15, 185.95, 148.67, 146.09, 129.24, 122.11, 121.06, 114.74, 110.09, 53.31, 50.16, 49.46, 30.49, 28.36, 27.58, 21.29. MS, *m/z*: 366.3 ($M^+$), 364.5 ($M^-$). Anal. Calcd. (%) for $C_{23}H_{27}NO_3$: C, 75.59; H, 7.45; N, 3.83; found: C, 75.48; H, 7.50; N, 3.93.

(*E*)-2-(3-(4-(*N*,*N*-di([1,1'-biphenyl]-4-yl)amino)phenyl)-1-hydroxyallylidene)-5,5-dimethylcyclohexane-1,3-dione (**19**), red solid, Yield 31%, m.p. = 221–222 °C. FT-IR, (KBr, $cm^{-1}$): 3032, 2952, 2869, 1655, 1584, 1486, 1170. $^1$H NMR (300 MHz, $CDCl_3$, ppm): δ = 8.23 (1H, d, $J$ = 13.9 Hz), 7.98 (1H, d, $J$ = 13.9 Hz), 7.64–7.57 (10H, m), 7.49–7.44 (4H, m), 7.38 (2H, d, $J$ = 6.2 Hz), 7.28–7.26 (4H, m), 7.14 (2H, d, $J$ = 6.2 Hz), 2.58 (2H, s), 2.45 (2H, s), 1.12 (6H, s). $^{13}$C NMR (75 MHz, $CDCl_3$, ppm): δ = 201.91, 196.04, 187.13, 150.32, 146.20, 145.81, 140.36, 137.08, 128.83, 128.35, 128.18, 127.18, 126.83, 125.69, 121.73, 119.75, 110.63, 53.27, 49.01, 30.48, 28.28. MS, *m/z*: 590.6 ($M^+$), 588.9 ($M^-$). Anal. Calcd. (%) for $C_{41}H_{35}NO_3$: C, 83.50; H, 5.98; N, 2.38; found: C, 83.15; H, 5.98; N, 2.43.

2-((2*E*,4*E*)-5-(4-(*N*,*N*-dimethylamino)phenyl)-1-hydroxypenta-2,4-dien-1-ylidene)-5,5-dimethylcyclohexane-1,3-dione (**20**), purple crystals, Yield 52%, m.p. = 166–167 °C. FT-IR, (KBr, $cm^{-1}$): 3089, 2963, 2944, 2825, 1655, 1584, 1548, 1415, 1400, 1146. $^1$H NMR (300 MHz, $CDCl_3$, ppm): δ = 7.88–7.71 (2H, m), 7.42 (2H, d, $J$ = 6.5 Hz), 7.03–6.88 (2H, m), 6.69 (2H, d, $J$ = 6.5 Hz), 3.05 (6H, s), 2.55 (2H, s), 2.43 (2H, s), 1.10 (6H, s). $^{13}$C NMR (75 MHz, $CDCl_3$, ppm): δ = 202.06, 195.96, 186.35, 151.38, 148.74, 148.69, 144.47, 129.43, 124.10, 123.30, 122.61, 112.01, 110.37, 53.28, 49.26, 40.19, 30.42, 28.27.MS, *m/z*: 340.3 ($M^+$), 338.5 ($M^-$). Anal. Calcd. (%) for $C_{21}H_{25}NO_3$: C, 74.31; H, 7.42; N, 4.13; found: C, 73.98; H, 7.51; N, 4.23.

## 3. Results and discussion

### 3.1. Synthesis and characterization of luminophores

Schemes 1 and 2 show synthetic routes of luminophores **11**–**20**. (*E*)-3-(4-(*N*,*N*-dimethylamino)phenyl)acrylaldehyde (**3**) was obtained with moderate yield in a single step acid catalyzed aldol condensation between acetaldehyde (**2**) and 4-*N*,*N*-dimethylaminobenzaldehyde (**1**). It is worth to point out, that other methods for synthesis of cinnamaldehyde with *N*,*N*-dimethylamino donor in *para* position of phenyl ring includes multiple steps (for example, Wittig reaction between benzaldehyde derivative and Wittig reagent, which is followed by Vilsmeir reaction between obtained alkene and Vilsmeir reagent) or expensive reagents (for example, 1,3-dioxan-2-yl-tributylphosponium bromide, which is necessary in Wittig oxopropenylation reaction). $^1$H NMR spectra of compounds **3** characterizes with large *trans* constant ($J$ = 13.1 Hz) for double bond protons of cinnamoyl moiety.

Aldehyde **7** was obtained in two-step synthesis from 4-*N*,*N*-diphenylamino-benzaldehyde (**4**). In the first stage the compound was iodinated with $KIO_3$/KI mixture and the 4-(bis(4-iodophenyl) amino)benzaldehyde (**5**) was obtained. Afterwards in Pd(0) catalyzed Suzuki coupling reaction between compound **5** and phenylboronic acid (**6**), aldehyde **7** with 61% yield was synthesized.

All luminophores **11**–**20** were synthesized through Claisen-Schmidt condensation reaction between 2-acetyl-1,3-indandione **8** or 2-acetyldimedone **9** and aldehydes **1**,**3**,**4**,**7**,**10** in the presence of 5 mmol piperidine. $^1$H, $^{13}$C NMR, FT-IR characteristics as well as X-Ray analysis data for 2-cinnamoyl-1,3-indandiones **11**–**13** were reported in our previous work [22].

2-Cinnamoyldimedones **16**–**20** showed similar characteristics to compounds **11**–**15**. In $^1$H NMR spectra large coupling constants ($J$ = 13.3–15.0 Hz) were found for double bond protons of cinnamoyl fragment, indicating *trans* configuration for these compounds. However, to get unquestionable evidence, that compounds **16**–**20**

similar to cinnamoyl-1,3-indandiones exist in exocyclic enol form, a single crystal of compound **16** was obtained by slow evaporation from saturated ethanol solution for X-ray analysis.

In accordance with the X-ray diffraction data the asymmetric unit of **16** contains two independent molecules, one of them is illustrated in Fig. 1. Table 1 lists the principal bond lengths in molecular structure **16**. Due to the fact that bond lengths in two independent molecules are identical within the errors the arithmetical mean values are given in Table 1. X-ray diffraction data confirms, that derivative of 2-cinamoyldimedone **16** in solid state exist in exocyclic enol form, which is stabilized by very strong intramolecular hydrogen bond between carbonyl group oxygen atom (O1) from dimedone fragment and hydroxyl group (O9–H9) from allylidene fragment. The hydrogen bond (O1···H9–O9) is characterized with very short bond length, which is equal 2.386(7) Å (O1···H9 = 1.59 Å, O1···H9–O9 = 138°) for one of independent molecules and 2.401(7) Å (O1···H9 = 1.48 Å, O1···H9–O9 = 149°) for the second. Due to intramolecular hydrogen bond following structural parameters are presented in the molecule – bond lengths for C3–C2 are longer than for C1–C2, meaning that bond C3–C2 has less double bond order. Moreover, comparing carbonyl groups bond lengths C3–O2 and C1–O1, the latter ones are significantly longer, showing more single bond character. These data lead to conclusion, that there is extended resonance system between atoms O1–C1–C2–C9–O9 stabilized by the intramolecular hydrogen bond presented in the molecule, similarly that it was reported to the 2-cinnamoyl-1,3-indandione **13** [22]. Unfortunately, a bad quality of the crystals **16** does not permit to provide a detailed analysis of the molecular geometry.

Interestingly, compound **16** does not show any intermolecular hydrogen bonds between molecules, like it was observed for compound **13** [22]. Dihedral angles between least-squares planes of dimedone and 4-*N*,*N*-dimethylaminophenyl moiety are 7.4 and 13.2° for two independent molecules. These values indicate that molecule **16** are almost planar.

### 3.2. Thermal properties

In order to investigate thermal behavior of luminophores **11**–**20**, thermogravimetric (TG) analysis were carried out between 30 and 550 °C in nitrogen atmosphere. Table 2 displays decomposition temperatures ($T_{5\%}$) of investigated compounds and TG curves of some luminophores are depicted in Fig. 2. Obtained results from TG analysis indicate, that all 10 dyes are thermally stable up to 200 °C. Identical order in the decrease of thermal stability depending on donor group was found for both 2-cinnamoyl derivatives **11**–**14** and **16**–**19** and can be arranged in the following order: $N(BPh)_2$>$N(Ph)_2$>$N(Me)_2$>Julolidyl. This sequence indicates that the thermal destruction of compounds begins with the destruction of the donor part.

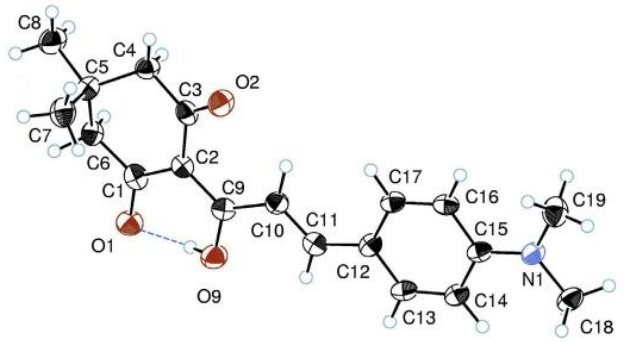


**Fig. 1.** ORTEP drawing of compound **16** with the atom numbering scheme. All non-hydrogen atoms are drawn as 50% probability ellipsoids.

**Table 1**
Principal bond lengths in the structure **16**.

| Bond | Bond length, Å |
|---|---|
| C1–O1 | 1.276(7) |
| C1–C2 | 1.427(7) |
| C2–C3 | 1.478(7) |
| C2–C9 | 1.433(7) |
| C3–O2 | 1.218(6) |
| C9–O9 | 1.309(7) |

**Table 2**
Thermal and electrochemical properties of compounds **11**–**20**.

| Code | $T_{5\%}$[a], °C | $E_{ox}$, V | $E_{red}$, V |
|---|---|---|---|
| **11** | 218 | 0.80 | −1.17 |
| **12** | 283 | 1.05 | −1.07 |
| **13** | 216 | 0.60 | −1.21 |
| **14** | 290 | 0.98 | −1.04 |
| **15** | 238 | 0.66 | −1.04 |
| **16** | 233 | 0.81 | −1.32 |
| **17** | 271 | 1.07 | −1.19 |
| **18** | 219 | 0.61 | −1.36 |
| **19** | 288 | 0.96 | −1.18 |
| **20** | 234 | 0.67 | −1.15 |

[a] $T_{5\%}$ is temperature of 5% weight loss, respectively.

Investigation of TG curves also confirms conclusion, that thermal degradation pattern is influenced by amino donor group. Compounds with amino donors containing alkyl chains, julolidine shows lower $T_{5\%}$ values than those with phenyl or biphenyl groups. Compounds **11**,**13**,**15** as well as **16**,**18**,**20** starts to decompose at ~215–230 °C and the first possible volatile fragments are the alkyl chains on the nitrogen atom. The alkyl chain replacement with phenyl rings leads to increased $T_{5\%}$ (270–290 °C), similar observations was reported for tricyanovinyldihydrofuran D-π-A dyes with different amino donors [33].

2-Cinnamoyl-1,3-indandione **14** and 2-cinnamoyl-dimedone **19** with bulky $N(BPh)_2$ substituent exhibit the highest $T_{5\%}$ over 280 °C, which can be explained with their higher molecular mass, and additional π-π stackings. Prolonging the π-bridge by one more double bond between donor and acceptor (**11** → **15** and **16** → **20**) leads to slight increase in $T_{5\%}$, for example compound **11** $T_{5\%}$ is 218 °C, but for its analogue **15** decomposition temperature is increased to 238 °C. As it can be seen from Fig. 2(**a**) compounds with julolidine donor (**13** and **18**) as well as ones with $N(BPh)_2$ group (**14** and **19**) shows two-step weight loss TG curves. On the other hand TG curves of dyes with $N(Me)_2$ donor group (**11**,**15**,**16**,**20**) can be characterized with one-step decomposition. The acceptor group shows no influence on the form of TG curve. The TG analysis results show, that all compounds have good enough thermal stability for the application in optoelectronic devices.

### 3.3. Electrochemical properties

Cyclic voltammetry was employed for all synthesized compounds to investigate their redox behavior. The results are summarized in Table 2 and some compounds cyclic voltammograms in acetonitrile are shown in Fig. 3. For all studied compounds both electrode processes - cathodic reduction as well as anodic oxidation are electrochemically irreversible in acetonitrile.

The structure of the electron acceptor moieties (1,3-indandione or dimedone) has a negligible influence (10–20 mV) on the

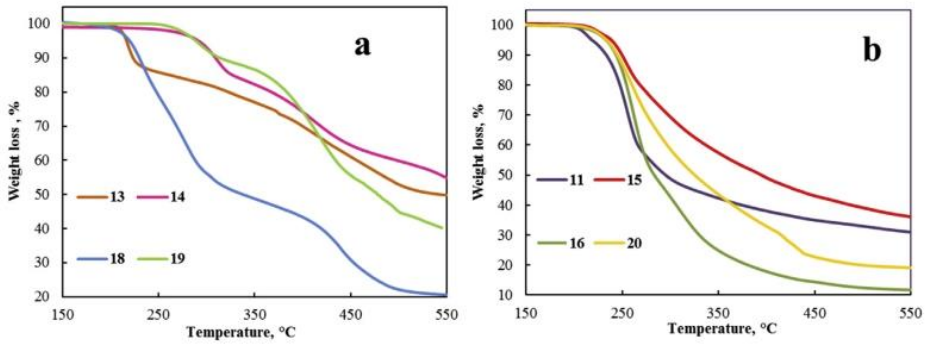


**Fig. 2.** TG curves of compounds **13**,**14**,**18**,**19** (**a**) and compounds **11**,**15**,**16**,**20** (**b**).

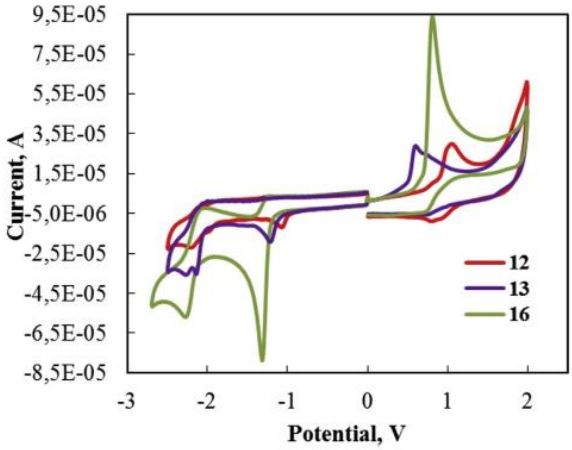


**Fig. 3.** Cyclic voltammograms of compounds **12**,**13**,**16** in acetonitrile solutions.

oxidation potentials of the dyes (**11**/**16**; **12**/**17**; **13**/**18**; **14**/**19**), while prolongation of the olefinic linker facilitates anodic oxidation for 140 mV (**11**/**15**; **16**/**20**). Similar effects on oxidation properties caused by elongation of planar π-bridge were reported for imidazole moiety containing dyes [34]. The oxidation potentials of the luminophores are affected mainly by the substituents attached directly to the nitrogen atom. Independently from acceptor moiety (1,3-indandione or dimedone) electron-rich julolidine fragment undergoes oxidation at 0.60 V. Furthermore, dyes **11** and **16** with two electron-donating methyl groups at the nitrogen atom undergo oxidation 200 mV more anodically. For the luminophores **12**, **17**, **14** and **19** conjugation between the nitrogen lone electron pair and the π-electron system of the aromatic rings results in the highest oxidation potential values.

The electrochemical reduction process of compounds **11**–**20** are localized on their acceptor moieties. Cathodic peak potentials of the compounds **16**–**20** are 110–150 mV more negative than those of **11**–**15**, confirming that 1,3-indandione possesses stronger electron-acceptor strength than dimedone moiety.

### 3.4. Absorption properties

In order to gain information about compounds structure-property relationship, UV–Vis absorption spectra (c~$1.5\cdot10^{-5}$ M) in a series of solvents with different dielectric constants and thin films were investigated. The data of absorption band maxima ($\lambda_{abs}$) are summarized in Table 3 and some compounds absorption spectra are depicted in Fig. 4. All compounds **11**–**20** in chloroform show intense visible light absorption with band maxima from 466 to 540 nm. The absorption bands are wide and correspond to intramolecular charge transfer (ICT) transitions $\pi(D)\rightarrow\pi^*(A)$ between donor and acceptor groups in the molecule. For compounds **14** and **19** with $N(BPh)_2$ substituent in cinnamoyl fragment second absorption band around 341 nm are observed and can be attributed to $\pi\rightarrow\pi^*$ transitions of the aminodibiphenylamino moiety. Due to the difference in acceptor groups the ICT band occurs in the different spectral range – from 466 to 509 nm for dimedone derivatives and from 502 to 540 nm for 1,3-indandione derivatives. Amino donor groups based on their structure and strength also shows some effect on ICT band position. By varying the donor moiety on 1,3-indandione and dimedone derivatives, ICT band is red shifted in the order: $N(Me)_2$~$N(Ph)_2$<$N(BPh)_2$<Julolidyl. $N(Me)_2$ and $N(Ph)_2$ shows similar donor strength based on absorption data. However, it is known, that $N(Ph)_2$ could have stronger donor character than $N(Me)_2$ group [9], but due to nitrogen atom lone pair conjugation with π-electrons of phenyl rings, the donor strength is reduced and $\lambda_{abs}$ does not show the expected red shift. Furthermore, change of the donor unit from $N(Ph)_2$ to $N(BPh)_2$ results in bathochromic shift of $\lambda_{abs}$ (+10 nm) for both dimedone and 1,3-indandione compounds. This fact could be explained with nitrogen atom lone pair weaker conjugation with biphenyl than phenyl group, which results in enhanced donor character for $N(BPh)_2$ group. This assumption was confirmed by theoretical chemical calculations (Section 3.6). Among all investigated amino groups julolidyl moiety shows the most red shift of $\lambda_{abs}$, which can be explained with its rigid character and probably, more effective p-π conjugation, which ensures stronger electron-donating effect than other amino substituents. Furthermore, prolongation of the π-bridge between D and A moieties (**11** → **15** and **16** → **20**) also shows some effect on ICT bands position in the spectra. As expected red shift of the $\lambda_{abs}$ was observed in the absorption spectra - 1,3-indandione derivative (**15**) shows +17 nm shift, but dimedone derivative (**20**) +20 nm bathochromic shift. It was concluded, that the strongest impact on absorption spectra position is due to the acceptor unit and π-bridge length between A and D moieties and amino donor group strength shows lesser effect.

Only four luminophores (**12**,**14**,**17**,**19**) with $N(Ph)_2$ and $N(BPh)_2$ donor groups formed thin films from chloroform solutions. As it can be seen from Fig. 4(**b**) in solid state compounds **12**,**14**,**17**,**19** absorption bands are wider and slight effect on absorption band maxima are observed compared to data obtained from solution samples.

The investigation of solvatochromic behavior of the newly synthesized dyes was also conducted, $\lambda_{abs}$ in different solvents are summarized in Table 3. Unfortunately, some compounds were

**Table 3**
Absorption and emission characteristics of compounds **11**–**20** in a series in solutions and thin films.

| Solvent | Dye | $\lambda_{abs}$, nm | $\lambda_{em}$, nm | $\lambda_{sts}$[a], $cm^{-1}$ | $\Phi$[b] | Dye | $\lambda_{abs}$, nm | $\lambda_{em}$, nm | $\lambda_{sts}$[a], $cm^{-1}$ | $\Phi$[b] |
|---|---|---|---|---|---|---|---|---|---|---|
| Toluene | **11** | 499 | 548 | 1762 | 0.12 | **12** | 499 | 568 | 2434 | 0.52 |
| THF | | 499 | 575 | 2649 | <0.01 | | 492 | 624 | 4300 | 0.49 |
| $CHCl_3$ | | 503 | 566 | 2212 | 0.03 | | 502 | 621 | 3817 | 0.76 |
| MeCN | | 500 | – | – | – | | –[c] | – | – | – |
| MeOH | | 501 | 582 | 2779 | <0.01 | | –[c] | – | – | – |
| Thin film | | – | – | – | – | | 501 | 643 | 4407 | 0.07 |
| Toluene | **13** | 532 | 577 | 1466 | 0.15 | **14** | 506 | 586 | 2698 | 0.93 |
| THF | | 536 | 601 | 2018 | <0.01 | | 502 | 662 | 4815 | 0.10 |
| $CHCl_3$ | | 540 | 595 | 1712 | <0.01 | | 512 | 663 | 4448 | 0.21 |
| MeCN | | 540 | – | – | – | | 494 | – | – | – |
| MeOH | | 537 | – | – | – | | 499 | – | – | – |
| Thin film | | – | – | – | – | | 500 | 667 | 5008 | 0.13 |
| Toluene | **15** | 511 | 613 | 3256 | 0.12 | **16** | 454 | 528 | 3087 | 0.05 |
| THF | | 517 | 664 | 4282 | 0.31 | | 456 | 546 | 3615 | 0.19 |
| $CHCl_3$ | | 520 | 647 | 3775 | 0.25 | | 467 | 548 | 3165 | 0.15 |
| MeCN | | 514 | – | – | – | | 459 | 571 | 4273 | 0.02 |
| MeOH | | 518 | 680 | 4599 | <0.01 | | 466 | 570 | 3915 | 0.01 |
| Thin film | | – | – | – | – | | – | – | – | – |
| Toluene | **17** | 456 | 549 | 3715 | 0.40 | **18** | 497 | 552 | 2005 | 0.31 |
| THF | | 452 | 624 | 6098 | 0.56 | | 496 | 575 | 2770 | 0.32 |
| $CHCl_3$ | | 466 | 612 | 5119 | 0.78 | | 509 | 577 | 2315 | 0.36 |
| MeCN | | 449 | 675 | 7457 | <0.01 | | 503 | 593 | 3017 | <0.01 |
| MeOH | | 451 | 643 | 6621 | <0.01 | | 510 | 600 | 2941 | <0.01 |
| Thin film | | 466 | 600 | 4793 | 0.17 | | – | – | – | – |
| Toluene | **19** | 465 | 572 | 4023 | 0.79 | **20** | 478 | 593 | 4057 | 0.05 |
| THF | | 460 | 636 | 6016 | 0.16 | | 476 | 635 | 5260 | 0.22 |
| $CHCl_3$ | | 476 | 654 | 5718 | 0.16 | | 487 | 624 | 4508 | 0.15 |
| MeCN | | 453 | 666 | 7060 | <0.01 | | 475 | 662 | 5947 | 0.13 |
| MeOH | | –[c] | – | – | – | | 483 | 666 | 5689 | 0.05 |
| Thin film | | 478 | 626 | 4946 | 0.13 | | – | – | – | – |

[a] Stokes shifts.
[b] Absolute photoluminescence quantum yield.
[c] Insoluble.

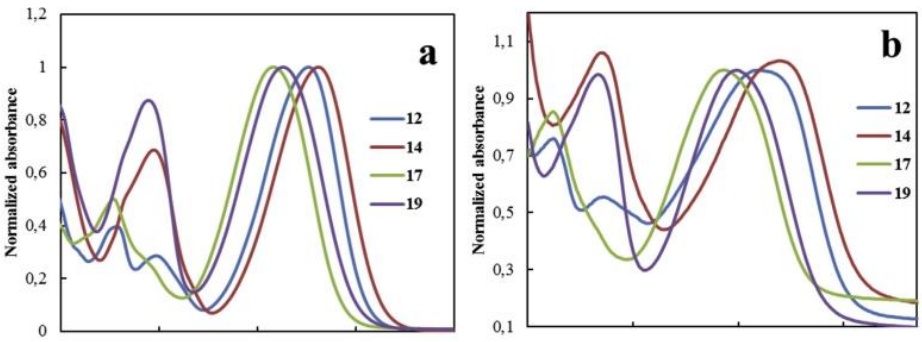


**Fig. 4.** Absorption spectra of compounds **12**,**14**,**17**,**19** in chloroform (c~$1.5 \cdot 10^{-5}$ M) solutions (**a**) and in thin films (**b**).

insoluble in polar solvents (MeCN and MeOH) and full solvatochromic outlook was not obtained. From the data depicted in Table 3 it was concluded, that these dyes did not show notable solvatochromism and upon changing the solvents polarity from non-polar toluene to polar MeCN, only small $\lambda_{abs}$ shifts (1–12 nm) were observed.

### 3.5. Emission properties

Emission properties of synthesized compounds were examined in series of solvents solutions (c~$1.5 \cdot 10^{-5}$M) and in thin films. The data of emission band maxima ($\lambda_{em}$), Stokes shifts ($\lambda_{sts}$), and absolute photoluminescence quantum yields ($\Phi$) are summarized in Table 3.

The emission color of solutions of **11**–**20** covers a very wide spectral range from bright green to red light region. In non-polar toluene emission color varies from green to red light region, but in polar solvents it shifts from yellow to red region. Emission spectra of dyes **11**–**20** are characterized with wide emission bands (Fig. 5), and emission band maxima $\lambda_{em}$ is influenced by many factors, including dyes structure. Due to the difference in acceptor groups the $\lambda_{em}$ position in chloroform solutions shifts – from 548 to 654 nm for dimedone compounds and from 566 to 663 nm for 1,3-indandione derivatives. This red shift of $\lambda_{em}$ for 1,3-indandione derivatives compared to the same analogues with dimedone cycle (**11**/**16**; **12**/**17**; **13**/**18** etc) can be explained with additional phenyl

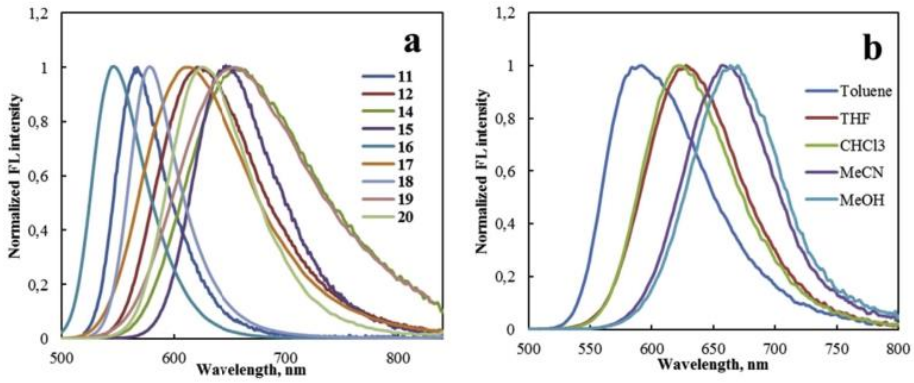


**Fig. 5.** (**a**) – Emission spectra of compounds **11**–**20** in chloroform (c~1.5·10$^{-5}$ M) solutions; (**b**) – solvatofluorochromism of dye **20.**

ring of 1,3-indandione moiety, which ensures more extend π-conjugation in the molecules. Moreover, amino donor group structure and strength show major impact on $\lambda_{em}$ position in the spectra. By varying the donor moiety $\lambda_{em}$ is red shifted in the following order: $N(Me)_2$<Julolidyl < $N(Ph)_2$<$N(BPh)_2$. $N(Me)_2$ group having the weakest donor character from all amino substituents shows the $\lambda_{em}$ at 566 nm (dye **11**) and at 548 nm (dye **16**), while dyes containing $N(BPh)_2$ substituent shows ~100 nm red shift and emits red light at 663 nm (dye **14**) and 654 nm (dye **19**) in chloroform solutions. All investigated compounds based on their amino donor structures can be divided into two groups - compounds containing amino donors with alkyl chains (Julolidyl, $N(Me)_2$) and phenyl groups ($N(BPh)_2$, $N(Ph)_2$). There is essential difference in the Stokes shifts for these groups – first group show smaller $\lambda_{sts}$ (in the range from 1466 to 2779 cm$^{-1}$ for 1,3-indandione derivatives, and 2005-4273 cm$^{-1}$ for dimedone derivatives) than second group. Smallest $\lambda_{sts}$ was obtained for julolidyl group containing compounds and can be explained with similar dipole moment from ground and excited state for these dyes. Similar observations were found for other D-π-A dyes [15]. Observed relatively large Stokes shifts ($\lambda_{sts}$) for compounds **12**,**14**,**15** as well as for **17**,**19**,**20** indicates, that after excitation these molecules undergo some structural reorientation, for example, excited state intramolecular proton transfer (ESIPT), which is common for compounds with strong intramolecular hydrogen bond in the molecules [35]. Large Stokes shifts are a huge advantage for dyes for OLED application, because it decreases the possibility of self-absorption, which can reduce the total emission efficiency.

The extension of the π-linker between D and A parts (**11** → **15** and **16** → **20**) also has an impact on $\lambda_{em}$ position in the spectra. As expected longer conjugation bridge leads to bathochromic shift of $\lambda_{em}$, for example, $\lambda_{em}$ **11** → **15** is red shifted for 81 nm in chloroform solutions.

Another factor, which greatly influences the $\lambda_{em}$ position in the spectra, is the solvents polarity. Strong positive solvatofluorochromism was observed by all investigated compounds. Upon changing the solvents polarity from non-polar (toluene) to polar (MeOH), $\lambda_{em}$ shifts in range from 24 to 126 nm. Among the compounds investigated dyes with the diphenyl and dibiphenyl substituents exhibit largest emission shifts due to considerably stronger donor groups in the molecules, for example, dye **17** shows the maximum $\lambda_{em}$ shift +126 nm going from toluene to MeCN. It is common for D-π-A dyes, which exhibit ICT, to have bathochromic shift of $\lambda_{em}$ [8,9] in polar solvents and can be explained with excited state more polar character than ground state. Therefore, $\lambda_{em}$ shows larger shifts with solvents polarity change, than $\lambda_{abs}$.

Also the absolute fluorescence quantum yields (Φ) are largely dependent on the solvents polarity. With the increase in solvents polarity (MeOH, MeCN) the decrease in Φ was observed and almost all dyes except **16** and **20** were non-emissive in polar environment. In non-polar toluene dyes with $N(BPh)_2$ donor group (**14**, **19**) shows high Φ values (0.93 and 0.79), dyes **11**–**13**,**15**,**17**,**18** - moderate Φ ranging from 0.12 to 0.52, however remaining compounds **16**,**20** exhibit relatively low quantum yields (0.05). Moreover, moderate to high quantum yields (0.10–0.78) were obtained in THF and $CHCl_3$ solvents. Obtained quantum yield data in different solvents demonstrates that emission properties of investigated dyes are affected more by the solvents polarity than nature of the donor group. Low emission intensity in polar media can be explained with interactions between dyes and polar solvent in polar excited state, which leads to pronounced non-radiative deactivation [9,36].

Photoluminescence spectra of thin films for compounds **12**,**14**,**17** and **19** can be characterized as wide emission bands with maximum $\lambda_{em}$ in the range of 600–667 nm and with quantum yields Φ from 0.07 to 0.17. Decrease in Φ could be explained with concentration quenching, due to intermolecular interactions in solid state. In the future to increase Φ values in thin films, these dyes need to be doped in polymer matrix. However, still acquired Φ values in thin films are notable, indicating, that compounds **12**,**14**,**17** and **19** might be the promising red light emitting optical materials for optoelectronic devices.

From all synthesized compounds, dye **17** with dimedone cycle as acceptor, $N(Ph)_2$ as donor and 1-hydroxyallylidene as π-bridge shows the most promising optical properties for application in OLED. Intense visible light absorption at ~455 nm, large Stokes

**Table 4**
Calculated HOMO/LUMO energy levels and band gaps of luminophores **11**–**20**.

| Code | HOMO, eV | LUMO, eV | $Eg^{DFT}$, eV[a] | $E_g^{Opt}$, eV[b] | $E_g$, V[c] |
|---|---|---|---|---|---|
| **11** | −5.37 | −2.28 | 3.09 | 2.25 | 1.97 |
| **12** | −5.34 | −2.47 | 2.87 | 2.22 | 2.12 |
| **13** | −5.11 | −2.19 | 2.92 | 2.11 | 1.81 |
| **14** | −5.27 | −2.50 | 2.77 | 2.16 | 2.02 |
| **15** | −5.22 | −2.43 | 2.79 | 2.04 | 1.70 |
| **16** | −5.38 | −2.16 | 3.22 | 2.37 | 2.13 |
| **17** | −5.33 | −2.37 | 2.96 | 2.30 | 2.26 |
| **18** | −5.16 | −2.11 | 3.05 | 2.21 | 1.97 |
| **19** | −5.26 | −2.40 | 2.86 | 2.26 | 2.14 |
| **20** | −5.21 | −2.34 | 2.87 | 2.15 | 1.82 |

[a] Calculated from DFT calculations: $Eg^{DFT}$ = LUMO−HOMO.
[b] Optical band gap $E_g^{Opt}$ calculated from UV–Vis spectra in $CHCl_3$ solution: $E_g^{Opt} = 1240/\lambda_{onset}$ (nm).
[c] Electrochemical band gap $E_g$ calculated from cyclic voltammograms: $E_g = E_{ox} - E_{red}$.

shifts (3715-6098 $cm^{-1}$) and bright yellow or orange-light emission in non-polar solvents as well as in thin film with moderate to high quantum yields (0.17–0.78) is characteristic for these dye. However, due to the demand for intense red-light emitting organic materials dye **14** with 1,3-indandione as acceptor unit, $N(BPh)_2$ as donor and 1-hydroxyallylidene as π-bridge show some potential application, due to its emission profile ($\lambda_{em}$~663 nm with $\Phi = 0.13–0.21$) in THF, $CHCl_3$ and in thin film.

### 3.6. Quantum-chemical calculation of electronic structures

To better understand the effect of the electronic structure on different photophysical properties of synthesized dyes, the density functional theory (DFT) was performed using ORCA program and Gaussian 09 *ab initio* quantum chemical software package. The calculated HOMO and LUMO energy levels of all dyes are depicted in Table 4. The obtained optimized geometries reveal that compounds with alkyl amino substituents (**11**,**13**,**15** and **16**,**18**,**20**) have nearly planar structure. However, dyes with phenyl amino groups ($N(Ph)_2$, $N(BPh)_2$) shows out of plane twisting. In compounds **12**, **14** as well as in **17**, **19** phenyl and biphenyl groups are twisted out of the plane of the cinnamoyl fragment with dihedral angles of −30.3, −31.2, −30.1 and −32.1°, respectively. Comparison of these dihedral angles of luminophores with $N(Ph)_2$ and ones with

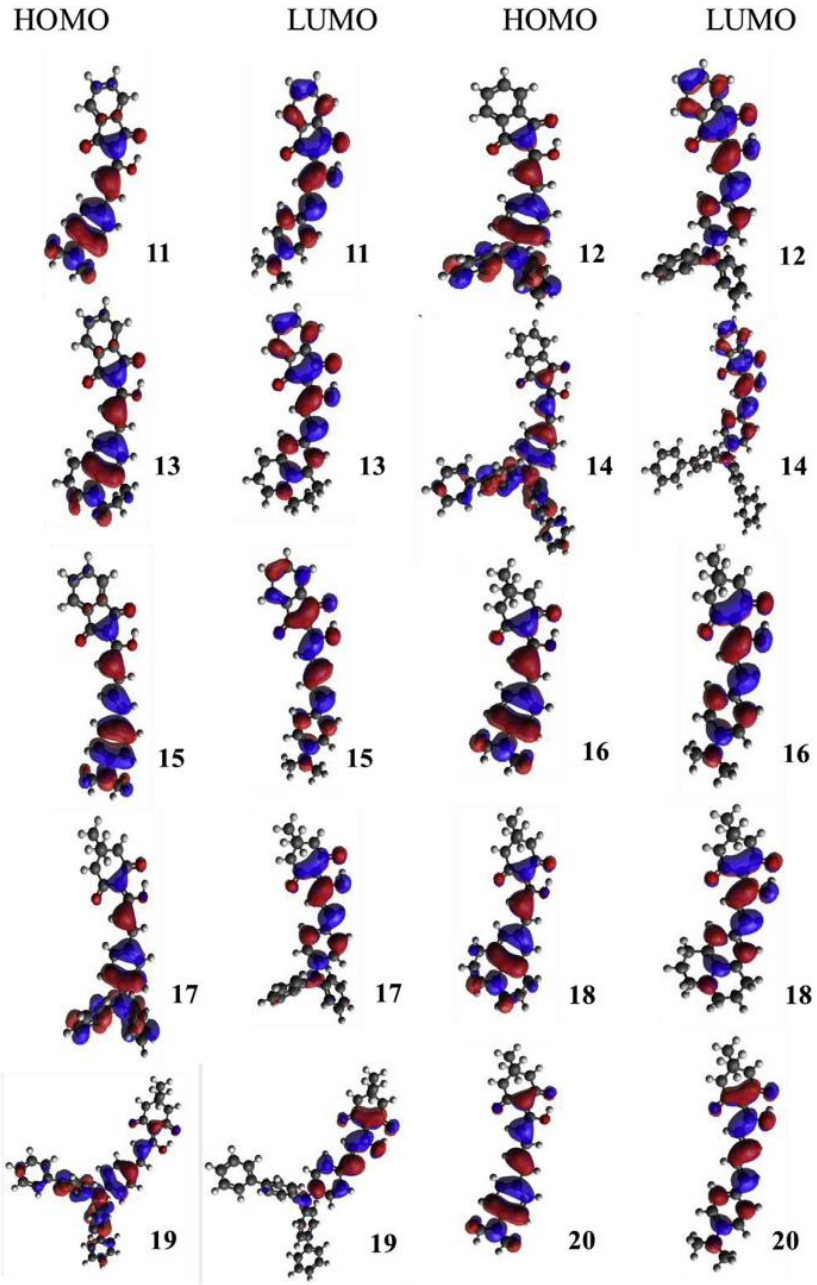


**Fig. 6.** HOMO and LUMO orbitals of optimized ground state structures of compounds **11**–**20**, obtained using B3LYP 6-311G** set.

$N(BPh)_2$ donor group (**12**/**14**, **17**/**19**), leads to the fact, that latter ones have less planar donor moiety, and nitrogen atom lone pair conjugation with biphenyl group is weaker, which results in enhanced donor character for $N(BPh)_2$. This conclusion is in agreement with absorption data of these luminophores. Moreover, such twisting out of the plane for these four compounds could lead to lowered absorption maxima, which was observed in $CHCl_3$ solutions (see paragraph 3.4.) and disarranged the order of donor strength based on absorption maxima. Similar observations were reported for different amino donor containing 4-pyridylbutadienes [8].

Fig. 6 shows the HOMO and LUMO orbitals of optimized ground state structures. HOMO orbitals of compounds **11**–**20** are mainly localized on the donor unit and cinnamoyl part of the molecule and the delocalization is not influenced by acceptor moiety. On contrary LUMO orbitals are localized on the acceptor and cinnamoyl moiety. Such a charge distribution leads to conclusion, that there is noticeable intramolecular charge transfer presented in HOMO→LUMO transition. Similar localization of molecular orbitals and charge distribution was reported for derivatives of cinnamoyl pyrones [17].

Optical ($E_g^{Opt}$) and electrochemical ($E_g$) bandgap, as well as bandgap ($Eg^{DFT}$) calculated from theoretically obtained HUMO/LUMO levels are depicted in Table 4. From the data of electronic levels, it can be seen that, band gap ($Eg^{DFT}$) calculated with DFT method are in the range from 2.77 to 3.22 eV and reduces with the increase of strength of the donor groups, for example, compound **11** has the largest difference between HOMO-LUMO levels and weakest donor group character. Moreover, there is relationship between conjugation length of D-π-A system and band gap – molecules with larger HOMO-LUMO band gap have shorter conjugation length, for example, luminophores **15** and **20** with longer π-spacer between A and D units presents the smallest $Eg^{DFT}$ values.

Optical and electrochemical band gaps are in the range 2.04–2.37 eV and 1.70–2.26 eV, respectively. The difference between calculated $Eg^{DFT}$ and experimentally obtained $E_g^{Opt}$ and $E_g$ band gap values can be explained with use of different methods and conditions for experiments. All three method results shows, that compounds with prolonged π-bridge and $N(Me)_2$ donor (**15**, **20**) has the smallest band gap value and, from the other hand compounds (**11**, **16**) with same donor unit and shorter conjugation length exhibit the largest band gap values.

## 4. Conclusions

In summary, the synthesis of ten D-π-A dyes containing different amino substituents as donors (D), 1,3-indandione or dimedone as acceptors (A) and 1-hydroxyallylidene or 1-hydroxypenta-2,4-dien-1-ylidene as π-bridge are reported. Donor, acceptor and π-bridge influence on absorption, emission, electrochemical and thermal properties are investigated. Investigated dyes exhibit high thermal stability above 200 °C, negligible solvatochromic behavior and noticeable solvatofluorochromism changing solvents polarity as well as intense green, yellow, orange and red light luminescence with quantum yields from 0.03 to 0.93 in non-polar solvents. Prolongation of π-bridge by one double bond in 2-cinnamoyl-1,3-indandione and dimedone derivatives leads to red shift of absorption and emission, enhanced photoluminescence quantum yield and decomposition temperature, as well as reduced oxidation potential. Substitution of a strong, bulky amino donor groups (diphenylamino and dibiphenylamino) in dyes structures leads to higher quantum yields, red-shifted emission, and large Stokes shifts.

For practical application in OLED dye **17** with dimedone cycle as acceptor, $N(Ph)_2$ as donor and 1-hydroxyallylidene as π-bridge, and dye **14** with 1,3-indandione as acceptor unit, $N(BPh)_2$ as donor and 1-hydroxyallylidene as π-bridge shows the most promising properties among all investigated compounds. These two dyes showed high thermal stability with $T_{5\%}$>270 °C, film forming properties and excellent optical properties. Compound **17** is characterized with intense visible light absorption at ~455 nm, large Stokes shifts (3715-6098 $cm^{-1}$) and bright yellow (~549 nm) or orange-light (~620 nm) emission in non-polar solvents as well as in thin film with moderate to high quantum yields (0.17–0.78). However, due to the demand for intense red-light emitting organic materials dye **14** show some potential application, due to its emission profile ($\lambda_{em}$~663 nm with $\Phi$ = 0.10–0.21) in THF, $CHCl_3$ and in thin film.

## Acknowledgements

This work was supported by the doctoral studies grants of Material Science and Applied Chemistry of Riga Technical University (Grant Nr. 34-14000-DOK.MLĶF) and the National research program of Latvia "IMIS2". The authors thank Ms. Chem. I. Mihailovs for his help with DFT calculations.

## Supplementary material

The deposition number CCDC 1510493 for compound **16** contains the supplementary crystallographic data for this paper. These data can be obtained free of charge at www.ccdc.cam.ac.uk/data_request/cif or from the Cambridge Crystallographic Data Centre (CCDC), 12 Union Road, Cambridge CB2 1EZ, UK; fax: +44 (0) 1223 336033; email:deposit@ccdc.cam.ac.uk.

## References

[1] Bai D, Benniston AC, Clift S, Baisch U, Steyn J, Everitt N, et al. Low molecular weight Neutral Boron Dipyrromethene (Bodipy) dyads for fluorescence-based neural imaging. J Mol Struct 2014;1065–6:10–5. http://dx.doi.org/10.1016/j.molstruc.2014.02.026.
[2] Bobe SR, Gupta A, Rananaware A, Bilic A, Xiang W, Li J, et al. Insertion of a naphthalenediimide unit in a metal-free donore acceptor organic sensitizer for efficiency enhancement of a dye-sensitized solar cell. Dyes Pigm 2016;134:83–90. http://dx.doi.org/10.1016/j.dyepig.2016.06.038.
[3] Yao YS, Zhou QX, Wang XS, Wang Y, Zhang BW. A DCM-Type Red-fluorescent dopant for high-performance organic electroluminescent devices. Adv Funct Mater 2007;17:93–100. http://doi.wiley.com/10.1002/adfm.200600055.
[4] Yoon JY, Lee JS, Yoon SS, Kim YK. Red fluorescent Donor-π-Acceptor type materials based on chromene moiety for organic light-emitting diodes. Bull Korean Chem Soc 2014;35:1670–4. http://dx.doi.org/10.5012/bkcs.2014.35.6.1670.
[5] Hwang DH, Lee JD, Lee MJ, Lee C. Organic light-emitting diode using a new DCM derivative as an efficient orange–red doping molecule. Curr Appl Phys 2005;5:244–8. http://dx.doi.org/10.1016/j.cap.2004.02.009.
[6] Chang YJ, Chow TJ. Highly efficient red fluorescent dyes for organic light-emitting diodes. J Mater Chem 2011;21:3091–9. http://dx.doi.org/10.1039/c0jm03109g.
[7] Yang Y, Bo S, Wang H, Liu F, Liu J, Qiu L, et al. Novel chromophores with excellent electro-optic activity based on double-donor chromophores by optimizing thiophene bridges. Dyes Pigm 2015;122:139–46. http://dx.doi.org/10.1016/j.dyepig.2015.06.012.
[8] Agnihotri H, Mahalingavelar P, Mande H, Ghalsasi P, Kanvah S. Amino substituted 4-pyridylbutadienes: synthesis and fluorescence investigations. Dyes Pigm 2015;123:341–8. http://dx.doi.org/10.1016/j.dyepig.2015.08.018.
[9] Palakollu V, Kanvah S. α-Cyanostilbene based fluorophores: aggregation-induced enhanced emission, solvatochromism and the pH effect. New J Chem 2014;38:5736–46. http://dx.doi.org/10.1039/c4nj01103a.
[10] Zhao P, Tang H, Zhang Q, Pi Y, Xu M, Sun R, et al. The facile synthesis and high efficiency of the red electroluminescent dopant DCINB: a promising alternative to DCJTB. Dyes Pigm 2009;82:316–21. http://dx.doi.org/10.1016/j.dyepig.2009.01.01.
[11] Kim SH, Lee SY, Gwon SY, Son YA, Bae JS. D–p–A solvatochromic charge transfer dyes containing a 2-cyanomethylene-3-cyano-4,5,5-trimethyl-2,5-dihydrofuran acceptor. Dyes Pigm 2010;84:169–75. http://dx.doi.org/10.1016/j.dyepig.2009.07.012.
[12] Li H, Guo Y, Li G, Xiao H, Lei Y, Huang X, et al. Aggregation-Induced fluorescence emission properties of Dicyanomethylene-1,4-dihydropyridine derivatives. J Phys Chem C 2015;119:6737–48. http://dx.doi.org/10.1021/

jp511060k.
[13] Behramand B, Molin F, Gallardo H. 2,1,3-Benzoxadiazole and 2,1,3-benzothiadiazole-based fluorescent compounds: synthesis, characterization and photophysical/electrochemical properties. Dyes Pigm 2012;95:600–5. http://dx.doi.org/10.1016/j.dyepig.2012.06.001.
[14] Genin E, Hugues V, Clermont G, Herbivo C, Castro MCR, Comel A, et al. Fluorescence and two-photon absorption of push–pull aryl(bi)thiophenes:structure–property relationships. Photochem Photobiol Sci 2012;11:1756–66. http://dx.doi.org/10.1039/c2pp25258a.
[15] Fulopova A, Magdolen P, Sigmundova I, Zahradnik P, Rakovsky E, Cigan M. Benzotristhiazole based chromophores for nonlinear optics. J Mol Struct 2012;1027:70–80. http://dx.doi.org/10.1016/j.molstruc.2012.06.018.
[16] Mitsuya M, Suzuki T, Koyama T, Shirai H, Taniguchi Y, Satsuki M, et al. Bright red organic light-emitting diodes doped with a fluorescent dye. Appl Phys Lett 2000;77:3272–4. http://dx.doi.org/10.1063/1.1326491.
[17] Tykhanov DA, Sanin EV, Serikova II, Yaremenko FG, Roshal AD. Cinnamoyl pyrones in proton-donating media: electronic structure and spectral properties of protolytic forms. Spectrochim Acta A Mol Biomol Spectrosc 2011;83:221–30. http://dx.doi.org/10.1016/j.saa.2011.08.022.
[18] Zyabrev K, Dekhtyar M, Vlasenko Y, Chernega A, Slominskii Y, Tolmachev A. New 2,2-difluoro-1,3,2(2H)oxazaborines and merocyanines derived from them. Dyes Pigm 2011;92:749–57. http://dx.doi.org/10.1016/j.dyepig.2011.05.025.
[19] Ahmedova A, Atanasov V, Marinova P, Stoyanov N, Mitewa M. Synthesis, characterization and spectroscopic properties of some 2-substituted 1,3-indandiones and their metal complexes. Cent Eur J Chem 2009;7:429–38. http://dx.doi.org/10.2478/s11532-009-0039-6.
[20] Ahmedova A, Pavlovic G, Zhiryakova D, Šišak D, Stoyanov N, Springborg M, et al. Experimental and theoretical study on the structure and optical properties of 2-acyl-1,3-indandiones – conformational effects. J Mol Struct 2010;981:10–20. http://dx.doi.org/10.1016/j.molstruc.2010.07.008.
[21] Ahmedova A, Marinova P, Pavlovic G, Guncheva M, Stoyanov N, Mitewa M. Structure and properties of a series of 2-cinnamoyl-1,3-indandiones and their metal complexes. J Iran Chem Soc 2012;9:297–306. http://dx.doi.org/10.1007/s13738-011-0024-9.
[22] Malina I, Kampars V, Turovska B. Synthesis, optical and electrochemical properties of substituted 2-cinnamoyl-1,3-indandione o-methyl ethers. J Mol Struct 2016;1115:241–9. http://dx.doi.org/10.1016/j.molstruc.2016.02.090.
[23] Nesse F. The ORCA program system. Wiley Interdiscip Rev Comput Mol Sci 2011;2:73–8. http://dx.doi.org/10.1002/wcms.81.
[24] Frisch MJ, Trucks GW, Schlegel HB, Scuseria GE, Robb MA, Cheeseman JR, et al. Gaussian 09, revision D.01. Wallingford CT: Gaussian, Inc.; 2009.
[25] Hanwell MD, Curtis DE, Lonie DC, Vandermeerschd T, Zurek E, Hutchison GR. Avogadro: an advanced semantic chemical editor, visualization, and analysis platform. J Cheminform 2012;4:17–34. http://dx.doi.org/10.1186/1758-2946-4-17.
[26] Krishnan R, Binkley JS, Seeger R, Pople JA. Self-consistent molecular orbital methods. XX. A basis set for correlated wave functions. J Chem Phys 1980;72:650–6. http://dx.doi.org/10.1063/1.438955.
[27] Altomare A, Burla M, Cammali M, Cascarano G, Giacovazzo C, Guagliardi A, et al. SIR97: a new tool for crystal structure determination and refinement. J Appl Cryst 1999;32:115–9. http://dx.doi.org/10.1107/S0021889898007717.
[28] Sheldrick GM. A short history of SHELX. Acta Cryst 2008;A64:112–22. http://dx.doi.org/10.1107/S0108767307043930.
[29] Mackay S, Dong W, Edwards C, Henderson A, Gilmore CJ, Stewart N, et al. maXus, integrated crystallography software. Bruker-Nonius and University of Glasgow; 2003.
[30] Teotonio EES, Brito HF, Viertler H, Faustino WM, Malta OL, deSá GF, et al. Synthesis and luminescent properties of $Eu^{3+}$-complexes with 2-acyl-1,3-indandionates (ACIND) and TPPO ligands: the first X-ray structure of Eu–ACIND complex. Polyhedron 2006;25:3488–94. http://dx.doi.org/10.1016/j.poly.2006.06.035.
[31] Akhrem AA, Lakhvich FA, Budai SI, Khlebnicova TS, Petrusevish II. A new simple synthesis of 2-acylcyclohexane-1,3-diones. Synthesis 1978;12:925–7. http://dx.doi.org/10.1055/s-1978-24943.
[32] Heoa J, Oha JW, Ahna HI, Leec SB, Choc SE, Kimc MR, et al. Synthesis and characterization of triphenylamine-based organic dyes for dye-sensitized solar cells. Synth Met 2010;160:2143–50. http://dx.doi.org/10.1016/j.synthmet.2010.08.001.
[33] Liu F, Yang Y, Wang H, Liu J, Hu C, Huo F, et al. Comparative studies on structure-nonlinearity relationships in a series of novel second-order nonlinear optical chromophores with different aromatic amine donors. Dyes Pigm 2015;120:347–56. http://dx.doi.org/10.1016/j.dyepig.2015.05.003.
[34] Kulhánek J, Bures F, Mikysek T, Ludvík J, Pytela O. Imidazole as a central p-linkage in Y-shaped push pull chromophores. Dyes Pigm 2011;90:48–55. http://dx.doi.org/10.1016/j.dyepig.2010.11.004.
[35] Enchev V, Bakalova S, Ivanova G, Stoyanov N. Excited state intramolecular proton transfer an 2-acetylindan-1,3-dione. Chem Phys Lett 1999;314:234–8. http://dx.doi.org/10.1016/S0009-2614(99)01160-4.
[36] Gupta VD, Tathe AB, Padalkar VS, Umape PG, Sekar N. Red emitting solid state fluorescent triphenylamine dyes: synthesis, photo-physical property and DFT study. Dyes Pigm 2013;97:429–39. http://dx.doi.org/10.1016/j.dyepig.2012.12.024.

3.pielikums

**Malina I,** Juhnevics N, Kampars V. Study of thermal and optical properties of dibenzoyl-methane Eu(III) organic complexes. *Proc. Est. Acad. Sci.*, **2017**, *66*(4), 493-500.

DOI: doi.org/10.3176/proc.2017.4.11

© 2017, Estonian Academy Publishers. This manuscript version is made available under the CC BY-NC 4.0 License http://creativecommons.org/licenses/by-nc/4.0/

Proceedings of the Estonian Academy of Sciences,
2017, **66**, 4, 493–500
https://doi.org/10.3176/proc.2017.4.11
Available online at www.eap.ee/proceedings

FUNCTIONAL MATERIALS

# Study of thermal and optical properties of dibenzoylmethane Eu(III) organic complexes

Ilze Malina*, Nikolajs Juhnevics, and Valdis Kampars

Institute of Applied Chemistry, Riga Technical University, Paula Valdena Str. 3, Riga, LV-1048, Latvia

Received 28 April 2017, revised 14 July 2017, accepted 21 August 2017, available online 30 November 2017

© 2017 Authors. This is an Open Access article distributed under the terms and conditions of the Creative Commons Attribution-NonCommercial 4.0 International License (http://creativecommons.org/licenses/by-nc/4.0/).

**Abstract.** Two Europium(III) organic complexes (*ternary* complex $Eu(DBM)_3(PHEN)$ and *tetrakis* complex $[Eu(DBM)_4]N(Et)_4$, where DBM is dibenzoylmethane and PHEN is 1,10-phenantroline) were synthesized and their structures proven with $^1$H-NMR spectroscopy, elemental analysis, FT-IR and mass spectroscopy. Their photophysical properties have been investigated in solution, solid-state and in poly-*N*-vinylcarbazole (PVK) films varying complex composition from 1 to 15 wt%. Both complexes exhibit intense UV light absorption and bright red-light emission with maximum wave length at 612 nm. It was shown that *tetrakis* complex in solution, solid-state and PVK films have enhanced photoluminescence properties compared to *ternary* complex due to four DBM molecules in $Eu^{3+}$ coordination sphere, which leads to more effective excited energy transfer to $Eu^{3+}$ ion. In THF solutions both complexes are characterized with low photoluminescence quantum yields (4% and 6%), in PVK films – moderate quantum yields (14–48%), but in solid state with high quantum yields (56% and 75%). Thermal properties for pure complexes and their PVK films were studied with thermogravimetric analysis. Both complexes exhibit high thermal degradation temperatures of 304 °C for *ternary* and 267 °C for *tetrakis* complex, but their PVK films show even higher degradation temperature (over 370 °C).

**Key words:** optical materials, europium, dibenzoylmethane ligands, luminescence, Poly-*N*-vinylcarbazole films.

## 1. INTRODUCTION

Unique optical properties such as narrow emission bands, high photoluminescence quantum yields, large Stokes shifts and long excited state lifetimes mark out $Eu^{3+}$ organic complexes among other organic red-light emitting materials for technological application in solid-state lighting and flat panel displays [1]. Luminescence of complexes arises from efficient excited energy transfer from organic ligand molecules to central metal ion, resulting in bright emission of $Eu^{3+}$. Investigation of effective ligands for $Eu^{3+}$ organic complexes mainly focuses on β-diketones due to their intense UV absorption (high extinction coefficient), relatively easy synthesis, good solubility in commonly used solvents and good thermal stability. Dibenzoylmethane (DBM) is one of the most used ligand for $Eu^{3+}$ organic complexes. Many scientific articles report DBM $Eu^{3+}$ *ternary* complexes, where $Eu^{3+}$ is coordinated with three DBM ligands and one secondary ligand, such as 1,10-phenantroline (PHEN) [2,3]. This complex and its poly-*N*-vinylcarbazole films have been fully examined as emitting layers in organic light emitting diodes (OLED) [4,5]. However, to our knowledge there are only 3 works devoted to investigate *tetrakis* $Eu^{3+}$ complexes with DBM ligands with general structure $[Eu(DBM)_4]^-$ ($Eu^{3+}$ complex is anionic and charge neutralization is required by quaternary ammonium ion countercation) [6–8]. $Eu^{3+}$ *tetrakis* complexes usually exhibit higher luminescence efficiency and chemical stability as well as better solubility in solvents than

* Corresponding author, malina.ilze1@gmail.com

*ternary* complexes. There are no data in the literature dealing with comparison of *ternary* and *tetrakis* complexes bearing the same β-diketone ligands, therefore in this work DBM is synthesized, and two $Eu^{3+}$ complexes – *ternary* complex $Eu(DBM)_3(PHEN)$ and *tetrakis* complex $[Eu(DBM)_4]N(Et)_4$ are characterized and their thermal and optical properties are reported. However, pure organic complexes display low thermal- and photo-stability as well as poor mechanical properties and film formability, which limits their practical use. Therefore, another objective of this work is the investigation of optical and thermal properties of poly-*N*-vinylcarbazole (PVK) films containing different concentration of the $Eu^{3+}$ complexes.

## 2. EXPERIMENTAL SECTION

### 2.1. Materials and methods

$EuCl_3 \cdot 6H_2O$ (99.99%) was purchased from Acros Organics, 1,10-phenantroline (99%), ammonium tetraethylbromide (98%), acetophenone (>96%), ethylbenzoate (>99%) – from Alfa Aesar and poly-*N*-vinylcarbazole (PVK) from ABCR (GmbH&Co).

$^1$H-NMR spectra were recorded in $CDCl_3$ and $(CD_3)_2CO$ solutions (~5–7 mg/ml) on a Brucker Avance 300 MHz spectrometer. CHN elemental analyses were performed on Euro Vector EA 3000 analyser. The FT–IR spectra were recorded on a Perkin–Elmer Spectrum 100 FTIR spectrometer using KBr pellets. Low resolution mass spectra were determined on a Waters EMD 1000MS mass detector (ESI mode, voltage 30 V). Thermal properties of solid complexes and PVK films were determined on a Perkin Elmer STA 6000 instrument. Solid complexes were heated from 30–900 °C with heating rate 10 °C/min, but PVK films from 30–700 °C with heating rate 3 °C/min in nitrogen atmosphere. The UV-Vis absorption spectra (solutions and films) were determined on Perkin–Elmer 35 UV/Vis spectrometer. Emission and excitation spectra were measured on QuantaMaster 40 steady state spectrofluorometer (Photon Technology International, Inc.). Absolute photoluminescence quantum yields were determined using 6 inch integrating sphere by LabSphere coupled to the spectrofluorometer. The values reported are the average of three independent measurements for each sample. PVK thin films were obtained with Laurell WS-400B-NPP/LITE spin coater.

### 2.2. Synthesis

The synthesis of DBM (**3**) and its *ternary* $Eu(DBM)_3(PHEN)$ **C1** and *tetrakis* complexes $[Eu(DBM)_4]N(Et)_4$ **C2** are shown in Fig. 1. DBM was synthesized as in reference [9].

**C1**: To a solution of DBM (**3**) (0.0963 g, 0.429 mmol, 3 eq.) and 1,10-phenantroline (0.0258 g, 0.143 mmol, 1 eq.) in 15 ml ethanol 10% NaOH solution was added until pH~7–8. Then, 2 ml distilled water solution

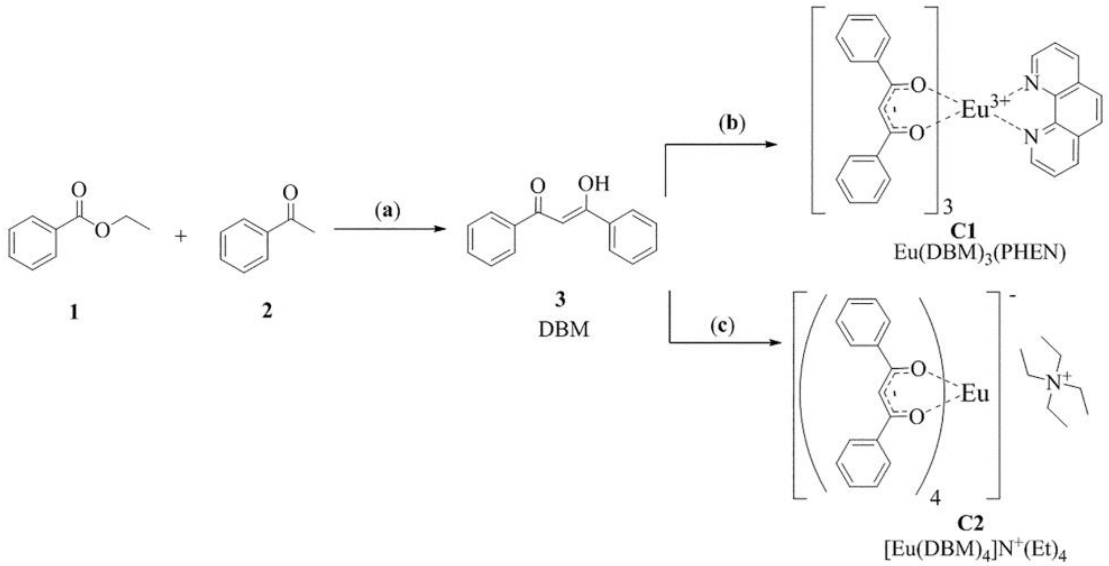


**Fig. 1.** Synthesis of complexes **C1** and **C2**; (a) – 1) NaH, THF, 65 °C; 2) 10% HCl; (b) – 10% $NaOH/H_2O/EtOH$, 1,10-Phenantroline, $EuCl_3 \cdot 6H_2O$; (c) – 10% $NaOH/H_2O/EtOH$, $N(Et)_4Br$, $EuCl_3 \cdot 6H_2O$.

containing $EuCl_3 \cdot 6H_2O$ (0.0525 g, 0.143 mmol, 1 eq.) was added dropwise and resulting solution was refluxed and stirred for 2 hours. Formed precipitate was separated by suction filtration, washed with ethanol (10 ml) and distilled water (10 ml) and dried in vacuum at 50 °C for 24 hours. Light yellow powder, yield 75%; $^1$H-NMR (300 MHz, $CDCl_3$, ppm): 10.98 (2H, d, PHEN-H), 10.59 (2H, br s, PHEN-H), 9.95 (2H, br s, PHEN-H), 8.95 (2H, br s, PHEN-H), 6.82-6.75 (18H, m, Ar-H), 5.95-5.93 (12H, m, Ar-H), 2.88 (3H, s, C=CH). Anal. Calcd. For $EuC_{57}H_{41}N_2O_6$: C, 68.33; H, 4.12; N, 2.80; found C, 67.67; H, 4.41; N, 2.75; FT-IR (KBr, cm$^{-1}$): 3059, 3026, 2925 ($\nu_{Csp2H}$); 1595 ($\nu_{C=O}$); 1550, 1528, 1478 ($\nu_{C=C}$); 1411 ($\nu_{C=N}$); ESI(+)-MS: (*m/z*) 181.1 [PHEN+H]$^+$; 821.4 [$^{151}$Eu(DBM)$_3$+H]$^+$; 823.3 [$^{153}$Eu(DBM)$_3$+H]$^+$.

**C2**: Solution of DBM (**3**) (0.1504 g, 0.671 mmol, 3 eq.) in 15 ml ethanol was stirred until complete dissolution. Then ammonium tetraethylbromide (0.0528 g, 0.252 mmol, 1.5 eq.) in 2 ml ethanol was added. 10% NaOH was added to the solution until pH~7–8. Afterwards, 2 ml distilled water solution containing $EuCl_3 \cdot 6H_2O$ (0.0617 g, 0.168 mmol, 1 eq.) was added dropwise and resulting solution was stirred for 2 hours in the room temperature. Formed precipitate was separated by suction filtration, washed with ethanol (10 ml) and distilled water (10 ml), then crystallized from acetonitrile and dried in vacuum at 50 °C for 24 hours. Light orange needles, yield 85%; $^1$H-NMR (300 MHz, $(CD_3)_2CO$, ppm): 7.78-7.75 (16H, br m, Ar-H), 7.22-7.14 (24H, br m, Ar-H), 4.00 (8H, br q, $(CH_3\text{-}C\underline{H}_2)_4N^+$), 2.85 (4H, s, C=CH), 1.65 (12H, br t, $(\underline{C}H_3\text{-}CH_2)_4N^+$). Anal. Calcd. For $EuC_{68}H_{64}NO_8$: C, 69.50; H, 5.49; N, 1.19; found C, 69.57; H, 5.67; N, 1.52; FT-IR (KBr, cm$^{-1}$): 3056, 3026 ($\nu_{Csp2H}$); 2988, 2926 ($\nu_{Csp3H}$); 1600 ($\nu_{C=O}$); 1557, 1513, 1478,1417 ($\nu_{C=C}$); 1307, 1278($\nu_{C\text{-}N}$); ESI(+)-MS: (*m/z*) 130.1 [N(Et)$_4$]$^+$; ESI(-)-MS: (*m/z*) 1043.8 [$^{151}$Eu(DBM)$_4$]$^-$; 1045.0 [$^{153}$Eu(DBM)$_4$]$^-$.

### 2.3. Fabrication of PVK films

PVK and required amount of complexes **C1** or **C2** were dissolved in 1 ml THF and the resulting mixture was heated at 40 °C for 0.5 h. Afterwards polymer film was spin-coated on a glass substrate using following parameters: speed 800 rpm, acceleration 800 rpm/sec 1 min. Then obtained films were dried in 45 °C for 2 h.

## 3. RESULTS AND DISCUSSION

### 3.1. Molecular structure confirmation

The elemental analysis, $^1$H-NMR spectroscopy and mass spectra data of complex **C1** (Eu(DBM)$_3$(PHEN)) demonstrates that mole ratio of $Eu^{3+}$:DBM:PHEN is 1:3:1, but for complex **C2** ([Eu(DBM)$_4$]N(Et)$_4$) $Eu^{3+}$:DBM:N(Et)$_4$ is 1:4:1. Mass spectra analysis of **C1** shows peaks with *m/z*: 181.1; 821.4 and 823.3 corresponding to [PHEN+H]$^+$; [$^{151}$Eu(DBM)$_3$+H]$^+$; [$^{153}$Eu(DBM)$_3$+H]$^+$, which confirms that $Eu^{3+}$ is coordinated with three DBM molecules. In the $^1$H-NMR spectra of complex **C1** four signals at 10.98, 10.59, 9.95 and 8.95 ppm corresponding to eight protons from 1,10-phenantroline molecule were observed. Furthermore, in the higher fields two multiplets (~6.80 and 5.94 ppm) and singlet (2.88 ppm) corresponding to 33 protons from three DBM molecules were observed, proving, that ratio of proton signals of PHEN and DBM molecules are 8:33, supplementing evidence, that **C1** is *ternary* complex with DBM:PHEN being 3:1. Furthermore, the $^1$H-NMR spectra of complex **C1** show some changes compared to ligands DBM (**3**) spectra, due to coordination to paramagnetic metal. All signals are broader and show shift to higher field, for example, methine group signal (C=CH) exhibited a shift from 6.88 ppm and showed signal at 2.88 ppm.

For complex **C2** mass spectra analysis show mass peaks with *m/z*: 130.1; 1043.8 and 1045.0 corresponding to [N(Et)$_4$]$^+$; [$^{151}$Eu(DBM)$_4$]$^-$; [$^{153}$Eu(DBM)$_4$]$^-$, which establishes, that complex is with *tetrakis* structure. Moreover, $^1$H-NMR spectra of **C2** shows two muliplets (~7.77 and 7.18 ppm) and one singlet (2.85 ppm) corresponding to 44 protons of four DBM molecules, but in higher fields quartet at 4 ppm and triplet at 1.65 ppm corresponding to 20 protons of $N^+(Et)_4$ molecule were observed, leading to conclusion, that $Eu^{3+}$ is coordinated with four DBM and one $N^+(Et)_4$ molecule.

### 3.2. Thermal properties

To evaluate **C1** and **C2** thermal durability, thermogravimetric (TG) analysis were conducted in nitrogen atmosphere from 30–900 °C and TG curves are shown in Fig. 2. Both complexes **C1** and **C2** exhibit high thermal decomposition temperatures $T_{5\%}$ ($T_{5\%}$ is temperature of 5% weight loss) – 304 and 267 °C, respectively. TG curve of complex **C1** consist of two mass loss steps around 310–443, and 444–556 °C. First mass loss step (45%) corresponds to the loss of two DBM molecules, second stage (22%) – to one DBM molecule. Further thermal decomposition from 557 to 900 °C leads to loss of PHEN molecule and residual weight of 20%. Similar thermal degradation pattern was reported for other $Eu^{3+}$ complexes with DBM derivatives and PHEN ligands [10]. Whereas TG curve of **C2** exhibits three thermal degradation stages: 268–295, 296–451, 452–590 °C, with mass losses of 19%, 30% and 19%, corresponding to loss of one DBM molecule, then one DBM and $N^+(Et)_4$ molecule, and lastly one DBM molecule, respectively. Further thermal decomposition from 591 to 900 °C

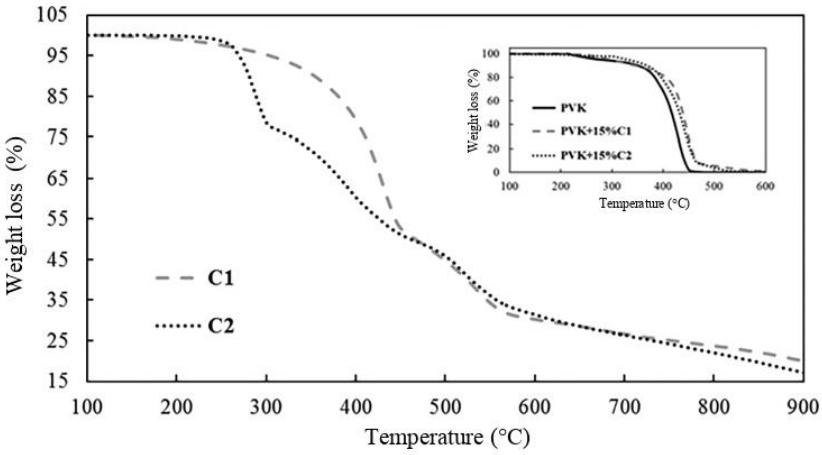


**Fig. 2.** Thermogravimetric curves of $Eu^{3+}$ complexes **C1** and **C2**. Inset shows TG curves of pure PVK and PVK thin film containing 15% complex **C1** or **C2**.

leads to loss of last DBM molecule and residual weight of 17%. Although $T_{5\%}$ of complex **C2** is lower, compared to **C1**, it is still higher for 50 °C than other $Eu^{3+}$*tetrakis* complexes with β-diketone ligands and quaternary ammonium ions [11,12].

It is known, that thermal properties can be improved by incorporating complexes in polymer matrixes, therefore TG analysis of PVK films containing 15% **C1** or **C2** were also conducted. TG curves of pure PVK film and films containing complexes are depicted in inset of Fig. 2. Pure PVK film shows small mass loss till 300 °C, which can be assigned to entrapped solvent removal from polymer films. Degradation of polymer occurs in a narrow temperature interval (366–453 °C). However, PVK films blended with complexes **C1** or **C2** show slight increase in thermal degradation temperature interval. For PVK+15% **C1** major degradation occurs at 392–467 °C, but for PVK+15% **C2** at 379–467 °C. The thermal degradation data indicate that incorporation of **C1** or **C2** in PVK leads to polymer films with high thermal decomposition endurance.

### 3.3. UV-Vis absorption properties

The UV-Vis absorption bands of pure DBM and complexes **C1** and **C2** were measured in THF solutions ($c \sim 1.5 \cdot 10^{-5}$M), and are depicted in Fig. 3. Absorption spectra of DBM shows broad band with maximum at

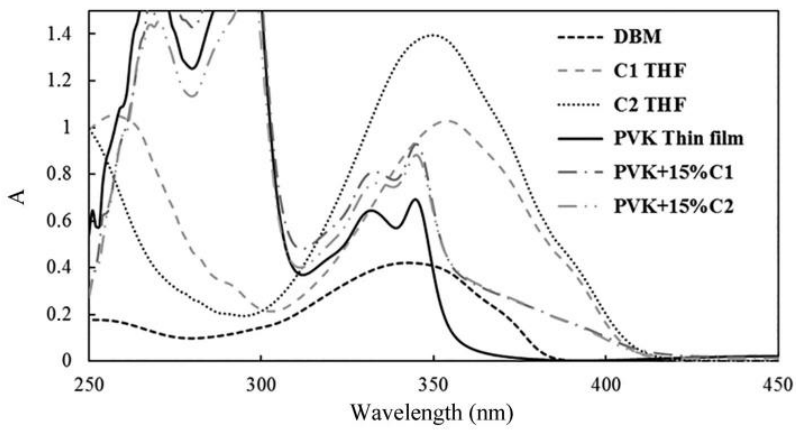


**Fig. 3.** UV-Vis absorption spectra of DBM, **C1**, **C2** in THF solutions ($\sim 1.5 \cdot 10^{-5}$M), pure PVK films and PVK thin films containing 15% of complexes **C1** and **C2**.

343 nm, which is assigned to enolic π-π* transitions of the β-diketone moiety. Furthermore, DBM exhibit high molar absorbance coefficient $\varepsilon$ –26287.5 $M^{-1}\cdot cm^{-1}$. The absorption spectra of complexes **C1** and **C2** in THF solutions are similar to the one of free DBM molecule, confirming that coordination with $Eu^{3+}$ ions do not affect ligands singlet excited states. Similar observations were reported for other β-diketones and their $Ln^{3+}$complexes [7,11]. The small red-shift (7–11 nm) of absorption band maximum for **C1** and **C2** compared to DBM can be explained with the more effective conjugation of π-electrons in $Eu^{3+}$ complexes. Furthermore, absorption intensity is enhanced in the complexes **C1** and **C2** due to expanded π-conjugated system, which forms, when $Eu^{3+}$ coordinates with DBM and PHEN molecules. The $\varepsilon$ of **C1** and **C2** reaches 68553 and 92967 $M^{-1}\cdot cm^{-1}$, which are 2.61 and 3.54 times higher than DBM molar absorptivity, suggesting, that these complexes exhibit strong ability to absorb light in the 320–380 nm region.

Figure 3 also shows absorption spectra of pure PVK and PVK thin films containing 15% of complexes **C1** or **C2**. Pure PVK film shows complicated band shape with absorption maxima at 271, 297, 332 and 346 nm, which can be assigned to π-π* and n-π* transitions. Absorption spectra of PVK films with **C1** and **C2** exhibit almost the same absorption profile as pure PVK film, only absorption intensity is increased at 332 and 346 nm due to overlap of PVK and complexes absorption spectra. Furthermore, new non-pronounced absorption band arises from 356 to 410 nm, which can be assigned to ligands absorption of complexes **C1** and **C2**.

### 3.4. Photoluminescence properties in solutions and solid state

Photoluminescence properties of $Eu^{3+}$ complexes were investigated in THF solutions (~$1.5\cdot10^{-5}$M) and in solid-state. The excitation spectra of $Eu^{3+}$ complexes monitoring $Eu^{3+}$ transition at 612 nm are displayed in Fig. 4. The excitation spectra of **C1** and **C2** exhibit broad band between 300–425 nm in THF (Fig. 4(a)) and 300–480 nm in solid-state (Fig. 4(b)), which can be assigned to absorption of DBM ligands. As absorption spectra of DBM and excitation spectra of complexes overlap, one can conclude that in synthesized complexes energy transfer occurs from DBM ligands to $Eu^{3+}$ ions. The maximums of excitation spectra for **C1** and **C2** in THF are at 373 and 384 nm, but in solid state a red shift to 402 and 403 nm occurs. This red shift of excitation wavelength maxima could be explained with the presence of strong π-π interactions between ligands in the solid-state. The absorption bands of *f-f** transitions of $Eu^{3+}$ ion (at 296, 362, 381, 394, 415, 466 and 527 nm) are not present in the excitation spectra of THF solutions, however in solid-state spectra transition at 466 nm ($^7F_0\rightarrow{}^5D_2$ transition) is clearly seen. This transition is usually observed for $Eu^{3+}$ complexes in solid state [6,7].

Emission spectra of **C1** and **C2** in THF solutions as well as in solid-state shows characteristic $Eu^{3+}$ $^5D_0\rightarrow{}^7F_J$ ($J$=0–4) transitions at 580, 593, 612, 651 and 703 nm. The highest intensity is observed for $^5D_0\rightarrow{}^7F_2$ transition at 612 nm, which is induced electric dipole transition and its intensity is dependent on coordination environment of $Eu^{3+}$ ion. As it was expected *tetrakis* $Eu^{3+}$ complex **C2** exhibits higher intensity for $^5D_0\rightarrow{}^7F_2$ transition than *ternary* complex **C1** in THF and in solid-state due to fact, that coordination sphere of $Eu^{3+}$ in **C2** is filled with four DBM ligands, which efficiently transfer the excitation energy to central metal ion and also provides better shielding of metal ion from surrounding environment. Furthermore, it is known that in *ternary* complexes PHEN is coordinated weakly to $Eu^{3+}$ ion, which could lead to dissociation of PHEN from some complex molecules and formation of *tris* complex $Eu(DBM)_3$.

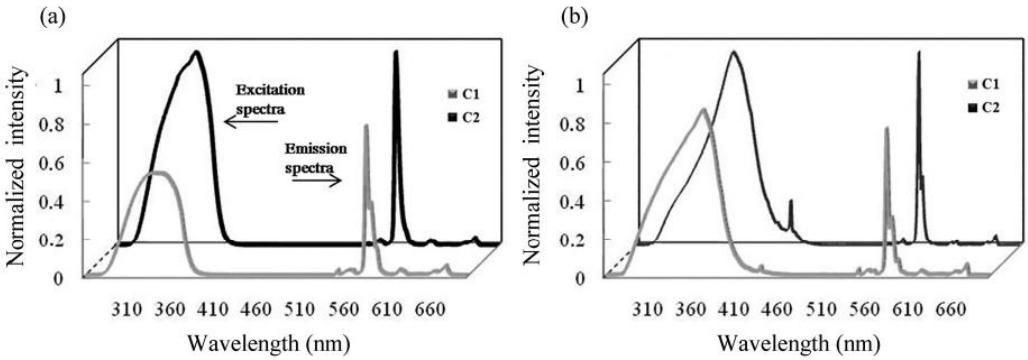


**Fig. 4.** Excitation ($\lambda_{mon}$=612 nm) and emission ($\lambda_{em}$=354 nm) spectra of complexes **C1** and **C2** in THF solutions (a) and in solid-state (b).

Formation of some *tris* complexes could also decrease luminescence intensity for **C1** complex. Furthermore, emission band at 612 for complex **C1** in both solution and solid-state is split and has secondary maximums at 618 and 622 nm. However, for complex **C2** in solution the emission band is broadened with one maximum at 612 nm. Similar observation was reported for other *tetrakis* $Eu^{3+}$ complex with DBM ligands and trioctylmethylphosphionium as counteraction [7] and was explained by interactions between $[Eu(DBM)_4]^-$ and counteraction ions in solution.

The absolute photoluminescence quantum yields were 4% for *ternary* **C1** complex and 6% for *tetrakis* **C2** complex in $1.5 \cdot 10^{-5}$M THF solutions. Furthermore, in a solid-state photoluminescence quantum yield reached 56% for **C1** and 75% for **C2**. Such luminescence quantum yield enhancement in solid-state compared to solutions can be explained with deactivation of ligand molecules in solvent medium by collisions. For $Eu^{3+}$ complexes with β-diketone ligands it is common to have higher luminescence quantum yields in solid-state rather than in solutions [7,10,12,14]. In conclusion, comparison of emission properties of *ternary* and *tetrakis* $Eu^{3+}$ complexes shows that *tetrakis* complex $[Eu(DBM)_4]N(Et)_4$ has enhanced emission properties in solid-state and has considerable potential for light emitting materials.

### 3.5. Photoluminescence properties in PVK thin films

In this work PVK was used as polymer matrix for $Eu^{3+}$ complexes due to its excellent hole-transporting properties. Furthermore, only few polymers have been established as good hosts for organic lanthanide complexes and PVK is one of them due to good match between triplet energy level of the polymer host and complex and also suitable overlap between emission spectra of polymer and absorption spectra of $Eu^{3+}$ complex. PVK thin films doped with 1, 4, 8 and 15 wt% of complex **C1** or **C2** were prepared by spin-coating method from THF. Excitation spectra of polymer films with complex **C1** and pure PVK thin film are shown in Fig. 5, inset shows emission spectra of pure PVK film. Excitation spectra of doped polymer films overlaps with pure PVK emission spectra, indicating possibility of absorbed excitation energy transfer from polymer host to $Eu^{3+}$ complex. Such energy transfer would give an advantage for thin PVK films, because polymer host would provide additional excitation energy for complex, which would lead to enhancement for film emission intensity.

The excitation spectra of PVK films shows broad bands in region from 300 to 410 nm with maximum at 348 nm, which corresponds to absorption of PVK matrix. However excitation bands have shoulder at 370 nm, which corresponds to absorption of **C1**.

The emission spectra of polymer films (depicted in Fig. 6) exhibit the same emission bands as those for complexes in THF solutions or solid-state. PVK films with 1% **C1** or **C2** also shows a weak polymer emission band from 360 till 560 nm indicating, that energy transfer from PVK to complexes is incomplete. This is due to great distance between polymer chain and complex in these films. However, for PVK films with higher complex concentration, the energy is completely transferred and no emission band of PVK is observed in spectra. Similar observations were reported for PVK films with *tetrakis* and *ternary* Eu(III) complexes with 2-thenoyltrifluoroacetonato ligands [15,16].

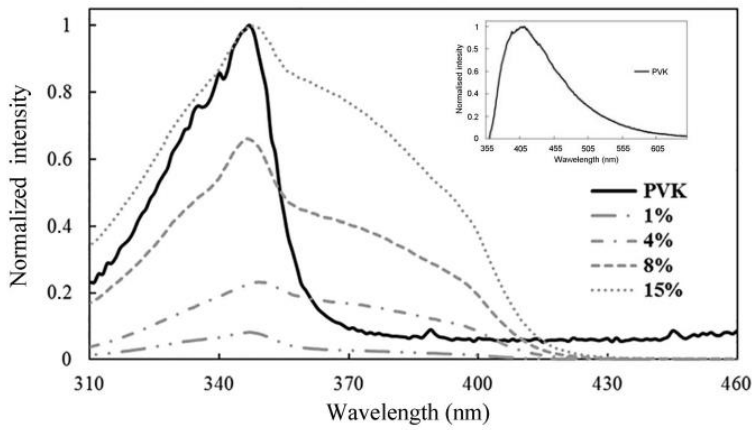


**Fig. 5.** Excitation spectra of pure PVK ($\lambda_{mon}$ = 435 nm) and PVK thin films ($\lambda_{mon}$ = 612 nm) containing 1, 4, 8 and 15 wt% complex **C1**. Inset shows emission spectra of pure PVK film.

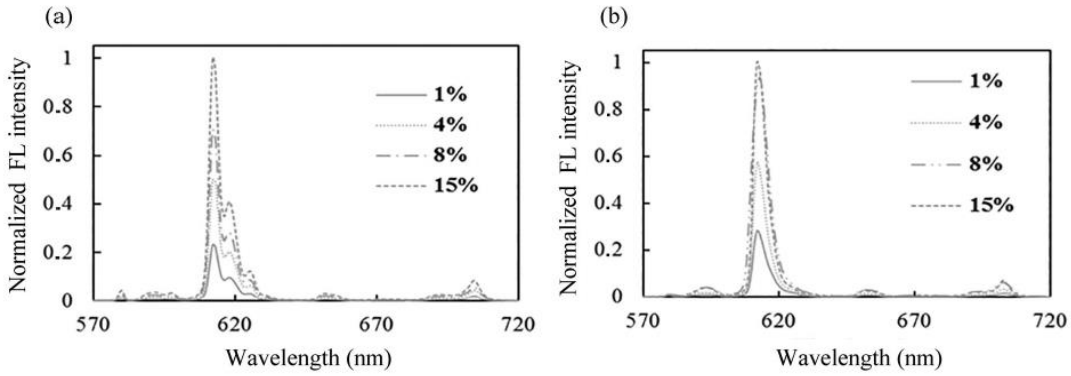


**Fig. 6.** Emission spectra of PVK films doped with 1, 4, 8 and 15 wt% of **C1** (a) and of **C2** (b).

Intensity of emission band at 612 nm and absolute photoluminescence quantum yields increases with increasing complex concentration in PVK matrix. The quantum yields for series of *ternary* complex **C1** PVK films (1, 4, 8, 15 wt%) increase in following order 14%, 21%, 26% and 30%, respectively, but for *tetrakis* complex **C2** films (1, 4, 8, 15 wt%) – 17%, 30%, 46% and 48%. For *tetrakis* complex **C2** increasing complex mass in the PVK from 8% to 15% has an insignificant effect on $^5D_0 \rightarrow {}^7F_2$ (612 nm) transition intensity and quantum yield. This can be explained with the fact that in film with high $Eu^{3+}$ ion concentration an energy transfer between $Eu^{3+}$ ions occurs as a non-radiative process. Therefore intensity of complex luminescence does not increase and sometimes even decreases in films with high complex concentration [13,17]. Registered quantum yield values for investigated PVK films are at the same level as the ones for the known films of $Eu^{3+}$ β-diketone complexes in other polymers [18]. It can be concluded, that *tetrakis* complex $[Eu(DBM)_4]N(Et)_4$ exhibits more intense emission not only in solution and solid-state, but also in PVK films.

## 4. CONCLUSIONS

In summary *ternary* and *tetrakis* $Eu^{3+}$ complexes with general structures $Eu(DBM)_3(PHEN)$ and $[Eu(DBM)_4]N(Et)_4$ were prepared and their structures were confirmed by elemental analysis, FT-IR, $^1$H-NMR and mass spectroscopy. Investigation of photoluminescence properties of complexes in THF, solid-state and PVK films shows that emission spectra contains characteristic $Eu^{3+}$ ion emission lines with the most intense transition at 612 nm. Excitation window for both complexes lies in the near-UV region (300–400 nm), providing large Stokes shifts. Enhanced emission intensity and photoluminescence quantum yields were found for both complexes in solid-state (quantum yields 56% and 75%). PVK polymer films containing $Eu^{3+}$ DBM complexes also showed moderate quantum yields (14–48%). The luminescence intensity and quantum yields increased with increasing complex concentration in PVK films and reached maximum at doping concentration of 15 wt%. *Tetrakis* complex $[Eu(DBM)_4]N(Et)_4$ in solution, solid-state and PVK films have enhanced photoluminescence properties compared to *ternary* complex due to four DBM molecules in $Eu^{3+}$ coordination sphere, which leads to more effective excited energy transfer to $Eu^{3+}$ ion. The results of thermogravimetric analysis of complexes revealed that they exhibit high thermal degradation temperatures.

## ACKNOWLEDGEMENTS

This work was supported by the doctoral studies grants of Riga Technical University (grant No. 34-14000DOK.MLĶF/16) and the National Research Program of Latvia "IMIS2". The authors thank MCs Chem. Kristine Lazdovica for help with themogravimetric analysis. The publication costs of this article were covered by the Estonian Academy of Sciences and the University of Tartu.

## REFERENCES

1. Binnemans, K. Lanthanide-Based Luminescent Hybrid Materials. *Chem. Rev.*, 2009, **109**, 4283–4374.
2. Singh, A. K., Singh, S. K., Mishra, H., Prakash, R., and Rai, S. B. Structural, Thermal, and Fluorescence Properties of $Eu(DBM)_3Phen_3$Complex Doped in PMMA. *J. Phys. Chem. B*, 2010, **114**, 13042–13051.

3. Liang, H., Xie, F., Liu, M., Jin, Z., Luo, F., and Zhang, Z. Luminescence studies of europium chelates with increasing benzene ring substituents ligand-doped polymer. *Spectrochim. Acta, Part A*, 2008, **71**, 588–591.
4. Ma, D.-G., Wang, D.-K., Hong, Z.-Y., Zhao, X.-J., Jing, X.-B., Song, F., et. al. Bright red electroluminescent devices based on a soluble lanthanide complex $Eu(DBM)_3$(phen). *Chin. J.Chem.*, 1998, **16**(1), 1–6.
5. Santos, G., Fonseca, F. J., and Andrade, A. M. The dependence of OLED external efficiency on the mass concentration of europium(III) dispersed in PVK. *ECS Trans.*, 2011, **39**(1), 475–480.
6. Mech, A., Karbowiak, M., Görller-Walrand, C., and Van Deun, R. The luminescence properties of three tetrakis dibenzoylmethaneeuropium(III) complexes with different counter ions. *J. Alloys Compd.*, 2008, **451**, 215–219.
7. Malba, C. M., Enrichi, F., Facchina, M., Demitric, N., Plaisier, J. R., Natile, M. M., Selva, M., Riello, P., Perosa, A., and Benedetti, A. Phosphonium-based tetrakis dibenzoylmethane Eu(III) and Sm(III) complexes: synthesis, crystal structure and photoluminescence properties in a weakly coordinating phosphonium ionic liquid. *RSC Adv.*, 2015, **5**, 60898–60907.
8. Zhou, D., Huang, C., Yaong, G., Bai, J., and Li, T. Luminescent europium-dibenzoylmethane complexes and their Langmuir–Blodgett films, *J. Alloys Compd.*,1996, **235**, 156–162.
9. Zawadiak, J. and Mrzyczek, M. Influence of substituent on UV absorption and keto–enol tautomerism equilibrium of dibenzoylmethane derivatives. *Spectrochim. Acta Part A Mol. Biomol. Spectrosc.*, 2012, **96**, 815–819.
10. Wang, D., Zheng, C., Fan, L., Zheng, J., and Wei, X. Preparation and fluorescent properties of europium(III) complexes with β-diketone ligand and 1,10-phenantroline. *Synth. Met.*, 2012, **162**, 2063–2068.
11. Biju, S., Xu, L.-J., Sun, C.-Z., and Chen, Z.-N. White OLEDs based on a novel $Eu^{III}$-tetrakis-β-diketonate doped into 4,4'-N,N'-dicarbazlebiphenyl as emitting material. *J. Mater. Chem. C*, 2015, **3**, 5775–5782.
12. Biju, S., Freire, R. O., Eom, Y. K., Scopelliti, R., Bunzli, J.-C.G., and Kim, H. K. A $Eu^{III}$ tetrakis (β-diketonate) dimeric complex: photophysical properties, structural elucidation by sparkle/AM1 calculations, and doping into PMMA films and nanowires. *Inorg. Chem.*, 2014, **53**, 8407–8417.
13. Li, W., Yan, P., Hou, G., Li, H., and Li, G. Efficient red emission from PMMA films doped with 5,6-DTFI europium(III) complexes: synthesis, structure and photophysical properties. *Dalton Trans.*, 2013, **42**, 11537–11547.
14. Ma, Q., Zheng, Y., Armaroli, N., Bolognesi, M., and Accorsi, G. Synthesis and photoluminescence properties of asymmetrical europium(III) complexes involving carbazole, phenanthroline and bathophenanthroline units. *Inorg. Chem. Acta*, 2009, **362**, 3181–3186.
15. Yu, G., Liu, Y., Wu, X., and Zhu, D. Soluble europium complexes for light-emitting diodes. *Chem. Mater.*, 2000, **12**, 2537–2541.
16. Deichmann, V. A. F., Novo, J. B. M., Cirpan, A., Karasz, F. E., and Akcelrud, L. Photo- and electroluminescent behaviour of $Eu^{3+}$ ions in blends with poly(vinyl-carbazole). *J. Braz. Chem. Soc.*, 2007, **18**(2), 330–336.
17. Raj, D. B. A., Francis, B., Reddy, M. L. P., Butorac, R. R., Lynch, V. M., and Cowley, A. H. Highly luminescent poly(methyl methacrylate)-incorporated europium complex supported by a carbazole-based fluorinated β-diketonate ligand and a 4,5-bis(diphenylphosphino)-9,9-dimethylxanthene oxide co-ligand. *Inorg. Chem.*, 2010, **49**, 9055–9063.
18. Forster, P. L., Parra, D. F., Lugao, A. B., Kai, J., and Brito, H. F. Highly luminescent polycaprolactone films doped with diaquatris (thenoyltrifluoroacetonate) europium(III) complex. *J. Lumin.*, 2015, **167**, 85–90.

## Dibensoüülmetaan-Eu(III) orgaaniliste komplekside termilised ja optilised omadused

Ilze Malina, Nikolajs Juhnevics ja Valdis Kampars

Sünteesiti kaks euroopium(III) orgaanilist kompleksi (kolmikkompleks $Eu(DBM)_3$(PHEN) ja nelikkompleks $[Eu(DBM)_4]N(Et)_4$), kus DBM on dibensoüülmetaan ning PHEN on 1,10-fenantroliin. Nende struktuur tõestati, kasutades $^1$H-NMR-spektroskoopiat, elementanalüüsi, FT-IR- ja mass-spektroskoopiat. Komplekside fotofüüsikalisi omadusi uuriti lahuses, tahkel kujul ja polü-*N*-vinüülkarbasool- (PVK) kiles, varieerides kompleksi kontsentratsiooni vahemikus 1 kuni 15 massiprotsenti. Mõlemad kompleksid on head UV neelajad ja kiirgavad eredalt punases spektri piirkonnas kiirgusriba keskpunktiga 612 nm. Näidati, et lahuses, tahkel kujul ja PVK-kiles on nelikkompleksil kolmikkompleksiga võrreldes võimendatud fotoluminestsentsomadusi tänu neljale DBM-molekulile $Eu^{3+}$ koordinatsioonisfääris, mis põhjustavad efektiivsemat energia ülekannet $Eu^{3+}$ ioonile. THF-lahuses olid mõlemad kompleksid madala kvantefektiivsusega (4% ja 6%), PVK-kiles keskmise kvantefektiivsusega (14–48%) ning tahkel kujul kõrge kvantefektiivsusega (56% ja 75%). Mõlema kompleksi termilisi omadusi PVK-kiles uuriti termogravimeetriameetoditega. Mõlemal kompleksil on kõrge termilise lagunemise temperatuur: kolmikkompleksil 304 °C ja nelikkompleksil 267 °C. PVK-kiles on vastav temperatuur aga mõlemal juhul üle 370 °C, seega veel kõrgem.

4.pielikums

**Malina I,** Kampars V. Comparison of luminescent properties in solid-state and polymer films of Eu(III) complexes containing 2-acylindandione ligands. *Key Eng. Mater.*, **2018**, *762*, 239-243.

DOI: 10.4028/www.scientific.net/KEM.762.239

Reprinted with permission from Trans Tech Publications Ltd.
Copyright © 2018, Trans Tech Publications Ltd.

*Key Engineering Materials*
*ISSN: 1662-9795, Vol. 762, pp 239-243*
*doi:10.4028/www.scientific.net/KEM.762.239*
*© 2018 Trans Tech Publications, Switzerland*
*Submitted: 2017-08-10*
*Revised: 2017-09-07*
*Accepted: 2017-10-15*
*Online: 2018-02-05*

# Comparison of Luminescent Properties in Solid-State and Polymer Films of Eu(III) Complexes Containing 2-Acylindandione Ligands

Ilze Malina[a]*, Valdis Kampars[b]

Institute of Applied Chemistry, Riga Technical University, P. Valdena 3/7, Riga, Latvia

[a]Ilze.Malina_1@rtu.lv, [b]Valdis.Kampars@rtu.lv

**Keywords:** Europium complexes, doped films, red-light emission

**Abstract.** The Europium(III) ternary complexes $Eu(BID)_3(PHEN)$ and $Eu(MBID)_3(PHEN)$ (BID – 2-benzoyl-1,3-indandione, MBID - 2-(4-methylbenzoyl)-1,3-indandione and PHEN – 1,10-Phenantroline) were synthesized, characterized and incorporated into poly methyl methacrylate (PMMA) and poly-*N*-vinylcarbazole (PVK) matrices. Emission properties in solid-state and polymer films were investigated through excitation spectra, emission spectra and absolute photoluminescence quantum yields (PLQY). Both complexes in their solid-state and films exhibited red-light luminescence with narrow bands corresponding to Eu(III) ion emission. In solid-state complexes were characterized with PLQY of 6% and 10%, in PVK matrices quantum yield dropped down to 4%, however, in PMMA films exhibited similar PLQY as in solid-state.

## Introduction

Since the first discovery about intensively luminescent Eu (III) organic complexes reported by Weismann [1] in 1942, the investigation and application fields for these compounds have grown enormously. Different ligands containing Eu(III) complexes have found application in polymer organic light emitting diodes (PLEDs) [2], laser materials, photovoltaic cells [3] as well as amplifiers [4] and bioprobes [5]. The most important part in designing new ligands for Eu(III) complexes is to obtain excellent compatibility between energy levels of ligands and Eu(III) ion. In order for complex to emit light, it is necessary that the triplet energy level of the binding ligand is close or even higher than the resonance energy level of Eu(III) ion. Certainly, there are other requirements for organic ligands, such as intense UV/Vis absorption, high thermal and chemical stability, as well as simple and inexpensive synthesis. The most popular ligands for Eu(III) complexes are β-diketones, such as derivatives of dibenzoylmethane (DBM) or acetlyacetone. Comparatively few reports are devoted towards investigation of Eu(III) complexes with β-diketone ligands with more rigid structure, where one carbonyl group is incorporated in cycle [6, 7]. These complexes showed promising optical and electrooptical properties for practical application, therefore continuing these investigations we present two new Eu(III) *ternary* complexes with rigid ligands – 2-benzoyl-1,3-indandione (BID) and 2-(4-methylbenzoyl)-1,3-indandione (MBID). Furthermore, to increase the emission intensity for these complexes a secondary ligand - 1,10-phenantroline was introduced in their structures affording Eu(III) complexes with coordination number of eight (Scheme 1). The optical property investigation results of these complexes will be described in detail in this report.

## Materials and Methods

$^1$H-NMR spectra were recorded in $CDCl_3$ solutions (7 mg/ml) on a *Brucker Avance 300 MHz* spectrometer at 300 MHz for $^1$H nuclei. The FT-IR spectra (4000 to 650 $cm^{-1}$) were recorded on a *Perkin-Elmer Spectrum 100 FTIR* spectrometer using KBr pellets. Low resolution mass spectra were acquired on a *Waters EMD 1000MS* mass detector (ESI+ mode, voltage 30 V). The UV-Vis absorption spectra were acquired using *Perkin-Elmer 35* UV/Vis spectrometer. Emission and excitation spectra were measured on *QuantaMaster 40* steady state spectrofluorometer (*Photon Technology International, Inc.*). Absolute photoluminescence quantum yields were determined

All rights reserved. No part of contents of this paper may be reproduced or transmitted in any form or by any means without the written permission of Trans Tech Publications, www.scientific.net. (#114722595, Riga Technical University, Riga, Latvia-16/05/19,19:38:25)

using *QuantaMaster 40* steady state spectrofluorometer (*Photon Technology International, Inc.*) equipped with 6 inch integrating sphere by *LabSphere*.

**Synthesis**. The synthetic routes of ligands (**4**,**5**) and complexes **6**,**7** are shown in Scheme 1. 2-Benzoyl-1,3-indandione (**4**) and 2-(4-methylbenzoyl)-1,3-indandione (**5**) were synthesized as described in reference [7].

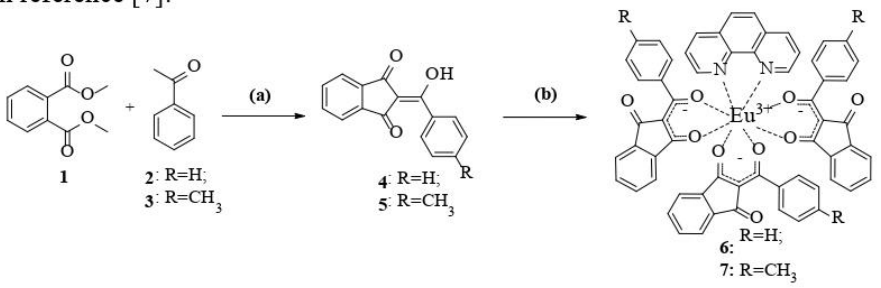


Scheme 1. Synthesis of ligands **4**,**5** and Eu(III) complexes **6**,**7** ; **(a)** – 1) $NaOCH_3$, Toluene, 80 °C; 2) $H_2O$, 10% HCl; **(b)** – 10% NaOH/$H_2O$, 1,10-Phenantroline, $EuCl_3{\cdot}6H_2O$

**6**: To a solution of 2-benzoyl-1,3-indandione (**4**) (1.08 mmol, 3 eq.) in 10 ml distilled water, which had been neutralized with 10% NaOH solution, an ethanol solution (5 ml) containing 1,10-phenantroline (0.36 mmol, 1 eq.) was added. The mixture was heated to 50 °C until complete dissolvation of the compounds. Afterwards, obtained solution was added drop-wise to a 10 ml distilled water containing $EuCl_3{\cdot}6H_2O$ (0.36 mmol, 1 eq.). Instantly yellow precipitates were formed and obtained suspension was stirred for 4 hours in room temperature. Afforded precipitates were separated by suction filtration, crystallized from methanol solution and dried in vacuum at 50 °C for 24 hours. Yellow powder, Yield 41%; $^1$H-NMR (300 MHz, ppm): 10.03 (2H, d, H-PHEN), 9.41 (2H, br s, H-PHEN), 7.86-7.77 (4H, m, H-PHEN), 7.60-7.47 (6H, br m, 1,3-Indand. H), 6.83-6.80 (6H, br m, 1,3-Indand. H), 6.55 (6H, br s, H-Ph), 6.24 (3H, br s, H-Ph), 5.29 (6H, s, H-Ph); Anal. Calcd.For $EuC_{60}H_{35}N_2O_9$: C, 66.73; H, 3.24; N, 2.59; found C, 67.14; H, 3.55; N, 2.59; FT-IR (KBr, $cm^{-1}$): 3054 ($\nu_{Csp2H}$); 1690, 1615 ($\nu_{C=O}$); 1586, 1566, 1519($\nu_{C=C}$);1447 ($\nu_{C=N}$); ESI(+)-MS: (*m/z*) 181.2 $[PHEN+H]^+$; 899.6 $[^{151}Eu(2BID)_3+H]^+$; 901.4 $[^{153}Eu(2BID)_3+H]^+$.

**7**: Complex was synthesized by the same procedure as for **6**, except 2-(4-methylbenzoyl)-1,3-indandione (**5**) was used instead of compound **4**.Yellow powder, Yield 31%; $^1$H-NMR (300 MHz, ppm): 10.02 (2H, d, H-PHEN), 9.43 (2H, br s, H-PHEN), 7.98-7.87 (4H, m, H-PHEN), 7.57-7.45 (6H, br m, 1,3-Indand. H), 6.84 (3H, brs, 1,3-Indand. H), 6.41-4.31 (9H, m, 1,3-Indand. H ,H-Ph), 5.27 (6H, br s, H-Ph), 2.24 (9H, s, Ph-$CH_3$); Anal. Calcd.For $EuC_{63}H_{41}N_2O_9$: C, 67.44; H, 3.66; N, 2.50; found C, 67.07; H, 3.82; N, 2.58; FT-IR (KBr, $cm^{-1}$): 3056, 3029 ($\nu_{Csp2H}$); 2919, 2864 ($\nu_{Csp3H}$); 1689, 1615 ($\nu_{C=O}$); 1584, 1563, 1512 ($\nu_{C=C}$); 1456 ($\nu_{C=N}$); ESI(+)-MS: (*m/z*) 181.1 $[PHEN+H]^+$; 941.6 $[^{151}Eu(MBID)_3+H]^+$; 943.4 $[^{153}Eu(MBID)_3+H]^+$.

**Preparation of Polymer Films**. PVK or PMMA (20 mg) and the required amount of complex **6** or **7** (1.6 mg) were dissolved in 1 mL THF and the resulting mixture was heated at 40 °C for 30 min. Afterwards polymer films were spin-coated on a glass substrate (parameters: speed 800 rpm, acceleration 800 rpm/sec for duration of 1 min). Obtained films were dried at 45 °C for 2 hours.

## Results and Discussion

**Characterization of Complexes**. To establish the structures of synthesized complexes – $^1$H-NMR, mass spectroscopy, as well as elemental analysis and FT-IR spectroscopy were employed. Elemental analysis data were in a good agreement with the proposed chemical structures, but $^1$H-NMR spectroscopy was used to prove the ratio of ligands in synthesized complexes. In $^1$H-NMR spectra of complexes **6** and **7** a three signals at δ 10.00, 9.40 and 7.90 ppm corresponding to eight protons from 1,10-phenantroline molecule were observed. Furthermore, in higher fields a signals corresponding to 27 protons from three 2-benzoyl-1,3-indandione ligands (**6**) or 33 protons from

three 2-(4-methylbenzoyl)-1,3-indandione ligands (**7**) were obtained, which verifies that in these complexes the ratio of PHEN:BID (or MBID) is 1:3. Moreover, due to the presence of paramagnetic metal ion – $Eu^{3+}$ in these complexes all proton signals are shifted to higher fields and shows peak broadening. Mass spectra of *ternary* complexes consists of three mass peaks, and for **6** they are *m/z* 181.2 $[PHEN+H]^+$, 899.6 $[^{151}Eu(BID)_3+H]^+$ and 901.4 $[^{153}Eu(BID)_3+H]^+$ establishing, that $Eu^{3+}$ and BID ratio in complex is 1:3. A similar mass spectrum was obtained for complex **7**. Both complexes show excellent solubility in $CH_2Cl_2$, $CHCl_3$, THF and MeOH.

**Emission Properties of Complexes in Solid-State**. Powder complexes excitation spectra were measured by monitoring Eu(III) emission at 613 nm (see Fig.1 (a)). The excitation spectra consist of broad band located between 250-500 nm, with maximum around 400 nm, indicating, that energy, which causes the emission, comes from π-π* absorption of the ligands. Furthermore, characteristic narrow Eu(III) ion absorption bands at 296, 362, 381, 394, 415, 466 nm can be barely observed as they are overlapped by much intense absorption band of the ligands. Independently from the used ligand (BID or MBID) excitation spectra are identical; meaning that substituent in benzoyl fragment has an insignificant effect on complex excitation spectra.

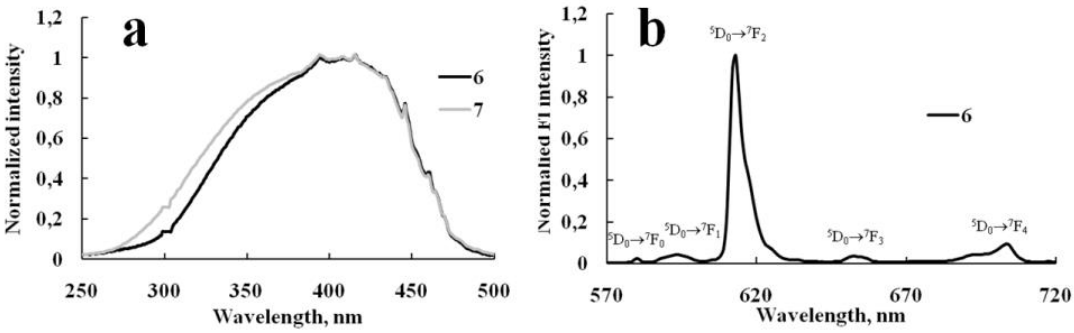


Fig. 1. (a) - Excitation spectra monitored at $\lambda_{exc}$=613 nm of complexes **6**, **7**; (b) - emission spectra ($\lambda_{exc}$=400 nm) of Eu(III) complex **6** in solid-state

Emission spectra were measured using 400 nm as the excitation wavelength. Since both complexes have identical emission spectra profile only compounds **6** emission spectra is shown (see Fig.1 (b)). Complex **6** exhibits multiple narrow emission bonds, which are characteristic of Eu(III) ion and corresponds to $^5D_0\rightarrow{}^7F_J$ ($J$=0-4) radiative deactivation transitions and lies at 580, 594, 613, 654 and 704 nm. Furthermore, emission spectra doesn't contain any broad emission band corresponding to ligands - PHEN, BID or MBID, therefore confirming, that excited energy transfer between these ligands and metal ion is efficient. Emission band at 580 nm ($^5D_0\rightarrow{}^7F_0$) is not splitted and shows only one peak, however, transition $^5D_0\rightarrow{}^7F_1$ (594 nm) shows three Stark components. Such observations are common for Eu(III) organic complexes and indicates, that there is a single environment around the central metal ion [8]. Moreover, band at 613 nm ($^5D_0\rightarrow{}^7F_2$) is hypersensitive transition and is intense. The ratio between intensities of transitions $^5D_0\rightarrow{}^7F_2$ and $^5D_0\rightarrow{}^7F_1$ are high R= ($I_{^5D_0\rightarrow{}^7F_2}/I_{^5D_0\rightarrow{}^7F_1}$)=24, meaning that Eu(III) occupies site without inversion symmetry [9]. Absolute photoluminescence quantum yields (Φ) for complex **6** (6%) and complex **7** (10%) were obtained with 400 nm excitation by using integrating sphere.

**Emission Properties for Complexes Doped in PMMA and PVK Films**. Eu(III) organic complexes are characterized with poor thin solid film formation ability, which is necessary for their practical application (for example, in OLEDs). Nevertheless, this drawback could be nullified by doping these complexes in polymers. The common used polymers for Eu(III) complexes are poly methyl methacrylate (PMMA) and poly-*N*-vinylcarbazole (PVK). Polymer films were prepared by spin-coating technique from THF solutions using 8 wt% doping mass of complexes. Absorption spectra of Eu(III) complexes **6** and **7** in the THF solutions as well as in the PVK and PMMA polymer matrixes are shown in Fig.2 (**a**). Complexes in THF solutions exhibit broad absorption

bands with maximums at 337 (**6**) and 340 nm (**7**), but for polymer films absorption spectra is different. PVK doped films exhibits two maximums at 332 and 345 nm, which corresponds to absorption of polymer matrix and it seems that both complexes absorption spectra are completely overlapped with PVK absorption spectra. However, PMMA films exhibits the same absorption profile than complexes in THF solutions due to fact, that PMMA is transparent over 250 nm.

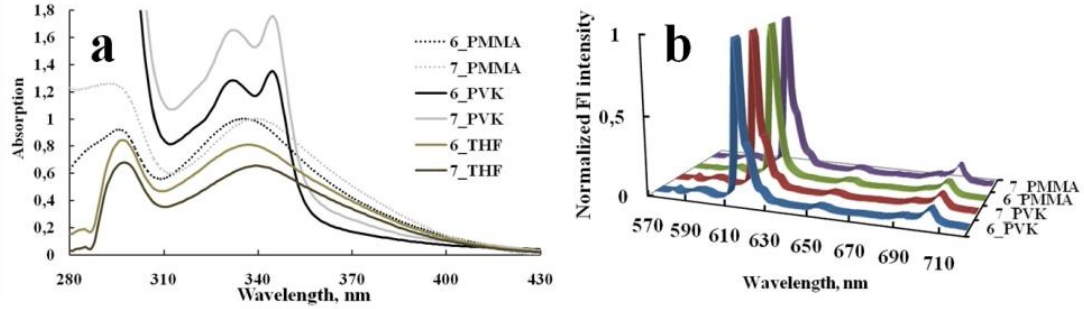


Fig. 2. (a) - absorption spectra of PMMA and PVK films doped with 8 wt% of Eu(III) complex **6** or **7** and absorption spectra of **6** and **7** in THF solutions (c~$1.5\cdot10^{-5}$M); (b) - emission spectra ($\lambda_{exc}$=350 nm) of PVK and PMMA films doped with 8 wt% of complex **6** or **7**

Emission spectra of produced complex **6** and **7** films are shown in Fig. 2 (b). All obtained films exhibits bright red-light emission with multiple emission bands, similarly as it was for solid-state samples. The emission band with the highest intensity for all polymer films was at 613 nm ($^5D_0\rightarrow{}^7F_2$). However, the ratio between intensities of transitions $^5D_0\rightarrow{}^7F_2$ and $^5D_0\rightarrow{}^7F_1$ are much higher (R= ($I^5D_0\rightarrow{}^7F_2/I^5D_0\rightarrow{}^7F_1$)~27) as it was for solid-state samples, meaning, that incorporation of Eu(III) complexes in polymers leads to increased the symmetry of coordination sphere of Eu(III) ion. Similar observations was reported for other films doped with Eu(III) complexes [10, 11].

Absolute PLQY for both PVK films were only 4%. Such low PLQY values can be explained with intense PVK absorption in the same region as complex. However, for PMMA films PLQY were higher – 6% for **6** and even 11% for **7**. From the obtained absolute photoluminescence quantum yield values, it can be seen, that synthesized complexes could find application in polymer optical fibers, where PMMA is often used rather than in OLED, where mostly PVK are produced.

## Conclusions

Newly synthesized Eu(III) complexes with structures $Eu(BID)_3(PHEN)$ and $Eu(MBID)_3(PHEN)$ are reported. Structures of complexes are proven with elemental analysis, $^1$H-NMR spectroscopy, mass spectroscopy and FT-IR spectroscopy. Investigation of emission properties in solid-state and poly methyl methacrylate and poly-*N*-vinylcarbazole films lead to conclusion, that the highest absolute photoluminescence quantum yields were obtained for PMMA film containing $Eu(MBID)_3(PHEN)$ (11%) , which could found application as polymer optical fibers.

## Acknowledgements

This work was supported by the doctoral studies grants of Riga Technical University (Grant Nr. 34-14000DOK.MLĶF/16).

## References


[1] S.I. Weissman, Intramolecular energy transfer. The fluorescence of complexes of Europium, J. Chem. Phys., 10 (1942), 214-217.

[2] Y. Liu , Y. Wang, C. Li, Y. Huang, D. Dang, M. Zhu, W. Zhu , Y. Cao, Red polymer light-emitting devices based on an oxadiazole functionalized europium(III) complex, Mater. Chem. Phys., 143 (2014), 1265-1270.

[3] H. Kataoka, T. Kitano, T. Takizawa, Y. Hirai, T. Nakanish, Y. Hasegawa, Photo- and thermo-stable luminescent beads composed of Eu(III) complexes and PMMA for enhancement of silicon solar cell efficiency, J. Alloys Compd., 601, (2014), 293-297.

[4] K. Kuriki, Y. Koike, Y. Okamoto, Plastic Optical Fiber Lasers and Amplifiers Containing Lanthanide Complexes, Chem. Rev., 102, (2002), 2347-2356.

[5] J. Sun, B. Song, Z. Ye, J. Yuan, Mitochondria Targetable Time-Gated Luminescence Probe for Singlet Oxygen Based on a β-Diketonate−Europium Complex, Inorg. Chem., 54(24), (2015), 11660-11668.

[6] W. Li, P. Yan, G. Hou, H. Li, G. Li. Efficient red emission from PMMA films doped with 5,6-DTFI europium(III) complexes: synthesis, structure and photophysical properties. Dalton Trans., 42, (2013), 11537-11547.

[7] E.E.S. Teotonio, H.F. Brito, H. Viertler, W.M. Faustino, O.L. Malta, G.F. de Sa, M.C.F.C. Felinto, R.H.A. Santos, M. Cremona, Synthesis and luminescent properties of Eu(III)-complexes with 2-acyl-1,3-indandionates (ACIND) and TPPO ligands: the first X-ray structure of Eu-ACIND complex, Polyhedron, 25, (2006), 3488-3494.

[8] S. Biju, D.B. Ambili Raj, M.L.P. Reddy, B.M. Kariuki. Synthesis, Crystal Structure, and Luminescent Properties of Novel $Eu^{3+}$ Heterocyclic *â*-Diketonate Complexes with Bidentate Nitrogen Donors. Inorg. Chem., 45, (2006), 10651-10660

[9] K. Binnemans, Rare-earth beta-diketonates. Handbook on the Physics and Chemistry of Rare Earths, Vol. 35, Elsevier, North Holland, 2005.

[10] D.B.A. Raj, B. Francis, M.L.P. Reddy, R.R. Butorac, V.M. Lynch, , A.H. Cowley, Highly Luminescent Poly(Methyl Methacrylate)-Incorporated Europium Complex Supported by a Carbazole-Based Fluorinated β-Diketonate Ligand and a 4,5-Bis(diphenylphosphino)-9,9-dimethylxanthene Oxide Co-Ligand. Inorg. Chem., 49, (2010), 9055-9063.

[11] H. Zhang, H. Song, B. Dong, L. Han, G. Pan, X. Bai, L. Fan, S. Lu, H. Zhao, F. Wang. Electrospinning preparation and luminescence properties of Europium complex/polymer composite fibers, J. Phys. Chem. C, 112, (2008), 9155-9162.

5.pielikums

**Malina I**, Kampars V, Belyakov S. Luminescence properties of 2-benzoyl-1,3-indandione based $Eu^{3+}$ ternary and tetrakis complexes and their polymer films. *Dyes and Pigments*, **2018**, *159*, 655-665.

DOI: 10.1016/j.dyepig.2018.07.003

© 2018, Elsevier. This manuscript version is made available under the CC-BY-NC-ND 4.0 license http://creativecommons.org/licenses/by-nc-nd/4.0

Grafiskais abstrakts/ Graphical abstract

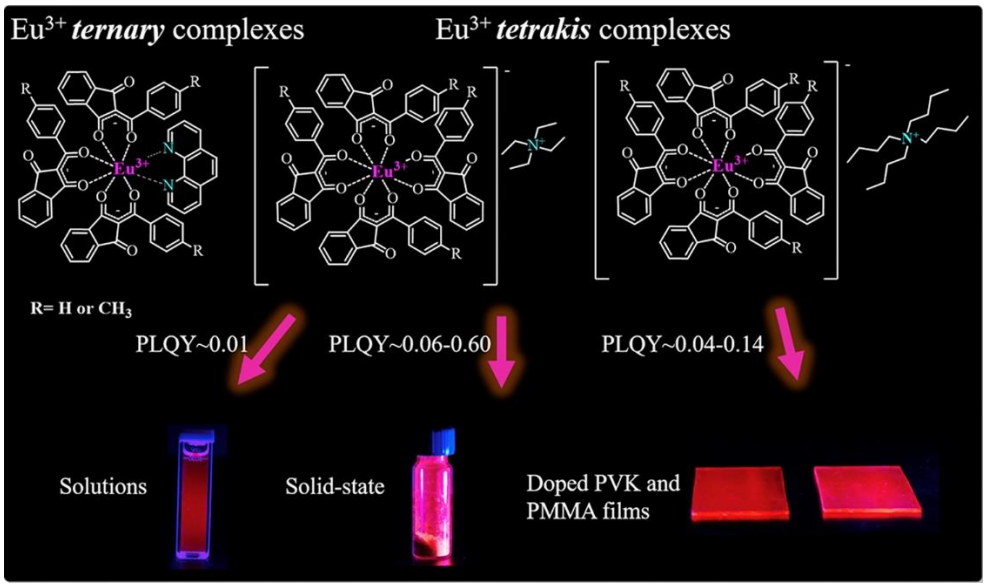

Dyes and Pigments 159 (2018) 655–665

Contents lists available at ScienceDirect

Dyes and Pigments

journal homepage: www.elsevier.com/locate/dyepig

# Luminescence properties of 2-benzoyl-1,3-indandione based $Eu^{3+}$ ternary and tetrakis complexes and their polymer films

Ilze Malina[a,*], Valdis Kampars[a], Sergey Belyakov[a,b]

[a] Riga Technical University, Institute of Applied Chemistry, Paula Valdena Str. 3, Riga, LV-1048, Latvia
[b] Latvian Institute of Organic Synthesis, Aizkraukles Str. 21, Riga, LV-1006, Latvia

ARTICLE INFO

*Keywords:*
Europium
Tetrakis complex
Ternary complex
Luminescent polymer films

ABSTRACT

Six new Europium (III) complexes with *ternary* and *tetrakis* structures - $Eu(BID)_3(PHEN)$, $Eu(MBID)_3(PHEN)$, $[Eu(BID)_4]^-N^+(Et)_4$, $[Eu(MBID)_4]^-N^+(Et)_4$, $[Eu(BID)_4]^-N^+(Bu)_4$, and $[Eu(MBID)_4]^-N^+(Bu)_4$ (BID – 2-benzoyl-1,3-indandionate, MBID - 2-(4-methylbenzoyl)-1,3-indandionate and PHEN – 1,10-phenantroline) are synthesized, characterized, and incorporated into poly-*N*-vinylcarbazole (PVK) and poly methyl methacrylate (PMMA) matrices. Complex structure shows significant effect on thermal properties and emission properties of complexes in solid-state. Used countercations ($N^+(Et)_4$ or $N^+(Bu)_4$) greatly affects complex solubility in solvents, absolute photoluminescence quantum yields and photoluminescence lifetimes in solid-state. Complexes exhibit red-light emission attributed to $^5D_0 \rightarrow {}^7F_J$ ($J$ = 0–4) transitions of $Eu^{3+}$ ion with moderate to high quantum yields (0.06–0.60), bi-exponential lifetimes and pure red-light CIE chromaticity coordinates (x = 0.670; y = 0.330) in solid-state. Incorporation of synthesized complexes in PVK matrices leads to significant emission intensity and quantum yield decrease.

However, doped PMMA films with synthesized complexes exhibit moderate PLQY (0.09–0.14) and longer lifetime values than in solid-state and could show potential application as polymer optical fibers or in OLED's and other devices.

## 1. Introduction

From all luminescent organic metal complexes with lanthanide ions ($Ln^{3+}$) trivalent Europium $Eu^{3+}$ compounds stand out due to bright red-light emission with high quantum yields and long lifetimes. Popularity of $Eu^{3+}$ complexes is so remarkable, that they have been investigated in wide range of fields and different type of materials, including nanoparticles for biomedical applications [1], mesoporous thin films for UV sensors and bio-sensing [2], as well as up-conversion luminescent thin films for wavelength-transfer imaging [3] and metal-organic framework microrods for colored optical waveguides [4] have been designed. Furthermore, due to noteworthy narrow emission line bandwidth, which defines the high red-light emission color purity, these compounds have been extensively investigated as emissive layers for organic/polymer light emitting diodes (OLEDs/PLEDs) [5].

To succeed with development of highly luminescent $Eu^{3+}$ complexes one must deliberate the design of attached organic ligands. For effective excited energy transfer from ligands to $Eu^{3+}$, compatibility between energy levels of ligands and $Eu^{3+}$ must be present in the complex. The main resonance level for $Eu^{3+}$ is 17 250 $cm^{-1}$ [6] and in order for complex to emit light, it is necessary that the triplet energy level of ligand is close or even higher than this resonance level. Other just as important requirements for organic ligands are intense UV/Vis absorption, high chemical and thermal stability and simple, inexpensive synthesis. Till now the most popular class of organic compounds for $Eu^{3+}$ chelating agents is β-diketones, which usually inherent above mentioned properties. However, structure of complex affects emission spectra profile and emission efficiency of $Eu^{3+}$ ion as much as utilized ligands. Different structure of complexes can be obtained using different ratio of ligands to $Eu^{3+}$ ion and utilization of secondary ligands. By using equimolar ratio of ligands to $Eu^{3+}$ ion 3:1 the equimolar *tris*-complexes ($Eu(\beta\text{-diketone})_3$) can be obtained, but usually, due to fact that coordination number of $Eu^{3+}$ is 8 [7], complexes with general structure of $Eu(\beta\text{-diketone})_3(Solvent)_2$ containing additional two solvent molecules are obtained instead. The coordination of these undesirable solvent molecules to $Eu^{3+}$ ion can divert using secondary ligands - N- or O-donor containing compounds, such as 1,10-phenantroline (PHEN), therefore obtaining *ternary* complexes with general structure of $Eu(\beta\text{-diketone})_3(PHEN)$. It is possible to divert solvent molecules using fourth β-diketone ligand and obtain anionic

* Corresponding author.
*E-mail addresses:* malina.ilze1@gmail.com, Ilze.Malina_1@rtu.lv (I. Malina).

https://doi.org/10.1016/j.dyepig.2018.07.003
Received 29 May 2018; Received in revised form 30 June 2018; Accepted 2 July 2018
Available online 07 July 2018
0143-7208/ © 2018 Elsevier Ltd. All rights reserved.

*tetrakis* complexes [Eu(β-diketone)$_4$]$^-$, which can be stabilized with countercations, such as quaternary ammonium ions and alkali metal ions.

Till now literature data about $Eu^{3+}$ organic complexes contains great amount of investigations about different ligand utilization for this lanthanide ion and their influence on emission properties. On the other hand, the data about comparison of different $Eu^{3+}$ complex structure – *tris*, *ternary* and *tetrakis* effect on complex optical properties are documented poorly. Likewise, information about comparison of different countercation utilization in $Eu^{3+}$ *tetrakis* complexes and their influence on the complex properties are limited [8,9]. Therefore, for the first time comparison of *ternary* and *tetrakis* complexes bearing the same β-diketone ligands are presented and full investigation about structure effect on thermal, absorption and emission properties are reported. Furthermore, two structurally similar counterions - tetraethylammonium and tetrabutylammonium cation are utilized in *tetrakis* complexes, therefore impact of counterion size on complex properties also are discussed. Lightly investigated rigid β-diketones - 2-benzoyl-1,3-indandione (HBID) and 2-(4-methylbenzoyl)-1,3-indandione (HMBID) with one carbonyl group in 1,3-indandione cycle are selected as ligands for $Eu^{3+}$ complexes. Only few similar rigid binding ligands such as indone [10,11] and 1,3-indandione [12,13] derivatives have been reported so far as excellent chelating compounds for $Eu^{3+}$ organic complexes. These type of compounds can magnify $Eu^{3+}$ complex luminescence efficiency due to restriction of thermal vibration by rigid ligand, which leads to reduction of non-radiative deactivation of whole complex. Selected ligands exhibit not only easy synthesis and excellent solubility in commonly used solvents, but also high molar absorptivity. The synthesis of HBID and HMBID, and six new $Eu^{3+}$ complexes with structures Eu(BID)$_3$(PHEN), Eu(MBID)$_3$(PHEN), [Eu(BID)$_4$]$^-$N$^+$(Et)$_4$, [Eu(MBID)$_4$]$^-$N$^+$(Et)$_4$, [Eu(BID)$_4$]$^-$N$^+$(Bu)$_4$ and [Eu(MBID)$_4$]$^-$N$^+$(Bu)$_4$ reported in this article are shown in Scheme 1. Characterization of complexes by $^1$H NMR and mass spectroscopy, FT-IR spectra, as well as X-Ray diffraction analysis are reported and optical properties in solutions and solid-state are investigated. Furthermore, different polymer thin films doped with complexes are obtained and their optical properties fully examined for practical evaluation of synthesized complexes in OLEDs.

## 2. Experimental section

### 2.1. Materials and instrumentation

$EuCl_3 \cdot 6H_2O$ (99.99%) and tetrabutylammonium bromide (98%), was purchased from *Acros Organics*, 1,10-phenantroline (99%), tetraethylammonium bromide (98%), acetophenone (96%) and 4-methylacetophenone (96%) were purchased from *Alfa Aesar*. Poly-*N*-vinylcarbazole (PVK) was purchased from *ABCR* (GmbH&Co), but poly (methyl methacrylate) (PMMA) from *Sigma Aldrich*. All substances were used without further purification. CHN elemental analyses were performed on Euro Vector EA 3000 analyzer. $^1$H NMR spectra were recorded in $CDCl_3$ or $CD_3CN$ solutions (7 mg/ml) on a Brucker Avance 300 MHz spectrometer at 300 MHz for $^1$H nuclei. Chemical shifts were expressed in parts per million (ppm) relative to solvent signal. The FT-IR spectra (4000–650 cm$^{-1}$) were recorded on a Perkin-Elmer Spectrum 100 FTIR spectrometer using KBr pellets. Thermal properties were determined on a Perkin Elmer STA 6000 instrument. Each sample was heated from 30-890 °C with heating rate 10 °C/min in nitrogen atmosphere. The purity of synthesized ligands was established on Waters 2695 HPLC using Waters 2996 Photodiode array UV-Vis detector. The chromatographic analyses were performed using Xterra® MS C18 (5 μm 2.1 × 100 mm) column, 50% Acetonitrile/0,1% formic acid solution as mobile phase and flow rate 0.2 ml/min. Low resolution mass spectra were acquired on a Waters EMD 1000MS mass detector (ESI + mode, voltage 30 V). The UV/Vis absorption spectra were acquired using Perkin-Elmer 35 UV/Vis spectrometer, emission and excitation spectra were measured on QuantaMaster 40 steady state spectrofluorometer (Photon Technology International, Inc.). Absolute photoluminescence quantum yields were determined using QuantaMaster 40 steady state spectrofluorometer (Photon Technology International, Inc.) equipped with 6 inch integrating sphere by LabSphere. The lifetime measurements were carried out in room temperature using QuantaMaster 40 steady state spectrofluorometer equipped with high power Xenon flash lamp as excitation source. Polymer films were obtained with Laurell WS-400 B-NPP/LITE spin coater. Diffraction data was collected on a Bruker-Nonius KappaCCD diffractometer using graphite monochromated Mo-Kα radiation (λ = 0.71073 Å). The crystal structure was solved by direct methods [14] and refined by full-matrix least squares [15] using maXus complex of programs [16]. The crystal data, details of data collection and refinement are given in Table 1.

### 2.2. Fabrication of PVK and PMMA films

PVK or PMMA (20 mg) and complexes **C1**-**C6** (1.6 mg) were dissolved in 1 ml THF and the resulting mixture was heated at 40 °C for 0.5 h. Afterwards polymer film was spin-coated on a glass substrate using following parameters: speed 800 rpm, acceleration 800 rpm/s for 1 min. Then obtained films were dried in 60 °C for 2 h.

### 2.3. Synthesis

The synthetic routes of compounds HBID and HMBID (**4**, **5**) and complexes **C1**-**C6** are shown in Scheme 1. 2-Benzoyl-1,3-indandione (**4**) and 2-(4-methylbenzoyl)-1,3-indandione (**5**) were synthesized as described in Ref. [13].

#### 2.3.1. Synthesis of ternary complexes C1-C2

**C1** Eu(BID)$_3$(PHEN): To a solution of 2-benzoyl-1,3-indandione (**4**) (1.08 mmol, 3 eq.) in 10 ml distilled water, which has been neutralized with 10% NaOH solution, an ethanol solution (5 ml) containing 1,10-phenantroline (0.36 mmol, 1 eq.) was added. The mixture was heated to 50 °C until complete dissolution of the compounds. Afterwards, obtained solution was added drop-wise to a 10 ml distilled water containing $EuCl_3 \cdot 6H_2O$ (0.36 mmol, 1 eq.). Instantly yellow precipitate was formed, which was allowed to stir for 4 h in room temperature. Then, precipitate was separated by suction filtration and crystalized from methanol solution and dried in vacuum at 50 °C for 24 h. Yellow powder, Yield 41%; $^1$H NMR (300 MHz, $CDCl_3$, ppm): 10.03 (2H, d, H-PHEN), 9.41 (2H, br s, H-PHEN), 7.86–7.77 (4H, m, H-PHEN), 7.60–7.47 (6H, br m, H-1,3-Indand.), 6.83–6.80 (6H, br m, H-1,3-Indand.), 6.55 (6H, br s, H-Ph), 6.24 (3H, br s, H-Ph), 5.29 (6H, s, H-Ph); Anal. Calcd. For $EuC_{60}H_{35}N_2O_9$: C, 66.73; H, 3.24; N, 2.59; found C, 67.14; H, 3.55; N, 2.59; FT-IR (KBr, cm$^{-1}$): 3054 ($\nu_{Csp2H}$); 1690, 1615 ($\nu_{C=O}$); 1586, 1566, 1519($\nu_{C=C}$); 1447 ($\nu_{C=N}$); ESI(+)-MS: (*m/z*) 181.2 [PHEN + H]$^+$; 899.6 [$^{151}$Eu(2BID)$_3$ + H]$^+$; 901.4 [$^{153}$Eu(2BID)$_3$ + H]$^+$.

**C2** Eu(MBID)$_3$(PHEN): Complex was synthesized by the same procedure as for **C1**, except 2-(4-methylbenzoyl)-1,3-indandione (**5**) was used instead of compound **4**. Yellow powder, Yield 31%; $^1$H NMR (300 MHz, $CDCl_3$, ppm): 10.02 (2H, d, H-PHEN), 9.43 (2H, br s, H-PHEN), 7.98–7.87 (4H, m, H-PHEN), 7.57–7.45 (6H, br m, H-1,3-Indand.), 6.84 (3H, br s, H-1,3-Indand.), 6.41–4.31 (9H, m, H-1,3-Indand., H-Ph), 5.27 (6H, br s, H-Ph), 2.24 (9H, s, Ph-$CH_3$); Anal. Calcd. For $EuC_{63}H_{41}N_2O_9$: C, 67.44; H, 3.66; N, 2.50; found C, 67.07; H, 3.82; N, 2.58; FT-IR (KBr, cm$^{-1}$): 3056, 3029 ($\nu_{Csp2H}$); 2919, 2864 ($\nu_{Csp3H}$); 1689, 1615 ($\nu_{C=O}$); 1584, 1563, 1512 ($\nu_{C=C}$); 1456 ($\nu_{C=N}$); ESI(+)-MS: (*m/z*) 181.1 [PHEN + H]$^+$; 941.6 [$^{151}$Eu(MBID)$_3$ + H]$^+$; 943.4 [$^{153}$Eu(MBID)$_3$ + H]$^+$.

#### 2.3.2. Synthesis of tetrakis complexes C3-C6

**C3** [Eu(BID)$_4$]$^-$N$^+$(Et)$_4$: To a solution of 2-benzoyl-1,3-indandione

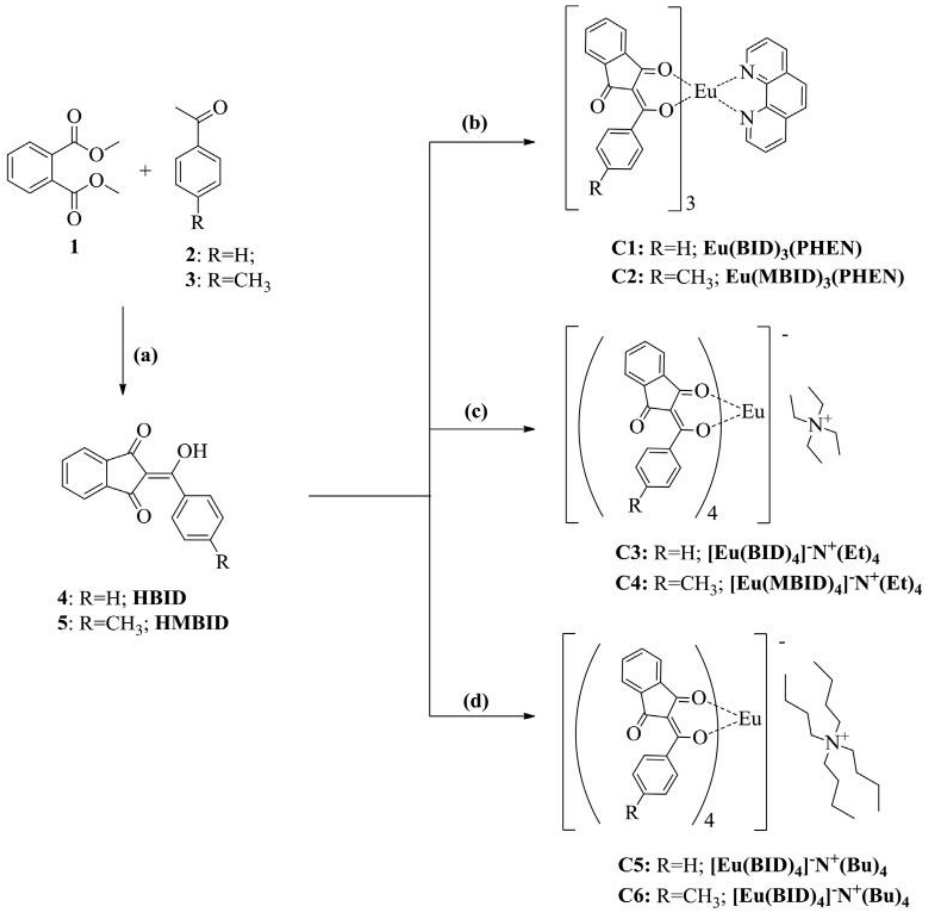


**Scheme 1.** Synthesis of complexes **C1**-**C6**; **(a)** – 1) $NaOCH_3$, toluene, 80 °C; 2) $H_2O$, 10% HCl; **(b)** – 10% NaOH/$H_2O$, 1,10-phenantroline, $EuCl_3{\cdot}6H_2O$; **(c)** – 10% NaOH/$H_2O$, $N(Et)_4Br$, $EuCl_3{\cdot}6H_2O$; **(d)** – 10% NaOH/$H_2O$, $N(Bu)_4Br$, $EuCl_3{\cdot}6H_2O$.

**Table 1**
Crystallographic data for complex **C4**.

| Parameters | $[Eu(MBID)_4]^-N^+(Et)_4$ |
|---|---|
| Formula | $C_{76}H_{64}EuNO_{12}$ |
| Formula weight | 1335.25 |
| Wavelength | 0.71073 Å |
| Crystal system | Monoclinic |
| Space group | C2/c |
| Unit cell dimensions | a = 27.2496 (4) Å |
| | b = 16.0957 (4) Å |
| | c = 20.2099 (5) Å |
| α | 90 deg |
| β | 132.2274 (10) deg |
| γ | 90 deg |
| Volume | 6563.7 (2) $Å^3$ |
| Z | 4 |
| Density (calculated) | 1.351 $g/cm^3$ |
| Absorption coefficient | 1.019 $mm^{-1}$ |
| F (000) | 2744 |
| Goodness-of-fit on $F^2$ | 1.861 |
| Data/restraints/parameters | 7778/0/407 |
| Final R indices [I > 2sigma(I)] | R1 = 0.1097, wR2 = 0.2783 |
| R indices (all data) | R1 = 0.1301, wR2 = 0.2859 |

(**4**) (1.08 mmol, 3 eq.) in 10 ml distilled water, which has been neutralized with 10% NaOH solution, distilled water solution (5 ml) containing tetraethylammonium bromide (0.54 mmol, 1.5 eq.) was added. The mixture was heated to 50 °C until complete dissolution of the compounds. Afterwards, obtained solution was added drop-wise to a 10 ml distilled water containing $EuCl_3{\cdot}6H_2O$ (0.36 mmol, 1 eq.). Instantly yellow precipitate was formed, which was allowed to stir for 4 h in room temperature. Then, precipitate was separated by suction filtration and crystalized from acetonitrile solution and dried in vacuum at 50 °C for 24 h. Yellow powder, Yield 55%; $^1H$ NMR (300 MHz, $CDCl_3$, ppm): 8.59 (4H, br s, H-1,3-Indand.), 7.70 (4H, br s, H-1,3-Indand.), 7.10 (8H, d, H-Ph), 6.78 (8H, m, H-1,3-Indand.), 6.46 (4H, br s, H-Ph), 5.96 (8H, br s, H-Ph), 4.27 (8H, br d, $(CH_3\text{-}CH_2)_4N^+$), 1.71 (12H, br s, $(CH_3\text{-}CH_2)_4N^+$). Anal. Calcd. For $EuC_{72}H_{56}NO_{12}$: C, 67.61; H, 4.38; N, 1.10; found C, 67.44; H, 4.41; N, 1.30; FT-IR (KBr, $cm^{-1}$): 3083, 3054, 3018 ($\nu_{Csp2H}$); 2997, 2977, 2948 ($\nu_{Csp3H}$); 1681, 1619 ($\nu_{C=O}$); 1589, 1574, 1451 ($\nu_{C=C}$); 1266, 1212 ($\nu_{C\text{-}N}$); ESI(+)-MS: (*m/z*) 130.2 $[N(Et)_4]^+$; 899.4 $[^{151}Eu(BID)_3+H]^+$; 901.4 $[^{153}Eu(BID)_3+H]^+$.

**C4** $[Eu(MBID)_4]^-N^+(Et)_4$: Complex was synthesized by the same procedure as for **C3**, except 2-(4-methylbenzoyl)-1,3-indandione (**5**) was used instead of compound **4**. Yellow crystals, Yield 44%; $^1H$ NMR (300 MHz, $CD_3CN$, ppm): 8.31 (4H, H-1,3-Indand., d, $J = 9$ Hz), 7.66 (4H, H-1,3-Indand., t, $J = 9$ Hz), 7.11 (4H, H-1,3-Indand., t, $J = 9$ Hz), 6.72 (8H, H-Ph, d, $J = 6$ Hz), 6.35 (4H, H-1,3-Indand., d, $J = 9$ Hz), 6.15 (8H, H-Ph, d, $J = 6$ Hz), 3.17 (8H, q, $(CH_3\text{-}CH_2)_4N^+$), 2.30 (12H, s, Ph-$CH_3$), 1.23 (12H, br t, $(CH_3\text{-}CH_2)_4N^+$). Anal. Calcd. For $EuC_{76}H_{64}NO_{12}$: C, 68.37; H, 4.80; N, 1.05; found C, 67.53; H, 4.88; N, 1.09; FT-IR (KBr, $cm^{-1}$): 3019 ($\nu_{Csp2H}$); 2924, 2802 ($\nu_{Csp3H}$); 1679, 1615 ($\nu_{C=O}$); 1585, 1563, 1492, 1432 ($\nu_{C=C}$); 1284($\nu_{C\text{-}N}$); ESI(+)-MS: (*m/z*) 130.2 $[N(Et)_4]^+$; 941.6 $[^{151}Eu(MBID)_3+H]^+$; 943.4 $[^{153}Eu(MBID)_3+H]^+$.

**C5** $[Eu(BID)_4]^-N^+(Bu)_4$: Complex was synthesized by the same

procedure as for **C3**, except tetrabutylammonium bromide was used instead of tetraethylammonium bromide. Yellow powder, Yield 50%; $^1$H NMR (300 MHz, $CDCl_3$, ppm): 7.02–6.87 (36H, m, H-1,3-Indand., H-Ph), 3.28 (8H, s, $(CH_3\text{-}CH_2\text{-}CH_2\text{-}CH_2)_4N^+$), 1.53 (8H, s, $(CH_3\text{-}CH_2\text{-}CH_2\text{-}CH_2)_4N^+$), 1.41 (8H, s, $(CH_3\text{-}CH_2\text{-}CH_2\text{-}CH_2)_4N^+$), 0.97 (12H, s, $(CH_3\text{-}CH_2\text{-}CH_2\text{-}CH_2)_4N^+$). Anal. Calcd. For $EuC_{80}H_{72}NO_{12}$: C, 69.06; H, 5.18; N, 1.00; found C, 68.23; H, 4.99; N, 1.07; FT-IR (KBr, $cm^{-1}$): 3056 ($\nu_{Csp2H}$); 2962, 2931, 2875 ($\nu_{Csp3H}$); 1767, 1688 ($\nu_{C=O}$); 1621, 1588, 1574, 1568, 1492 ($\nu_{C=C}$); 1260 ($\nu_{C\text{-}N}$); ESI(+)-MS: (*m/z*) 242.4 $[N(Bu)_4]^+$; 899.5 $[^{151}Eu(2BID)_3+H]^+$; 901.5 $[^{153}Eu(2BID)_3+H]^+$.

**C6** $[Eu(MBID)_4]^-N^+(Bu)_4$: Complex was synthesized by the same procedure as for **C3**, except 2-(4-methylbenzoyl)-1,3-indandione (**5**) was used instead of compound **4** and tetrabutylammonium bromide was used instead of tetraethylammonium bromide. Yellow powder, Yield 42%; $^1$H NMR (300 MHz, $CDCl_3$, ppm): 7.70–6.50 (32H, m, H-1,3-Indand., H-Ph), 4.02 (8H, br s, $(CH_3\text{-}CH_2\text{-}CH_2\text{-}CH_2)_4N^+$), 2.22 (12H, s, Ph-$CH_3$), 1.99 (8H, br s, $(CH_3\text{-}CH_2\text{-}CH_2\text{-}CH_2)_4N^+$), 1.72 (8H, br q, $(CH_3\text{-}CH_2\text{-}CH_2\text{-}CH_2)_4N^+$), 1.12 (12H, t, $(CH_3\text{-}CH_2\text{-}CH_2\text{-}CH_2)_4N^+$); Anal. Calcd. For $EuC_{84}H_{80}NO_{12}$: C, 69.71; H, 5.53; N, 0.97; found C, 69.19; H, 5.29; N, 1.00; FT-IR (KBr, $cm^{-1}$): 3034 ($\nu_{Csp2H}$); 2960, 2876 ($\nu_{Csp3H}$); 1739, 1683 ($\nu_{C=O}$); 1616, 1584, 1563, 1511, 1427 ($\nu_{C=C}$); 1282 ($\nu_{C\text{-}N}$); ESI(+)-MS: (*m/z*) 242.4 $[N(Bu)_4]^+$; 941.5 $[^{151}Eu(MBID)_3+H]^+$; 943.5 $[^{153}Eu(MBID)_3+H]^+$.

## 3. Results and discussion

### 3.1. Characterization of $Eu^{3+}$ complexes with BID and MBID ligands

To establish the structures of synthesized complexes – $^1$H NMR, mass spectroscopy, as well as element analysis and FT-IR spectroscopy were employed. Elemental analysis data were in a good agreement with proposed structures, but $^1$H NMR spectroscopy was used to prove ratio of ligands in synthesized complexes. $^1$H NMR spectra of *tetrakis* complex **C3** is shown in Fig. 1. Due to the presence of paramagnetic metal ion – $Eu^{3+}$ all proton signals are shifted to higher fields and shows peak broadening. In higher fields two signals corresponding to ethylene (8 protons, 4.25 ppm) and methyl (12 protons, 1.69 ppm) group protons from quaternary ammonium ion $N^+(Et)_4$ molecule were observed. Furthermore, at lower field six broad signals corresponding to 36 protons from four BID ligands were observed indicating, that in complex **C3** ratio of $N^+(Et)_4$ to BID is 1:4. Similar $^1$H NMR spectra were obtained for other *tetrakis* complexes **C4**-**C6**. Whereas in the $^1$H NMR spectra of *ternary* complexes **C1** and **C2** three signals at ~10.00, 9.40 and 7.90 ppm corresponding to eight protons from 1,10-phenantroline molecule were observed. Furthermore, in higher fields four broad signals corresponding to 27 protons from three BID ligands (**C1**) or five broad signals corresponding to 33 protons from three MBID ligands (**C2**) were obtained, which verifies that in these complexes ratio of PHEN:BID (or MBID) is 1:3.

Mass spectra of *ternary* complexes consists of three mass peaks, and for **C1** they are *m/z* 181.2 $[PHEN + H]^+$, 899.6 $[^{151}Eu(BID)_3+H]^+$ and 901.4 $[^{153}Eu(BID)_3+H]^+$ establishing, that $Eu^{3+}$ and BID ratio in complex is 1:3. Unfortunately, molar masses of ions of *tetrakis* complexes ($[Eu(BID)_4]^-$ or $[Eu(MBID)_4]^-$) were over the mass spectra detection limit and only *tris* ions ($[Eu(BID)_3+H]^+$ or $[Eu(MBID)_3+H]^+$) and quaternary ammonium ions (*m/z* 242.4 $[N(Bu)_4]^+$ or 130.2 $[N(Et)_4]^+$) were detected.

In the FT-IR spectra of complexes **C1**-**C6** absence of any broad band around 3500 $cm^{-1}$ ($\nu_{OH}$) indicates, that they are anhydrous and there are no solvent molecules in $Eu^{3+}$ coordination sphere. Furthermore, comparing complexes with BID ligands: *ternary* **C1** with *tetrakis* **C3** and **C5**, the latter two shows vibrations of $C_{sp3}H$ groups from $N^+(Et)_4$ or $N^+(Bu)_4$ ions in the range from 2800-3000 $cm^{-1}$, verifying that these complexes are with *tetrakis* structure. Furthermore, compound FT-IR spectra of HBID (**4**) contains sharp peak at 1713 $cm^{-1}$ and one at 1644 $cm^{-1}$ corresponding to symmetric and asymmetric stretching vibrations of carbonyl group ($\nu_{C=O}$). In the FT-IR spectra of complexes **C1**, **C3** and **C5** both of these peaks appears on lower frequencies (for 22-32 $cm^{-1}$). Similar observations were reported for other 2-acyl-1,3-indandione complexes [17].

*Ternary* complexes **C1** and **C2** and *tetrakis* complexes **C5** and **C6** with $N^+(Bu)_4$ cation shows excellent solubility in $CH_2Cl_2$, $CHCl_3$, THF, MeOH and MeCN. However, *tetrakis* complexes **C3** with $N^+(Et)_4$ cation exhibit slightly lower dissolution ability in commonly used solvents and **C4** is insoluble in non-polar solvents, but soluble in MeCN. It seems that, solubility of *tetrakis* complexes are mainly affected by used counterion ($N^+(Et)_4$ or $N^+(Bu)_4$) and complexes with $N^+(Bu)_4$ cation shows higher dissolution ability in polar and non-polar solvents.

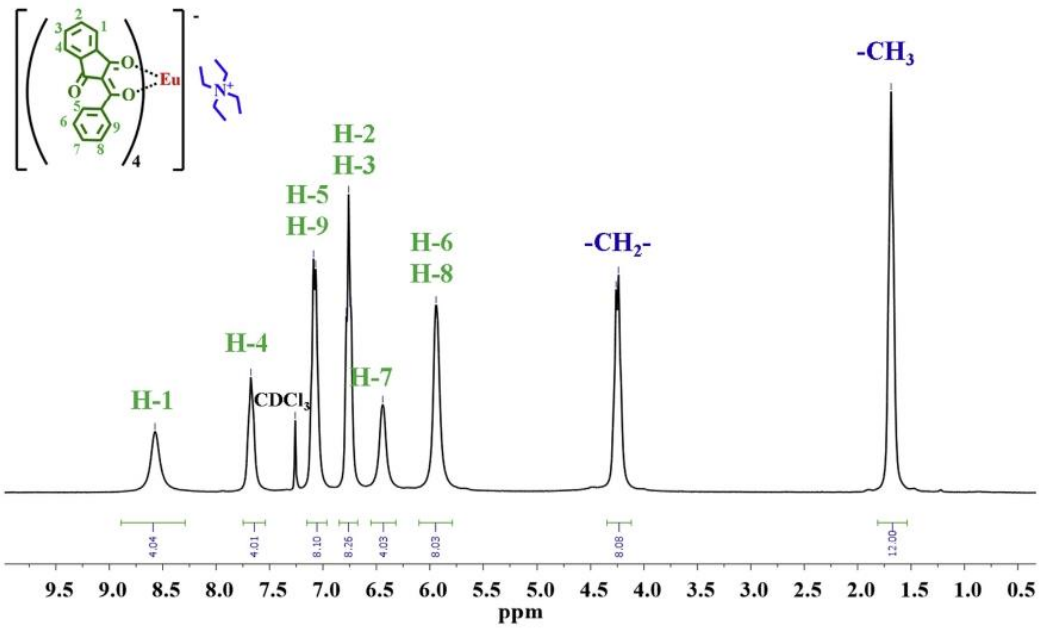


**Fig. 1.** $^1$H NMR spectra of *tetrakis* complex **C3** in $CDCl_3$ at 298 K.

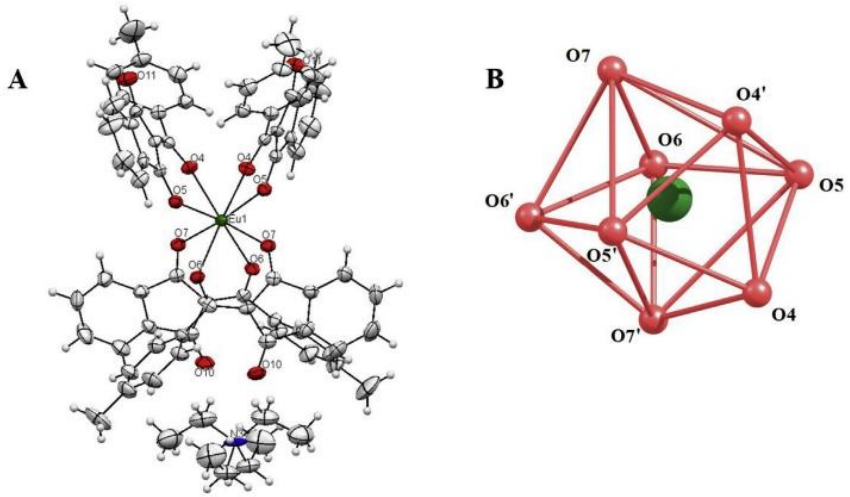


**Fig. 2.** (**A**) - X-Ray structure with 50% probability ellipsoids of crystal **C4** ($[Eu(MBID)_4]^-N^+(Et)_4$); (**B**) - Coordination polyhedron of europium in **C4**.

### 3.2. Crystal structure of complex C4

Crystal of complex **C4** was obtained by slow evaporation of MeCN solution. X-ray structure of complex **C4** is shown in Fig. 2 (**A**) and selected bond lengths and angles are given in Table 2. Important disorder contribution has been encountered in these Eu complex crystals. *Tetrakis* complex $[Eu(MBID)_4]^-N^+(Et)_4$ **C4** crystallizes in the monoclinic space group *C2/c*. In the crystal structure both cations and anions lie on twofold symmetry axes. Therefore, the structure of the molecular ions consists of two parts with identical bond length and angles. No MeCN molecules were found trapped in crystal packing of **C4**.

In the structure of complex **C4** each $Eu^{3+}$ ion is coordinated with eight oxygen atoms from four β-diketone moieties. The mean bond length of Eu-O is 2.390 Å, which is a close value to other previously reported Eu-O bond lengths of $Eu^{3+}$ *tetrakis* complexes with β-diketone ligands [18–20]. Furthermore, mean bond angle around central metal atom (O-Eu-O, where both oxygen atoms are from one β-diketone molecule) is 72.35°, which is very close to reported value (72.23°) for other $Eu^{3+}$ complex with 2-acyl-1,3-indandionate ligands [13]. The geometrical arrangement of oxygen atoms in the first coordination sphere of $Eu^{3+}$ ion can be described as trigondodecahedron (see Fig. 2 (**B**)).

### 3.3. Thermal properties of $Eu^{3+}$ complexes with BID and MBID ligands

The high thermal stability is necessary for practical application of organic luminescent materials in optoelectronic devices. Therefore, thermal stability of $Eu^{3+}$ complexes was examined by thermogravimetric analysis (TGA) in the inert atmosphere and obtained thermal decomposition temperatures $T_d$ are depicted in Table 3. TGA shows that the starting decomposition temperatures of *ternary* complexes **C1** and **C2** are 240 and 247 °C, respectively, and are lower than ones for *tetrakis* complexes **C3**-**C6** (299–307 °C). It seems, that introduction of secondary ligand PHEN in $Eu^{3+}$ ion coordination sphere leads to reduction of $T_d$ and can be explained with lower thermal stability of PHEN (start of $T_d \sim 240$ °C) [21] than used β-diketonates BID and MBID. However, obtained $T_d$ values for **C1** and **C2** are close to other previously reported destruction temperatures of $Eu^{3+}$ *ternary* complexes with rigid β-diketone ligands [11]. On the other hand, for *tetrakis* complexes **C3**-**C6** thermal decomposition temperatures are higher by 52–67 °C. Moreover, decomposition temperatures of *tetrakis* complexes is not influenced by used counterion ($N^+(Et)_4$ or $N^+(Bu)_4$) and obtained $T_d$ values differs for only 3–5 °C. It can be concluded that synthesized *tetrakis* complexes exhibit ones of the highest thermal stabilities from currently reported *tetrakis* $Eu^{3+}$ β-diketone complexes [19,22], which usually do not exceed 300 °C.

Destruction pattern of complexes was studied through obtained termogramms (Fig. 3). Termogramms of *ternary* complexes **C1** and **C2** consists of two rapid weight losses in the steps around 240–452, 453–570 °C (**C1**) and 247–426, and 427–580 °C (**C2**), which corresponds to the loss of organic ligands - one PHEN and one BID or MBID molecule. Further destruction of complex has followed by complicated decomposition and carbonization reactions, which lead to rather high residual weight – 46% and 49%, respectively. Similarly, *tetrakis* complexes **C3**-**C6** exhibits two rapid weight loss stages in TGA curve, and for complex **C5** they are at 299–410, 411–572 °C. The first stage can be signed to loss of counterion ($N^+(Bu)_4$) and one MBID molecule and second stage – to one MBID molecule. Similar destruction pattern was reported for *tetrakis* $Eu^{3+}$ complexes with dibenzoylmethane ligands and hexadecyltrimethyl ammonium or octadecyltriethyl ammonium counterions [23]. In the end of TGA (at 890 °C) high residual weight of *tetrakis* complexes (40–48%) are obtained similarly than for *ternary* complexes. Solid residue of all complexes was analyzed by CHN elemental analysis, and for complex **C6** it showed C, 65.31; H, 0.85; N, < 0.30, which points to formation of solid residue with high fracture of carbon. Probably in high temperatures carbonization reactions takes place with remaining β-diketone ligands and remaining europium forms different inorganic compounds, for example $Eu_2O_3$. All obtained complexes exhibits proper thermal decomposition temperatures for application in the electronic devices.

**Table 2**
Selected bond lengths (Å) and angles (°) for complex $[Eu(MBID)_4]^-N^+(Et)_4$ **C4**.

| Bond lengths | | | | Bond angles | |
|---|---|---|---|---|---|
| Bond | Value, Å | Bond | Value, Å | Bond angle | Value, ° |
| Eu(1)-O (4) | 2.410 (6) | Eu(1)-O (4) | 2.410 (6) | O (4)-Eu(1)-O (5) | 72.40 (19) |
| Eu(1)-O (5) | 2.375 (6) | Eu(1)-O (5) | 2.375 (6) | O (4)-Eu(1)-O (5) | 72.40 (19) |
| Eu(1)-O (6) | 2.410 (6) | Eu(1)-O (6) | 2.410 (6) | O (6)-Eu(1)-O (7) | 72.30 (2) |
| Eu(1)-O (7) | 2.378 (6) | Eu(1)-O (7) | 2.379 (6) | O (6)-Eu(1)-O (7) | 72.30 (2) |

**Table 3**
Thermal decomposition temperatures ($T_d$), absolute photoluminescence quantum yields (PLQY) and CIE coordinates calculated from emission spectra of complexes **C1-C6** in MeCN solutions ($c \sim 1.5 \cdot 10^{-5}$ M) and in solid-state, luminescence lifetime ($\tau_1$ and $\tau_2$) of complexes **C1-C6** in solid-state.

| | In MeCN solutions | | | | In solid-state | | |
|---|---|---|---|---|---|---|---|
| | PLQY | CIE 1931 coordinates x; y | $\tau_1$, μs | $\tau_2$, μs | PLQY | CIE 1931 coordinates x; y | $T_d$, °C |
| **C1** | < 0.01 | 0.669; 0.331 | 121 ± 4 (6%) | 42 ± 1 (94%) | 0.06 | 0.670; 0.330 | 240 |
| **C2** | < 0.01 | 0.669; 0.331 | 122 ± 3 (5%) | 39 ± 1 (95%) | 0.10 | 0.670; 0.330 | 247 |
| **C3** | 0.01 | 0.669; 0.331 | 233 ± 2 (22%) | 54 ± 1 (78%) | 0.29 | 0.673; 0.329 | 302 |
| **C4** | 0.01 | 0.668; 0.331 | 203 ± 17 (25%) | 118 ± 5 (75%) | 0.60 | 0.673; 0.327 | 307 |
| **C5** | 0.01 | 0.669; 0.331 | 118 ± 4 (4%) | 37 ± 1 (96%) | 0.12 | 0.670; 0.330 | 299 |
| **C6** | 0.11 | 0.669; 0.331 | 115 ± 6 (2%) | 34 ± 1 (98%) | 0.01 | 0.670; 0.330 | 302 |

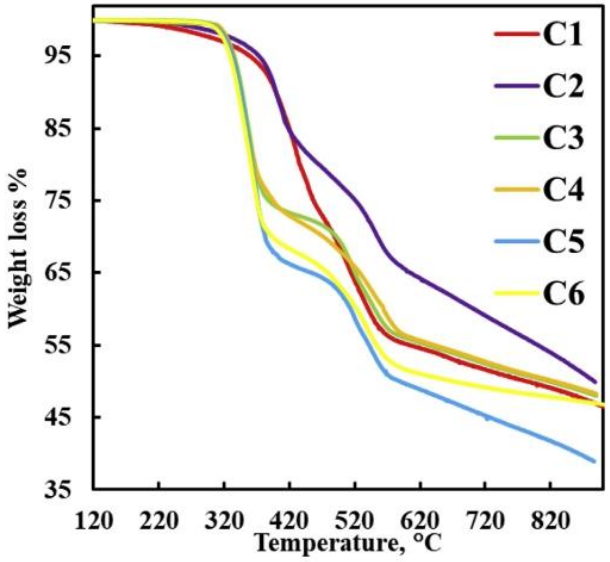


**Fig. 3.** TG curves of $Eu^{3+}$ complexes **C1-C6** obtained in the nitrogen atmosphere with heating rate of 10 °C/min.

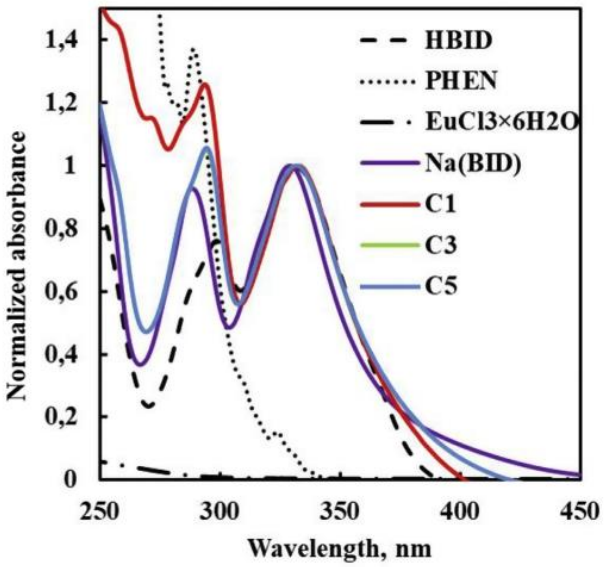


**Fig. 4.** UV/Vis absorption spectra of compounds HBID, PHEN, and $Eu^{3+}$ complexes **C1**, **C3**, **C5** in MeCN solutions ($c \sim 1.5 \cdot 10^{-5}$ M) and $EuCl_3 \cdot 6H_2O$ ($c \sim 1.0 \cdot 10^{-3}$ M) and Na complex with BID ligand Na(BID) ($c \sim 1.5 \cdot 10^{-5}$ M) in EtOH solutions.

### 3.4. UV/Vis absorption properties of $Eu^{3+}$ complexes with BID and MBID ligands

UV/Vis absorption spectra of compounds HBID, HMBID, PHEN and their $Eu^{3+}$ complexes were recorded in MeCN solutions ($c \sim 1.5 \cdot 10^{-5}$ M), also $EuCl_3 \cdot 6H_2O$ ($c \sim 1.0 \cdot 10^{-3}$ M) and Na complexes with BID and MBID ligands (Na(BID), Na (MBID)) ($c \sim 1.5 \cdot 10^{-5}$ M) were measured in EtOH solutions. Spectra of $EuCl_3 \cdot 6H_2O$, PHEN, HBID and its Na and $Eu^{3+}$ complexes are shown in Fig. 4. $EuCl_3 \cdot 6H_2O$ dissolved in EtOH exhibits very weak absorption in UV light region, however secondary ligand PHEN shows intense absorption below 300 nm, with maximum at 290 nm ($\varepsilon \sim 50881\ M^{-1}\ cm^{-1}$). Compounds HBID and HMBID exhibit broad UV-light absorption between 275-400 nm with maximums at 297 and 331 for HBID and 299 and 336 nm for HMBID. Absorption at 297 and 299 nm attributes to $\pi \rightarrow \pi^*$ transitions in 1,3-indandione, however lower energy bands corresponds to $\pi \rightarrow \pi^*$ enolic transitions from β-diketone fragment [11]. Substituent ($-CH_3$) in benzoyl fragment has negligible effect on absorption maximum, and for HMBID $\lambda_{abs\ max}$ is shifted for 5 nm, compared to HBID $\lambda_{abs\ max}$. Molar absorptivity ε are 25625 (HBID) and 24306 (HMBID) $M^{-1} \cdot cm^{-1}$, respectively. Furthermore, solutions containing Na complexes Na(BID) and Na(MBID) exhibits the same absorption profile as compounds HBID and HMBID with small blue-shift of $\lambda_{abs\ max}$ (2 nm). Similar observations, that Na complexes with rigid β-diketones exhibit almost identical absorption spectra as free ligands were reported previously [10,11].

Furthermore, coordination with $Eu^{3+}$ ion leads to some changes in UV/Vis spectra. MeCN solutions containing *ternary* complexes **C1** and **C2** exhibit absorption at region 250–294 nm, which attributes to the absorption of secondary ligand PHEN. However, lower energy bands location are not noticeably influenced by the presence of lanthanide ion and $\lambda_{abs\ max}$ lies at 332 nm for **C1** and 333 nm for **C2**. Molar absorptivity for complexes **C1**, **C2** as expected are considerably higher ($\varepsilon \sim 56385$ and $56131\ M^{-1}\ cm^{-1}$) than for free ligands confirming fact, that complexes contains several ligands in their structures. MeCN solutions containing *tetrakis* complexes **C3-C6** shows exact absorption band shape as HBID and HMBID and since used countercations ($N^+(Et)_4$ and $N^+(Bu)_4$) does not exhibit absorption in 250–400 nm range, the absorption bands for pairs **C3** and **C5**, and **C4** and **C6** even overlaps with each other. Similarly to *ternary* complexes, $\lambda_{abs\ max}$ for solutions containing *tetrakis* complexes differs from HBID and HMBID for 1–2 nm, but ε coefficients are in the range from 92370 to $94007\ M^{-1}\ cm^{-1}$. It can be concluded, that absorption spectra patterns of the solutions containing complexes **C1-C6** are almost identical to the ones observed for compounds HBID and HMBID, suggesting that coordination with $Eu^{3+}$ ion shows negligible effect on $\pi \rightarrow \pi^*$ transitions of the ligands. Similar conclusions were reported for other *ternary* and *tetrakis* $Eu^{3+}$ complexes with β-diketone ligands [10,18,22,24].

### 3.5. Photoluminescence properties of $Eu^{3+}$ complexes

Photoluminescence properties of synthesized complexes were

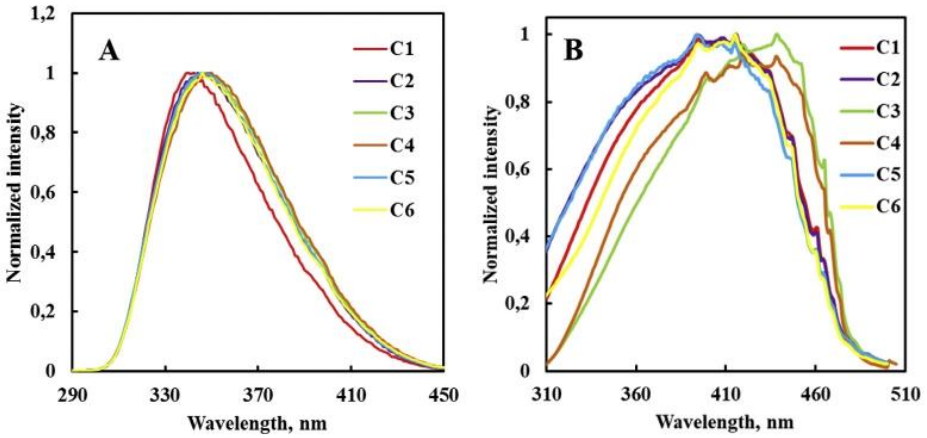


**Fig. 5.** (**A**) - Excitation spectra ($\lambda_{mon}$ = 611 nm) of $Eu^{3+}$ complexes **C1**- **C6** in MeCN solutions (c ~ 1.5·10$^{-5}$ M); (**B**) - Excitation spectra ($\lambda_{mon}$ = 611 nm) of complexes **C1**-**C6** in solid-state.

investigated in MeCN solutions and solid-state through excitation and emission spectra. Excitation spectra (monitored at $Eu^{3+}$ emission at 611 nm) of MeCN solutions (c ~ 1.5·10$^{-5}$ M) containing complexes **C1**-**C6** exhibits broad bands ranging from 300 to 440 nm (Fig. 5. (**A**)) with $\lambda_{exc}$ at ~350 nm, which attributes to π→π* transitions of coordinated ligands BID and MBID. Excitation bands match very well with absorption spectra of corresponding complexes, therefore confirming fact, that $Eu^{3+}$ emission arise from energy absorbed by coordinated BID or MBID ligands. Furthermore, excitation spectra of *ternary* complexes **C1** and **C2** does not exhibit bands below 300 nm, where the secondary ligand PHEN absorbs the light, meaning that direct energy transfer from PHEN to $Eu^{3+}$ ion is not present in these complexes.

Excitation spectra of complexes in solid-state (Fig. 5. (**B**)) contains much broader bands in 300–480 nm range with maximums at 408 nm for complexes **C1**,**C2**,**C5**,**C6**, and 425 nm for *tetrakis* complexes **C3** and **C4** with $N^+(Et)_4$ counterion. Such red shift of $\lambda_{exc}$ in solid-state compared to solutions spectra is common for $Eu^{3+}$ β-diketone complexes [18] and explained with the presence of strong π-π interactions between ligands in the solid-state. Furthermore, solid-state excitation spectra of **C1**-**C6** contains some of $Eu^{3+}$ ion sharp absorption lines of *f*-*f** transitions at 394, 415 and 465 nm. However, these transitions are almost completely overlapped with excitation bands of complexes, therefore confirming, that excitation of $Eu^{3+}$ ion through attached organic ligands is more efficient than direct excitation of $Eu^{3+}$ absorption bands. In conclusion, excitation window for all six complexes in solid-state has been extended to the visible region (up to 480 nm), which is favorable property for $Eu^{3+}$ complexes, due to frequently observed low stability of β-diketones in UV light.

Emission of complexes **C1**-**C6** was investigated in MeCN solutions and solid-state, but due to fact, that emission profile is identical for complexes with similar structure (*ternary* or *tetrakis*) only one *ternary* complex **C2** and one *tetrakis* complex **C3** emission spectra are shown as examples (Fig. 6). In MeCN solutions, when excited with 350 nm, complexes exhibit weak red-light emission with characteristic $Eu^{3+}$ ion narrow emission bands, which lies at 580, 594, 611, 652 and 701 nm and attributes to $^5D_0 \rightarrow {}^7F_J$ ($J$ = 0–4) transitions. Analogue, but more intense emission spectra profiles were obtained for complexes in solid-state, when excited with 408 or 425 nm. Commonly reported observations in the literature about emission profile of $Eu^{3+}$ β-diketone complexes are also present for our newly synthesized complexes **C1**-**C6**: Emission bands at 580 and 652 nm shows weak intensity due to fact, that their corresponding transitions ($^5D_0 \rightarrow {}^7F_0$, $^5D_0 \rightarrow {}^7F_3$) are forbidden by electric dipole and magnetic dipole moments. Furthermore, transition $^5D_0 \rightarrow {}^7F_1$ (594 nm) is forbidden by electric dipole moment, but allowed by magnetic dipole moment and is almost insensitive from

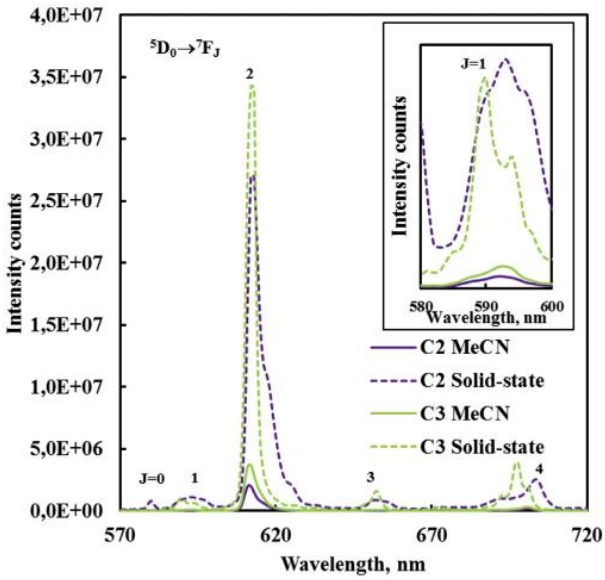


**Fig. 6.** Emission spectra of $Eu^{3+}$ complexes **C2** and **C3** in MeCN solutions (c ~ 1.5·10$^{-5}$ M) ($\lambda_{exc}$ = 350 nm) and solid-state ($\lambda_{exc}$ = 425 nm). Inset shows splitting of $^5D_0 \rightarrow {}^7F_1$ transition in the solid-state.

coordination environment around $Eu^{3+}$ ion. This transition shows splitting (Inset, Fig. 6). Moreover, band at 611 nm ($^5D_0 \rightarrow {}^7F_2$) is hypersensitive transition, which exhibit the highest intensity and is giving the red emission color for complexes. It is electric dipole allowed transition and very sensitive to coordination environment of central metal ion. Therefore ratio of intensities between transitions $^5D_0 \rightarrow {}^7F_2$ and $^5D_0 \rightarrow {}^7F_1$ shows the nature and symmetry of the first coordination sphere of $Eu^{3+}$ organic complexes. For all complexes in MeCN solutions and solid-state the intensity ratio between these two transitions is extremely high meaning that, strong coordination interactions are present in complexes **C1**-**C6** and $Eu^{3+}$ occupies site without inversion symmetry. Moreover, the higher is the intensity ratio, the more intense is the red emission from the complex [25]. CIE chromaticity coordinates for complexes **C1**-**C6** (Table 3) calculated from their emission spectra are situated in explicit red region and completely corresponds to standard red color of NTSC (x = 0.67; y = 0.33) therefore being a promising candidates for application in OLEDs. Similar CIE coordinates with 100% red color purity were reported for Eu *tetrakis* complex with butyl-methoxy-dibenzoyl-methane ligands and $NH_4^+$ as counterion

[26].

Furthermore, Fig. 6 also shows, that emission spectra shape is slightly affected by the complex structure. For, *ternary* complex **C2** emission band at 611 nm are much wider and shows shoulders at 615 and 625 nm. However, the same band of *tetrakis* complex **C3** exhibit one sharp line. $Eu^{3+}$ ion *ternary* complexes with PHEN as secondary ligand usually display splitting of $^5D_0 \rightarrow ^7F_2$ transition [8,27], which could be explained with less ordered environment around central metal ion than in *tetrakis* complexes [19,28].

To further establish the efficiency of the emission from complexes in MeCN solutions and in solid-state, absolute photoluminescence quantum yields (PLQY) were determined using integrating sphere. The data are shown in Table 3. Two relationships can be seen from PLQY:

(1) PLQY in solid state for all complexes shows higher values, than in MeCN solutions. Lower PLQY in solutions of $Eu^{3+}$ organic complexes arise from undesirable, high frequency CH vibrational oscillators of solvent (MeCN) molecules in the surrounding environment of the complex, which effectively lowers the emission transition probabilities of central metal ion [29]. PLQY of complexes **C1**-**C3**,**C5**, **C6** were also measured in THF and $CHCl_3$ solutions and again low values (~0.01) were obtained. It is possible, that some dissociation processes of complexes are present in solutions. It is known, that in non-polar solvents *tetrakis* complexes dissociate into corresponding *tris*-complexes (for example $Eu(BID)_3$) and a β-diketonate salt (for example, $BID^-N^+(Et)_4$) [30]. First coordination sphere of $Eu^{3+}$ ion is not fulfilled in *tris*-complexes, therefore, for $Eu^{3+}$ to obtain coordination number 8 two solvent molecules are attached to metal. Having high frequency CH vibrational oscillators in first coordination sphere greatly lowers emission intensity and PLQY of $Eu^{3+}$ complexes.

(2) In MeCN and solid-state *ternary* complexes **C1**, **C2** show lower PLQY than their analogues *tetrakis* complexes **C3**-**C6.** In MeCN solutions differences in PLQY between *ternary* and *tetrakis* complexes are insignificant due to low emission intensity. However, in solid-state PLQY for *tetrakis* complexes **C3** and **C4** are five to six times higher than for *ternary* complexes **C1**, **C2** and almost three to six times higher than for *tetrakis* complexes **C5**, **C6.** *Tetrakis* complexes usually are characterized with higher intensity of emission compared to analogue *ternary* complexes [6] due to due to larger cross section of photon absorption. Furthermore, in *tetrakis* complexes $Eu^{3+}$ ion is fenced by four coordinated benzoyl-1,3-indandione ligands, which provides better shielding from surrounding environment than for *ternary* complexes.

The luminescence decay of $Eu^{3+}$ emission related to $^5D_0 \rightarrow ^7F_2$ (611 nm) transition of complexes **C1**-**C6** were determined in solid-state under pulsed laser excitation at 408 or 425 nm. The obtained lifetime values ($\tau_1$ and $\tau_2$) are listed in Table 3. All decay curves were fitted by bi-exponential functions and have two lifetime components $\tau_1$ and $\tau_2$, indicating on the presence of two sites of symmetry around the $Eu^{3+}$. Usually $Eu^{3+}$ complexes with two lifetime components exhibits broadening of transition $^5D_0 \rightarrow ^7F_0$ at emission spectra [27,31], which also points to two sites of symmetry around central metal ion. All complexes **C1**-**C6** in solid-state shows slightly broad, featureless band at 580 nm, which attributes to $^5D_0 \rightarrow ^7F_0$ transition. Different symmetry around $Eu^{3+}$ ions probably forms from different distances between emitting $Eu^{3+}$ ions in the solid-state. When distance between two emitting $Eu^{3+}$ ion sites are short, some interactions between $Eu^{3+}$-$Eu^{3+}$ centers take place, which could lead to two different chemical environment formation around $Eu^{3+}$ ions. Longest decay lifetimes were obtained for *tetrakis* complexes with $N^+(Et)_4$ cation and are 233 and 54 μs for **C3** and 203 and 118 μs for **C4**.

From obtained PLQY and lifetime values, we can draw a conclusion, that the used countercation ($N^+(Et)_4$ or $N^+(Bu)_4$) affects emission properties of synthesized complexes more than complex structure in solid-state. For ternary complexes **C1**, **C2** and *tetrakis* complexes **C5**, **C6** with $N^+(Bu)_4$ cation obtained PLQY and lifetime values were close. However, complexes with $N^+(Et)_4$ as counteraction exhibits three (BID ligand) or even six times (MBID) higher PLQY values than their analogues with $N^+(Bu)_4$ cation. Such difference in emission efficiency could be as a result of different cation incorporation in the crystal structure of complex in solid-state. Therefore, in MeCN solutions, where these long-range order is absent and complex exist as anion ($[Eu(BID)_4]^-$; $[Eu(MBID)_4]^-$) no difference in PLQY were observed. In solid-state counter cation size is the mayor factor, which influences the emission properties as it was shown in the report [9]. Increase in the counteraction size usually decrease complex emission efficiency and emission data of our newly synthesized complexes confirms this statement.

### 3.6. Photoluminescence from polymer films doped with $Eu^{3+}$ complexes

The mayor drawback for practical application of $Eu^{3+}$ organic complexes are their poor carrier-transporting ability and film formability. Therefore, to overcome this problem, complexes need to be doped in host materials, which could provide missing properties, for example, in polymers. Two polymers – *N*-polyvinylcarbazole (PVK) and poly methyl methacrylate (PMMA) were chose as host materials for our complexes. PVK owing excellent hole transporting properties as well as good match between its triplet energy state and energy levels of most $Eu^{3+}$ β-diketone complexes is one of the most used host materials for metal organic complexes. However, PMMA was chosen due to its low optical absorbance (it is transparent at wavelengths > 250 nm). The doping mass of polymer films was chosen 8 wt%, according to our [32] and other authors [11,24,33,34] reported investigations about relationship of doping mass – emission efficiency of doped PVK and PMMA films with $Eu^{3+}$ complexes. Lower doping mass (0.5–2 wt%) could lead to incomplete energy transfer between host and doping complex, however, high doping mass (> 12 wt%) could lead to non-radiative energy transfer between two metal ions ($Eu^{3+}$-$Eu^{3+}$), which decreases emission intensity of doped films. PVK and PMMA polymer films doped with 8 wt% of $Eu^{3+}$ complexes were prepared by spin-coating technique from THF solutions (due to complex **C4** low solubility in commonly used solvents, PVK film with 8 wt% of **C4** wasn't prepared, but PMMA film was obtained from MeCN solution). UV/VIS absorption spectra of prepared films are depicted in Fig. 7 (**A**) and Fig. 8 (**A**).

UV/Vis spectra of pure PVK film exhibit broad absorption in 250–350 nm range, with $\lambda_{abs\ max}$ at 271, 297, 327 and 348 nm, which can be assigned to π-π* and n-π* transitions of *N*-polyvinylcarbazole. Nevertheless, absorption profile of doped PVK films exhibits the same profile as pure thin film, which appoints to absorption overlap between host matrix and $Eu^{3+}$ complexes. However, in the spectral region from 350 to 400 nm new absorption band arises for doped PVK films and can be attributed to the absorption of ligands (BID, MBID). This band is particular pronounced for *tetrakis* complex **C3**, which also showed red-shift of excitation spectra in solid-state, compared to other complexes. Completely different situation is found for doped PMMA films (Fig. 8 (**A**)). These films exhibit pure complex absorption profile with two $\lambda_{abs\ max}$ at ~297 nm and ~337 nm (Table 4), which compared to $\lambda_{abs\ max}$ in MeCN solutions are shifted to longer wavelengths.

Excitation spectra of pure PVK film (Fig. 7 (**B**)) ($\lambda_{mon}$ = 435 nm) shows sharp band (300–360 nm) with maximum at 346 nm and corresponding doping films ($\lambda_{mon}$ = 611 nm) with complexes **C1**,**C2**,**C5**,**C6** exhibits the same maximum, but excitation bands shows shoulder at longer wavelengths rising from 360 to 420 nm. Only polymer film doped with *tetrakis* complex **C3** shows distinct excitation spectra from pure PVK film (350–460 nm with $\lambda_{exc}$ = 379 nm). Furthermore, all excitation spectra of PVK films doped with complexes **C1**-**C3**,**C5**, **C6** slightly overlaps with emission spectra of PVK (355–550 nm) (Fig. 7 (**B**)), which could also be advantageous for polymer films due to fact, that host would provide additional excitation energy for complex,

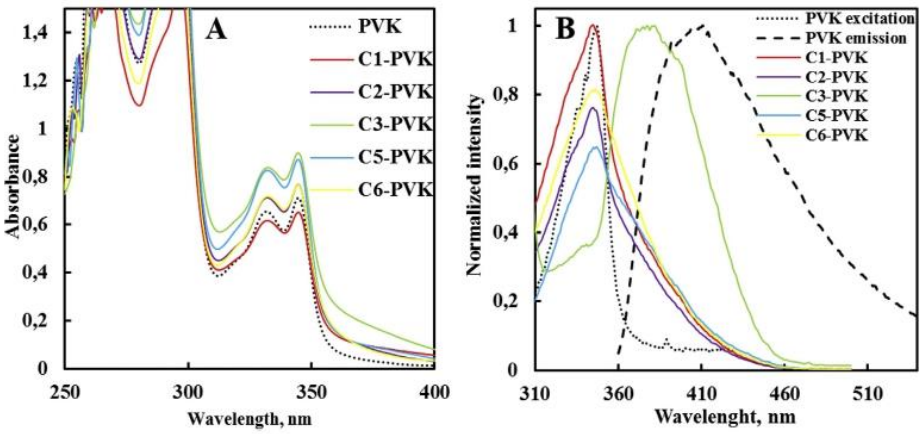


**Fig. 7.** (**A**) – UV/Vis absorption spectra of pure PVK film and PVK films containing 8 wt% of $Eu^{3+}$ complexes **C1-C3**,**C5**,**C6**; (**B**) - Excitation spectra ($\lambda_{mon\ PVK}$ = 435 nm) and emission spectra ($\lambda_{exc}$ = 346 nm) of pure PVK film and excitation spectra of PVK films containing 8 wt% of $Eu^{3+}$ complexes **C1-C3**,**C5**, **C6** ($\lambda_{mon}$ = 611 nm).

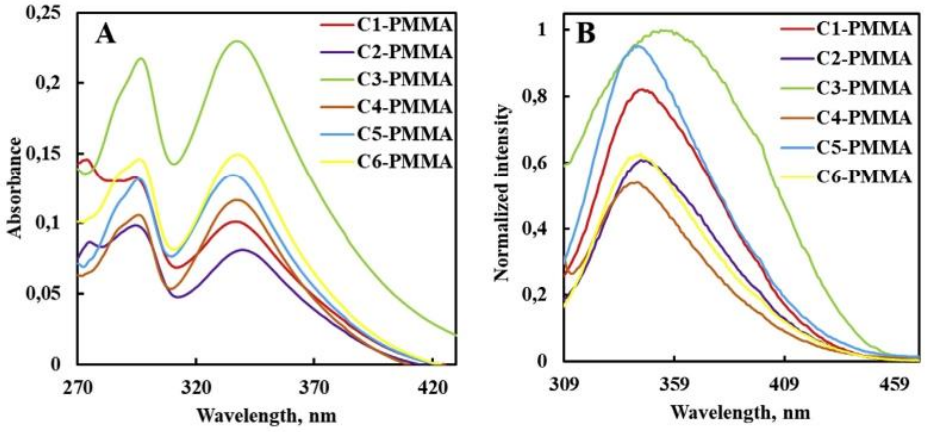


**Fig. 8.** (**A**) – UV/Vis absorption spectra of PMMA films containing 8 wt% of $Eu^{3+}$ complexes **C1-C6**; (**B**) – Excitation spectra of PMMA films containing 8 wt% of $Eu^{3+}$ complexes **C1-C6** ($\lambda_{mon}$ = 611 nm).

**Table 4**
Optical properties of PVK and PMMA films doped with 8 wt% of complexes **C1-C6**.

| | PVK films | | | | | PMMA films | | | | |
|---|---|---|---|---|---|---|---|---|---|---|
| | $\lambda_{abs}$, nm | $\lambda_{exc}$, nm | $\tau_1$, μs | $\tau_2$, μs | PLQY[b] | $\lambda_{abs}$, nm | $\lambda_{exc}$, nm | $\tau_1$, μs | $\tau_2$, μs | PLQY[c] |
| **C1** | 332, 345 | 344 | 47 ± 0.5 (92%) | 179 ± 3 (8%) | 0.04 | 337 | 347 | 75 ± 1 (83%) | 306 ± 8 (17%) | 0.12 |
| **C2** | 332, 345 | 345 | 50 ± 0.7 (95%) | 193 ± 7 (5%) | 0.04 | 341 | 347 | 74 ± 1 (90%) | 317 ± 14 (10%) | 0.11 |
| **C3** | 332, 345 | 377 | 60 ± 1 (95%) | 199 ± 14 (5%) | 0.08 | 337 | 353 | 56 ± 0.6 (85%) | 204 ± 2 (15%) | 0.14 |
| **C4** | -[a] | -[a] | -[a] | -[a] | -[a] | 339 | 342 | 68 ± 1 (88%) | 256 ± 7 (12%) | 0.10 |
| **C5** | 332, 345 | 347 | 40 ± 0.5 (94%) | 139 ± 2 (6%) | 0.05 | 336 | 342 | 72 ± 1 (85%) | 255 ± 6 (15%) | 0.14 |
| **C6** | 332, 345 | 346 | 42 ± 0.8 (97%) | 154 ± 9 (3%) | 0.04 | 339 | 345 | 53 ± 0.6 (88%) | 214 ± 2 (12%) | 0.09 |

[a] Film wasn't obtained due to complex **C4** low solubility in THF, $CHCl_3$.
[b] PLQY determined with $\lambda_{exc}$ = 370 nm.
[c] PLQY determined with $\lambda_{exc}$ = 340 nm.

therefore increasing emission efficiency. From these excitation spectra we can conclude, that PVK films can be excited not only through $\pi \rightarrow \pi^*$ transitions of the ligands, but also through host matrix transitions.

Furthermore, excitation spectra of PMMA films (Fig. 8. (**B**)) reveal wide bands in the range from 309 to 450 nm, with $\lambda_{exc}$ ~347 nm. Excitation spectra very well corresponds to absorption spectra, meaning that these bands can be attributed to $\pi \rightarrow \pi^*$ transitions of coordinated ligands. Slight shift of $\lambda_{abs}$ and $\lambda_{exc}$ in PMMA matrices compared to ones in MeCN solution, points out to some interactions between ligands from complexes **C1-C6** and PMMA matrix.

Emission spectra of doped polymer films are shown in Fig. 9. All five PVK films shows characteristic $Eu^{3+}$ ion emission lines, also no emission from matrix (PVK) in the range from 360 to 520 nm are observed indicating, that complete energy transfer process between host and complexes are present in these films. PLQY were determined using two excitation wavelengths. First, doped films were excited with 350 nm (through host matrix transitions) and obtained PLQY values were low (0.03–0.04). Second, doped PVK films were excited with 370 nm (through coordinated ligands transitions) and obtained PLQY were higher (0.04–0.08) (Table 4) indicating, that direct excitation through complex absorption region is more efficient, than through host matrix absorption region. Similar to emission properties in MeCN solutions and in solid-state, highest quantum yield was obtained for *tetrakis* complex **C3** with $N^+(Et)_4$ countercation, due to fact, that its

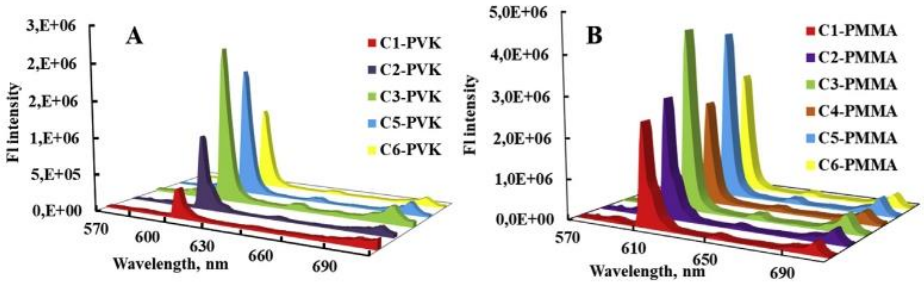


**Fig. 9.** (**A**) - Emission spectra of PVK films containing 8 wt% of $Eu^{3+}$ complexes **C1**-**C3**,**C5**,**C6**; (**B**) - Emission spectra of PMMA films containing 8 wt% of $Eu^{3+}$ complexes **C1**-**C6**.

excitation spectra show the largest overlap with host matrix emission spectra, which increases the efficiency of energy transfer process between host and doping substance. The obtained PLQY of doped PVK films are lower than other reported doped PVK films with ternary complexes [35].

Furthermore, all six PMMA doped films exhibit more intense red light emission (Fig. 9 (**B**)) with much higher quantum yields (0.09–0.14) than for PVK films confirming the assumption, that one of the main factors why PVK films showed low PLQY are undesirable absorption spectra overlap between matrix and complex. Yet again the highest PLQY were obtained for *tetrakis* complexes **C3** and **C5** – 0.14. The obtained PLQY of doped PMMA films are close or slightly lower than other reported doped PMMA films containing Eu complexes with rigid β-diketones [11].

The luminescence decay curves for all PVK and PMMA doped films were found to be bi-exponential and relevant time components $\tau_1$ and $\tau_2$ are given in Table 4. As it seems, both luminescence lifetime values for doped films are longer than it was in the solid-state and can be explained with greater distance between two emitting centers $Eu^{3+}$-$Eu^{3+}$ in polymer films, which reduces possibility of energy transfer between $Eu^{3+}$-$Eu^{3+}$ as a non-radiative process. Two lifetime components $\tau_1$ and $\tau_2$ for polymer films could be connected with complex interaction with hosts, which could lead to two different emitting sites – one being unbounded complex, other – complex bounded with polymers PMMA and PVK. Similar conclusions were reported for Eu $(DBM)_3$PHEN complex doped in PMMA matrix [21].

Herein we conclude, that PMMA matrix provides excellent, transparent film formability for $Eu^{3+}$ organic complexes with no influence on absorption or properties of doping complex. Obtained films exhibit moderate PLQY and lifetime values and could show potential in application as polymer optical fibers, which are being used in luminescent solar concentrators and luminescent biosensors.

## 4. Conclusions

Structures of newly synthesized *ternary* and *tetrakis* $Eu^{3+}$ complexes $Eu(BID)_3$(PHEN), $Eu(MBID)_3$(PHEN), $[Eu(BID)_4]^-N^+(Et)_4$, $[Eu(MBID)_4]^-N^+(Et)_4$, $[Eu(BID)_4]^-N^+(Bu)_4$ and $[Eu(MBID)_4]^-N^+(Bu)_4$ were neatly characterized with elemental analysis, $^1$H NMR spectroscopy, mass spectroscopy, FT-IR spectra and X-Ray diffraction analysis. Complex structure (*ternary* or *tetrakis*) did not affect excitation window (300–450 nm) and CIE chromaticity coordinates (x = 0.670; y = 0.330) for emission spectra in the solid-state and solution. However, complex structure greatly affects thermal properties and emission properties in the solid-state. *Tetrakis* complexes with structure $[Eu(BID)_4]^-N^+(Et)_4$ and $[Eu(MBID)_4]^-N^+(Et)_4$ showed higher PLQY values (0.29 and 0.60) than corresponding *ternary* complexes (0.06–0.10) in the solid-state. Countercation ($N^+(Et)_4$ or $N^+(Bu)_4$) size noticeably affects emission properties of *tetrakis* complexes. Increase in the countercation size decrease complex emission efficiency. For each complex two polymer films (PVK and PMMA) with doping mass of 8 wt% were prepared and optical properties investigated. Highest PLQY (0.09–0.14) and longest lifetime values ($\tau_1$ = 53–74 μs; $\tau_2$ = 203–316 μs) were obtained for doped PMMA films. Obtained PMMA films could show potential in application as polymer optical fibers or in polymer organic light emitting diodes.

## Supplementary material

The deposition number CCDC 1843401 for complex **C4** contains the supplementary crystallographic data for this paper. These data can be obtained free of charge at www.ccdc.cam.ac.uk/data_request/cif or from the Cambridge Crystallographic Data Centre (CCDC), 12 Union Road, Cambridge CB2 1EZ, UK; fax: +44 (0) 1223 336033; email:deposit@ccdc.cam.ac.uk.

## Acknowledgements

This work was supported by the doctoral studies grant of Riga Technical University (Grant Nr. 34-14000DOK.MLĶF/17) and the National Research Program of Latvia "IMIS2".

## References

[1] Syamchand SS, Sony G. Europium enabled luminescent nanoparticles for biomedical applications. J Lumin 2015;165:190–215https://doi.org/10.1016/j.jlumin.2015.04.042.
[2] Carlos LD, Ferreira RAS, de Zea Bermudez V, Ribeiro SJL. Lanthanide-containing light-emitting organic–inorganic hybrids: a bet on the future. Adv Mater 2009;21:509–34https://doi.org/10.1002/adma.200801635.
[3] Gao R, Zhao M, Guan Y, Fang X, Li X, Yan D. Ordered and flexible lanthanide complex thin films showing up-conversion and color-tunable luminescence. J Mater Chem C 2014;2:9579–86https://doi.org/10.1039/C4TC01213E.
[4] Yang X, Lin X, Zhao Y, Zhao YS, Yan D. Lanthanide metal–organic framework microrods: colored optical waveguides and chiral polarized emission. Angew Chem Int Ed 2017;56:7853–7https://doi.org/10.1002/anie.201703917.
[5] Liu Y, Wang Y, Li C, Huang Y, Dang D, Zhu M, Zhu W, Cao Y. Red polymer light-emitting devices based on an oxadiazole functionalized europium(III) complex. Mater Chem Phys 2014;143:1265–70https://doi.org/10.1016/j.matchemphys.2013.11.032.
[6] Binnemans K. Lanthanide-Based luminescent hybrid materials. Chem Rev 2009;109:4283–374.
[7] Cotton S. Lanthanide and actinide chemistry. England: John Wiley & Sons; 2006https://doi.org/10.1002/0470010088.
[8] Lunstroot K, Driesen K, Nockemann P, Viau L, Mutin PH, Vioux A, Binnemans K. Ionic liquid as plasticizer for europium(III)-doped luminescent poly(methyl methacrylate) films. Phys Chem Chem Phys 2010;12:1879–85https://doi.org/10.1039/B920145A.
[9] Mech A, Karbowiak M, Görller-Walrand C, Van Deun R. The luminescence properties of three tetrakis dibenzoylmethane europium(III) complexes with different counter ions. J Alloy Comp 2008;451:215–9https://doi.org/10.1016/j.jallcom.2007.05.019.
[10] Li J, Li H, Yan P, Chen P, Hou G, Li G. Synthesis, crystal structure, and luminescent properties of 2-(2,2,2-Trifluoroethyl)-1-indone lanthanide complexes. Inorg Chem 2012;51:5050–7https://doi.org/10.1021/ic202473b.
[11] Li W, Yan P, Hou G, Li H, Li G. Efficient red emission from PMMA films doped with 5,6-DTFI europium(III) complexes: synthesis, structure and photophysical properties. Dalton Trans 2013;42:11537–47https://doi.org/10.1039/C3DT50580D.
[12] Teotonio EES, Brito HF, Cremona M, Quirino WG, Legnani C, Felinto MCFC. Novel electroluminescent devices containing Eu3+-(2-acyl-1,3-indandionate) complexes with TPPO ligand. Opt Mater 2009;32:345–9https://doi.org/10.1016/j.optmat.

2009.08.015.
[13] Teotonio EES, Brito HF, Viertler H, Faustino WM, Malta OL, de Sá GF, et al. Synthesis and luminescent properties of $Eu^{3+}$-complexes with 2-acyl-1,3-indandionates (ACIND) and TPPO ligands: the first X-ray structure of Eu–ACIND complex. Polyhedron 2006;25:3488–94https://doi.org/10.1016/j.poly.2006.06.035.
[14] Altomare A, Burla M, Cammali M, Cascarano G, Giacovazzo C, Guagliardi A, Moliterni A. Spagna. SIR97: a new tool for crystal structure determination and refinement. J Appl Crystallogr 1999;32:115–9https://doi:10.1107/S0021889898007717.
[15] Sheldrick GM. A short history of SHELX. Acta Crystallogr 2008;A64:112–22https://doi.org/10.1107/S0108767307043930.
[16] Mackay S, Dong W, Edwards C, Henderson A, Gilmore CJ, Stewart N, Shankland K, Donald A. maXus, integrated crystallography software. Bruker-Nonius and University of Glasgow; 2003.
[17] Wang N, Tao X, Du FL, Feng M, Jiang LN, Shen YZ. Synthesis and characterization of organophosphine/phosphite stabilized silver(I) complexes bearing 2-acetyl-1,3-indandione ligand, crystal structure of $[Ph_3P{\cdot}AgC_{11}H_7O_3]$. Polyhedron 2010;29:1687–91https://doi.org/doi:10.1016/j.poly.2010.02.017.
[18] Biju S, Freire RO, Eom YK, Scopelliti R, Bunzli JCG, Kim HK. A $Eu^{III}$ tetrakis (β-diketonate) dimeric complex: photophysical properties, structural elucidation by Sparkle/AM1 calculations, and doping into PMMA films and nanowires. Inorg Chem 2014;53:8407–17https://doi.org/10.1021/ic500966z.
[19] Malba CM, Enrichi F, Facchina M, Demitri N, Plaisier JR, Natile MM, Selva M, Riello P, Perosa A, Benedetti A. Phosphonium-based tetrakis dibenzoylmethane Eu(III) and Sm(III) complexes: synthesis, crystal structure and photoluminescence properties in a weakly coordinating phosphonium ionic liquid. RSC Adv 2015;5:60898–907https://doi.org/10.1039/C5RA03947A.
[20] Sweeting LM, Rheingold AL. Crystal disorder and triboluminescence: triethylammonium tetrakis(dibenzoylmethanato)europate. J Am Chem Soc 1987;109:2652–8https://doi.org/10.1021/ja00243a017.
[21] Singh AK, Singh SK, Mishra H, Prakash R, Rai SB. Structural, thermal, and fluorescence properties of $Eu(DBM)_3Phen_x$ complex doped in PMMA. J Phys Chem B 2010;114:13042–51https://doi.org/10.1021/jp1050063.
[22] Biju S, Xu LJ, Sun CZ, Chen ZN. White OLEDs based on a novel $Eu^{III}$-tetrakis-β-diketonate doped into 4,4'-N,N'-dicarbazlebiphenyl as emitting material. J Mater Chem C 2015;3:5775–82https://doi.org/10.1039/C5TC00638D.
[23] Zhou D, Huang C, Yaong G, Bai J, Li T. Luminescent europium dibenzoylmethane complexes and their Langmuir-Blodgett films. J Alloy Comp 1996;235:156–62https://doi.org/10.1016/0925-8388(95)02159-0.
[24] Raj DBA, Francis B, Reddy MLP, Butorac RR, Lynch VM, Cowley AH. Highly luminescent poly(methyl methacrylate)-incorporated europium complex supported by a carbazole-based fluorinated β-diketonate ligand and a 4,5-Bis(diphenylphosphino)-9,9-dimethylxanthene oxide Co-Ligand. Inorg Chem 2010;49:9055–63https://doi.org/10.1021/ic1015324.
[25] Binnemans K. Rare-earth beta-diketonates. Handbook on the physics and chemistry of rare earths vol 35. North Holland: Elsevier; 2005.
[26] Adati RD, Lima SAM, Davolos MR, Jafelicci M. A new β-diketone complex with high color purity. J Alloy Comp 2006;418:222–5https://doi.org/10.1016/j.jallcom.2005.10.062.
[27] Malina I, Kampars V. Photoluminescent properties of novel tris, ternary and tetrakis Eu(III) organic complexes with 2-acetyl-1,3-indandione ligands. Materials, Methods & Technologies 2017;17:18–27.
[28] Seo SJ, Zhao D, Suh K, Shin JH, Bae BS. Synthesis and luminescence properties of mesophase silica thin films doped with in-situ formed europium complex. J Lumin 2008;128:565–72https://doi.org/10.1016/j.jlumin.2007.08.012.
[29] Ahmed Z, Iftikhar K. Efficient layers of emitting ternary lanthanide complexes for fabricating red, green, and yellow OLEDs. Inorg Chem 2015;54:11209–25https://doi.org/10.1021/acs.inorgchem.5b01630.
[30] Gao R, Koeppen C, Zheng G, Garito AF. Effects of chromophore dissociation on the optical properties of rare-earth-doped polymers. Appl Optic 1998;37:7100–6https://doi.org/10.1364/AO.37.007100.
[31] Liu HG, Park S, Jang K, Zhang WS, Seo HJ, Lee YI. Different photoluminescent properties of binary and ternary europium chelates doped in PMMA. Mater Chem Phys 2003;82:84–92https://doi.org/10.1016/S0254-0584(03)00216-5.
[32] Malina I, Juhnevics N, Kampars V. Study of thermal and optical properties of dibenzoyl-methane Eu(III) organic complexes. Proc Est Acad Sci 2017;66:493–500https://doi.org/10.3176/proc.2017.4.11.
[33] Zhang Y, Li C, Shi H, Du B, YangW Cao Y. Bright red light-emitting devices based on a novel europium complex doped into polyvinylcarbazole. New J Chem 2007;31:569–74https://doi.org/10.1039/B617612G.
[34] Deichmann VAF, Novo JBM, Cirpan A, Karasz FE, Akcelrud L. Photo-and electroluminescent behaviour of $Eu^{3+}$ ions in blends with poly(vinyl-carbazole). J Braz Chem Soc 2007;18:330–6https://doi.org/10.1590/S0103-50532007000200013.
[35] Knyazev AA, Krupin AS, Romanova KA, Galyametdinov YG. Luminescence and energy transfer in poly(Nvinylcarbazole) blends doped by a highly anisometric Eu (III) complex. J Coord Chem 2016;69:1473–83https://doi.org/10.1080/00958972.2016.1185781.

6.pielikums

**Malina I**, Traskovskis K, Lesiņa N, Vembris A. $Eu^{3+}$ ternary and tetrakis complexes with carbazole and methyl group substituted dibenzoylmethane derivatives: Induction of aggregation enhanced emission. *Dyes and Pigments*, **2019**, *163*, 257-266.

DOI: https://doi.org/10.1016/j.dyepig.2018.11.060

© 2019, Elsevier. This manuscript version is made available under the CC-BY-NC-ND 4.0 license http://creativecommons.org/licenses/by-nc-nd/4.0

Grafiskais abstrakts/ Graphical abstract

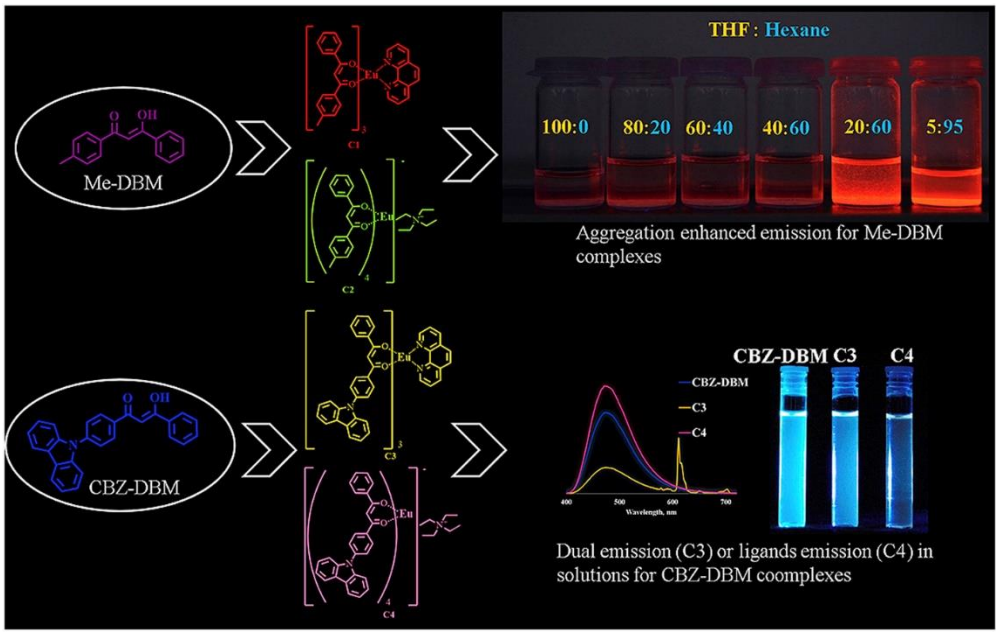

Dyes and Pigments 163 (2019) 257–266

Contents lists available at ScienceDirect

Dyes and Pigments

journal homepage: www.elsevier.com/locate/dyepig

# $Eu^{3+}$ ternary and tetrakis complexes with carbazole and methyl group substituted dibenzoylmethane derivatives: Induction of aggregation enhanced emission

Ilze Malina[a,*], Kaspars Traskovskis[a], Natalija Lesina[b], Aivars Vembris[b]

[a] Institute of Applied Chemistry, Riga Technical University, Paula Valdena Str. 3, Riga, LV-1048, Latvia
[b] Institute of Solid State Physics, University of Latvia, Kengaraga Str. 8, Riga, LV-1063, Latvia

ARTICLE INFO

*Keywords:*
Europium ternary complex
Europium tetrakis complex
Partial energy transfer process
Aggregation enhanced emission
Carbazole

ABSTRACT

Two dibenzoylmethane (DBM) derivatives with methyl (Me-DBM) or carbazole (CBZ-DBM) substituents at the *para*-position of the phenyl ring and their four novel *ternary* and *tetrakis* $Eu^{3+}$ complexes with 1,10-phenanthroline (PHEN) as a secondary ligand or tetraethylamonium ion ($N^+(Et)_4$) as the counter-cation were synthesized and characterized. The investigation of the optical properties of the complexes revealed that Me-DBM based compounds exhibit aggregation enhanced emission (AEE), while in the case of CBZ-DBM this effect is not observed. At the same time, the introduction of a carbazole substituent reduces the emission quantum yield of the complexes. The decrease in luminescence efficiency for CBZ-DBM based $Eu^{3+}$ complexes is mainly attributed to the closely situated $S_1$ and $T_1$ energy levels of the ligand that obstruct the intersystem crossing process.

## 1. Introduction

Over the previous years the research interest in $Eu^{3+}$ complexed β-diketones is not decreasing due to a wide variety of potential application directions found in amplifiers for optical communication [1], as luminescent probes in biological samples [2], in solar cells [3], as well as in the emissive layers of organic light emitting diodes (OLEDs) [4]. Also $Eu^{3+}$ complexes have been used to fabricate red or white light emitting diodes (LEDs) [5,6]. The utilization of $Eu^{3+}$ organic complexes in OLEDs and LEDs can be specifically outlined, because of their distinctive emission properties such as high emission efficiencies and sharp emission bands in the red-light region, which provide high color purity for the devices. Additionally, $Eu^{3+}$ complexes with β-diketone ligands usually have relatively simple and inexpensive steps of synthesis and purification.

In order to obtain a brightly luminescent $Eu^{3+}$ complex one must pay attention to the design of organic ligands, so that their electronic configuration is compatible to that of $Eu^{3+}$ ion. To observe a full energy transfer process between the attached ligands and the central metal ion, it is necessary that the triplet energy level of the ligand is higher than the resonance level of the $Eu^{3+}$ ion (17 250 $cm^{-1}$) [7]. Usually it means that absorption bands of ligands should lie in near-UV region, however there are some reports on the $Eu^{3+}$ organic complexes with blue light absorbing ligands [8,9]. Furthermore, for the purpose of practical applications it is also necessary, that the $Eu^{3+}$ complex exhibits a good solubility in commonly used solvents, so that the fabrication process of the thin films containing these compounds would be simpler and less costly. Finally, $Eu^{3+}$ organic complexes should exhibit high thermal and chemical stability.

In the recent years many authors have designed ligands, which contain organic substituents that provide good solubility, charge transporting properties and high thermal stability of the corresponding $Eu^{3+}$ complexes. Carbazole, being an inexpensive starting material and showing the previously discussed properties, is one of the most commonly used amongst such chemical building blocks. Many complexes, where carbazole is introduced to phenyltrifluorobutane-1,3-dione [10], biphenyltrifluorobutane-1,3-dione [11] and phenylpropane-1,3-dione [12] *para*-position through a nitrogen atom have been synthesized. Alternatively, $Eu^{3+}$ complexes containing ligands, where carbazole is attached to β-diketone through 2- [8,9,13] and 3- [14–16] position of carbazole ring, are reported. Some authors have chosen to attach the carbazole group in secondary ligands, for example in 1,10-phenanthroline unit [17,18]. Independently from the position of the attachment, $Eu^{3+}$ complexes with carbazole-functionalized β-diketone ligands usually exhibit bright red emission and they have potential application possibilities in biological imaging [14] and in fabrication of white organic light emitting diodes (WOLED) [11] and red-light OLEDs [10].

* Corresponding author.
*E-mail addresses:* malina.ilze1@gmail.com, Ilze.Malina_1@rtu.lv (I. Malina).

https://doi.org/10.1016/j.dyepig.2018.11.060
Received 4 October 2018; Received in revised form 28 November 2018; Accepted 30 November 2018
Available online 01 December 2018
0143-7208/ © 2018 Elsevier Ltd. All rights reserved.

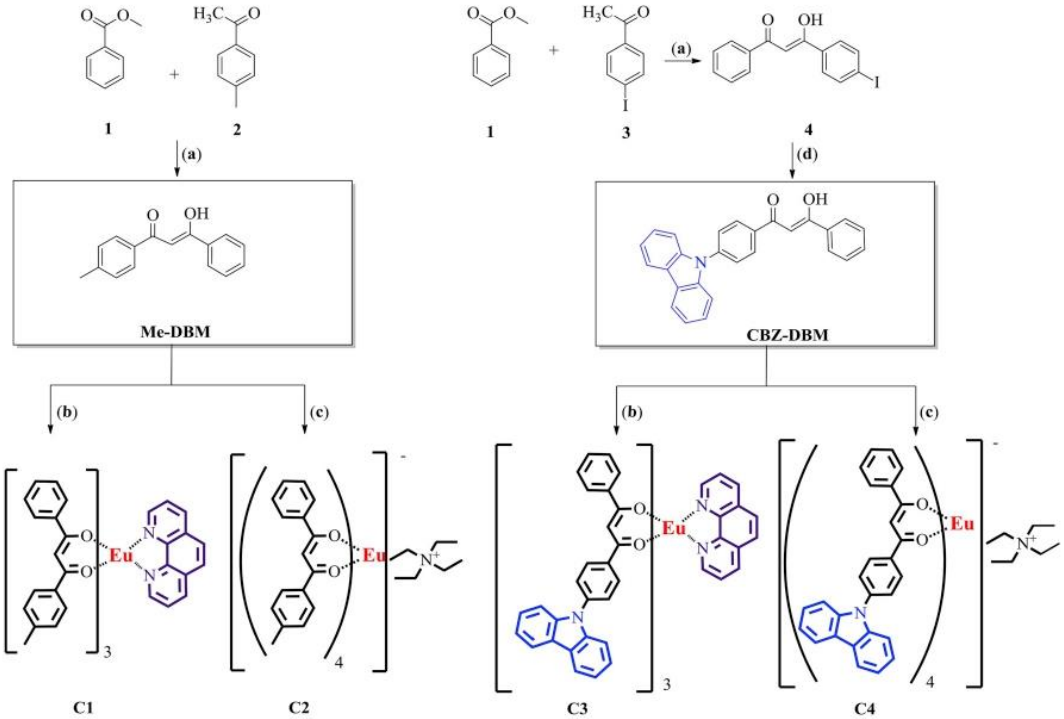


**Scheme 1.** Synthesis of ligands **Me-DBM, CBZ-DBM** and complexes **C1-C4**; **(a)** – 1) NaH, THF, 65 °C; 2) $H_2O$, 10% HCl; **(b)** – 10% NaOH/$H_2O$, 1,10-phenanthroline, $EuCl_3{\cdot}6H_2O$; **(c)** – 10% NaOH/$H_2O$, $N(Et)_4Br$, $EuCl_3{\cdot}6H_2O$; **(d)** Carbazole, Cu, 18-Crown-6, $K_2CO_3$, DMF, 155 °C.

Dibenzoylmethane (DBM), without the doubt, is one of the most used β-diketone type chelating ligands for the $Eu^{3+}$ organic complexes. However, the understanding of the consequences of carbazole group attachment to *para*-position of this molecule through N-atom (**CBZ-DBM**) and its effects on the corresponding $Eu^{3+}$ complexes is poor. Only one report characterizing $Eu^{3+}$ *tris* complex with this ligand can be found [19]. It is known that *ternary* and *tetrakis* $Eu^{3+}$ complexes usually exhibit higher photoluminescence quantum yields (PLQY), longer lifetimes [7] as well as higher thermal stability and solubility. This improvement is attributed to the replacement of the chelating solvent molecules in the complex by a secondary or the fourth β-diketone ligand. Furthermore, only two *tetrakis* $Eu^{3+}$ complexes with β-diketone ligands that contain carbazole group have been reported to date [10,11], but the mentioned compounds also contain a trifluorated methyl group in DBM fragment. This study consists of the synthesis of two DBM derivatives – 4-methyldibenzoylmethane (**Me-DBM**) and 4-carbazol-9-yl-dibenzoylmethane (**CBZ-DBM**) and the corresponding four novel $Eu^{3+}$ complexes **C1-C4** (Scheme 1), with an initial aim to assess the effects of the carbazole introduction. Structural characterization as well as investigation of optical properties in different media and evaluation for OLED application use is reported. Ground state and excited state energy level calculations are presented and discussed for ligands in order to explain the experimental observations. The acquired results show that the emissive properties of the compounds can be drastically changed depending on the structure of the used dibenzoylmethane derivative.

## 2. Experimental section

### 2.1. Materials and instrumentation

$EuCl_3{\cdot}6H_2O$ (99.99%) was purchased from *Acros Organics*, 1,10-phenanthroline (99%), tetraethylammonium bromide (98%), 4-methylacetophenone (96%), 4-iodoacetophenone from *Alfa Aesar*, methylbenzoate (99%) and carbazole (≥95%) from *Sigma Aldrich*, but poly(*N*-vinylcarbazole) (PVK) from *ABCR* (GmbH&Co). All substances were used without further purification.

$^1H$ NMR and $^{13}C$ NMR spectra were recorded on a Brucker Avance 300 MHz spectrometer in $CDCl_3$, DMSO-$D_6$ or $CD_3CN$ solutions. Chemical shifts were expressed in parts per million (ppm) relative to solvent signal. CHN elemental analysis was carried on Euro Vector EA 3000 analyzer. Infrared spectra were recorded on a Perkin-Elmer Spectrum 100 FTIR spectrometer using KBr pellets (4000–650 $cm^{-1}$). The thermogravimetric analysis was performed on a Perkin Elmer STA 6000 instrument. Each sample was heated from 30 to 900 °C with heating rate 10 °C/min in the nitrogen atmosphere. Low resolution mass spectra of ligands were acquired on a Waters EMD 1000MS mass detector (ESI + mode, voltage 30 V). The UV/Vis absorption spectra were acquired with Perkin-Elmer 35 UV/Vis spectrometer using 1 cm length quartz cuvettes. Emission and excitation spectra were measured on QuantaMaster 40 steady state spectrofluorometer (Photon Technology International, Inc.). For triplet level measurements low-temperature phosphorescence spectra were acquired at 77 K in 2-methyltetrahydrofuran solution on the same device. The singlet and triplet energy levels were determined at the emission band maxima. The lifetime measurements were carried out in room temperature using the same spectrofluorometer equipped with high power Xenon flash lamp as excitation source. Lifetime data were processed by OriginPro 8 program. Absolute photoluminescence quantum yields (PLQY) were determined using the same spectrofluorometer equipped with 6 inch integrating sphere by LabSphere and special holders for cuvette, film and powder samples. The PLQY were calculated by software supplied by Photon Technology International, Inc. Polymer films were obtained with Laurell WS-400B-NPP/LITE spin coater (Parameters: speed 800 rpm, acceleration 800 rpm/s for 1 min). Density functional theory (DFT) has been performed using ORCA program version 4.0.1 [20]. The geometry optimization of ligands was obtained using non-local functional B3LYP with 6-311G** [21] basis set. For singlet and triplet

energy level calculations def2-TZVP basis [22] and def2/J [23] auxiliary basis were used.

### 2.2. Synthesis

The synthesis of dibenzoylmethane derivatives as well as complexes **C1-C4** is shown in Scheme 1.

#### 2.2.1. Synthesis of compounds DBM derivatives

*(Z)-3-hydroxy-3-phenyl-1-(p-tolyl)-prop-2-en-1-one* **Me-DBM**. To a methyl benzoate (**1**) (1.15 g, 8.45 mmol), placed in two-neck round-bottom flask, dry THF (15 mL) and NaH 60% dispersion in mineral oil (0.34 g, 8.45 mmol) was added. Reaction mixture was refluxed until all $H_2$ is released from solution. Afterwards, 4-methylacetophenone (**2**) (1.03 g, 7.68 mmol) dissolved in dry THF (5 mL) was added dropwise with dropping funnel and resulting mixture was refluxed for 4 h. Then reaction mixture was cooled with ice bath to room temperature and neutralized with 10% HCl solution until pH ~7. Water (10 mL) and $CHCl_3$ (40 mL) was added and organic fraction was separated, washed with water (2 × 50 mL) and dried with anhydrous $Na_2SO_4$. The solution was filtered and filtrate was evaporated. Obtained precipitate was crystalized from *i*-PrOH (30 mL) and 1.01 g of compound **Me-DBM** was obtained as yellow powder. Yield 55%; m.p. = 80–81 °C. $^1$H NMR (300 MHz, DMSO-$D_6$, ppm): $\delta$ = 8.17 (2H, d, $J$ = 6.0 Hz, H-Ph); 8.12 (2H, d, $J$ = 6.0 Hz, H-Ph); 7.69–7.62 (1H, m, H-Ph); 7.58 (2H, d, $J$ = 9.0 Hz, H-Ph); 7.38 (2H, d, $J$ = 9.0 Hz, H-Ph); 7.32 (1H, s, −CH=C(OH)-); 2.41 (3H, s, $-CH_3$). $^{13}$C NMR (75 MHz, DMSO-$D_6$, ppm): $\delta$ = 186.1; 185.1; 144.0; 135.0; 133.4; 132.4; 129.9; 129.3; 128.0; 127.8; 93.4; 21.6. FT-IR, (KBr, cm$^{-1}$): 3129, 3066, 3038, 2924, 2855, 1599, 1520. MS, $C_{16}H_{14}O_2$ requires $[M+H]^+$ 239.10; found $[M+H]^+$ 239.2. Anal. Calcd. For $C_{16}H_{14}O_2$: C, 80.65; H, 5.92; found C, 80.44; H, 5.67.

*(Z)-3-hydroxy-3-(4-iodophenyl)-1-phenylprop-2-en-1-one* (**4**). Two-neck round-bottom flask containing dry THF (15 mL) and NaH 60% dispersion in mineral oil (1.60 g, 40.00 mmol) was purged with Argon and cooled to 0 °C with ice bath. Then methyl benzoate (**1**) (3.00 g, 22.00 mmol) was added. After 10 min 4-iodoacetophenone (**3**) (5.00 g, 20.00 mmol) dissolved in dry THF (5 mL) was added dropwise with dropping funnel and resulting mixture was refluxed for 6 h. Afterwards, ethylacetate (15 mL) and water (10 mL) was added and reaction mixture was neutralized with 10% HCl solution until pH ~7. Organic fraction was separated, washed with water (2 × 50 mL) and brine (2 × 25 mL), and dried with anhydrous $Na_2SO_4$. Solution was filtered and filtrate was evaporated. Obtained precipitate was crystalized from $CH_2Cl_2$: ethylacetate (2:1) system and 3.24 g of compound **4** was obtained as light brown powder. Yield 46%; m.p. = 105–107 °C. $^1$H NMR (300 MHz, $CDCl_3$, ppm): $\delta$ = 7.99 (2H, d, $J$ = 6.0 Hz, H-Ph), 7.85 (2H, d, $J$ = 9.0 Hz, H-Ph), 7.71 (2H, d, $J$ = 9.0 Hz, H-Ph), 7.61–7.48 (3H, m, H-Ph), 6.83 (1H, s, −CH=C(OH)-). $^{13}$C NMR (75 MHz, $CDCl_3$, ppm): $\delta$ = 186.1; 184.7; 138.0; 135.3; 135.0; 132.7; 128.8; 128.6; 127.2; 99.9; 93.0. FT-IR, (KBr, cm$^{-1}$): 3436, 3059, 2955, 2926, 1584, 1564, 1508. MS, $C_{15}H_{11}IO_2$ requires $[M+H]^+$ 350.98; found $[M+H]^+$ 351.1. Anal. Calcd. For $C_{15}H_{11}IO_2$: C, 51.45; H, 3.17; found C, 51.22; H, 2.97.

*(Z)-1-(4-(9H-carbazol-9-yl)phenyl)-3-hydroxy-3-phenylprop-2-en-1-one* **CBZ-DBM**. Two-neck round-bottom flask was purged with Argon and then diketone (**4**) (1.50 g, 4.29 mmol), carbazole (0.72 g, 4.29 mmol), $K_2CO_3$ (2.30 g, 16.80 mmol), activated Cu (0.53 g, 8.58 mmol), 18-Crown-6 (0.38 g, 1.43 mmol) and dry DMF (7.5 mL) were added. Reaction mixture was refluxed at 155 °C for 4 h. Then it was cooled to room temperature and water (10 mL) was added. Reaction mixture was extracted with $CH_2Cl_2$ (3 × 25 mL) and organic fraction was separated, evaporated and obtained precipitate was dissolved in $CH_2Cl_2$:MeOH (1:1) system. From this solution green precipitate was obtained, filtered and then dried in room temperature. Afterwards to green precipitate ethanol (30 mL) and 10% NaOH solution (5 mL) was added and resulting mixture was refluxed for 20 min. The insoluble precipitate was filtered off and filtrate was neutralized with 10% HCl solution. Yellow precipitate (0.24 g) was formed, filtered and dried. Yield 14%; m.p. = 126–129 °C. $^1$H NMR (300 MHz, $CDCl_3$, ppm): $\delta$ = 8.27 (2H, d, $J$ = 9.0 Hz, H-Ph-CBZ), 8.19 (2H, d, $J$ = 9.0 Hz, H-Ph), 8.07 (2H, d, $J$ = 6.0 Hz, H-Ph), 7.76 (2H, d, $J$ = 9.0 Hz, H-Ph-CBZ), 7.62–7.45 (7H, m, H-Ph-CBZ, H-Ph), 7.36 (2H, t, $J$ = 9.0 Hz, H-Ph-CBZ), 6.98 (1H, s, −CH=C(OH)-). $^{13}$C NMR (75 MHz, $CDCl_3$, ppm): $\delta$ = 186.0; 184.7; 141.6; 140.3; 135.4; 134.1; 132.7; 129.0; 128.8; 127.3; 126.7; 126.2; 123.9; 120.6; 120.4; 109.8; 93.2. FT-IR, (KBr, cm$^{-1}$): 3436, 3055, 2926, 1602, 1516, 1224. MS, $C_{27}H_{19}NO_2$ requires $[M+H]^+$ 390.14; found $[M+H]^+$ 390.3. Anal. Calcd. For $C_{27}H_{19}NO_2$: C, 83.27; H, 4.92; N, 3.60; found C, 83.01; H, 4.71; N, 3.72.

#### 2.2.2. Synthesis of complexes C1−C4

*Eu(Me-DBM)$_3$PHEN (C1)*. Solution of diketone **Me-DBM** (0.22 g, 0.92 mmol) in ethanol (10 mL) was refluxed until complete dissolution. 1,10- Phenanthroline (0.06 g, 0.31 mmol) in ethanol (3 mL) was added, followed by addition of 10% NaOH solution until pH ~ 7–8. Afterwards, distilled water solution (5 mL) containing $EuCl_3{\cdot}6H_2O$ (0.08 g, 0.31 mmol) was added dropwise and resulting solution was stirred for 2 h in the room temperature. Formed precipitate was separated by suction filtration, washed with ethanol (10 mL) and distilled water (10 mL) and dried in vacuum at 50 °C for 24 h. Complex **C1** was obtained as light yellow powder (0.18 g). Yield 56%. $^1$H NMR (300 MHz, $CDCl_3$, ppm): $\delta$ = 10.96 (2H, br s, H-PHEN), 10.58 (2H, br s, H-PHEN), 10.00 (2H, br s, H-PHEN), 8.97 (2H, br s, H-PHEN), 6.75 (9H, br s, H-Ph), 6.59 (6H, br s, H-Ph), 5.94 (12H, br s, H-Ph), 2.90 (3H, s, −CH=C(O)-), 2.40 (12H, s, $-CH_3$). FT-IR, (KBr, cm$^{-1}$): 3059, 3028, 2921, 1593, 1549, 1520, 1499, 1422. Anal. Calcd. For $EuC_{60}H_{47}N_2O_6$: C, 69.03; H, 4.54; N, 2.68; found C, 68.59; H, 4.32; N, 2.81.

*[Eu(Me-DBM)$_4$]$^-$N$^+$(Et)$_4$ (C2)*. Solution of diketone **Me-DBM** (0.25 g, 1.05 mmol) in ethanol (10 mL) was refluxed until complete dissolution. Tetraethylammonium bromide (0.06 g, 0.26 mmol) in ethanol (3 mL) was added, and then 10% NaOH solution was added until pH ~ 7–8. Afterwards, $EuCl_3{\cdot}6H_2O$ (0.07 g, 0.26 mmol) in distilled water (5 mL) was added dropwise and resulting solution was stirred for 2 h in the room temperature. Formed precipitate was filtrated, washed with ethanol (10 mL), distilled water (10 mL) and dried in vacuum at 50 °C for 24 h, then 0.19 g of light yellow powder (**C2**) was obtained. Yield 59%. $^1$H NMR (300 MHz, $CD_3CN$, ppm): $\delta$ = 7.70 (8H, br s, H-Ph), 7.65 (8H, d, $J$ = 9.0 Hz, H-Ph), 7.25 (12H, br s, H-Ph), 7.08 (8H, d, $J$ = 9.0 Hz, H-Ph), 5.93 (4H, s, −CH=C(O)-), 3.23 (8H, q, $(CH_3-CH_2)_4N^+$), 2.53 (12H, s, Ph-$CH_3$), 1.25 (12H, m, $(CH_3-CH_2)_4N^+$). FT-IR, (KBr, cm$^{-1}$): 3056, 3029, 2985, 2921, 2859, 1596, 1552, 1519, 1498, 1423, 1307, 1289. Anal. Calcd. For $EuC_{72}H_{72}NO_8$: C, 70.23; H, 5.89; N, 1.14; found C, 70.11; H, 5.75; N, 0.98.

*Eu(CBZ-DBM)$_3$PHEN (C3)*. Complex was synthesized by the same procedure as for **C1**, except diketone **CBZ-DBM** was used instead of compound **Me-DBM**. Light brown powder, Yield 67%. $^1$H NMR (300 MHz, $CDCl_3$, ppm): $\delta$ = 11.08 (2H, br d, H-PHEN), 10.67 (2H, br s, H-PHEN), 10.24 (2H, br s, H-PHEN), 9.08 (2H, br d, H-PHEN), 8.12–8.10 (6H, br d, H-Ph-CBZ), 7.34–7.21 (24H, m, H-Ph-CBZ, H-Ph), 6.95–6.90 (15H, m, H-Ph-CBZ, H-Ph), 6.44–6.08 (9H, m, H-Ph, −CH=C(O)-). FT-IR, (KBr, cm$^{-1}$): 3051, 2959, 2926, 2852, 1598, 1547, 1500, 1423. Anal. Calcd. For $EuC_{93}H_{62}N_5O_6$: C, 74.59; H, 4.17; N, 4.68; found C, 74.12; H, 4.32; N, 4.29.

*[Eu(CBZ-DBM)$_4$]$^-$N$^+$(Et)$_4$ (C4)*. Complex was synthesized by the same procedure as for **C2**, except diketone **CBZ-DBM** was used instead of compound **Me-DBM**. Light brown powder, Yield 30%. $^1$H NMR (300 MHz, $CDCl_3$, ppm): $\delta$ = 8.27 (8H, d, $J$ = 9.0 Hz, H-Ph-CBZ), 8.18 (8H, d, $J$ = 6.0 Hz, H-Ph-CBZ), 8.06 (8H, d, $J$ = 6.0 Hz, H-Ph-CBZ), 7.78 (8H, d, $J$ = 9.0 Hz, H-Ph-CBZ), 7.62–7.32 (36H, m, H-Ph), 6.97 (4H, s, −CH=C(O)-), 3.79–3.75 (8H, m, $CH_3-CH_2)_4N^+$), 1.32–1.24 (12H, m, $(CH_3-CH_2)_4N^+$). FT-IR, (KBr, cm$^{-1}$): 3057, 2926, 1596, 1548, 1500, 1306, 1226. Anal. Calcd. For $EuC_{116}H_{92}N_5O_8$: 75.89; H, 5.05; N, 3.81; found C, 75.44; H, 4.93; N, 4.08.

### 2.3. OLED preparation

Sandwich type samples with the pixel size of 16 $mm^2$ were prepared with the following structure ITO/PEDOT:PSS(40 nm)/**C1**(50 nm)/TPBi (20 nm)/LiF(1 nm)/Al(100 nm) for the host free device and ITO/PEDOT:PSS(40 nm)/PVK:**C1**(50 nm) (10 wt%)/TPBi(20 nm)/LiF(1 nm)/Al(100 nm) for hosted device, where Poly(3,4-ethylenedioxythiophene)-poly(styrenesulfonate) (PEDOT:PSS), 2,2′,2"-(1,3,5-Benzinetriyl)-tris(1-phenyl-1-H-benzimidazole) (TPBi) and LiF were used as hole-injection, electron transport and electron-injection layers, respectively, and poly(*N*-vinylcarbazole) (PVK) as hole-transporting host for the emitter. Indium Tin Oxide (ITO) glass (Präzisions Glas & Optik GmbH) with a sheet resistivity of 15 Ω/square was used as a substrate. A 12 mm wide ITO strip line was made by wet etching at the middle of the substrate. ITO substrates were cleaned by the following method: sonicated in $CHCl_3$; sonicated in acetone; 2x rinsed with deionized (DI) water; sonicated in water with 3 vol% of Hellmanex II detergent; rinsed with DI water; sonicated in DI water and isopropyl alcohol. Before deposition of PEDOT:PSS the ITO glass was blown dry with nitrogen and treated by UV-ozone for 20 min. ITO layer was covered with PEDOT:PSS (from H.C. Starck, Al4083) using spin coater Laurell WS650. Rotation lasted for 1 min with speed 2000 rpm. The sample was moved in a glovebox and heated at 200 °C for 10 min. The solution of emitting layer compounds with a concentration of 5 mg/mL was spin-coated on the PEDOT:PSS layer with 2000 rpm for 40 s and heated at 120 °C for 15 min afterwards. Further the samples were moved from glovebox to vacuum chamber, without the exposure to air, for thermal evaporation of electron transport TPBi (Sigma Aldrich 806781) electron-injection LiF (Sigma Aldrich 449903) and electrodes at the pressure $6{\cdot}10^{-6}$ Torr. The deposition speed was 1 Å/s, 0.1 Å/s and 5 Å/s for TPBi, LiF and Al, respectively. In the end the samples were encapsulated using two component epoxide. The current–voltage characteristics of the OLEDs were measured by the multimeter Keithley 2700 and the voltage source was Keithley 230 unit. The electroluminescence brightness was measured by Konica Minolta Luminance and Color Meter CS-150.

## 3. Results and discussion

### 3.1. Synthesis and characterization of ligands and $Eu^{3+}$ complexes

The synthetic route to the β-diketone ligands **Me-DBM** and **CBZ-DBM** and their $Eu^{3+}$ *ternary* and *tetrakis* complexes is shown in Scheme 1. The ligand **Me-DBM** was prepared by Claisen condensation reaction between methyl benzoate (**1**) and 4-methyl acetophenone (**2**) with a moderate yield – 55%. The other β-diketone **CBZ-DBM** was obtained by two-step synthesis. In the first stage 4-iododibenzoylmethane (**4**) was obtained in the Claisen condensation reaction between methyl benzoate (**1**) and 4-iodoacetophenone (**3**). Afterwards, **CBZ-DBM** was prepared in Cu catalyzed Ullman condensation reaction between 4-iododibenzoylmethane (**4**) and carbazole, with a relatively low yield (14%). $Eu^{3+}$ *ternary* complexes **C1** and **C3** were prepared by mixing ligands PHEN, **Me-DBM** or **CBZ-DBM** and $EuCl_3{\cdot}6H_2O$ in the ratio 1:3:1 in the presence of 10% NaOH. However, *tetrakis* complexes **C2** and **C4** were obtained by taking tetraethylammonium bromide, **Me-DBM** or **CBZ-DBM** and $EuCl_3{\cdot}6H_2O$ in the molar ratio 1:4:1 in the presence of 10% NaOH. The obtained ligands were analyzed by FT-IR, $^1$H NMR, $^{13}$C NMR spectroscopy and mass spectra data, but newly synthesized $Eu^{3+}$ complexes **C1-C4** by FT-IR, $^1$H NMR, elemental analysis data and thermogravimetric analysis (TGA). Comparison of $^1$H NMR spectra of the ligand **CBZ-DBM** and its $Eu^{3+}$ *ternary* complex **C3** are given in Fig. 1. As it can be seen from Fig. 1 **(a)** free ligand **CBZ-DBM** in $CDCl_3$ solution exists in enol form and methine proton (H4) shows a signal at 6.98 ppm. Enolic proton (—OH) was not observed, due to a rapid exchange of this proton with $H_2O$ (traces in $CDCl_3$), which usually render the signal too broad to be observed in $^1$H NMR spectra. Protons from carbazole cycle (H7—H10, H7'-H10') exhibit three well resolved signals at 8.27, 7.76 and 7.36 ppm with spin coupling constant of 9.0 Hz. However, signals of protons H8, H8′ overlap with protons from DBM fragment (H2, H2', H3, H6, H6') and form a multiplet at 7.53 ppm. Remaining protons H1, H1′ and H5, H5′ show two well resolved doublets at 8.19 and 8.07 ppm. $^1$H NMR spectra of ligand **CBZ-DBM** show changes upon complexation with $Eu^{3+}$ ion (Fig. 1 **(b)**). First of all, complexation with $Eu^{3+}$ ion leads to a proton signal broadening and shift to higher field. Four new broad signals at 11.08, 10.67, 10.24 and 9.08 ppm appear in the $^1$H NMR spectra and correspond to the protons from 1,10-phenanthroline molecule (H11—H14, H11'-H14'). Methine proton (H4) from **CBZ-DBM** molecule shows a shift to higher field at 6.19 ppm and overlaps with proton signals from phenyl group of DBM unit (H6 and H6'). Furthermore, proton signals from the carbazole cycle (H7—H10, H7'-H10') are not well resolved as it was for the free ligand and even overlaps with some proton signals of DBM unit. Two signals – a broad doublet (8.11 ppm) and multiplets at 7.28 ppm and 6.96 ppm were signed to protons H7—H10, H7'-H10'. Finally, remaining protons from DBM unit exhibit two broad multiplets at 7.28 and 6.96 ppm. In conclusion, $^1$H NMR spectra of complex **C3** confirms that ligand ratio of PHEN to **CBZ-DBM** is 1:3 (8 protons:54 protons). Similar $^1$H NMR spectra and the same ligand ratio was obtained for other newly synthesized *ternary* complex **C1**.

The $^1$H NMR spectra of *tetrakis* complexes **C2** and **C4** contain two signals at 3.23 and 1.25 ppm (**C2**) (3.79 and 1.28 ppm for **C4**) in higher field region, which correspond to the protons of ethylene and methyl group in $N^+(Et)_4$ unit. Moreover, six signals of four **Me-DBM** ligands with an integral intensity of 52 protons or seven signals of four **CBZ-DBM** ligands with an integral intensity of 68 protons were observed at lower field and confirmed that these complexes contain one tetraethylammonium cation and four DBM ligands.

FT-IR spectra of free ligands **Me-DBM** and **CBZ-DBM** exhibit a broad band around 3200-3600 $cm^{-1}$, which attributes to enolic —OH stretching vibrations. Carbonyl group (C=O) stretching vibrations were found at 1599 (**Me-DBM**) and 1601 $cm^{-1}$ (**CBZ-DBM**). The observed strong absorption bands at region 1573-1500 $cm^{-1}$ probably corresponds to enolic and aromatic C=C bond vibrations. However, for complexes **C1-C4** no broad band in the region above 3000 $cm^{-1}$ was observed, indicating that DBM derivatives are coordinated to $Eu^{3+}$ ion through diketone fragment. For *tetrakis* complexes **C2** and **C4** sharp absorption bands in the region 3060-2850 $cm^{-1}$ are observed and attributes to aliphatic C—H vibrations of $N^+(Et)_4$ unit. Furthermore, carbonyl group (C=O) stretching vibrations were found at lower frequencies – at 1593 and 1594 $cm^{-1}$ for complexes **C1** and **C2**, and at 1597 and 1596 $cm^{-1}$ for **C3** and **C4**. Similar changes between FT-IR spectra of the ligands and their $Eu^{3+}$ complexes were reported for other β-diketone complexes [24,25]. Elemental analysis data of complexes **C1-C4** were in a good agreement with the proposed structures.

Thermal stability of complexes **C1-C4** was investigated by thermogravimetric analysis (TGA) in inert atmosphere with a heating rate of 10 °C/min. Decomposition temperatures of complexes **C1** and **C2** (275 and 234 °C) with **Me-DBM** ligands are higher than the ones for complexes **C3** and **C4** with **CBZ-DBM** ligands (180 and 166 °C). It is apparent, that the introduction of carbazole moiety in DBM molecule slightly decreases the thermal stability of $Eu^{3+}$ complexes, independently from a complex structure. Although $T_d$ for complexes **C3** and **C4** are below 200 °C, these values are close to the reported decomposition temperatures (190–200 °C) for other $Eu^{3+}$ complexes with β-diketones that contain carbazole moiety [10,11].

*Ternary* and *Tetrakis* complexes **C1-C4** exhibit excellent solubility in commonly used solvents, such as $CH_2Cl_2$, THF, $CHCl_3$, MeCN, EtOH.

### 3.2. Absorption properties of ligands and $Eu^{3+}$ complexes

The UV/Vis absorption spectra of compounds PHEN, **Me-DBM**, **CBZ-DBM** and complexes **C1-C4** were measured in THF solutions ($c \sim 1.5{\cdot}10^{-5}$ M) and are shown in Fig. 2.

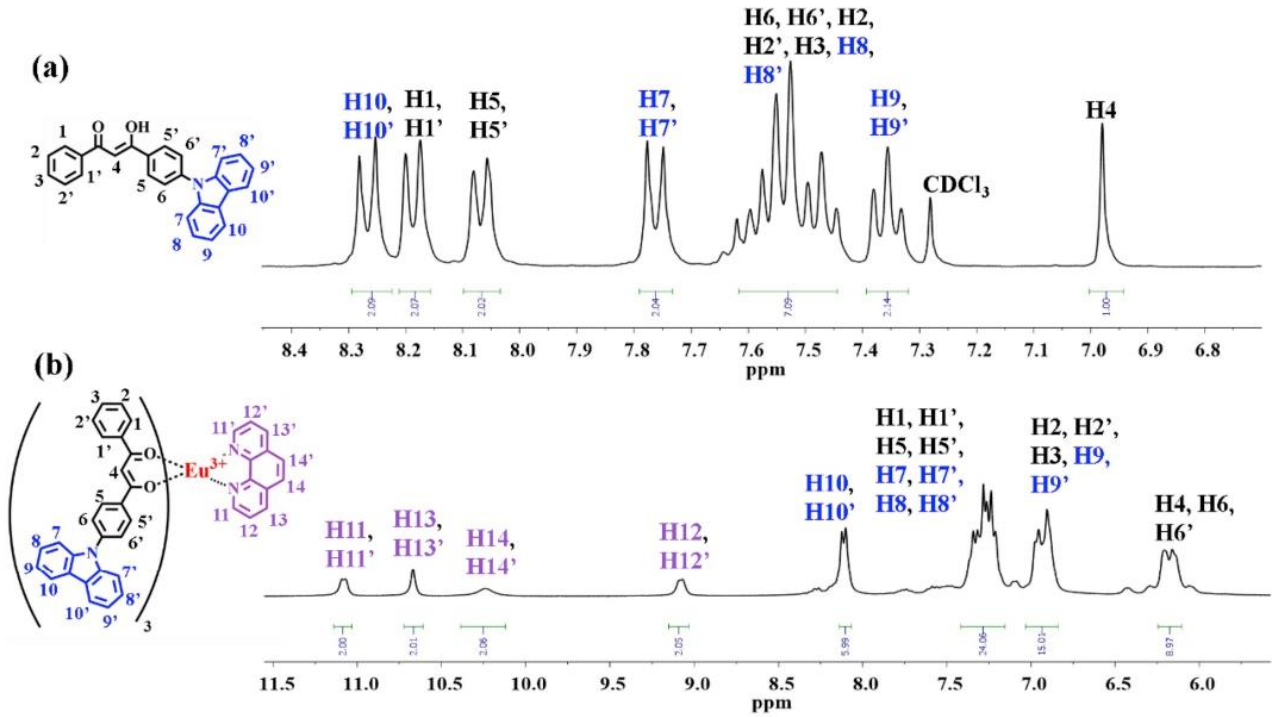


**Fig. 1.** **(a)** - $^1$H NMR spectra of compound **CBZ-DBM** in $CDCl_3$ at 298 K; **(b)** – $^1$H NMR spectra of $Eu^{3+}$ *ternary* complex **C3** in $CDCl_3$ at 298 K.

Secondary ligand PHEN shows a broad absorption band with maximum at 289 nm and high molar absorption coefficient $\varepsilon$ (Table 1). β-Diketone **Me-DBM** exhibits a broad absorption band in near UV region (300–380 nm), centered at 347 nm, which attributes to the π-π* enolic transitions from β-diketone fragment. Introduction of substituent (-Me) in DBM molecule leads to a small bathochromic shift of the absorption spectra maxima by 5 nm, compared to the value reported for DBM ($\lambda_{abs}$ = 343 nm in THF) [26]. Ligand **CBZ-DBM** exhibits a wide absorption band with maxima at 291 and 375 nm and two well separated low energy shoulders at 320 and 335 nm. These two low energy shoulders together with absorption at 291 nm correspond to π-π* transitions of carbazole moiety [27], whereas $\lambda_{abs}$ at 375 nm marks charge transfer (CT) transition due to a fact that carbazole moiety possesses electron donating but carbonyl groups – accepting properties.

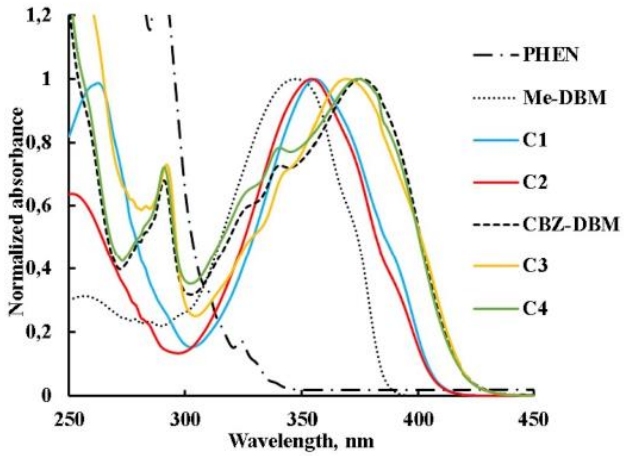


**Fig. 2.** UV/Vis absorption spectra of compounds PHEN, **Me-DBM**, **CBZ-DBM** and their $Eu^{3+}$ complexes **C1-C4** in THF solutions (c ~ $1.5 \cdot 10^{-5}$ M).

**Table 1**
UV/Vis absorption and luminescence spectral data of the ligands PHEN, **Me-DBM**, **CBZ-DBM** and their complexes **C1-C4** in THF (c ~ $1.5 \cdot 10^{-5}$ M).

| Compound | $\lambda_{abs}$, nm ($\varepsilon$, $10^4 M^{-1} cm^{-1}$) | $\lambda_{em}$, nm | PLQY | $I_2/I_1$ [a] | $\tau$ [b], μs |
|---|---|---|---|---|---|
| PHEN | 289 (5.09) | – | – | – | – |
| Me-DBM | 347 (2.45) | – | – | – | – |
| **C1** | 356 (7.11) | 611 | 0.03 | 29.8 | 143.60 ± 0.24 |
| **C2** | 354 (9.45) | 611 | 0.02 | 23.4 | 141.49 ± 0.35 |
| CBZ-DBM | 291, 326, 341, 375 (2.11) | 478 | 0.26 | – | – |
| **C3** | 292, 327, 342, 369 (6.34) | 475, 611 | 0.10 | 12.1 | 38.88 ± 0.22 |
| **C4** | 291, 326, 341, 374 (9.15) | 476 | 0.26 | – | – |

[a] intensity ratio between transitions $^5D_0 \rightarrow {}^7F_2/{}^5D_0 \rightarrow {}^7F_1$ from emission spectra.
[b] luminescence lifetime.

To prove this statement DFT calculation were carried for ligands **Me-DBM** and **CBZ-DBM** in order to obtain optimized ground state structure geometries as well as HUMO and LUMO orbitals (Fig. 3). HOMO orbital for **Me-DBM** are localized on 4-methylphenyl-β-diketone unit, while LUMO resides on the whole molecule, illustrating a large HOMO-LUMO overlap. However, for compound **CBZ-DBM** HOMO is localized on 1-(4-carbazolephenyl)-1,3-diketone unit and LUMO is contained on 3-phenyl-1,3-diketone part, what indicates that, upon the excitation, a CT transition is expected for **CBZ-DBM**.

The absorption spectra of $Eu^{3+}$ complexes **C1-C4** show a slightly different behavior between **Me-DBM** and **CBZ-DBM** based compounds. While the band shape in all cases almost completely mimics that of the free ligands, upon the complexation the absorption peak of **Me-DBM** experiences a redshift. For **CBZ-DBM** based **C4**, on the other hand, it remains almost unchanged, while for **C3**- slightly blueshifts. The explanation of this difference between the two ligands can, once again, be explained by CT nature of **CBZ-DBM**, as upon the complexation the

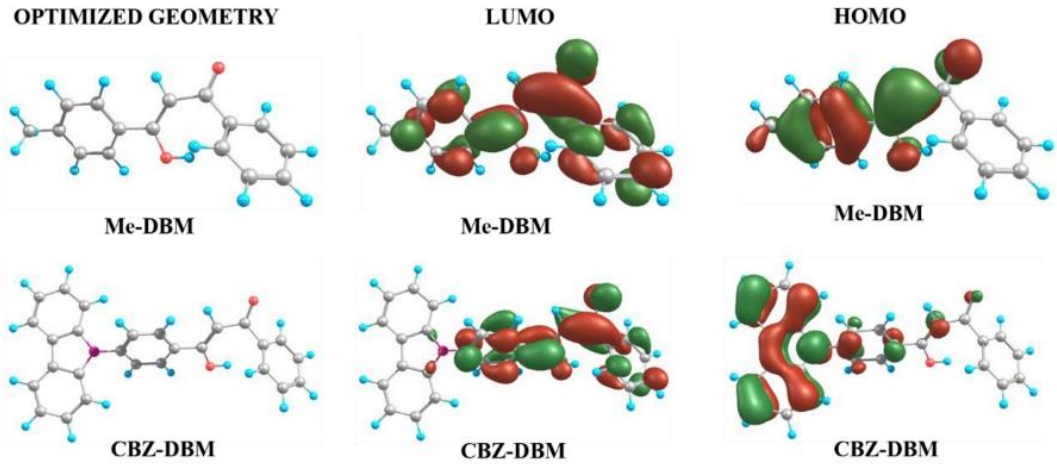


**Fig. 3.** HOMO and LUMO orbitals of optimized ground state structures of compounds **Me-DBM** and **CBZ-DBM**, obtained using B3LYP6-311G** set.

increased electron density in diketonate fragment reduces the push-pull character of the molecule, increasing the bandgap value. The complexation with $Eu^{3+}$ ion is accompanied with an increase in molar absorption coefficients for the lowest energy transitions: for *ternary* complexes **C1** and **C3** $\varepsilon$ is approximately three times higher, but for *tetrakis* complexes **C2** and **C4** ~ four times higher than the values measured for the free ligands, confirming yet again, that in complexes **C1**, **C3** $Eu^{3+}$ is coordinated with three β-diketone ligands, but in complexes **C2** and **C4** – with four β-diketone ligands.

### 3.3. Photoluminescence studies of $Eu^{3+}$ complexes in solution and solid state

Photoluminescence properties of the synthesized ligands and their $Eu^{3+}$ complexes were investigated in THF solutions ($c \sim 1.5 \cdot 10^{-5}$ M). Relevant data are summarized in Table 1 and emission spectra are shown in Fig. 4 **(a)**.

Ligand **Me-DBM** is completely non-emissive in THF solution. **CBZ-DBM**, on the other hand, exhibits bright cyan-blue emission (Fig. 4. **(b)**) with maxima at 478 nm and moderate absolute photoluminescence quantum yield (PLQY) of 0.26.

$Eu^{3+}$ *ternary* and *tetrakis* complexes **C1** and **C2** with **Me-DBM** ligand show only the narrow $Eu^{3+}$ ion emission bands with multiple maximums at 580, 594, 611, 650 and 703 nm, corresponding to $^5D_0 \rightarrow {}^7F_J$ ($J = 0$–4) transitions. The emission efficiencies are very low, with PLQY values in THF being 0.03 and 0.02 for **C1** and **C2**.

**CBZ-DBM** based $Eu^{3+}$ *ternary* and *tetrakis* complexes **C3** and **C4** in THF solutions exhibit quite different emission spectra. In the case of *ternary* complex **C3** the emission spectra show the characteristic red emission from $Eu^{3+}$ ion and also an emission band ranging from 400 to 600 nm that is attributed to the luminescence of **CBZ-DBM**. Intensity ratio between emission at 611 and 475 nm are 2:1. It is likely that the incomplete energy transfer process from ligand to $Eu^{3+}$ ion is a reason for such behavior. Similar observations were made for other $Eu^{3+}$ complexes with β-diketone ligands containing carbazole groups [17,19,28]. PLQY for complex **C3** in THF solution is 0.10 and CIE color coordinates (x = 0.26; y = 0.28) lie in cyan blue region, respectively. Complex **C3** is also characterized with, relatively to **C1** and **C2**, short mono-exponential lifetime value (38.88 μm) for $^5D_0 \rightarrow {}^7F_2$ transition of $Eu^{3+}$. In the emission spectra of *tetrakis* complex **C4** no characteristic $Eu^{3+}$ ion emission bands are observed and only the emission of the ligand is present. This could be explained with a known tendency of *tetrakis* complexes to dissociate into *tris* complexes and the corresponding tetraethylammonium salt [29], what could greatly affect the emission intensity of the $Eu^{3+}$ ion and intensify the emission of the ligand.

Solid-state photoluminescence properties of the $Eu^{3+}$ complexes are summarized in Table 2 and photoluminescence excitation and emission

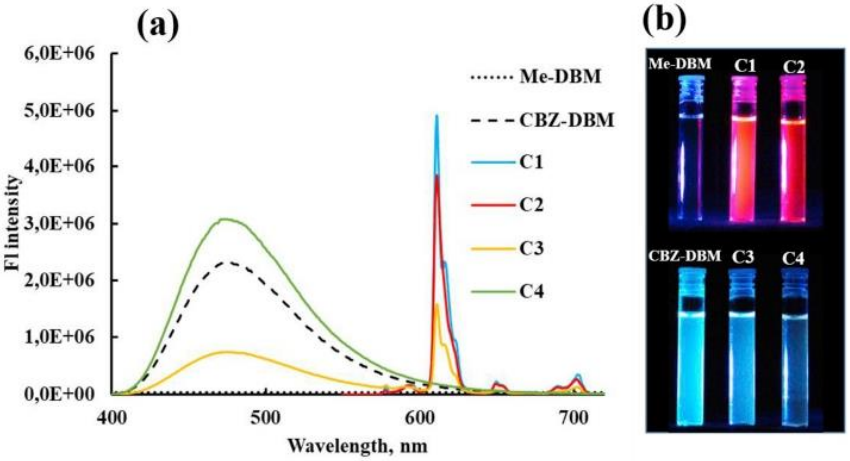


**Fig. 4. (a)** - Emission spectra of **Me-DBM**, **CBZ-DBM** and their $Eu^{3+}$ complexes **C1-C4** in THF solutions ($c \sim 1.5 \cdot 10^{-5}$ M); **(b)** – photograph of **Me-DBM**, **CBZ-DBM** and their $Eu^{3+}$ complexes **C1-C4** in THF solutions under excitation with 365 nm UV-lamp.

**Table 2**
Excitation and emission spectra maximums ($\lambda_{exc}$, $\lambda_{em}$), absolute photoluminescence quantum yields (PLQY), luminescence lifetimes ($\tau_1$, $\tau_2$) and intensity ratios $I_2/I_1$ between transitions $^5D_0 \rightarrow {}^7F_2/{}^5D_0 \rightarrow {}^7F_1$ of complexes **C1-C4** in solid-state and doped PVK films.

| Compound | $\lambda_{exc}$, nm | $\lambda_{em}$, nm | PLQY | $I_2/I_1$ | $\tau_1$, μs | $\tau_2$, μs |
|---|---|---|---|---|---|---|
| **C1** | 399 | 611 | 0.53 | 29.3 | 431 ± 2 (67%) | 157 ± 4 (33%) |
| **C2** | 399 | 611 | 0.57 | 29.9 | 410 ± 1 (68%) | 124 ± 2 (32%) |
| **C3** | 412 | 611 | 0.09 | 28.1 | 170 ± 2 (13%) | 51 ± 1 (87%) |
| C4 | 398 | 611 | 0.10 | 29.7 | 191 ± 1 (15%) | 48 ± 0.5 (85%) |
| **C1-PVK** | 351 | 611 | 0.22 | 31.6 | 364 ± 1(71%) | 116 ± 1(29%) |
| **C2-PVK** | 361 | 611 | 0.18 | 27.3 | 354 ± 1(67%) | 104 ± 1(33%) |
| **C3-PVK** | 346, 379 | 611 | 0.07 | 22.9 | 362 ± 17(23%) | 93 ± 3 (77%) |
| **C4-PVK** | 346, 379 | 611 | 0.09 | 23.4 | 295 ± 2 (26%) | 84 ± 1 (74%) |

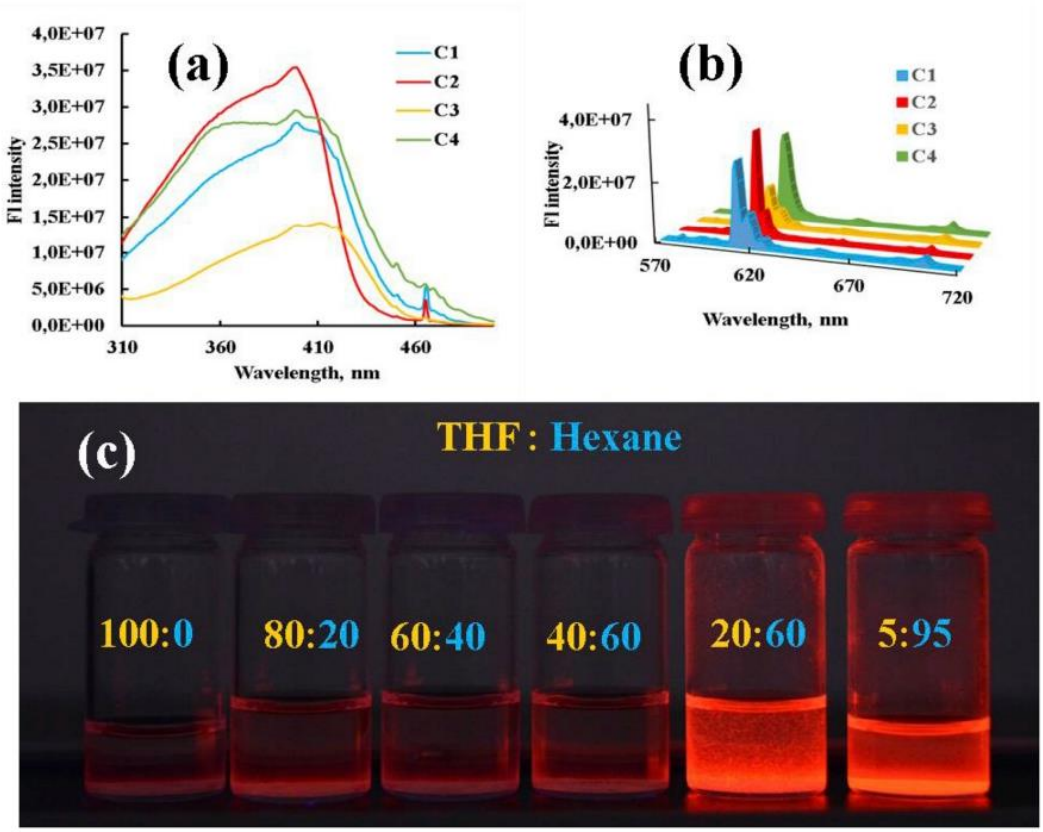


**Fig. 5. (a)** – Excitation spectra ($\lambda_{em}$ = 611 nm) of powders of complexes **C1-C4**; **(b)** – Emission spectra ($\lambda_{exc}$ = 400 nm) of **C1-C4** powders. **(c)** Aggregation enhanced emission of the compound **C2,** illustrated by UV irradiated solutions with different THF:hexane volume fractions.

spectra are shown in Fig. 5.

In solid powdered state all complexes exhibit wide excitation bands ranging from 300 to even 470 nm with maxima around 400 nm. These wide bands correspond very well to the absorption spectra of the complexes (Fig. 2), therefore confirming assumption that the emission of $Eu^{3+}$ ion arises from the energy that is absorbed by the coordinated ligands. Furthermore, the excitation spectra in solid-state also contains some $Eu^{3+}$ ion excitation bands at 396 ($^7F_0 \rightarrow {}^5G_4$), 417 ($^7F_0 \rightarrow {}^5L_6$) and 467 nm ($^7F_0 \rightarrow {}^5D_3$), which overlap with the much stronger excitation bands of the ligands. Excitation window for four newly synthesized complexes **C1-C4** in solid-state have been extended to the visible light region, what can be considered as an advantage, because $Eu^{3+}$ complexes with β-diketones usually show low stability under the UV-light irradiation.

Upon the excitation with 400 nm, the powders of complexes **C1-C2** show only the typical $Eu^{3+}$ ion emission bands, with a significant enhancement in emission efficiency (PLQY = 0.53 and 0.57) in comparison to the measurements in solution. Such behavior strongly infers that these compounds exhibit the aggregation enhanced emission (AEE). Indeed, this effect can be unambiguously demonstrated in the case of **C2** in the THF:hexane solvent system, where with an increasing hexane fraction a suspension of the complex particles forms, "turning-on" the bright red emission (Fig. 5 **(c)**). To the best of our knowledge, only one report has attributed aggregation induced emission (AIE) or AEE effects to $Eu^{3+}$ complexes, where the metal was sensitized with tetraphenylethene, a well-known AIE emitter [30]. At the same time, DBM and its close structural analogues, in their complexed state with boron trifluoride, are very well known frameworks for AIE-active compounds [31–34]. So it is not surprising, that the same molecular system, but complexed with $Eu^{3+}$ ion, would exhibit AEE effect.

Complexes **C3** and **C4** with **CBZ-DBM** ligands, which in solution spectra showed the emission of ligand or the combination of emission of

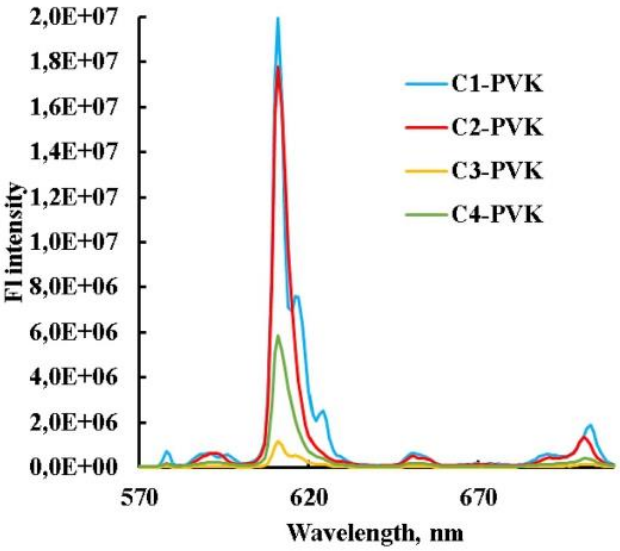


**Fig. 6.** Emission spectra of PVK films doped with 8 wt% of complexes **C1-C4**.

ligand and $Eu^{3+}$ ion, in solid-state exhibit only metal centered luminescence. This can be explained by a combination of two effects: a stronger bonding between ligand and metal takes place in the solid-state and the emission of the ligand is completely quenched due to the aggregation. In comparison to **Me-DBM** based counterparts, no enhancement is observed in emission efficiency of the **C3** and **C4**. The relatively low PLQY values of these compounds, once more, point to a poor excitation transfer between the ligand and $Eu^{3+}$ ion.

Emission spectra of complexes **C1-C4** in solid-state contains five typical $Eu^{3+}$ ion emission lines in the range from 575 to 720 nm. Emission band at ~580 nm ($^5D_0 \rightarrow {}^7F_0$) shows a weak intensity due to the fact, that its corresponding transition is forbidden by electric dipole and magnetic dipole moments. Unlike in the solution spectra, this transition is not observed as a sharp peak, but rather than a poorly resolved wide band. Transition $^5D_0 \rightarrow {}^7F_1$ (594 nm), which is forbidden by electric dipole moment but allowed by magnetic dipole moment, shows two to three Stark components. Emission spectra is dominated by sharp, hypersensitive electric dipole allowed transition at 611 nm ($^5D_0 \rightarrow {}^7F_2$) with full half width of ~6 nm, likewise it was observed for solution samples. It is known, that electric dipole transitions of lanthanide ions are quite sensitive to ligand field. Usually strongly asymmetric or strongly interacting ligand fields lead to relatively intense electric dipole transitions [35]. In our case the intensity ratio $I_2/I_1$ between transitions $^5D_0 \rightarrow {}^7F_2/{}^5D_0 \rightarrow {}^7F_1$ are very high (28.1–29.9), which shows, that not only $Eu^{3+}$ ion is located in a site without an inversion symmetry, but strong coordination interactions also take place. Moreover, $I_2/I_1$ in solid-state is higher than in solutions, pointing to weaker interactions between ligands and central metal ion in the dissolved state. Similar observations about $I_2/I_1$ in different states were reported for other $Eu^{3+}$ complexes [36,37]. Such intensity of $^5D_0 \rightarrow {}^7F_2$ transition in comparison to the intensity of other $Eu^{3+}$ emission lines is the reason why emission color of all four complexes is in red region, with CIE x = 0.67; y = 0.33.

To further understand the photoluminescence behavior, luminescence lifetimes of $^5D_0$ excited state of $Eu^{3+}$ ion were determined by monitoring the transition at 611 nm at room temperature. All luminescence decay curves were fitted with bi-exponential functions and have two decay time values $\tau_1$ and $\tau_2$ (Table 2). Bi-exponential lifetimes point to the presence of two sites of symmetry around central metal ion. This hypothesis is confirmed by the relatively broad emission of $^5D_0 \rightarrow {}^7F_0$ transition, observed at 580 nm. The splitting of the bands, marking this transition in photoluminescence spectra, points to different non-equivalent sites in $Eu^{3+}$ complexes [38]. In solid-state the distance between two emitting $Eu^{3+}$ ion sites are relatively short and the interaction between $Eu^{3+}$- $Eu^{3+}$ centers can take place. Multiple aggregated forms of the compound with alternative local chemical environments would lead to species with different emission kinetics. Bi-exponential lifetime in solid-state were also reported for other $Eu^{3+}$ *ternary* and *tetrakis* complexes [25,37,39,40]. As it is the case for PLQY, lifetime values are not greatly affected by the structure of complexes (*ternary* or *tetrakis*) and $\tau_1$ and $\tau_2$ values vary in the range from 3 to 33 μs, if the same ligands are present.

### 3.4. $Eu^{3+}$ complex behavior in host materials and OLEDs

The incorporation of $Eu^{3+}$ complexes in practically applicable devices often involves a use of guest-host systems, where the emitting molecule is dispersed in polymeric or molecular matrix. This has to be done in order to improve optical transparency and ensure plasticity to the initially crystalline materials. Additionally, a host material with charge transporting properties is a necessity in order to acquire efficient OLEDs with $Eu^{3+}$ based emitters [10,11]. To investigate the effects of dispersion in polymer matrix, the synthesized compounds were dispersed in a conventional hole-transporting material, poly(*N*-vinylcarbazole) (PVK). Four PVK films doped with 8 wt percent (wt%) of complexes **C1-C4** were prepared by spin coating technique from THF solutions.

Emission spectra of doped PVK films are shown in Fig. 6 and the relevant emission data (PLQY, $\tau_1$ and $\tau_2$) are collected in Table 2. When excited at 380 nm, all doped films exhibit only characteristic $Eu^{3+}$ ion emission bands in the red-light region and no emission from PVK are detected in shorter wavelengths. The films with complexes **C1** and **C2** exhibit moderate PLQY of 0.22 and 0.18, but complexes **C3** and **C4** - 0.07 and 0.09. These values give an important insight about the differences in the emission characteristics between the two subsets of compounds. The dispersion in polymer matrix causes a drop in PLQY by more than 50% for **Me-DBM** based complexes, while **CBZ-DBM** shows no significant change in comparison to the emission efficiency in the powdered form. This difference in the behavior can be explained by the fact that **C1** and **C2** exhibits an AEE effect, while the emission of **C3** and **C4**, apparently, is not affected by a solid state packing arrangement. The dispersion in polymer can be considered as a pseudo-solvation, where molecules are encapsulated by the host material. However, for solution-processed guest-host systems, unless the polar guest is completely encapsulated by isolating groups, a large portion of the dispersed molecules still forms aggregates [41]. This is an explanation for the PLQY drop for guest-host systems of **C1** and **C2**, where only the aggregated fraction of the molecules emit, while the emission in the isolated molecules is quenched. In **C3** and **C4** the both fractions of the molecules are able to emit, hence no apparent change in PLQY is observed.

Regarding the discussed difference between the emissive properties of **Me-DBM** and **CBZ-DBM** based compounds, it can be attributed to the dissimilar electronic nature of these ligands. It is known that AIE and AEE effects largely take place due to the restriction of the emission-quenching intramolecular rotation, when the molecules are packed in crystal lattice [42]. In **Me-DBM** this rotation, most likely, can be related to the torsion changes between phenyl ring and diketone fragment. As discussed previously, in **CBZ-DBM** the lowest energy electronic transition has CT character that involves the push-pull system consisting of carbazole electron donating group and diketone acceptor. As it is well known, the conjugation energy in push-pull molecules causes their planarization and reduces conformational freedom. This can be considered as the reason why the compounds based on **CBZ-DBM** do not exhibit AEE effect and this ligand is strongly emissive in solution, while **Me-DBM** does not emit.

In order to evaluate a possible enhancement in solid-state emission quenching for **CBZ-DBM** based compounds, PLQY for this ligand in a host-free film was measured, yielding a value - 0.05. While a steep drop

in PL efficiency can be seen for **CBZ-DBM** in comparison to solution, indicating a strong concentration quenching, solid phase emission efficiency notably increases for **CBZ-DBM** based $Eu^{3+}$ complexes. In addition, PLQY of **C3** and **C4** is almost identical in host-free and PVK-dispersed samples, showing no significant concentration dependence. These observations let assume that, while **CBZ-DBM** is highly susceptible to photoinduced electron transfer quenching, this effect is suppressed by the complexation to $Eu^{3+}$. This can be explained by a fast excited state migration to the metal center, which is sterically encapsulated by the ligands.

Taking into the consideration the previously discussed results, two OLEDs were prepared containing complex **C1** as the emitter, where this compound was either dispersed in PVK host [ITO/PEDOT:PSS(40 nm)/PVK:**C1**(50 nm)(10 wt%)/TPBi(20 nm)/LiF(1 nm)/Al(100 nm)] or used in a host-free layer [ITO/PEDOT:PSS (40 nm)/**C1**(50 nm)/TPBi (20 nm)/LiF(1 nm)/Al(100 nm)]. In the presence of the host material no characteristic $Eu^{3+}$ emission band was observed in the spectra of the device, as it emitted only blue light, associated with the electroluminescence (EL) of the charge transporting compounds. On the other hand, the host-free OLED showed only red $Eu^{3+}$ related emission. The lack of the host and the poor charge transporting characteristics of the compound determines that the device exhibits low maximal brightness of 10 cd/m$^2$, with current efficiency 0.004 cd/A and turn-on voltage 9 V. These results reaffirm that due to AEE effect the ability to emit is greatly reduced for **Me-DBM** based complexes, as they are dispersed in host material.

### 3.5. Energy transfer between ligands and $Eu^{3+}$ ion

To better understand the observed partial and complete energy transfer between ligands **CBZ-DBM** or **Me-DBM** and $Eu^{3+}$ ion, the singlet and triplet excited-state energy levels were determined experimentally in the case of **CBZ-DBM** and using the ORCA quantum chemical calculation program in the case of **Me-DBM**. A simplified energy transfer process between ligands and $Eu^{3+}$ ion can be expressed as a following exited state transition sequence: $S_1$–$T_1$–Eu*. First, energy from the excited singlet state ($S_1$) of ligand is transferred to its excited triplet state ($T_1$). Second, energy from $T_1$ state is transferred onto the excited states of the $Eu^{3+}$ ion (usually $^5D_0$). Some authors have proposed interaction mechanisms involving these energy states to evaluate the effectiveness of the excitation transfer process: (**1**) Reinhoudt empirical rule [43] states, that for an efficient transfer between $S_1$-$T_1$ levels, the energy difference between these two states should be around 5000 cm$^{-1}$; (**2**) however, for effective energy transfer between $T_1$–Eu*, the difference needs to be in the range 2500–5500 cm$^{-1}$ (Latva empirical rule) [44].

For ligand **Me-DBM** singlet and triplet energy levels are located at 28 218 and 21 928 cm$^{-1}$, and for ligand **CBZ-DBM** at 21 929 and 18 416 cm$^{-1}$, respectively (Fig. 7). All energy levels are higher than the $^5D_0$ energy level of $Eu^{3+}$ ion (17 250 cm$^{-1}$). In the case of **Me-DBM** ligand, the difference between levels $S_1$–$T_1$ is 6290 cm$^{-1}$ and $T_1$–Eu* – 4678 cm$^{-1}$. This means that the both empirical rules discussed previously are fulfilled and the energy transfer process is efficient. High emission PLQY values in the solid-state for complexes **C1** and **C2** confirms this statement. For ligand **CBZ-DBM** the situation is different and the obtained energy gap values for $S_1$–$T_1$ and $T_1$–Eu* are smaller than those for **Me-DBM** – 3513 and 1166 cm$^{-1}$, respectively. The difference between the excited singlet and triplet energy states of **CBZ-DBM** is less than 5000 cm$^{-1}$, what could indicate a non-efficient intersystem crossing in this molecule. This is probably the reason, why the emission of the ligand is also observed in the luminescence spectra of complexes **C3** and **C4** in THF solutions. Not all energy from $S_1$ level is transferred to $T_1$ level and some part of it manifests as the ligand fluorescence. Furthermore, energy difference between triplet state of **CBZ-DBM** and $^5D_0$ energy level of $Eu^{3+}$ ion is notably lower than the preferable value (2500-5500 cm$^{-1}$) [43]. In the cases, where the gap is less than 3500 cm$^{-1}$, the energy back-transfer from $^5D_0$ energy level of $Eu^{3+}$ ion to $T_1$ level of the ligand could occur. This is another likely cause for the low PLQY values of **CBZ-DBM** based complexes.

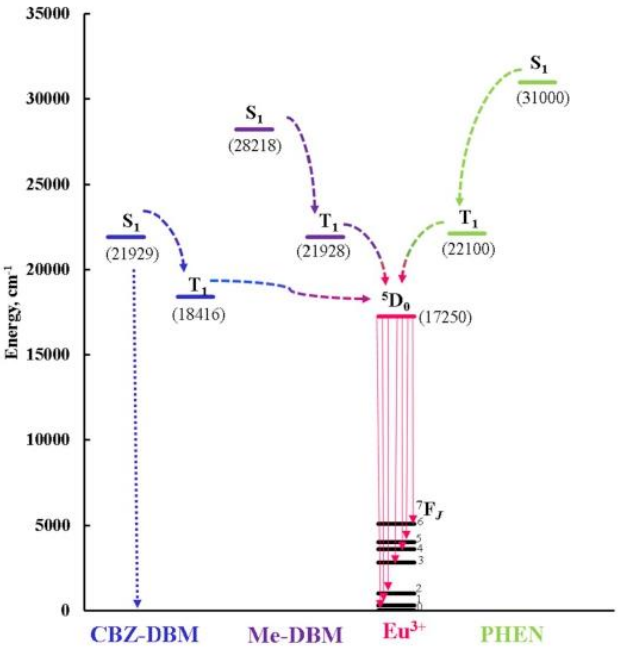


**Fig. 7.** Schematic energy level diagram of energy transfer processes: **Me-DBM**-to-$Eu^{3+}$, **CBZ-DBM**-to-$Eu^{3+}$ and PHEN-to- $Eu^{3+}$.

Fig. 7 also shows the transfer process between the energy levels of secondary ligand PHEN and resonance level of the $Eu^{3+}$ ion. It is known, that singlet and triplet energy levels of PHEN are located at 31 000 and 22 100 cm$^{-1}$ [45]. After a comparison of singlet and triplet energy levels of β-diketone ligands to those of PHEN, we can conclude that the energy levels of the latter one are located at higher energies, therefore secondary ligand PHEN can transfer absorbed excited energy not only directly to resonance level ($^5D_0$) of $Eu^{3+}$ ion, but also to $S_1$ and $T_1$ levels of ligands **CBZ-DBM** and **Me-DBM**.

## 4. Conclusions

Two β-diketones with methyl and carbazole substituents attached to dibenzoylmethane (**Me-DBM**, **CBZ-DBM**) and their corresponding novel $Eu^{3+}$ *ternary* ($Eu(Me\text{-}DBM)_3PHEN$ **C1**, $Eu(CBZ\text{-}DBM)_3PHEN$ **C2**) and *tetrakis* ($[Eu(Me\text{-}DBM)_4]N^+(Et)_4$ **C3**, $Eu(CBZ\text{-}DBM)_4]N^+(Et)_4$ **C4**) complexes were synthesized, fully characterized with $^1$H NMR, $^{13}$C NMR, FT-IR spectroscopy methods, elemental analysis and thermogravimetric analysis.

The photophysical properties of the compounds were investigated in solution and solid-state. The acquired results show that the complexes based on **Me-DBM** ligand exhibit strong AEE behavior, with very low emission efficiency in solutions and moderately high PLQY values of 0.53 and 0.57 in powders. **CBZ-DBM** based complexes in solution show either dual $Eu^{3+}$ and ligand centered emission (**C3**) or only ligand emission (**C4**), while in the solid state only $Eu^{3+}$ emission is detected. At the same time the measured solid-state PLQY values of **CBZ-DBM** based compounds are notably lower (0.09 and 0.10). The results of quantum chemical modeling show that this decrease in luminescence efficiency is mainly attributed to the close situated $S_1$ and $T_1$ energy levels of **CBZ-DBM** that obstruct the intersystem crossing process. Additionally, no AEE behavior was observed for **C3** and **C4** due to CT nature of **CBZ-DBM** that reduces the conformational freedom of the molecule.

Taking into account the practical application aspects of the synthesized compounds, the molecular design of **Me-DBM** based

complexes can be considered as more promising, due to increased emission efficiency. AEE characteristics of these compounds can be exploited towards the development of environment-sensitive luminescent probes. The potential use of these compounds in OLEDs is limited due to the fact that the dispersion in charge transporting host reduces emission efficiency through the obstructed aggregation ability of the molecules.

## Acknowledgements

This work is supported by the ERDF 1.1.1.1. activity project Nr. 1.1.1.1/16/A/131 "Design and Investigation of Light Emitting and Solution Processable Organic Molecular Glasses".

## References

[1] Kuriki K, Koike Y, Okamoto Y. Plastic optical fiber lasers and amplifiers containing lanthanide complexes. Chem Rev 2002;102:2347–56https://doi.org/10.1021/cr010309g.
[2] Sun J, Song B, Ye Z, Yuan J. Mitochondria targetable time-gated luminescence probe for singlet oxygen based on a β-diketonate-europium complex. Inorg Chem 2015;54:11660–8https://doi.org/10.1021/acs.inorgchem.5b02458.
[3] Kataoka H, Kitano T, Takizawa T, Hirai Y, Nakanishi T, Hasegawa Y. Photo- and thermo-stable luminescent beads composed of Eu(III) complexes and PMMA for enhancement of silicon solar cell efficiency. J Alloy Comp 2014;601:293–7https://doi.org/10.1016/j.jallcom.2014.01.165.
[4] Martins JP, Martín-Ramos P, Coya C, Silva MR, Eusebio MES, de Andrés A, Álvarez ÁL, Martín-Gil J. Highly luminescent pure-red-emitting fluorinated β-diketonate europium(III) complex for full solution-processed OLEDs. J Lumin 2015;159:17–25https://doi.org/10.1016/j.jlumin.2014.10.020.
[5] Singh K, Boddula R, Vaidyanathan S. Versatile luminescent europium(III) – β-Diketonate-imidazo-bipyridyl complexes intended for white LEDs: a detailed photophysical and theoretical study. Inorg Chem 2017;6:9376–90https://doi.org/10.1021/acs.inorgchem.7b01565.
[6] Boddula R, Vaidyanathan S. White light emissive bipolar ligand and their $Eu^{III}$ complex for white/red light emitting diodes. J Photochem Photobiol, A 2017;347:26–40https://doi.org/10.1016/j.jphotochem.2017.07.008.
[7] Binnemans K. Lanthanide-based luminescent hybrid materials. Chem Rev 2009;109:4283–374https://doi.org/10.1021/cr8003983.
[8] Francis B, Heering C, Freire RO, Reddy MLP, Janiak C. Achieving visible excitation in carbazole-based $Eu^{3+}$-β-diketonate complexes via molecular engineering. RSC Adv 2015;5:90720–30https://doi.org/10.1039/C5RA18819A.
[9] Liu SG, Pan RK, Zhou XP, Wen XL, Chen YZ, Wang S, Shi XB. Blue light excitable europium(III) complex based on deprotonated 1-(9-ethyl-6,8-dimethyl-9H-carbazol-2-yl)-4,4,4-trifluorobutane-1,3-dionate and 1,10-phenanthroline. Inorg Chim Acta 2013;395:119–23https://doi.org/10.1016/j.ica.2012.10.026.
[10] Biju S, Xu LJ, Alves MAH, Freire RO, Chen ZN. Bright orange and red light-emitting diodes of new visible light excitable tetrakis-Ln-β-diketonate (Ln = Sm3+, $^{Eu}$3+) complexes. New J Chem 2017;41:1687–95https://doi.org/10.1039/C6NJ03450K.
[11] Biju S, Xu LJ, Sun CZ, Chen ZN. White OLEDs based on a novel $Eu^{III}$-Tetrakis-β-Diketonate doped into 4,4'-N,N'-Dicarbazlebiphenyl as emitting material. J Mater Chem C 2015;3:5775–82https://doi.org/10.1039/C5TC00638D.
[12] Ma Q, Zheng Y, Armaroli N, Bolognesi M, Accorsi G. Synthesis and photoluminescence properties of asymmetrical europium(III) complexes involving carbazole, phenanthroline and bathophenanthroline units. Inorg Chim Acta 2009;362:3181–6https://doi.org/10.1016/j.ica.2009.02.014.
[13] He P, Wang HH, Yan HG, Hu W, Shi JX, Gong ML. A strong red-emitting carbazole based europium(III) complex excited by blue light. Dalton Trans 2010;39:8919–24https://doi.org/10.1039/C0DT00424C.
[14] Hu ZJ, Tian XH, Zhao XH, Wang P, Zhang Q, Sun PP, Wu JY, Yanga JX, Tian YP. Efficient two-photon-sensitized luminescence of a novel europium(III) β-diketonate complex and application in biological imaging. Chem Commun 2011;47:12467–9https://doi.org/10.1039/C1CC14968G.
[15] Liu J, Liang QB, Wu HB. Synthesis, photophysics, electrochemistry, thermal stability and electroluminescent performances of a new europium complex with bis(β-diketone) ligand containing carbazole group. Luminescence 2017;32:460–5https://doi.org/10.1002/bio.3206.
[16] Räsänen M, Takalo H, Rosenberg J, Mäkelä J, Haapakka K, Kankare J. Study on photophysical properties of Eu(III) complexes with aromatic β-diketones – role of charge transfer states in the energy migration. J Lumin 2014;146:211–7https://doi.org/10.1016/j.jlumin.2013.09.076.
[17] Rajamouli B, Sivakumar V. Eu(III) complexes for LEDs based on carbazole- and fluorene-functionalized phenanthro-imidazole ancillary ligands: detailed photophysical and theoretical study. Chemistry Select 2017;2:4138–49https://doi.org/10.1002/slct.201700266.
[18] Rajamouli B, Viswanath CSD, Giri S, Jayasankar CK, Sivakumara V. Carbazole functionalized new bipolar ligand for monochromatic red light emitting Europium (III) complex: combined experimental and theoretical study. New J Chem 2017;41:3112–23https://doi.org/10.1039/C6NJ03947B.
[19] Nie D, Chen Z, Bian Z, Zhou J, Liu Z, Chen F, Zhao Y, Huang C. Energy transfer pathways in the carbazole functionalized β-diketonate europium complexes. New J Chem 2007;31:1639–46https://doi.org/10.1039/B705666D.
[20] Nesse F. The ORCA program system. Wiley Interdiscip Rev Comput Mol Sci 2011;2:73–8https://doi.org/10.1002/wcms.81.
[21] Krishnan R, Binkley JS, Seeger R, Pople JA. Self-consistent molecular orbital methods. XX.A basis set for correlated wave functions. J Chem 1980;72:650–6https://doi.org/10.1063/1.438955.
[22] Weigend F, Ahlrichs R. Balanced basis sets of split valence, triple zeta valence and quadruple zeta valence quality for H to Rn: design and assessment of accuracy. Phys Chem Chem Phys 2005;7:3297–305https://doi.org/10.1039/B508541A.
[23] Weigend F. Accurate Coulomb-fitting basis sets for H to Rn. Phys Chem Chem Phys 2006;8:1057https://doi.org/10.1039/B515623H.
[24] Wang D, Luo Z, Liu Z, Wang D, Fan L, Yin G. Synthesis and photoluminescent properties of Eu(III) complexes with fluorinated β-diketone and nitrogen heterocyclic ligands. Dyes Pigments 2016;132:398–404https://doi.org/10.1016/j.dyepig.2016.05.026.
[25] Malina I, Kampars V, Belyakov S. Luminescence properties of 2-benzoyl-1,3-indandione based $Eu^{3+}$ ternary and tetrakis complexes and their polymer films. Dyes Pigments 2018;159:655–65https://doi.org/10.1016/j.dyepig.2018.07.003.
[26] Malina I, Juhnevics N, Kampars V. Study of thermal and optical properties of dibenzoyl-methane Eu(III) organic complexes. Proc Est Acad Sci 2017;66:493–500https://doi.org/10.3176/proc.2017.4.11.
[27] Siraj N, Das S, Hasan F, Lu C, Kiruri LW, Gall KES, Warner IM. Enhanced S2 emission in carbazole-based ionic liquids. RSC Adv 2015;5:9939–45https://doi.org/10.1039/C4RA12362J.
[28] Li L, Liu Y, Guo H, Wang Y, Cao Y, Liang A, Tan H, Qi H, Zhu M, Zhu W. Synthesis, optophysical and electrochemical properties of bipolar-transporting europium(III) complexes with carbazole and oxadiazole units. Tetrahedron 2010;66:7411–7https://doi.org/10.1016/j.tet.2010.07.003.
[29] Gao R, Koeppen C, Zheng G, Garito AF. Effects of chromophore dissociation on the optical properties of rare-earth-doped polymers. Appl Opt 1998;37:7100–6https://doi.org/10.1364/AO.37.007100.
[30] Zhu Z, Song B, Yuan J, Yang C. Enabling the triplet of tetraphenylethene to sensitize the excited state of europium(III) for protein detection and time-resolved luminescence imaging. Adv Sci 2016;3:1600146https://doi.org/10.1002/advs.201600146.
[31] Hu J, He Z, Wang Z, Li X, You J, Gao G. A simple approach to aggregation-induced emission in difluoroboron dibenzoylmethane derivatives. Tetrahedron Lett 2013;54:4167–70https://doi.org/10.1016/j.tetlet.2013.05.099.
[32] Galer P, Korošec RC, Vidmar M, Šket B. Crystal structures and emission properties of the BF2 complex 1-Phenyl-3-(3,5-dimethoxyphenyl)-propane-1,3-dione: multiple chromisms, aggregation- or crystallization-induced emission, and the self-assembly effect. J Am Chem Soc 2014;136:7383–94. 1 https://doi.org/10.1021/ja501977a.
[33] Yoshii R, Hirose A, Tanaka K, Chujo Y. Functionalization of boron diiminates with unique optical properties: multicolor tuning of crystallization-induced emission and introduction into the main chain of conjugated polymers. J Am Chem Soc 2014;136:18131–9https://doi.org/10.1021/ja510985v.
[34] Butler T, Morris WA, Samonina-Kosicka J, Fraser CL. Mechanochromic luminescence and aggregation induced emission of dinaphthoylmethane β-diketones and their boronated counterparts. ACS Appl Mater Interfaces 2016;8:1242–51https://doi.org/10.1021/acsami.5b09688.
[35] Werts MHV. Making sense of lanthanide luminescence. Sci Prog 2005;88:101–31https://doi.org/10.3184/003685005783238435.
[36] Yang C, Xu J, Ma J, Zhu D, Zhang Y, Lianga L, Lu M. The effect of two additional $Eu^{3+}$ lumophors in two novel trinuclear europium complexes on their photoluminescent properties. Photochem Photobiol Sci 2013;12:330–8https://doi.org/10.1039/c2pp25284h.
[37] Lunstroot K, Driesen K, Nockemann P, Viau L, Mutin PH, Vioux A, Binnemans K. Ionic liquid as plasticizer for europium(III)-doped luminescent poly(methyl methacrylate) films. Phys Chem Chem Phys 2010;12:1879–85https://doi.org/10.1039/B920145A.
[38] Binnemans K. Rare-earth beta-diketonates. Handbook on the physics and chemistry of rare earths vol. 35. North Holland: Elsevier; 2005.
[39] Mech A, Karbowiak M, Görller-Walrand C, Van Deun R. The luminescence properties of three tetrakis dibenzoylmethane europium(III) complexes with different counter ions. J Alloy Comp 2008;451:215–9https://doi.org/10.1016/j.jallcom.2007.05.019.
[40] Lunstroot K, Driesen K, Nockemann P, Görller-Walrand C, Binnemans K, Bellayer S, Le Bideau J, Vioux A. Luminescent ionogels based on europium-doped ionic liquids confined within silica-derived networks. Chem Mater 2006;18:5711–5https://doi.org/10.1021/cm061704w.
[41] Xu X, Yang X, Zhao J, Zhou G, Wong W-Y. Recent advances in solution-processible dendrimers for highly efficient phosphorescent organic light-emitting diodes (PHOLEDs). Asian J Org Chem 2015;4:394–429https://doi.org/10.1002/ajoc.201402266.
[42] Hong Y, Lam JWY, Tang BZ. Aggregation-induced emission. Chem Soc Rev 2011;40:5361–88https://doi.org/10.1039/C1CS15113D.
[43] Steemers FJ, Verboom W, Reinhoudt DN, van der Tal JEB, Verhoeven JW. New sensitizer-modified calix[4]arenes enabling near-UV excitation of complexed luminescent lanthanide ions. J Am Chem Soc 1995;117:9408–14https://doi.org/10.1021/ja00142a004.
[44] Latva M, Takalo H, Mukkala VM, Matachescu C, Rodriguez-Ubis JC, Kankare J. Correlation between the lowest triplet state energy level of the ligand and lanthanide(III) luminescence quantum yield. J Lumin 1997;75:149–69https://doi.org/10.1016/S0022-2313(97)00113-0.
[45] Li J, Li H, Yan P, Chen P, Hou G, Li G. Synthesis, crystal structure, and luminescent properties of 2-(2,2,2-Trifluoroethyl)-1-indone lanthanide complexes. Inorg Chem 2012;51:5050–7https://doi.org/10.1021/ic202473b.